STUDIES ON THE MECHANISMS UNDERLYING ACTIVITY IN THE SUBTHALAMIC NUCLEUS - GLOBUS PALLIDUS NETWORK

PETER JAMES MAGILL

Trinity College

Thesis submitted for the degree of Doctor of Philosophy at the University of Oxford

Hilary Term 2001



STUDIES ON THE MECHANISMS UNDERLYING ACTIVITY IN THE SUBTHALAMIC NUCLEUS - GLOBUS PALLIDUS NETWORK

PETER JAMES MAGILL
Trinity College, Oxford
Thesis submitted for the degree of Doctor of Philosophy, Hilary Term 2001

ABSTRACT

The reciprocally-connected network of neurons of the subthalamic nucleus (STN) and globus pallidus (GP) plays a pivotal role in basal ganglia function and dysfunction. A series of *in vivo* and *in vitro* electrophysiological studies were performed in order to elucidate the mechanisms underlying activity in the STN-GP network.

To characterise the relationship of activity in the normal STN-GP network to activity in the cerebral cortex, the principal excitatory afferent of the basal ganglia, single and multiple unit activity in STN and/or GP were recorded together with cortical electroencephalogram in anaesthetised rats during various states of cortical activation and inactivation. The data suggested that: (1) the rate and pattern of firing of STN and GP neurons are intimately related to coincident cortical activity and hence, the sleep-wake cycle; (2) oscillatory activity in the STN-GP network in health and disease may be driven by the cortex; and (3) activity of the network is regulated in space and time in a complex manner.

To provide insight as to whether the relationship between the STN-GP network and the cortex is altered in Parkinson's disease (PD), a similar study was undertaken using a well established model of experimental PD, the unilateral 6-hydroxydopamine-lesioned rat. The results indicated that: (1) activity in the STN-GP network is dramatically altered by the chronic loss of dopamine from the forebrain; (2) the impact of the cortex on the network is modulated by dopamine and thus, pathological oscillatory activity in the basal ganglia in PD may be caused by the inappropriate processing of rhythmic cortical input; (3) the classical indirect pathway is abnormally augmented during activation of the parkinsonian brain; and (4) the relative contributions of firing rate and pattern to information coding in the STN-GP network and the basal ganglia is related to the state of cortical activation.

To examine the dynamics of GABAergic inhibition in the STN and to test whether $GABA_A$ receptor-mediated synaptic input from the GP could generate rebound burst-firing in STN neurons, a phenomenon which may contribute to normal and abnormal activity in the STN-GP network, the equilibrium potential of $GABA_A$ receptor-mediated current, the reversal potential of $GABA_A$ receptor-mediated inhibitory post-synaptic potentials, and the degree of membrane hyperpolarisation required for rebound burst-firing were determined using perforated patch-clamp recordings *in vitro*. An extension of this study investigated the responses of STN neurons to different patterns of inhibitory synaptic input. The findings implied that: (1) active chloride homeostasis ensures a large net driving force for $GABA_A$ receptor-mediated events in STN neurons; (2) asynchronous and irregular inhibitory input from the GP has a profound influence on activity in the STN; and (3) synchronous, bursting activity in the parkinsonian GP could contribute to pathological oscillatory activity in the BG by generating rebound burst-firing in STN neurons.

In conclusion, the three studies have identified a number of key mechanisms underlying the activity of the STN-GP network. The importance of the corticosubthalamic projection in driving the activity of the STN-GP network has been established, suggesting that the STN should not be viewed as a simple relay station along the indirect pathway, but rather as a second important entry point for cortical information in the basal ganglia. Furthermore, the activity of STN and GP neurons was coupled, albeit to varying degrees, and thus, the reciprocal connections between these neurons are of great importance in shaping the activity of the network.

For My Mother

Christine P. Magill BSc.

ACKNOWLEDGEMENTS

First and foremost, I would like to thank my two co-supervisors, Dr. Mark Bevan and Professor Paul Bolam, for their boundless patience, help, advice and friendship during my studentship. I consider myself very fortunate to have been able to work with them. What a formidable team we made!

I would like to express my gratitude to Professor Peter Somogyi for the excellent facilities at the MRC Anatomical Neuropharmacology Unit and for sharing his views on the importance of "discoveries". I would also like to acknowledge the financial assistance of the Medical Research Council and the European Community.

I gratefully acknowledge the excellent technical assistance of Caroline Francis, Paul Jays and Liz Norman, and the secretarial assistance of Jo Gregory, Sandra Knowles and Pam Twynam. I also thank Drs. Edward Stern and Yoshiki Kaneoke for their help with data analysis, and Drs. Gordon Arbuthnott, Jochen Roeper and Charles Wilson for their invaluable comments and discussions.

Thank you to all of the "crazy kids" of the Unit, past and present, for their friendship and their enthusiastic attempts at stopping me becoming a complete square, especially (in alphabetical order to avoid arguments!) Adrian, Alison, André, Boother, Ed, Fen, Izumi, Jakob, Jason, Justin, Kerrie, Lizbuff, Marge, Nick, Philip, Sankari, TC, Txema, and Wai.

I would like to give my heartfelt thanks to my loving family for their seemingly tireless support over the years. I reserve my last thanks for Mary, my muse, whose love and encouragement have enriched my life beyond measure and have ensured that this thesis was completed. Annie Lennox, a childhood heroine of mine, once sang, "Behind every great man, there has to be a great woman". Well, that's certainly true in my case!

CONTENTS

ABSTRACT ii

ACKNOWLEDGEMENTS iv

TABLE OF CONTENTS v

ABBREVIATIONS x

CHAPTER 1. GENERAL INTRODUCTION 1

1.1 Introduction to the basal ganglia 2

1.2 Neostriatum 4

1.2.1 Projection neurons 4

1.2.2 Interneurons 8

1.3 Globus pallidus 9

1.4 Subthalamic nucleus 13

1.5 Entopeduncular nucleus 18

1.6 Substantia nigra 20

1.6.1 Substantia nigra *pars reticulata* 20

1.6.2 Substantia nigra *pars compacta* 22

1.7 The direct/indirect pathway model of information flow through the basal ganglia 25

1.8 Movement disorders 29

1.8.1 Parkinson's disease 29

1.9 Subthalamic nucleus - globus pallidus network 32

1.9.1 Functional organisation of the network 33

1.9.1.1 Anatomical considerations 33

1.9.1.2 Physiological considerations 36

1.9.2 Functions of the network in health 38

1.9.3 Functions of the network in disease 40

1.10 Aims of thesis studies 44

CHAPTER 2. MATERIALS AND METHODS 45

2.1 Electrophysiological recordings *in vivo* 46

2.1.1 Animals 46

2.1.2 Anaesthesia, analgesia and surgical procedures 46

2.1.3 Electroencephalogram 47
2.1.4 Extracellular recording of single and multiple units 48
2.1.5 Juxtacellular labelling of recorded units 49
2.1.6 Survival time and perfusion fixation 50
2.2 Unilateral lesion of midbrain dopaminergic neurons with 6-hydroxydopamine 52
2.2.1 Animals 52
2.2.2 Pretreatments, anaesthesia, analgesia and surgery 53
2.2.3 Postoperative care and recovery 54
2.2.4 Testing for successful unilateral 6-OHDA lesions 54
2.3 Histochemistry and immunocytochemistry 55
2.3.1 Histochemical verification of recording sites and juxtacellularly-labelled neurons for light and electron microscopic analysis 55
2.3.2 Immunocytochemical verification of 6-OHDA lesions 56
2.4 Acquisition and analysis of *in vivo* data 57
2.4.1 Data acquisition 57
2.4.2 Data sampling 58
2.4.3 Data analysis 58
2.4.3.1 Power spectra, auto-and cross-correlograms, phase shifts, spike-triggered waveform averages, mean rates of firing, coefficients of variation, 59
2.4.3.2 Lomb periodograms 61
2.4.3.3 Determination of firing pattern 62
2.4.4 Statistical analysis 62
2.5 Electrophysiological recordings *in vitro* 62
2.5.1 Animals 62
2.5.2 Anaesthesia and preparation of brain slices 62
2.5.3 Perforated patch-clamp recordings 63
2.5.4 Pharmacological manipulations 66
2.5.5 Verification of recording sites 66
2.6 Acquisition and analysis of *in vitro* data 67
2.6.1 Data acquisition 67
2.6.2 Data analysis 67
2.6.2.1 Determination of the equilibrium potential of $GABA_A$ receptor-mediated current 68

2.6.2.2 Determination of the reversal potential of $GABA_A$ receptor-mediated IPSPs 70
2.6.2.3 Determination of the level of membrane hyperpolarisation required for rebound burst-firing 70
2.6.3 Statistical analysis 71

CHAPTER 3. RELATIONSHIP OF ACTIVITY IN THE NORMAL SUBTHALAMIC NUCLEUS – GLOBUS PALLIDUS NETWORK TO ACTIVITY IN THE CEREBRAL CORTEX *IN VIVO* 72

3.1 Introduction 73
3.2 Experimental procedures 75
3.2.1 Electrophysiological recording and labelling of neurons in the STN-GP network of anaesthetised rats 75
3.2.2 Cortical spreading depression 77
3.2.3 Activation of the forebrain by somatosensory stimulation 78
3.3 Results 79
3.3.1 Juxtacellularly-labelled STN and GP neurons 79
3.3.2 Characterisation of EEG activity 81
3.3.3 Physiological characteristics of STN neurons 81
3.3.4 Physiological characteristics of GP neurons 87
3.3.5 Simultaneously-recorded STN and GP neurons 90
3.3.6 Simultaneously-recorded pairs of STN neurons 93
3.3.7 Simultaneously-recorded pairs of GP neurons 96
3.4 Discussion 98

CHAPTER 4. RELATIONSHIP OF ACTIVITY IN THE DOPAMINE-DEPLETED SUBTHALAMIC NUCLEUS – GLOBUS PALLIDUS NETWORK TO ACTIVITY IN THE CEREBRAL CORTEX *IN VIVO* 106

4.1 Introduction 107
4.2 Experimental procedures 110
4.2.1 Electrophysiological recording and labelling of neurons in the normal and dopamine-depleted STN-GP network of anaesthetised rats 110

4.2.2 Transection of the corpus callosum 111
4.2.3 Acute cortical ablation 112
4.2.4 Activation of the forebrain by somatosensory stimulation 113
4.2.5 Local field potential recordings 113
4.3 Results 115
4.3.1 Histochemical, immunocytochemical and histological observations 115
4.3.1.1 Location of recorded neurons 115
4.3.1.2 Extent of unilateral 6-OHDA lesions 115
4.3.1.3 Verification of callosal transections and cortical ablations 115
4.3.2 Characterisation of EEG activity 117
4.3.3 Firing properties of STN and GP neurons in normal animals before and after cortical ablation 118
4.3.4 Firing properties of STN and GP neurons in 6-OHDA-lesioned animals before and after cortical ablation 123
4.3.5 Responses of STN and GP neurons to global activation in normal animals before and after cortical ablation 129
4.3.6 Responses of STN and GP neurons to global activation in 6-OHDA-lesioned animals before and after cortical ablation 130
4.3.7 Characterisation of local field potentials in the STN and GP 134
4.3.8 Firing properties and response profiles of substantia nigra *pars reticulata* neurons in a 6-OHDA-lesioned animal before and after cortical ablation 140
4.4 Discussion 145

CHAPTER 5. $GABA_A$ RECEPTOR – MEDIATED INPUT TO SUBTHALAMIC NUCLEUS NEURONS *IN VITRO* 154
5.1 Introduction 155
5.2 Experimental procedures 158
5.2.1 Determination of $E_{GABA\text{-}A}$ and $E_{IPSP\text{-}A}$ 158
5.3 Results 159
5.3.1 Electrophysiological characteristics of STN neurons *in vitro* 159
5.3.2 Equilibrium potential of $GABA_A$ current in STN neurons 161
5.3.3 Rebound burst-firing of STN neurons 162

5.3.4 Reversal potential of $GABA_A$ receptor-mediated IPSPs in STN neurons 162
5.3.5 Responses of STN neurons to irregular synaptic barrage and bursts of IPSPs 165
5.4 Discussion 170

CHAPTER 6. GENERAL DISCUSSION 177
6.1 Summary and concluding remarks 178
6.2 Technical considerations 180
6.2.1 *In vivo* studies 181
6.2.2 *In vitro* study 185
6.3 Future studies 187
6.3.1 *In vivo* studies 188
6.3.2 *In vitro* studies 190
6.3.3 Anatomical studies 192

BIBLIOGRAPHY 193

ABBREVIATIONS

4-AP	4-aminopyridine
6-OHDA	6-hydroxydopamine
ABC	avidin-biotin peroxidase complex
AC	auto-correlogram
ACSF	artificial cerebrospinal fluid
AHP	afterhyperpolarising potential
AMPA	α-amino-3-hydroxy-5-methyl-4-isoxazoleproprionic acid
APV	D(-)-2-amino-5-phosphonovaleric acid
AvLFP	spike-triggered average of local field potential
AvWv	spike-triggered average of electroencephalogram
Ca^{2+}	calcium ion
CC	cross-correlogram
CGP 55845A	[3-[[1-(S)-(3,4-dichlorophenyl) ethyl]amino]-2-(S)-hydroxypropyl](phenyl-methyl)-phosphinic acid hydrochloride
Cl^-	chloride ion
Cm-Pf	centromedian-parafascicular thalamic complex
CNS	central nervous system
CV	coefficient of variation of the interspike interval
D1	dopamine receptor, subtype 1
D2	dopamine receptor, subtype 2
DAB	3, 3'-diaminobenzidine tetrahydrochloride
d.c.	direct current
DNQX	6,7-dinitroquinoxaline-2,3-dione
DRN	dorsal raphe nucleus
E_{Cl}	equilibrium potential of chloride
EEG	electroencephalogram
E_{GABA-A}	equilibrium potential of $GABA_A$ receptor-mediated current
EGTA	ethylene glycol-bis(B-aminoethyl ether)-N,N,N′,N′-tetraacetic acid
E_{IPSP-A}	reversal potential of $GABA_A$ receptor-mediated IPSPs
EM	electron microscope (microscopic)
EP	entopeduncular nucleus
EPSP	excitatory post-synaptic potential
g	gram(s)
GΩ	gigohm(s)
GABA	γ-aminobutyric acid
$GABA_A$	GABA receptor, subtype A
$GABA_B$	GABA receptor, subtype B
GP	globus pallidus
GPe	globus pallidus, external segment
GPi	globus pallidus, internal segment
HCO_3^-	bicarbonate ion
hr	hour
HEPES	4-(2-hydroxyethyl)-1-piperazineethane sulphonic acid
Hz	Hertz (cycles/events per second)
I	current
I_A	A-type potassium current
I_h	hyperpolarisation-activated mixed-cation current
I_{Kir}	inwardly-rectifying potassium current

ABBREVIATIONS (Cont.)

i.m.	intramuscular
i.p.	intraperitoneal
IPSP	inhibitory post-synaptic potential
IR-DIC	infrared differential interference contrast (microscopy)
ISI	interspike interval
I_T	T-type (low-threshold) calcium current
K^+	potassium ion
kHz	kiloHertz
$KMeSO_4$	potassium methylsulphate
L-DOPA	3,4-dihydroxy-L-phenylalanine
LFO	low-frequency oscillatory
LFP	local field potential
LM	light microscope (microscopic)
Lomb	Lomb periodogram
LTS	low-threshold spike
µA	microampere(s)
µg	microgram(s)
µm	micrometer(s)
µs	microsecond(s)
µV	microvolt(s)
MΩ	megaohm(s)
mACSF	modified artificial cerebrospinal fluid
mg	milligram(s)
MPTP	1-methyl-4-phenyl-1,2,3,6-tetrahydropyridine
min	minute(s)
MTg	mesopontine tegmentum
mV	millivolt(s)
n	number of observations
Na^+	sodium ion
nA	nanoampere(s)
NMDA	N-methyl-D-aspartate
NS	neostriatum
O.D.	outside diameter
pA	picoampere(s)
PB	phosphate buffer
PBS	phosphate-buffered saline
PD	Parkinson's disease
pEEG	power spectrum of the electroencephalogram
pLFP	power spectrum of the local field potential
PPN	pedunculopontine nucleus
psi	pounds per square inch
PV	parvalbumin
R_{series}	series resistance
s	second
s.c.	subcutaneous
SC	superior colliculus
SD	standard deviation
SN	substantia nigra

ABBREVIATIONS (Cont.)

SNpc	substantia nigra *pars compacta*
SNpr	substantia nigra *pars reticulata*
STN	subthalamic nucleus
SWA	slow-wave activity
T-channel	T-type calcium channel
TH	tyrosine hydroxylase (EC 1.14.16.2)
Tris	2-amino-2-(hydroxymethyl)propane-1,3-diol
TRN	thalamic reticular nucleus
V	voltage or potential difference
VL	ventrolateral nucleus of the thalamus
VM	ventromedial nucleus of the thalamus
VP	ventral pallidum
VTA	ventral tegmental area
WvCC	cross-correlogram of two waveforms

CHAPTER 1.

GENERAL INTRODUCTION

1.1 Introduction to the basal ganglia

The basal ganglia are a large group of subcortical nuclei intimately involved in a variety of processes including motor, associative, cognitive and mnemonic functions. The "dorsal" division of the basal ganglia consists of the neostriatum (NS, or caudate-putamen), the globus pallidus (GP) and its equivalent in primates, the external (or lateral) segment of the globus pallidus (GPe), the entopeduncular nucleus (EP) and its homologue in primates, the internal (or medial) segment of the globus pallidus (GPi), the subthalamic nucleus (STN) and the substantia nigra (SN). The latter structure is divided into two main parts, the dorsal *pars compacta* (SNpc) and the more ventral *pars reticulata* (SNpr). In addition to these structures, which are associated with motor and associative functions, there is a "ventral" division of the basal ganglia (ventral striatum or nucleus accumbens, olfactory tubercle, ventral pallidum (VP) and ventral tegmental area) that is associated with limbic functions.

The anatomy of the basal ganglia connections suggest that, at least in part, these structures operate as part of recurrent circuits (loops) with the cerebral cortex. In very simplistic terms, the basal ganglia receives cortical inputs, processes these inputs and feeds information back to the cortex via connections through the midbrain and thalamus. Broad subdivisions exist within these cortico-basal ganglia-thalamocortical loops suggesting that different loops operate in relation to different types of cortical function (Alexander and Crutcher, 1990; Parent and Hazrati, 1995a; Joel and Weiner, 1997). The importance of the "motor circuit" of the basal ganglia, just one of the family of cortico-basal ganglia thalamocortical loops, in cortical function is particularly apparent since neurodegenerative diseases of the basal ganglia result in profound movement disorders, including Parkinson's disease, Huntington's disease, and (hemi) ballismus (DeLong, 1990, Albin, 1995).

Virtually the whole of the cortical mantle projects onto the basal ganglia in a highly topographical manner. The main point of entry of this cortical information into the basal

ganglia is the neostriatum, although there are also substantial cortical projections to the STN. In what is now considered the classical view of the basal ganglia circuitry (Albin et al., 1989b; DeLong, 1990; see section 1.7), the functional organisation of the basal ganglia is such that cortical information carried by the corticostriatal projection is processed within the NS, integrated with the many other inputs to the basal ganglia (*e.g.* from the intralaminar thalamic nuclei, amygdala and dorsal raphe nucleus), and then the processed information is transmitted to the "output nuclei of the basal ganglia", the EP/GPi and the SNpr. The basal ganglia then influence motor-related behaviour via output nuclei projections to the ventral thalamus, which in turn, projects back to the cortex, or via projections to "premotor" subcortical regions, including the superior colliculus, the pedunculopontine nucleus of the mesopontine tegmentum, or the reticular formation (see Albin et al., 1989b; DeLong, 1990; Gerfen and Wilson, 1996; Smith et al., 1998 for recent reviews).

The studies detailed in this thesis were confined to the dorsal (associative and motor function-related) aspects of the basal ganglia and the interpretation and discussion of these data is focused on the motor-related functions of the basal ganglia. Thus, the ventral region of the basal ganglia, which has connectional features similar to those of its dorsal homologue (see Groenewegen et al., 1991; Groenewegen and Berendse, 1994 and references therein), will not be referred to further here, except for some discussion of the connections of the VP. Since rodents were used exclusively in these studies, terminology applicable to the rodent basal ganglia will be used. Thus, the term "globus pallidus" (GP) will not only refer to that structure in rodents (and cats) but includes the primate equivalent, the GPe. The term "basal ganglia output nuclei" will refer to the EP or the primate equivalent, the GPi, and the SNpr. The term "targets of the basal ganglia" refers to the main structures innervated by the basal ganglia *i.e.* the ventral tier of the thalamus, the lateral habenula, the superior colliculus, the mesopontine tegmentum and the reticular formation.

1.2 Neostriatum

The neostriatum is the largest component of the basal ganglia and is the main recipient of afferents to the basal ganglia from the cerebral cortex and thalamus. Studies on the cellular organisation of the NS have shown that it contains both projection neurons and several populations of interneurons (for recent reviews, see Bolam and Bennett, 1995; Kawaguchi et al., 1995; Gerfen and Wilson, 1996; Kawaguchi, 1997).

1.2.1 Projection neurons

The majority (90-95%) of the total population of neostriatal neurons, which has been estimated to be ~ 2.79 million neurons in each hemisphere in the rat (Oorschot, 1996), are projection neurons. The major type of projection neuron is the medium-size densely spiny neuron (hereafter referred to as "spiny projection neurons"). These neurons utilise γ-aminobutyric acid (GABA) as a neurotransmitter and are subdivided into two major populations on the basis of their projection targets, pattern of axonal collateralisation and their neurochemical content (for comprehensive reviews, see Smith and Bolam, 1990a; Bolam and Bennett, 1995; Parent and Hazrati, 1995a; Gerfen and Wilson, 1996; Smith et al., 1998; Bolam and Bevan, 2000). One subpopulation preferentially projects to the output nuclei of the basal ganglia (some neurons send a collateral to the GP; Kawaguchi et al., 1990; Parent et al., 1995) and expresses, in addition to GABA, the neuropeptide co-transmitters substance P and dynorphin (hereafter referred to as "striatonigral/entopeduncular neurons"). The second subpopulation only projects to the GP and expresses, in addition to GABA, enkephalin (hereafter referred to as "striatopallidal neurons"). There is considerable evidence from immunocytochemical as well as *in situ* hybridisation studies that the two major subtypes of dopamine receptor, the D1 subtype and the D2 subtype, are preferentially expressed in the striatonigral/entopeduncular and

striatopallidal projection neurons, respectively (Gerfen et al., 1990; Yung et al., 1995; Le Moine and Bloch, 1995; Ince et al., 1997; Aubert et al., 2000). It should be noted, however, that correlated anatomical, molecular biological and physiological studies suggest that D1 and D2 receptors are co-localised in a significant proportion of neostriatal projections neurons (Surmeier et al., 1996; Aizman et al., 2000). In addition to innervating extrinsic targets in the basal ganglia, the axons of spiny projection neurons also give rise to extensive local axon collaterals that target other spiny neurons and some types of interneuron (Bolam and Bennett, 1995; Gerfen and Wilson, 1996).

Although spiny projection neurons can be divided into two major populations using the criteria described above, studies *in vitro* and *in vivo* have demonstrated that the two subpopulations possess almost identical intrinsic physiological properties, which include: (1) a relatively hyperpolarised resting membrane potential (~ –75 to –90 mV), which is due to a powerful inwardly-rectifying potassium current (I_{Kir}); (2) a high action potential threshold (~ –42 mV); (3) fast, anomalous inward rectification that dominates responses to hyperpolarising current pulses (also due to I_{Kir}); (4) slow ramp-like response to depolarising current pulses, which is governed by fast and slow A-type potassium currents; and (5) the ability to fire action potentials at moderate to high rates (up to 70 Hz) with very little frequency adaptation (Calabresi et al., 1987, 1990; Kawaguchi et al., 1989; Tepper and Trent, 1993; Nisenbaum and Wilson, 1995; Wilson and Kawaguchi, 1996; Kawaguchi, 1997; Plenz and Kitai, 1998; Koós and Tepper, 1999).

The cerebral cortex provides the major excitatory input to the neostriatum. This input originates from most cortical areas, including: primary and secondary sensory areas; motor, premotor and prefrontal regions; as well as from limbic cortical areas (for reviews, see Alexander and Crutcher, 1990; Parent and Hazrati, 1995a; Gerfen and Wilson, 1996). These cortical inputs are topographically organised and remain, at least to some extent, functionally segregated within the NS and thus, impart functional organisation to the other

nuclei in the basal ganglia (Gerfen and Wilson, 1996). Indeed, functionally diverse information arising from the cerebral cortex is classically thought to be processed in the basal ganglia by parallel and segregated cortical-basal ganglia-thalamocortical loops (Alexander and Crutcher, 1990; Joel and Weiner, 1997). However, it should be noted that the basal ganglia are well suited to integrate information derived from different cortical regions to generate context-dependent, goal-directed patterns of behaviour (Graybiel et al., 1994; Graybiel 1995; Schultz et al., 1997).

All corticostriatal neurons are glutamatergic pyramidal neurons and can be divided into at least three major types based on their intracortical connections, laminar origin and pattern of striatal arborisation: (1) pyramidal tract neurons in deep layer V of motor cortex; (2) bilaterally-projecting corticocortical corticostriatal neurons in superficial layer V and deep layer III of premotor cortex; and (3) "corticothalamic" neurons in superficial layer VI of somatomotor cortex (Wilson, 1986; Cowan and Wilson, 1994; Kincaid and Wilson, 1996; Gerfen and Wilson, 1996). Consistent with the asymmetrical character of corticostriatal synapses onto spiny projection neurons, electrophysiological studies have shown that corticostriatal input evokes a monosynaptic excitatory post-synaptic potential (EPSP; Ryan et al., 1986; Wilson, 1986; Calabresi et al., 1990, 1996; Tepper and Trent, 1993), which is mediated by both α-amino-3-hydroxy-5-methyl-4-isoxazoleproprionic acid (AMPA)/kainate receptors and N-methyl-D-aspartate (NMDA) receptors (Kita, 1996). The excitatory cortical input to spiny projection neurons may be modulated by a host of other inputs, including those from extrinsic sources and from local interneurons (see Smith and Bolam, 1990a; Bolam and Bennett, 1995; Gerfen and Wilson, 1996; Kawaguchi, 1997 for reviews of the synaptology of spiny neurons). Extrinsic sources of input to spiny projection neurons include the dopaminergic input from the SNpc (Fallon and Moore, 1978; Beckstead et al., 1979; Freund et al., 1984; Gerfen et al., 1987; Hanley and Bolam, 1997; Joel and Weiner, 2000), serotonergic input from the dorsal raphe nucleus (DRN; Mori et al., 1985b;

Soghomonian et al., 1989; Lavoie and Parent, 1990) and GABAergic input from the GP (Staines et al., 1981; Beckstead, 1983a; Walker et al., 1989; Bevan et al., 1998; Kita et al., 1999). In addition, spiny projection neurons also receive glutamatergic inputs from the amygdala (Kita and Kitai, 1990; McDonald, 1991), and the rostral (centrolateral and paracentral) and caudal (centromedian-parafascicular complex) nuclei of the intralaminar thalamus (Beckstead, 1984; Dubé et al., 1988; Xu et al., 1991; Sadikot et al., 1992; Féger et al., 1994; Sidibé and Smith, 1996). Intrinsic sources of input to spiny projection neurons include afferents from the local axon collaterals of other spiny projection neurons (Wilson and Groves, 1980; Somogyi et al., 1981; Yung et al., 1996) and inputs from a variety of interneurons (see section 1.2.2).

Cortical input is a critical determinant for the complex activity observed in the neostriatum during movement. Intracellular recordings *in vivo* have shown that membrane potential shifts from a hyperpolarised ("down") state (~ –75 to –90 mV) to a depolarised ("up") state (~ –50 to –55 mV) appear to be necessary for action potential firing in spiny projection neurons (Calabresi et al., 1990; Wilson and Kawaguchi, 1996; Wickens and Wilson, 1998). These up state transitions are caused by the synchronous discharge of corticostriatal neurons (Cowan and Wilson, 1994; Wilson and Kawaguchi, 1996; Stern et al., 1997). In the absence of cortical input, the potassium current I_{Kir} ensures that the membrane potential remains in the down state and thus, far below the threshold for firing (Kawaguchi et al., 1989). Thus, in awake animals that are behaviourally inactive, spiny projection neurons typically exhibit very low rates (< 5 Hz) of spontaneous activity (DeLong, 1973; Soltysik et al., 1975; Garcia-Rill et al., 1979; Wilson and Groves, 1981; Schultz and Romo, 1988; Gardner and Kitai, 1992) and a large proportion of spiny projection neurons do not exhibit spontaneous activity at all (Wilson and Groves, 1981; Kiyatkin and Rebec, 1999). However, the preparation, initiation, execution or termination of particular movements is associated with increased corticostriatal output and brief episodes or "bursts" of action

potential firing in striatal neurons (De Long, 1973; Soltysik et al., 1975; Schultz and Romo, 1988; Gardner and Kitai, 1992; Jaeger et al., 1993, 1995; Kiyatkin and Rebec, 1999).

1.2.2 Interneurons

Neostriatal interneurons, which extend axons within but not out of the NS, make up approximately 5-10% of the rat neostriatal cell population. Four main classes of interneurons have been identified using cytochemical, physiological and morphological methods (for review see Kawaguchi et al., 1995). They are: (1) large cholinergic aspiny neurons; (2) parvalbumin-containing GABAergic aspiny neurons; (3) somatostatin/nitric oxide synthase/neuropeptide Y-containing GABAergic aspiny neurons; and (4) calretinin-containing GABAergic neurons. Small numbers of cholecystokinin- and vasoactive intestinal polypeptide-positive aspiny neurons have also been described. Many roles have been attributed to the various classes of interneuron in orchestrating the responses of spiny projection neurons to cortical input (see Kita, 1993; Kawaguchi et al., 1995 for reviews). For reasons of brevity, only the salient functions of parvalbumin-containing GABAergic interneurons (PV interneurons) will be related here since these neurons are the major targets of pallidostriatal projection neurons (Bevan et al., 1998; see section 1.3) and thus, are likely to be important effectors of GP output activity.

The GABAergic control of spiny neuron excitability is critical for normal motor behaviour (Yoshida et al., 1991; Yamada et al., 1995). Since inhibition arising from the local collaterals of spiny neurons is weak or nonexistent (Jaeger et al., 1994), the feed-forward inhibition of spiny neurons during periods of cortical activation is thought to be principally mediated by PV interneurons (Jaeger et al., 1994, Kita, 1993; 1996; Plenz and Kitai, 1998). These interneurons are well suited to this role because they receive monosynaptic input from the cortex (Lapper et al., 1992; Bennett and Bolam, 1994), display the ability to fire at high rates in response to depolarising input (Kawaguchi, 1993; Plenz and

Kitai, 1998) and establish frequent synaptic contact with spiny projection neurons (Kita et al., 1990; Bennett and Bolam, 1994). Indeed, the results of a recent study *in vitro* suggest that inhibitory post-synaptic potentials (IPSPs) generated by input from single PV interneurons are sufficiently powerful to shunt, delay and/or synchronise the discharge of many projection neurons simultaneously (Koós and Tepper, 1999). Thus, despite the relatively small number of neurons and boutons that comprise the pallidostriatal pathway (Bevan et al., 1998), pallidostriatal neurons are in a position to powerfully control the activity of the NS by selective innervation of PV interneurons, which in turn, control the activity of the spiny projection neurons.

1.3 Globus pallidus

The GP of the rat is the second largest nucleus of the basal ganglia and lies medial to the NS and posterior to the anterior commissure. Most of the ~ 46000 neurons that constitute the rat GP (Oorschot, 1996) are projection neurons that utilise GABA as their neurotransmitter (Oertel and Mugnaini, 1984; Smith et al., 1987). The neuronal population of the GP is heterogeneous and can be divided into two major subtypes on the basis of intrinsic physiological and morphological properties (Park et al., 1982; Millhouse, 1986; Kita and Kitai, 1991, 1994; Nambu and Llinás, 1994, 1997; Pang et al., 1998; Stanford and Cooper, 1999; Cooper and Stanford, 2000). Type I neurons constitute ~ 65% of the total cell population and exhibit the following intrinsic electrophysiological properties: (1) time- and voltage-dependent inward rectification in response to membrane hyperpolarisation, which is due to a hyperpolarisation-activated mixed-cation current (I_h) (2) a voltage- and Ca^{2+}-dependent low-threshold spike (LTS); and (3) the ability to fire action potentials at high frequencies (up to 350 Hz) with moderate frequency adaptation and little or no spike accommodation. Furthermore, approximately half of all type I neurons spontaneously

discharge at a moderate rate (5-10 Hz) and with a regular pattern in the absence of synaptic input. Type II neurons make up ~ 30% of the neuronal population and do not possess I_h or a LTS. Other distinguishing physiological characteristics include: (1) spontaneous firing (10-15 Hz) in an irregular manner in the absence of synaptic input; and (2) the ability to fire action potentials at very high frequencies (up to 440 Hz) with weak frequency adaptation and spike accommodation. Studies in guinea pig have suggested that the GP contains a small subpopulation of interneurons (4% of population) and an unusual type of projection neuron that displays Ca^{2+}-dependent, low-frequency (1-8 Hz) membrane oscillations in response to membrane depolarisation (Nambu and Llinás, 1994, 1997). However, the existence of interneurons or oscillatory projection neurons has not been confirmed in rat GP (Kita and Kitai, 1991; Stanford and Cooper, 1999; Cooper and Stanford, 2000).

The predominant inhibitory input to GP neurons is provided by the GABAergic spiny projection neurons of the NS (Noda et al., 1968; Levine et al., 1974; Ohye et al., 1976; Chang et al., 1981; Park et al., 1982; Wilson and Phelan, 1982; Totterdell et al., 1984; Gerfen, 1985; Nakanishi et al., 1985; Kita and Kitai, 1991; Kawaguchi et al., 1990; Yoshida et al., 1993; Parent et al., 1995; Shink and Smith, 1995). Globus pallidus neurons also receive an inhibitory input from the local axon collaterals of other GP neurons (Park et al., 1982; Millhouse, 1986; Kita and Kitai, 1994; Shink et al., 1996; Nambu and Llinás, 1997; Bevan et al., 1998; Stanford and Cooper, 1999; Bolam et al., 2000; Ogura and Kita, 2000; Sato et al., 2000a). The main excitatory input to the GABAergic neurons of the GP arises from the STN (Deniau et al., 1978a; Perkins and Stone, 1980; Kita et al., 1983a; Kita and Kitai, 1987, 1991; Robledo and Féger, 1990; Féger and Robledo, 1991; Soltis et al., 1994). The GP is reciprocally-connected to the STN by a series of open and closed loops (Kita and Kitai, 1987; Smith et al., 1990; Parent and Hazrati, 1995b; Shink et al., 1996; Joel and Weiner, 1997; Smith et al., 1998); the functional organisation of this network of STN and GP neurons is discussed in section 1.9.1. Additional extrinsic sources of excitatory input

include a topographic projection from the centromedian-parafascicular complex (Cm-Pf) of the intralaminar thalamus (Noda et al., 1968; Levine et al., 1974; Kincaid et al., 1991b; Deschênes et al., 1996; Mouroux et al., 1997) and minor projections from the cerebral cortex (Naito and Kita, 1994b; Lévesque et al., 1996; Lévesque and Parent, 1998). The GP is also known to receive a sparse dopaminergic projection from the SNpc (Fallon and Moore, 1978; Lindvall and Björklund, 1979; Lavoie et al., 1989; Charara and Parent, 1994; Gauthier et al., 1999; Hedreen, 1999; Jan et al., 2000; Smith and Kieval, 2000), which may have an excitatory and/or inhibitory effect on activity (Perkins and Stone, 1981; Bergstrom and Walters, 1984; Nakanishi et al., 1985). Furthermore, projections from the mesopontine tegmentum (MTg; an area defined by the cholinergic neurons of the pedunculopontine nucleus (PPN), the glutamatergic and GABAergic neurons of the midbrain extrapyramidal area, and to a lesser extent, the cholinergic neurons of the laterodorsal tegmental nucleus) are also likely to have mixed excitatory and inhibitory effects on GP neurons (Saper and Loewy, 1982; Gonya-Magee and Anderson, 1983; Jackson and Crossman, 1983; Woolf and Butcher, 1986; Lee et al., 1988; Charara and Parent, 1994). Although the serotonergic neurons of the DRN are known to send their axons to the GP (Mori et al., 1985b; Lavoie and Parent, 1990; Charara and Parent, 1994), physiological studies suggest that serotonin is unlikely to have a direct effect on GP neurons (Perkins and Stone, 1983).

Physiological analyses (responses to antidromic activation/invasion) and anterograde tract-tracing experiments have demonstrated that the efferents of the GP variously target all regions of the dorsal aspect of the basal ganglia, including STN (see section 1.9.1), EP (Kincaid et al., 1991a; Bolam and Smith, 1992; Bolam et al., 1993; Bevan et al., 1994b, 1997), SNpr (Totterdell et al., 1984; Smith and Bolam, 1989, 1990b; Kita and Kitai, 1991; Bolam et al., 1993; Bevan et al., 1996), and SNpc (Hattori et al., 1975; Smith and Bolam 1990b; Bevan et al., 1996). Furthermore, a subpopulation of GP neurons provide a feed-back inhibitory projection to the NS (Staines et al., 1981; Beckstead, 1983a; Staines and

Fibiger, 1984; Walker et al., 1989; Kita and Kitai, 1991; Spooren et al., 1996; Nambu and Llinás, 1994; Kita et al., 1999), which is known to preferentially target PV interneurons (Bevan et al., 1998; see section 1.2.2). Single-cell labelling studies of GP neurons in rodents and monkeys have provided evidence for a high degree of collateralisation of the axons of individual GP neurons (Kita and Kitai, 1994; Nambu and Llinás, 1997; Bevan et al., 1998; Bolam et al., 2000; Sato et al., 2000a). Indeed, the axon collaterals of a single GP neuron may establish synaptic contact with every nucleus in the basal ganglia (Bevan et al., 1998; Bolam et al., 2000). In addition to providing feed-forward and feed-back GABAergic projections to basal ganglia regions, the GP can also act as an output station of the basal ganglia that can influence the activity of thalamocortical neurons by virtue of a projection to the thalamic reticular nucleus (TRN; Asanuma and Porter, 1990; Hazrati and Parent, 1991; Gandia et al., 1993).

The GP also contains a number of cell types that do not target the STN, NS or output nuclei. A minor population (less than 15%) of non-cholinergic GP neurons do not project to the STN and send their axons to the cortex (van der Kooy and Kolb, 1985; Détári and Vanderwolf, 1987). Furthermore, a small number of cholinergic corticopetal neurons (Ingham et al., 1985; Moriizumi and Hattori, 1992), which are thought to be displaced neurons from the nucleus basalis of Meynert (Armstrong et al., 1983), are also scattered throughout the GP. The efferents of neurons located in caudal GP differ from those of rostral GP in that they project to extensive territories in posterior thalamus and the brainstem (Moriizumi and Hattori, 1992; Shammah-Lagnado et al., 1996). Thus, it appears that corticopetal neurons in rostral GP and most neurons in caudal GP are not closely related to the basal ganglia and will not be discussed further.

In contrast to the low level of spontaneous activity that is observed in the NS of awake rats, cats and non-human primates during periods of behavioural inactivity, most GP neurons are tonically active during these "resting" conditions and discharge at high rates (20-

70 Hz) with regular, irregular or (occasionally) bursting firing patterns (Noda et al., 1968; DeLong, 1971; Ohye et al., 1976; Garcia-Rill et al., 1979; Georgopoulos et al., 1983; DeLong et al., 1985; Sachdev et al., 1989; Filion and Tremblay, 1991; Gardner and Kitai, 1992; Cheruel et al., 1994; Boraud et al., 1998; Ruskin et al., 1999; Urbain et al., 2000). The discharge of many (but not all) GP neurons is selectively modulated in response to passive movements or during the planning, initiation, execution, and/or termination of voluntary movements. However, the relationship of neuronal activity to sensory and motor events is complex and inconsistent since neurons may exhibit phasic increases and/or decreases in firing rate, with or without a change in firing pattern, depending on the specifics of the movement and whether cognitive components are involved (DeLong, 1971; Soltysik et al., 1975; Georgopoulos et al., 1983; DeLong et al., 1985; Nambu et al., 1990; Anderson and Turner, 1991; Brotchie et al., 1991b, c; Mink and Thatch, 1991a, b; Gardner and Kitai, 1992; Cheruel et al., 1994; Jaeger et al., 1995).

1.4 Subthalamic nucleus

The STN is a small, lens-shaped nucleus that lies, as its name implies, below the thalamus and zona incerta, on the medial and inferior pole of the cerebral peduncle. In the rat, the STN is an "open" nucleus and consists of a homogeneous collection of ~ 13600 densely-packed neurons (Oorschot, 1996). Subthalamic nucleus neurons are unique within the basal ganglia in that they utilise glutamate as a neurotransmitter (Smith and Parent, 1988; Albin et al., 1989a; Rinvik and Ottersen, 1993). Intracellular labelling and Golgi-impregnation studies in rat, cat and primates have shown that the STN is composed of a single species of projection neuron (Yelnick and Percheron, 1979; Hammond and Yelnick, 1983; Kita et al., 1983a; Afsharpour, 1985a). In good agreement with these morphological data, the intrinsic physiological properties of STN neurons have been demonstrated to be largely homogeneous

(Kita et al., 1983b; Nakanishi et al., 1987a; Yung et al., 1991; Overton and Greenfield, 1995; Beurrier et al., 1999, 2000; Bevan and Wilson, 1999; Wigmore and Lacey, 2000) and include: (1) a prominent I_h; (2) a voltage- and Ca^{2+}-dependent LTS; (3) a non-inactivating (persistent) Na^+ current; (4) a persistent, outwardly rectifying K^+ current; (5) the ability to fire action potentials at very high frequencies (up to 500 Hz) with weak frequency adaptation and little or no spike accommodation; and (6) spontaneous single-spike firing of a moderate rate (5-40 Hz) and highly regular pattern in the absence of synaptic input. Whilst almost all STN neurons exhibit spontaneous single-spike firing (Yung et al., 1991; Overton and Greenfield, 1995; Bevan and Wilson, 1999), about half of the neuronal population exhibit a switch in spontaneous firing mode to rhythmic, bursting activity upon membrane hyperpolarisation or following application of metabotropic glutamate receptor agonists (Beurrier et al., 1999, 2000; Awad et al., 2000).

The main inhibitory input to the STN arises from the GABAergic projection neurons of the GP and VP (Carpenter et al., 1968, 1981; Tsubokawa and Sutin, 1972; Ohye et al., 1976; Rouzaire-Dubois et al., 1980; van der Kooy et al., 1981; Kita et al., 1983b; Canteras et al., 1990; Carpenter and Jayaraman, 1990; Bell et al., 1995; Maurice et al., 1998b). Whilst dorsomedial regions of rat STN are predominantly innervated by axons originating in the subcommisural regions of VP (Groenewegen and Berendse, 1990; Groenewegen et al., 1993; Bell et al., 1995; Bevan et al., 1997), the remainder receives a massive and topographically-organised projection from GP (Groenewegen and Berendse, 1990; Smith et al., 1990; Bevan et al., 1997). Moreover, the STN is functionally coupled to the pallidum by a series of open and closed loops (Carpenter et al., 1981; Kita and Kitai, 1987; Groenewegen and Berendse, 1990; Smith et al., 1990; Parent and Hazrati, 1995b; Shink et al., 1996; Joel and Weiner, 1997; Smith et al., 1998); the functional organisation of the STN-GP network is discussed in greater detail in section 1.9.1.

One of the major excitatory inputs to the STN is provided by the cerebral cortex. Anatomical studies in rat (Afsharpour, 1985b; Canteras et al., 1988, 1990; Féger et al., 1994; Bevan et al., 1995), cat (Romanski et al., 1979) and monkey (Hartmann-von Monakow et al., 1978; Nambu et al., 1996, 1997; Inase et al., 1999) have shown that the STN receives substantial, topographically-organised projections from several districts of the ipsilateral cerebral cortex, including prefrontal regions, primary motor cortex, and primary somatosensory cortex. The exact cellular origin and degree of collateralisation of the corticosubthalamic pathway are still poorly understand. However, retrograde labelling in the rat has shown that corticosubthalamic neurons are pyramidal in shape, are mainly located in layer V, and that many of them send axon collaterals to the NS (Canteras et al., 1988, 1990; Féger et al., 1994). Other studies in cats suggest that part of the corticosubthalamic pathway is derived from the axon collaterals of pyramidal tract neurons (Giuffrida et al., 1985). In good agreement with these anatomical data, brief electrical stimulation of the cortex evokes a powerful excitation of STN neurons (Kitai and Deniau, 1981; Rouzaire-Dubois and Scarnati, 1985; Fujimoto and Kita, 1993; Maurice et al., 1998a), which is probably mediated by both AMPA/kainate (Rouzaire-Dubois and Scarnati, 1987; Maurice et al., 1999) and NMDA receptors (Nakanishi et al., 1988; Nambu et al., 2000). Taken together, these data indicate that the STN may receive a copy of the commands that the motor cortex issues to the NS (see section 1.2.1 for detailed description of corticostriatal neurons) and spinal motor centres, and further suggest that the STN represents a crucial second entry point of cortical information into the circuitry of the basal ganglia.

Another prominent excitatory input to the STN is derived from the intralaminar thalamus (Sugimoto et al., 1983; Carpenter and Jayaraman, 1990; Groenewegen and Berendse, 1990; Sadikot et al., 1992; Féger et al., 1994; Bevan et al., 1995; Deschênes et al., 1996). Indeed, electrical or pharmacological stimulation of glutamatergic projection neurons in Cm-Pf evokes marked excitatory responses in STN neurons *in vivo* (Mouroux and Féger,

1993; Mouroux et al., 1995). It is also likely that cholinergic and glutamatergic projections from the MTg (Saper and Loewy, 1982; Jackson and Crossman, 1983; Woolf and Butcher, 1986; Lee et al., 1988; Charara and Parent, 1994; Bevan and Bolam, 1995) exert an excitatory influence on the STN since acetylcholine alone (Féger et al., 1979; Flores et al., 1996), or stimulation of the PPN (Hammond et al., 1983a; Rouzaire-Dubois and Scarnati, 1987), exerts a potent excitatory effect on STN neurons. Subthalamic nucleus neurons may also receive direct excitatory input from their neighbours since the axons of a subpopulation of projection neurons emit sparse local collaterals before exiting the nucleus (Hammond and Yelnik, 1983; Kita et al., 1983a; Shink et al., 1996). Furthermore, electrophysiological studies *in vitro* (Flores et al., 1995) suggest that the diffuse projection from the DRN to the STN (Mori et al., 1985a; Canteras et al., 1990; Lavoie and Parent, 1990; Charara and Parent, 1994) may also predominantly excite STN neurons. Although it is now well established that the dopaminergic SNpc neurons send their axons to the STN (Brown et al., 1979; Campbell et al., 1985; Lavoie et al., 1989; Flores et al., 1993; Charara and Parent, 1994; Hassani et al., 1997; Gauthier et al., 1999; Hedreen, 1999; Smith and Kieval, 2000), the functional role of dopamine in the STN is controversial. Indeed, local administration of dopamine or dopamine receptor agonists into the STN may lead to an increase (Campbell et al., 1985; Mintz et al., 1986; Rouzaire-Dubois and Scarnati, 1987; Kreiss et al., 1996) and/or a decrease (Campbell et al., 1985; Hassani and Féger, 1999) in the firing rates of STN neurons *in vivo*.

Anterograde and retrograde tract-tracing experiments have demonstrated that the STN projects to all of the nuclei in the dorsal division of the basal ganglia, including GP (see section 1.9.1), EP (Ricardo, 1980; Carpenter et al., 1981; Kita and Kitai, 1987; Parent and Smith, 1987; Bevan et al., 1994b), SNpr (Ricardo, 1980; Kita and Kitai, 1987; Parent and Smith, 1987; Bevan et al., 1994a), and SNpc (Kita and Kitai, 1987), as well as projecting to the VP (Ricardo, 1980; Kita and Kitai, 1987; Groenewegen and Berendse, 1990).

Furthermore, a small number of STN neurons send their axons to the NS (Beckstead, 1983b; Kita and Kitai, 1987; Parent and Smith, 1987; Takada et al., 1988) and the PPN (Jackson and Crossman, 1981, 1983; Hammond et al., 1983a; Kita and Kitai, 1987; Parent and Smith, 1987; Takada et al., 1988). Intracellular labelling (Hammond and Yelnick, 1983; Kita et al., 1983a), electrophysiological analyses (Deniau et al., 1978a; Hammond et al., 1983b; Kita et al., 1983b), and tracing experiments (van der Kooy and Hattori, 1980; Smith and Bolam, 1991; Bolam and Smith, 1992; von Krosigk et al., 1992; Bolam et al., 1993) in the rat have consistently demonstrated that most STN neurons are highly collateralised and that single STN neurons send axon collaterals to the GP, EP and SNpr. The situation is different in primates because whilst the majority (83%) of single axons projecting from STN arborise in GPe, only 25% of these axons also send collaterals to the GPi and SNpr (Sato et al., 2000b). Furthermore, it has been proposed that primate STN neurons can be divided into at least five subtypes based on their pattern and degree of axonal collateralisation (Sato et al., 2000b).

In awake animals that are behaviourally inactive or in anaesthetised animals, STN neurons are tonically active and exhibit moderate (10-40 Hz) and regular or irregular (and occasionally bursting) spontaneous firing (Tsubokawa and Sutin, 1972; Rouzaire-Dubois et al., 1980; Georgopoulos et al., 1983; DeLong et al., 1985; Robledo and Féger, 1990; Féger and Robledo, 1991; Bergman et al., 1994; Cheruel et al., 1996; Hassani et al., 1996; Kreiss et al., 1996, 1997; Maurice et al., 1998b; Urbain et al., 2000). The discharge of many (but not all) STN neurons is selectively modulated in response to passive limb manipulations or during the initiation, execution, and/or termination of voluntary skeletomotor movements. As is the case for the GP, the relationship of neuronal activity in the STN to motor events appears to be complex since neurons can exhibit monophasic, biphasic and/or triphasic fluctuations in firing rate during movement, depending on the specifics of the motor task and whether cognitive or sensory components are involved (Georgopoulos et al., 1983; DeLong et al., 1985; Matsumura et al., 1992; Wichmann et al., 1994a; Cheruel et al., 1996).

However, in contrast to the GP, monophasic excitation is by far the most common response to limb movement (Wichmann et al., 1994a; Cheruel et al., 1996). Whilst the activity of STN neurons is inconsistently modulated during skeletomotor tasks, the activity of a small group of neurons in the ventral sector of monkey STN is always increased during the performance of specific visual and oculomotor tasks (Matsumura et al., 1992).

1.5 Entopeduncular nucleus

The EP of the rat is a small nucleus consisting of ~ 3200 neurons (Oorschot, 1996) and is located among the fibres of the rostral aspect of the cerebral peduncle. All EP neurons are projection neurons that utilise GABA as their neurotransmitter (Oertel and Mugnaini, 1984; Smith et al., 1987). The EP neuron population can be divided into two mayor subtypes using physiological and morphological criteria (Nakanishi et al., 1990, 1991). Type I neurons constitute ~ 80% of the total cell population and are electrophysiologically characterised as possessing: (1) a marked I_h; (2) a LTS; (3) the ability to spontaneously discharge (5-30 Hz) in a regular or irregular manner in the absence of synaptic input; and (4) the ability to fire action potentials at high frequencies (up to 300 Hz) with little or no frequency adaptation or spike accommodation. Type II neurons do not spontaneously fire and do not possess I_h or a prominent LTS, but typically display a ramp depolarisation attributable to a A-type potassium current (I_A) (Nakanishi et al., 1990).

The EP receives a massive inhibitory GABAergic input from the NS (van der Kooy and Carter, 1981; Bolam and Smith, 1992; Bolam et al., 1993; Fink-Jensen and Mikkelsen, 1989; Rajakumar et al., 1993; Bevan et al., 1994b), the GP (Kincaid et al., 1991a; Bolam and Smith, 1992; Bolam et al., 1993; Bevan et al., 1994b; 1997, 1998; Kita and Kitai, 1994) and the VP (Bevan et al., 1997). Furthermore, the EP can be regarded a site of integration of functionally diverse information within the basal ganglia since the synaptic terminals of

neostriatal and pallidal afferents, as well as those of GP and VP afferents, converge on individual EP neurons (Bolam and Smith, 1992; Bolam et al., 1993; Bevan et al., 1994b; 1997). The principal excitatory afferents to the EP are derived from the glutamatergic neurons of the STN (Deniau et al., 1978a; Kita et al., 1983a; Kita and Kitai, 1987; Robledo and Féger, 1990; Féger and Robledo, 1991; Nakanishi et al., 1991; Bevan et al., 1994b). In addition, the EP receives excitatory glutamatergic and cholinergic inputs from the MTg (Saper and Loewy, 1982; Gonya-Magee and Anderson, 1983; Jackson and Crossman, 1983; Woolf and Butcher, 1986; Lee et al., 1988; Clarke et al., 1996, 1997) as well as sparse dopaminergic and serotonergic inputs from the SNpc and DRN, respectively (Mori et al., 1985b; Lavoie and Parent, 1990; Charara and Parent, 1994; Gauthier et al., 1999).

The EP and the substantia nigra *pars reticulata* (see section 1.6.1) are the output nuclei of the basal ganglia and thus, constitute the last link in the chain of basal ganglia nuclei that contribute to the cortico-basal ganglia-thalamocortical loops. These nuclei act as an active interface through which cortically-derived information that has been previously processed by the basal ganglia is relayed to target structures in order to influence behaviour. Whilst the PV-containing projection neurons of the caudal two thirds of the EP send their axons to the ventrolateral (VL), ventromedial (VM) and Cm-Pf thalamic nuclei and/or the PPN, the PV-negative projection neurons in the rostral third of the EP principally target the lateral habenula nucleus (Carter and Fibiger, 1978: Filion and Harnois, 1978; Parent et al., 1981; van der Kooy and Carter 1981; Rajakumar et al., 1994). The axons of EP neurons do not emit local collaterals (Nakanishi et al., 1991).

Studies of EP and GPi activity *in vivo* have shown that neurons in these nuclei generally discharge in a tonic, moderate- to high-frequency (20-80 Hz) fashion, with regular and/or irregular firing patterns, during periods of behavioural inactivity or under anaesthesia (DeLong, 1971; Garcia-Rill et al., 1979; Georgopoulos et al., 1983; DeLong et al., 1985; Sachdev et al., 1989; Robledo and Féger, 1990; Féger and Robledo, 1991; Filion and

Tremblay, 1991; Cheruel et al., 1994; Boraud et al., 1998; Ruskin et al., 1999; Wichmann et al., 1999). The discharge of many (but not all) EP and GPi neurons is specifically modulated during passive movements or during the planning, initiation, execution, and/or termination of voluntary movements. However, the relationship of neuronal activity to motor-related events is complex and inconsistent since neurons may display decreases and/or increases in firing rate, with or without a change in firing pattern, and responses may vary according to the specifics of the movement and whether cognitive or sensory components are also involved (DeLong, 1971; Soltysik et al., 1975; Georgopoulos et al., 1983; DeLong et al., 1985; Nambu et al., 1990; Anderson and Turner, 1991; Brotchie et al., 1991b, c; Mink and Thatch, 1991a, b; Cheruel et al., 1994; Jaeger et al., 1995; Boraud et al., 2000a).

1.6 Substantia nigra

The substantia nigra lies just caudal to the STN and is generally divided into two major nuclei, the *pars reticulata* and the *pars compacta*.

1.6.1 Substantia nigra *pars reticulata*

The SNpr is an ovoid-shaped nucleus located ventral to the SNpc and consists of ~ 26000 loosely-packed neurons (Oorschot, 1996). The SNpr neuron population can be divided into two very distinct subtypes using physiological and morphological criteria (Nakanishi et al., 1987b; Richards et al., 1997). Type I neurons account for the large majority of the total cell population in the SNpr and are GABAergic projection neurons (Oertel and Mugnaini, 1984; Smith et al., 1987). In marked contrast to the intrinsic physiological properties of type II neurons (see below), type I neurons do not posses a prominent I_h or LTS, and display neither inward or outward rectification. Additional electrophysiological hallmarks include: (1) a short duration action potential (~ 0.5 ms halfwidth) with a small biphasic

afterhyperpolarisation (AHP); (2) the ability to spontaneously discharge (5-30 Hz) in a regular or irregular manner in the absence of ordered synaptic input; and (3) the ability to fire action potentials at high frequencies (up to 200 Hz) with little or no frequency adaptation or spike accommodation. Type II neurons are dopaminergic projection neurons and have physiological and morphological traits that are indistinguishable to those of dopaminergic SNpc neurons (Nakanishi et al., 1987b; Richards et al., 1997; see section 1.6.2).

The SNpr receives a highly-ordered, inhibitory GABAergic input from the spiny projection neurons of the NS (Precht and Yoshida, 1971; Bunney and Aghajanian, 1976; Dray et al., 1976; Chevalier et al., 1985; Gerfen, 1985; Grace and Bunney, 1985; Bolam et al., 1993; Bevan et al., 1994a; Deniau et al., 1996). Additional inhibitory inputs originate in the GP (Totterdell et al., 1984; Smith and Bolam, 1989, 1990b; Bolam et al., 1993; Bevan et al., 1996, 1998) and the VP (Bevan et al., 1996; Zahm et al., 1996). Furthermore, these functionally diverse inhibitory inputs have been shown to converge at the level of single projection neurons in the SNpr (Smith and Bolam, 1991; von Krosigk et al., 1992; Bolam et al., 1993; Bevan et al., 1996). Although there is some anatomical evidence that the SNpr receives a monosynaptic projection from the prefrontal cortex (Bunney and Aghajanian, 1976; Kornhuber et al., 1984; Naito and Kita, 1994a), the major excitatory input to the SNpr is almost certainly derived from the STN (Deniau et al, 1978a; Hammond et al., 1978a, 1983b; Kita et al., 1983a; Chang et al., 1984; Kita and Kitai, 1987; Nakanishi et al., 1987b; Robledo and Féger, 1990; Féger and Robledo, 1991; Rinvik and Ottersen, 1993; Bevan et al., 1994a). The SNpr also receives input from the cholinergic and non-cholinergic neurons of the MTg (Woolf and Butcher, 1986; Beninato and Spencer, 1988; Lee et al., 1988; Bolam et al., 1991), and input from the serotonergic neurons of the DRN (Lavoie and Parent, 1990; Corvaja et al., 1993).

The SNpr in one of the output nuclei of the basal ganglia. The efferents of the SNpr target extensive regions of the thalamus (VM, Cm-Pf, mediodorsal, lateral dorsal, and

paracentral nuclei) as well as the superior colliculus, PPN, and mesencephalic reticular formation (Faull and Mehler, 1978; Deniau et al., 1978b; Chevalier et al., 1981; Beckstead et al., 1979; Bentivoglio et al., 1979; Grofová et al., 1982; Deniau and Chevalier, 1992; von Krosigk et al., 1992). A small population (5-8%) of GABAergic SNpr neurons project to the NS (Rodríguez and González-Hernández, 1999). The axons of most, if not all, SNpr neurons emit local collaterals that extensively ramify within the SNpr and the SNpc (Deniau et al., 1982; Grofová et al., 1982; Damlama et al., 1993).

The activity of SNpr (presumably GABAergic projection) neurons in awake, but immobile animals (Wilson et al., 1977; DeLong et al., 1983; Waszczak et al., 1984; Schwarz et al., 1984; Schultz, 1986; Magariños-Ascone et al., 1992; Ruskin et al., 1999; Wichmann et al., 1999) or in anaesthetised animals (Dray et al., 1976; Deniau et al., 1978b; Chevalier et al., 1985; Robledo and Féger, 1990; MacLeod et al., 1990; Féger and Robledo, 1991; Fujimoto and Kita, 1992; Burbaud et al., 1995; Murer et al., 1997) is typified by a tonic, regular or irregular discharge at moderate to high rates (15-70 Hz). The relationship of activity in the SNpr to motor and sensory events is convoluted and appears to be highly variable because phasic increases and/or decreases in activity have been reported to accompany the planning, initiation and/or execution of skeletomotor and oculomotor commands (DeLong et al., 1983; Schwarz et al., 1984; Schultz, 1986; Nishino et al., 1985; Magariños-Ascone et al., 1992).

1.6.2 Substantia nigra *pars compacta*

The SNpc is a small nucleus that lies along the dorsomedial aspect of the SNpr and consists of ~ 7200, densely-packed neurons (Oorschot, 1996). The majority (> 95%) of SNpc neurons are dopaminergic projection neurons (Gerfen and Wilson, 1996; Joel and Weiner, 2000). The morphological and physiological of dopaminergic SNpc neurons are readily distinguishable from those of GABAergic SNpr neurons (Grace and Bunney, 1983b, 1984a;

Kita et al., 1986; Tepper et al., 1987; Richards et al., 1997; Iribe et al., 1999). The defining intrinsic physiological properties of SNpc neurons include: (1) a prominent I_h and I_A; (2) a long duration action potential (~ 1.5 ms halfwidth) with a large single AHP; (3) a regular ("pacemaker-like") spontaneous discharge at low rates (< 5 Hz) in the absence of synaptic input; and (4) strong frequency adaptation and spike accommodation during sustained firing (typically cannot maintain firing much above 15 Hz). Furthermore, more than 50% of SNpc neurons exhibit an LTS or similar "pacemaker-like slow depolarisation".

The projection neurons of the SNpc receive a topographically organised, inhibitory GABAergic input from NS (Dray et al., 1976; Grace and Bunney, 1985; Gerfen et al., 1985; Tepper et al., 1990; Bolam and Smith, 1991). Additional GABAergic input to the SNpc is provided by the GP (Smith and Bolam 1990b; Bevan et al., 1996, 1998), the VP (Bevan et al., 1996; Zahm et al., 1996), and the local axon collaterals of SNpr neurons (Grofová et al., 1982; Grace and Bunney, 1985; Damlama et al., 1993; Tepper et al., 1995; Celada et al., 1999; Paladini and Tepper, 1999). The SNpc receives an excitatory input from the STN; although the projection from the STN to the SNpc is relatively sparse (Ricardo, 1980; Kita and Kitai, 1987), a wealth of physiological data indicate that this input exerts a powerful effect on the activity of SNpc neurons (Hammond et al., 1978a; Nakanishi et al., 1987b; Robledo and Féger, 1990; Smith and Grace, 1992; Chergui et al., 1994; Kang and Futami, 1999; Iribe et al., 1999). The SNpc also receives excitatory inputs from the MTg, which has both cholinergic and glutamatergic components (Scarnati et al., 1986; Woolf and Butcher, 1986; Beninato and Spencer, 1987; Lee et al., 1988; Bolam et al., 1991), and the cortex (Naito and Kita, 1994a), as well as a serotonergic input from the DRN (Lavoie and Parent, 1990; Corvaja et al., 1993).

The dopaminergic innervation of the basal ganglia plays a central role in a wide variety of motor, cognitive and emotional functions ascribed to these nuclei. The functional importance of this innervation is exemplified by the marked motor and cognitive

disturbances that occur in Parkinson's disease and in animal models of Parkinson's disease involving the selective destruction of dopaminergic nigral neurons (see section 1.8.1). Although the major target of the dopaminergic nigral projection system is the NS (Fallon and Moore, 1978; Beckstead et al., 1979; Gerfen et al., 1987; Hanley and Bolam, 1997), SNpc neurons also send their axons to the EP, GP and STN (for comprehensive reviews of the anatomy of the dopaminergic innervation of the basal ganglia (see Joel and Weiner, 2000; Smith and Keival, 2000).

In anaesthetised animals, or in awake animals that are behaviourally inactive, most dopaminergic SNpc neurons are spontaneously active and typically discharge at a slow (2-8 Hz) rate and in an irregular manner, although regular (pacemaker) or bursting firing patterns are also sometimes observed (Wilson et al., 1977; Deniau et al., 1978b; DeLong et al., 1983; Grace and Bunney, 1983a, b, 1984a, b, 1985; Freeman et al., 1985; Diana et al., 1989; Schultz, 1986; Tepper et al., 1987, 1995; Magariños-Ascone et al., 1992; Dai and Tepper, 1998; Paladini and Tepper, 1999; Ruskin et al., 1999). Clear covariations in the firing rate and pattern of SNpc activity with limb and eye movements have only been observed in a small subpopulation of dopaminergic neurons; these neurons tend to fire bursts of action potentials during the initiation and execution of movements (DeLong et al., 1983; Freeman et al., 1985; Diana et al., 1989; Romo and Schultz, 1990; Magariños-Ascone et al., 1992). By contrast, it has been found that dopaminergic neurons are activated in a very distinctive manner by the rewarding characteristics of a wide range of somatosensory, visual and auditory stimuli (Romo and Schultz, 1990; Schultz and Romo, 1990). Thus, it has been proposed that dopaminergic neurons label environmental stimuli with appetitive value, predict and detect rewards and signal alerting and motivational events (reviewed by Schultz, 1998).

1.7 The direct/indirect pathway model of information flow through the basal ganglia

It is clear that the nuclei of basal ganglia are heavily interconnected and that many different combinations of feed-forward and feed-back circuits probably underlie the complex spatiotemporal sequences of activity that are observed in the basal ganglia during movement. The highly complex nature of the functional organisation of the basal ganglia has inevitably hampered the development of consolidated hypotheses of basal ganglia function that take into account data derived from different disciplines. However, the continued correlation of *post mortem* human anatomical and neurochemical findings with data derived from experimental models of basal ganglia disease has facilitated the construction of a unifying model of the functional organisation of the basal ganglia that accounts for both normal and abnormal motor function (Albin et al., 1989b). This model, which has been expanded, elaborated and updated by many authors since its conceptualisation (Alexander and Crutcher, 1990; DeLong, 1990; Chesselet and Delfs, 1996; Gerfen and Wilson, 1996; Wichmann and Delong, 1996; Levy et al., 1997; Smith et al., 1998; Obeso et al., 2000b), is based on the so-called "*direct*" and "*indirect*" pathways of cortical information flow through the basal ganglia. The direct/indirect pathway model of the motor circuit of the basal ganglia, just one of a family of cortico-basal ganglia thalamocortical loops, is schematically illustrated in Fig. 1.1*A*. According to this model of the basal ganglia motor circuit, cortical information impinging on the NS is processed and subsequently transmitted to the output nuclei of the basal ganglia via two routes; either directly from the NS to the output nuclei or indirectly via the GP and STN (Fig. 1.1*A*). When the basal activity of basal ganglia neurons (*i.e.* the rates and patterns of firing exhibited during periods of behavioural inactivity) and the nature of the neurotransmitters utilised by these neurons are both taken into account, it becomes apparent that the consequences of activation of the direct and indirect pathways are

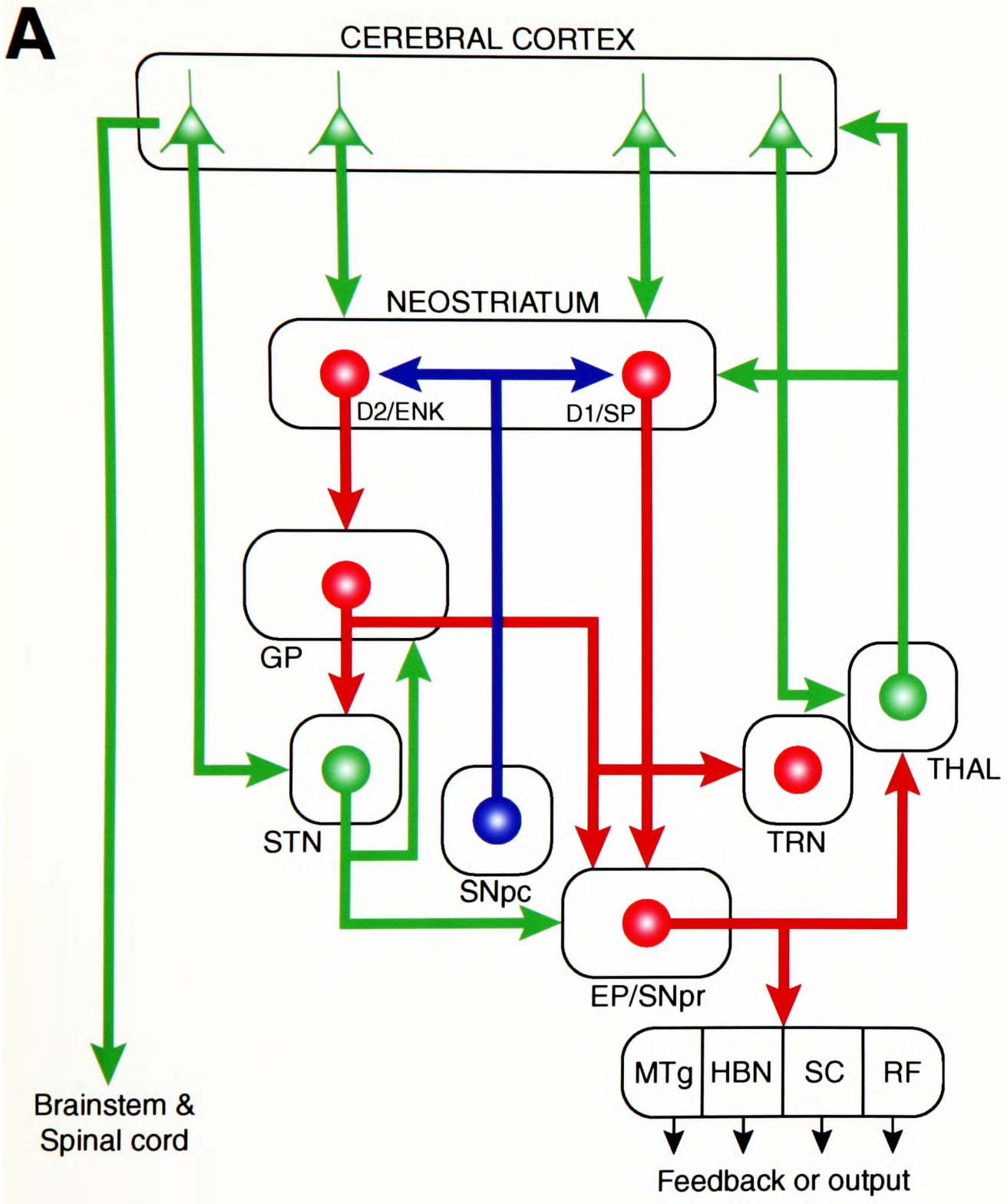
functionally opposite in the target regions of the basal ganglia (Fig. 1.1*A*; Albin et al., 1989b; DeLong, 1990). In short, activation of the direct pathway leads to a disinhibition of neurons in the targets of the basal ganglia, whereas activation of the indirect pathway leads to an inhibition of neurons in the target regions.

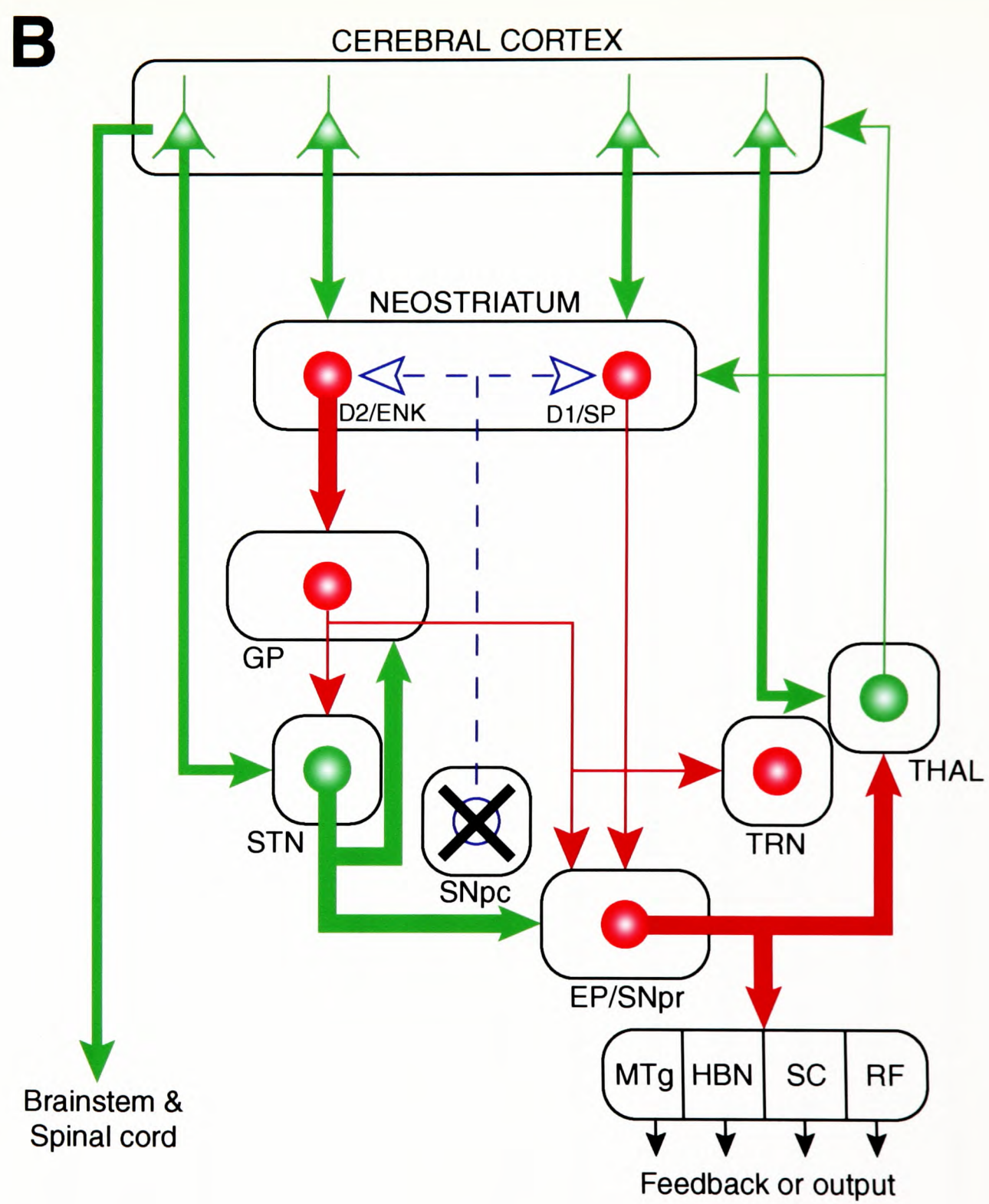
According to the model, the diametrically opposed influences of the direct and indirect pathways on the targets of the basal ganglia are dependent on the excitation of spiny projection neurons, which are typically quiescent at rest, and the subsequent propagation of signals through the basal ganglia via feed-forward connections. Activation of glutamatergic corticostriatal neurons, which could be expected to occur during the preparation or initiation of movement, concurrently increases the firing of spiny projection neurons that give rise to the direct and indirect pathways. Increased activity of spiny projection neurons that give rise to the direct pathway leads, by virtue of their GABAergic nature, to the inhibition of tonically active neurons in the output nuclei. A reduction in the tonic activity of the GABAergic neurons in the output nuclei leads to a reduction in the inhibition of, or a disinhibition of, neurons in the targets of the basal ganglia. The phenomenon of disinhibition of the targets of the basal ganglia is central to the physiology of the cortico-basal ganglia-thalamocortical loops (reviewed by Chevalier and Deniau, 1990). In particular, disinhibition of ventral thalamic targets facilitates the flow of information through these regions and provides a positive feed-back signal to the premotor and motor cortices, from which much of the movement-related activity within the basal ganglia arises. In contrast to this, activation of those spiny neurons that project to the GP, *i.e.* neurons that give rise to the indirect pathway, leads to the opposite functional effect in the targets of the basal ganglia. Activation of corticostriatal fibres will result in the increased activity of striatopallidal neurons which, in turn, inhibit the tonically active neurons in the GP. Inhibition of these neurons disinhibits neurons in the STN. Since STN neurons are glutamatergic, their increased activity leads to increased firing of neurons in the output

Figure 1.1. Schematic diagram of the direct/indirect pathway model of the cortico-basal ganglia-thalamocortical motor circuitry under (*A*) normal conditions and in (*B*) Parkinson's disease. Inhibitory (GABAergic) projections are depicted as *red arrows*, and excitatory (glutamatergic) projections as *green arrows*.

A, According to this model, cortical information that reaches the neostriatum during movement is conveyed to the output nuclei of the basal ganglia, the entopeduncular nucleus (EP) and the substantia nigra *pars reticulata* (SNpr), via two pathways, a direct inhibitory projection from the neostriatum to EP/SNpr and an indirect pathway, which involves an inhibitory projection from the neostriatum to globus pallidus (GP), an inhibitory projection from the GP to subthalamic nucleus (STN), and an excitatory projection from the STN to EP/SNpr. The information is then transmitted back to the cerebral cortex via a relay in the thalamus (THAL) or conveyed to various brain stem structures: The EP projects to the pedunculopontine nucleus of the mesopontine tegmentum (MTg) and the lateral habenular nucleus (HBN), whereas the SNpr innervates the MTg, the superior colliculus (SC) and the reticular formation (RF). Thus, activation of the direct pathway leads to a disinhibition of neurons in the targets of the basal ganglia, whereas activation of the indirect pathway leads to an inhibition of neurons in the target regions. The direct and indirect pathways largely arise from different populations of neostriatal spiny projection neurons that contain different peptides and preferentially express different subtypes of dopamine receptor. The dopaminergic projection from the substantia nigra *pars compacta* (SNpc; *blue arrows*) exerts a net excitatory effect on spiny projection neurons giving rise to the direct pathway by the activation of D1 receptors, and a net inhibitory effect on spiny projection neurons giving rise to the indirect pathway by activation of D2 receptors. Thus, in effect, the overall influence of dopamine within the neostriatum may be to reinforce any cortically-initiated activation of the motor circuit by both facilitating conduction though the circuit's direct pathway and suppressing conduction through the indirect pathway. Cortical information can also reach the basal ganglia via the corticosubthalamic projection. Note the extensive projections of the GP and the reciprocal connections between the GP and STN.

B, In Parkinson's disease, the loss of dopaminergic neurons in SNpc (represented by *black cross* and *dashed blue arrows*) results in an imbalance in the activity of the direct and indirect pathway in favour of the indirect pathway. Relative increases in activity are indicated by *thickening* of arrows and relative decreases in activity by *thinning* of arrows as compared to *A*. The net result of this imbalance is the overactivity of GABAergic neurons in the output nuclei, which leads to excessive inhibition and, effectively, to shutdown of the targets of the basal ganglia. The excessive thalamic inhibition leads to suppression of the cortical motor system, possibly resulting in akinesia, rigidity, and tremor, whereas the overactive inhibitory projection to the brainstem locomotor areas may contribute to abnormalities of gait and posture. It should be noted that these diagrams are a simplification as many connections have not been indicated. ENK, enkephalin; SP, substance P; TRN, thalamic reticular nucleus. Modified from Fig. 12 in Smith et al., 1998 and Fig. 1 in DeLong, 1990.


A
CEREBRAL CORTEX
NEOSTRIATUM
D2/ENK
D1/SP
GP
STN
SNpc
TRN
THAL
EP/SNpr
MTg
HBN
SC
RF
Brainstem &
Spinal cord
Feedback or output


B
CEREBRAL CORTEX
NEOSTRIATUM
D2/ENK
D1/SP
GP
STN
SNpc
TRN
THAL
EP/SNpr
MTg
HBN
SC
RF
Brainstem &
Spinal cord
Feedback or output

nuclei and hence, because neurons in the output nuclei are GABAergic, leads to a greater inhibition of neurons in the target nuclei. The increased inhibition of neurons in the target nuclei provides negative feed-back to the cortex and is likely to be associated with the cessation of selected movements and the suppression of non-selected movements (Albin et al., 1989b; DeLong, 1990).

The model predicts that one of the most important functions of the dopaminergic input to the basal ganglia is to exert a dual effect on the spiny projection neurons of the NS; exciting D1-expressing striatonigral/entopeduncular neurons and inhibiting D2-expressing striatopallidal neurons (Fig. 1.1*A*; see Albin et al., 1989b; DeLong, 1990; Alexander and Crutcher, 1990). Thus, in effect, the overall influence of dopamine within the NS may be to reinforce any cortically-initiated activation of the motor circuit by both facilitating conduction though the circuit's direct pathway and suppressing conduction through the indirect pathway. It should be noted however, that this scheme is only a gross approximation of the role of dopamine within the NS. In reality, the functions of dopamine within the basal ganglia appear to be highly complex and many issues remain unresolved (see recent reviews by Greengard et al.,1999; Nicola et al., 2000; Obeso et al., 2000b; Smith and Kieval, 2000 and references therein).

The proposed direct/indirect pathway model has been used to advance two possible functions of the motor circuit, the "scaling" and "focusing" of movements. To achieve scaling of movement parameters and termination of movements, neostriatal output must first inhibit the output nuclei via the direct pathway, thereby facilitating movement, and then, after a delay, disinhibit the same neurons in the output nuclei via the indirect pathway, leading to an inhibition of the ongoing movement (see review by Alexander et al., 1990). In the focusing model, by contrast, inhibition of neurons in the output nuclei via the direct pathway allows intended movements to proceed, whereas unintended (competing) movements are suppressed by concomitant increased excitatory input to other neurons in the

output nuclei via the indirect pathway (for reviews see Mink and Thatch, 1993; Mink, 1996). Both hypotheses are derived from the direct/indirect pathway model and are therefore, based on the implicit understanding that cortically-derived information is represented or encoded as a series of changes in the discharge rates of basal ganglia neurons. However, whilst the phenomenon of "rate coding" probably has great significance in basal ganglia function, it also likely that the pattern and synchronisation of neuronal discharge is of at least equal importance (Bergman et al., 1998; also see section 1.9.3).

1.8 Movement disorders

The direct/indirect pathway model serves as a basis for understanding the pathophysiology of disorders of movement associated with diseases of the basal ganglia (Albin et al., 1989b; DeLong, 1990; Albin, 1995; Wichmann and DeLong, 1996; Obeso et al., 2000b). Since the increased activity of the direct pathway is associated with facilitation of movement and increased activity of the indirect pathway is associated with inhibition of movement, it follows that hypokinetic motor disorders, of which Parkinson's disease is the archetype (see below), may be the result of an imbalance in the activity of the direct and indirect pathway in favour of the indirect pathway. On the other hand, hyperkinetic motor disorders, of which Huntington's disease is the archetype, could be the product of an imbalance in favour of the direct pathway. For reasons of brevity, only Parkinson's disease will be discussed further.

1.8.1 Parkinson's disease

Overlying the apparent feed-forward organisation of the basal ganglia are many feed-back pathways. One of the major feed-back projections is provided by the dopaminergic neurons of the SNpc. The pivotal role played by dopaminergic neurons in the modulation of information flow through the cortico-basal ganglia-thalamocortical loops is exemplified by

the devastating symptoms of Parkinson's disease (PD), a disease which becomes clinically manifest when 50-70% of the neuronal population of the SNpc is lost (for comprehensive reviews on PD see Lang and Lozano, 1998a, b). Parkinson's disease is an age-related neurodegenerative disorder of unknown cause with an average onset age of 60 years. Although the exact pathogenic mechanisms responsible for the preferential degeneration of the nigral dopaminergic neuron population in PD remain unknown, a myriad of factors have been implicated (for review see Lozano et al., 1998). In the initial stages of disease evolution, the neurodegenerative process is mainly confined to dopaminergic fibres innervating the dorsolateral putamen and therefore, the clinical manifestations are primarily motor. As the disease progresses, dopamine loss extends to involve the entire NS (Hornykiewicz, 1998; Lang and Lozano, 1998a;), both segments of the pallidum (Hornykiewicz, 1998; Jan et al., 2000), and the STN (Hornykiewicz, 1998). Furthermore, neurons in other brain regions, including the cerebral cortex, brainstem and spinal cord, may also be progressively lost (Lang and Lozano, 1998a). The cardinal features of PD are tremor at rest, rigidity and akinesia (Lang and Lozano, 1998a, b). Resting tremor arises as a consequence of rhythmic, alternating discharges of agonist and antagonist muscle groups (typically at a frequency of 4-6 Hz) and is so-called because it disappears when a voluntary movement is performed. Rigidity is characterised by a pathological increase in passive muscle tone in both flexor and extensor muscle groups that extends throughout the range of movement. Akinesia strictly means absence of movement, but in PD it usually refers to a slowness in movement execution (bradykinesia) or a poverty of spontaneous movements (hypokinesia). Other common symptoms of PD include postural instability, gait disturbances and a host of non-motor features (dementia, depression, and excessive sleepiness to name but a few).

The direct/indirect pathway model of the functional organisation of the basal ganglia accounts for the pathological alterations of basal ganglia activity that may underlie

hypokinetic movement disorders, such as PD (Albin et al., 1989b; DeLong, 1990; Albin, 1995; Wichmann and DeLong, 1996). As stated above, a central feature of the model of basal ganglia function and dysfunction is that dopamine has a differential effect on the spiny projection neurons in the NS that give rise to the direct and indirect pathways, *i.e.* that the dopaminergic nigrostriatal feed-back projection to the NS has a net excitatory effect on the D1-expressing striatonigral/entopeduncular neurons (the origin of the direct pathway), and a net inhibitory effect on the D2-expressing striatopallidal neurons (the origin of the indirect pathway). The model further predicts that a dopamine deficiency results in overactivity of the striatopallidal projection and reduced activity of the striatonigral/entopeduncular projection (Fig. 1.1*B*). The former situation leads to excessive inhibition of GP neurons and hence, abnormal and inappropriate disinhibiton of STN neurons, ultimately resulting in excessive glutamatergic drive to the output nuclei (Fig. 1.1*B*). Reduced activity of the direct pathway serves to further disinhibit the output nuclei. Thus, an imbalance in activity of the direct and indirect pathways occurs in favour of the indirect pathway (Fig. 1.1*B*). Since the output nuclei are GABAergic, hyperactivity in these structures leads to excessive inhibition and, effectively, to shutdown of the targets of the basal ganglia. The excessive thalamic inhibition leads to suppression of the cortical motor system, possibly resulting in akinesia, rigidity, and tremor, whereas the overactive inhibitory projection to the brainstem locomotor areas may contribute to abnormalities of gait and posture.

In keeping with the predictions of the model, data obtained from experimental animal models of PD (Filion, 1979; Filion et al., 1988; Bergman et al., 1990, 1994; Filion and Tremblay, 1991; Hollerman and Grace, 1992; Rothblat and Schneider, 1995; Hassani et al., 1996; Kreiss et al., 1997; Boraud et al., 1998, 2000b; Raz et al., 2000; Vila et al., 2000) have implicated a relative overactivity of the indirect pathway in Parkinson's disease. Furthermore, pharmacological manipulations or surgical interventions that restore the balance between the two pathways alleviate abnormal motor activity (Bergman et al., 1990;

Aziz et al., 1991, 1992; Greenamyre et al., 1991; Brotchie et al., 1991a; Burbaud et al., 1995). The value of the model is further exemplified by the application of this type of intervention to the treatment of idiopathic Parkinson's disease (for recent reviews, see Lang and Lozano, 1998b; Lozano et al., 1998; Kupsch and Earl, 1999).

The model asserts that dopamine is a key factor in maintaining the balance between the direct and indirect pathways. However, the notion that dopamine has a disparate effect on the two major subpopulations of spiny projection neuron is difficult to reconcile with growing evidence that D1 and D2 receptors are co-localised on a substantial proportion of neostriatal neurons (see section 1.2.1). Regardless of the mechanism of dopamine action, it is clear that replacement of the dopamine that is lost in PD with the dopamine precursor 3,4-dihydroxy-L-phenylalanine (L-DOPA) remains the most effective treatment for the disease. Indeed, although a number of motor and non-motor complications are commonly associated with L-DOPA treatment, it is still regarded as the gold standard of antiparkinsonian drug therapy (Lang and Lozano, 1998b; Lozano et al., 1998; Obeso et al., 2000a).

1.9 Subthalamic nucleus – globus pallidus network

The current models of basal ganglia circuits have served a valuable role by providing testable hypotheses and have led to considerable advances in our understanding of the roles played by the basal ganglia in movement and in the treatment of movement disorders. However, there is no question that the functional organisation of the basal ganglia is far more complicated than is apparent from even the most elaborate variations of the model. The importance of the massive projection from the STN to the GP has recently been emphasised by several authors (Chesselet and Delfs, 1996; Levy et al., 1997; Smith et al., 1998). However, whilst the projection from the STN to GP has been incorporated into the direct/indirect pathway model, the role of this pathway within the essentially feed-forward

scheme of information flow remains controversial. In addition, the existence of a direct projection from the cortex to the STN is hard to reconcile with the scaling hypothesis and the direct/indirect pathway model since both are justifiably "striato-centric". The term "STN-GP network" (Smith et al., 1998) will be used here to counter the notion that the STN is simply a relay station in the feed-forward, striato-centric scheme of the indirect pathway.

1.9.1 Functional organisation of the network

1.9.1.1 Anatomical considerations

The projection from the GP to the STN represents part of the "classical" indirect pathway. Both the GP and VP give rise to massive and topographically-organised projections that terminate throughout the entire extent of the STN (Carpenter et al., 1968, 1981; Carter and Fibiger, 1978; Rinvik et al., 1979; van der Kooy et al., 1981; Canteras et al., 1990; Carpenter and Jayaraman, 1990; Smith et al., 1990; Groenewegen and Berendse, 1990; Shink et al., 1996; Bevan et al., 1997). In the STN of the rat, the terminals arising from neurons in the GP are distributed in a series of rich plexuses according to a mediolateral and rostrocaudal topography and are concentrated in the lateral (sensorimotor and associative) part of the nucleus (Smith et al., 1990; Bevan et al., 1997), whereas terminals from neurons in the VP are largely confined to more medial (limbic) aspects (Groenewegen and Berendse, 1990; Bevan et al., 1997; Maurice et al., 1998b). The large varicosities of pallidosubthalamic fibres are sometimes grouped to ensheath the perikarya and dendrites of STN neurons and, in addition, single GP axons may give rise to several varicosities apposed to a single neuron in the STN (Smith et al., 1990; Bevan et al., 1997). Ultrastructual analyses have established that pallidosubthalamic varicosities are GABA-positive and form synapses with all parts of STN neurons (Nakamura and Sutin, 1972; van der Kooy et al., 1981; Moriizumi et al., 1987; Smith et al., 1990; Shink and Smith, 1995; Bevan et al., 1995, 1997). Furthermore, in the

rat, it has been estimated that 31% of pallidal terminals form synapses with perikarya, 39% with large (presumably proximal) dendrites and 30% with small (presumably distal) dendrites (Smith et al., 1990). Taken together, these anatomical data indicate that the GP is in a position to powerfully control activity in the STN through this inhibitory GABAergic pathway. In support of this concept, electrical stimulation of pallidosubthalamic fibres has been shown to evoke profound inhibitory responses in STN neurons (Tsubokawa and Sutin, 1972; Ohye et al., 1976; Rouzaire-Dubois et al., 1980; Kita et al., 1983b; Nakanishi et al., 1987a; Bell et al., 1995; Maurice et al., 1998b). Pallidal inhibition of STN neurons has been suggested to be predominantly mediated by the activation of $GABA_A$ receptors (Rouzaire-Dubois et al., 1980; Kita et al., 1983b; Nakanishi et al., 1987a; Robledo and Féger, 1990; see Chapter 5).

The projection from the STN to the GP is not part of the classical indirect pathway and thus, is often omitted from representations of the motor circuit. However, the substantial size and topographic organisation of the subthalamopallidal pathway imply that this connection is important for basal ganglia function (Nauta and Cole, 1978; Ricardo, 1980; van der Kooy and Hattori, 1980; Carpenter et al., 1981; Kita and Kitai, 1987; Parent and Smith, 1987; Carpenter and Jayaraman, 1990; Groenewegen and Berendse, 1990; Parent and Hazrati, 1995b; Shink et al., 1996). In further support of this, single-axon tracing (Hammond and Yelnick, 1983; Kita et al., 1983a; Sato et al., 2000b) and electrophysiological (Deniau et al., 1978a; Hammond et al., 1983b; Kita et al., 1983b) studies have shown that the majority of STN neurons send an axon collateral to the GP. In the rat, STN efferents to the GP display a mediolateral and inverted dorsoventral topographic organisation and typically terminate in a diffuse plexus of fibres with *en passant* and terminal boutons (Kita and Kitai, 1987). The characteristically small boutons of subthalamopallidal fibres are enriched in glutamate and been shown to establish synaptic contact with the somata and dendrites of GP neurons (Kita and Kitai, 1987; Shink and

Smith, 1995; Shink et al., 1996). Furthermore, studies in primate have shown that terminals that are derived from the STN account for ~ 10% of the total population of terminals in the GP, and are evenly spread over perikarya and dendrites (Shink and Smith, 1995). Taken together, these anatomical data suggest that the STN may act as a powerful driving force of activity in the GP. Indeed, electrophysiological studies support this hypothesis (Perkins and Stone, 1980; Park et al., 1982; Kita and Kitai, 1991; Ryan and Clark, 1991; Kita, 1992; Robledo and Féger, 1990; Féger and Robledo, 1991; Soltis et al., 1994; Nambu et al., 1990, 2000).

The topographic organisation of the pallidosubthalamic and subthalamopallidal projections in rat and primate suggests that functionally related subregions of the STN and GP are interconnected (for reviews, see Parent and Hazrati, 1995b; Joel and Weiner, 1997; Smith et al., 1998). Indeed, dual anterograde-retrograde tracers and selective anterograde or retrograde tracers (for review of multimodal transport of these tracers, see Smith et al., 1998) have been used to demonstrate that many of the STN neurons that receive inputs from a specific pallidal region are highly likely to project back to the same region of GP, and vice versa (Kita and Kitai, 1987; Moriizumi et al., 1987; Canteras et al., 1990; Carpenter and Jayaraman, 1990; Groenewegen and Berendse, 1990; Smith et al., 1990; Shink et al., 1996), which indicates, therefore, that the relationship between neurons of the STN and the GP is, at least in part, reciprocal. In support of this, stimulation of the GP often leads to both antidromic activation and orthodromic inhibition of STN neurons (Rouzaire-Dubois et al., 1980; Kita et al., 1983b), and stimulation of the STN commonly evokes antidromic and orthodromic responses from GP neurons (Perkins and Stone, 1980, 1981). Both convergence and divergence are likely to exist in the STN-GP network since: (1) there are many more neurons in GP than in the STN (approximately 3:1 in rat; Oorschot, 1996); (2) the dendritic tree of a single STN neuron is extensive and can cover large expanses of the nucleus (Yelnick and Percheron, 1979; Hammond and Yelnick, 1983; Kita et al., 1983a;

Afsharpour, 1985a); and (3) the axons of individual GP and STN neurons may contact multiple neurons in their target nuclei (Kita et al., 1983a; Kita and Kitai, 1994; Bevan et al., 1998). Although absolute (unitary) reciprocity between STN and GP neurons has yet to be demonstrated, the strict reciprocal relationship between some elements of the STN and GP strongly suggests that the STN-GP network contains a number of "closed" loops; each closed loop effectively couples functionally corresponding subregions of the STN and GP. Furthermore, anatomical studies in primates have led some authors to suggest that the interconnections of STN-GP network support an additional series of "open" loops (for review, see Joel and Weiner, 1997). These open loops have been hypothesised to arise as a consequence of a non-reciprocal component of the subthalamopallidal pathway and are thought to couple functionally non-corresponding subregions of the pallidum via a disynaptic link with the STN (Joel and Weiner, 1997).

1.9.1.2 Physiological considerations

The functions that may be subserved by the reciprocal connections of the STN-GP network are largely a matter of conjecture. The widespread and sophisticated nature of these interconnections suggest that they play a prominent role in shaping the responses of STN and GP neurons to afferent synaptic activity and that they may partly provide the anatomical substrate for the complex sequences of inhibition and excitation that are observed in the network during normal movement (see sections 1.3 and 1.4). In support of this hypothesis, studies by several groups have demonstrated that the reciprocal connections between the STN and GP are actively engaged by descending cortical input (Levine et al., 1974; Kitai and Deniau, 1981; Toan and Schultz, 1985; Nambu et al., 1990, 2000; Ryan and Clark, 1991, 1992; Kita, 1992; Fujimoto and Kita, 1993; Yoshida et al., 1993; Maurice et al., 1998a). In contradiction to the predictions of the striato-centric direct/indirect pathway model, the first response of STN neurons to cortical stimulation or stimulation of

corticofugal fibres is a brief period of excitation (Ohye et al., 1976; Kitai and Deniau, 1981; Rouzaire-Dubois and Scarnati, 1985, 1987; Ryan and Clark, 1991, 1992; Fujimoto and Kita, 1993; Maurice et al., 1998a; Nambu et al., 2000). This excitatory effect has a short latency (< 6 ms) and is mediated by the glutamatergic corticosubthalamic pathway (Rouzaire-Dubois and Scarnati, 1985, 1987; Ryan and Clark, 1992; Fujimoto and Kita, 1993; Nambu et al., 2000), thus implying that the conduction speeds of this system are faster than those of the pathways flowing from the cortex through the NS. The response of most STN neurons to cortical stimulation is not monophasic; the brief excitatory response is swiftly followed by a short period of inhibition and then another, longer period of excitation (Ryan and Clark, 1991, 1992; Fujimoto and Kita, 1993; Maurice et al., 1998a; Nambu et al., 2000). The brief inhibitory component of this triphasic response likely results from the activation of a feed-back loop through the GP (Ryan and Clark, 1992; Fujimoto and Kita, 1993; Maurice et al., 1998a). In good agreement with this, the first phase of the typical triphasic response of GP neurons to cortical stimulation is most often a brief excitation (Noda et al., 1968; Levine et al., 1974; Toan and Schultz, 1985; Nambu et al., 1990, 2000; Kita and Kitai, 1991; Ryan and Clark, 1991; Kita, 1992; Yoshida et al., 1993). Furthermore, this early excitation is lost after lesion of the STN (Ryan and Clark, 1991; Kita, 1992) or following the blockade of corticosubthalamic transmission (Nambu et al., 2000). Thus, the subthalamopallidal pathway drives the short latency responses of GP neurons to cortical activation, which in turn, temper and sculpt the responses of STN neurons via the pallidosubthalamic projection. The feed-forward propagation of cortical impulses through the NS is probably responsible for the inhibition of GP neurons after their initial excitation by the neurons of the STN (Toan and Schultz, 1985; Nambu et al., 1990; Ryan and Clark, 1991; Kita, 1992; Yoshida et al., 1993; Maurice et al., 1998a). Inhibition of the GP by the NS leads to a disinhibition of the STN and thus, partly underlies the long-lasting late excitation of STN neurons (Ryan and Clark, 1992, Maurice et al., 1998a). Taken together, these data suggest that the

corticosubthalmic projection and the reciprocal connections of the STN-GP network play critical roles in mediating the responses of STN and GP neurons to cortical stimulation. Thus, the predominance of brisk increases in the discharge of STN neurons in response to movements (Georgopoulos et al., 1983; DeLong et al., 1985; Matsumura et al., 1992; Wichmann et al., 1994a; Cheruel et al., 1996) or somatosensory input (Hammond et al., 1978b; Mintz et al., 1986; Wichmann et al., 1994a) most likely result from corticosubthalamic activation, and the phasic decreases in discharge (Georgopoulos et al., 1983; DeLong et al., 1985; Wichmann et al., 1994a; Cheruel et al., 1996) probably arise as a consequence of pallidosubthalamic feed-back. It should be noted however, that the stimulation experiments also reported that a minority of STN neurons displayed a short-latency, long-lasting excitation, without an intermediate inhibitory component (Ryan and Clark, 1992; Fujimoto and Kita, 1993; Maurice et al., 1998a), and that a minority of GP neurons did not exhibit a short latency excitation (Noda et al., 1968; Levine et al., 1974; Toan and Schultz, 1985; Nambu et al., 1990; Ryan and Clark, 1991; Yoshida et al., 1993). These data corroborate the existence of a non-reciprocal component of the STN-GP network (Joel and Weiner, 1997). Thus, while brief increases in the discharge of GP neurons in response to movements or somatosensory stimuli (Georgopoulos et al., 1983; Nambu et al., 1990; Mink and Thatch, 1991a, b; Cheruel et al., 1994; Nambu et al., 2000) most likely result from subthalamopallidal activation, phasic decreases (DeLong et al., 1985; Brotchie et al., 1991b, c; Gardner and Kitai, 1992; Jaeger et al., 1995) may arise from a lack of subthalamopallidal input and a powerful striatopallidal input.

1.9.2 Functions of the network in health

The corticosubthalamic pathway and the reciprocal connections of the STN-GP network probably underlie, at least in part, the complex responses of STN and GP neurons that are observed during passive or voluntary movement. Furthermore, activity in the

corticosubthalamic pathway and within the STN-GP network is likely to have a profound influence on behaviour since the output nuclei receive extensive projections from both STN and GP. Previous electrophysiological experiments have shown that stimulation of corticofugal fibres evokes an early excitation, an inhibition, and late excitation in EP and SNpr neurons (Dray et al., 1976; Nambu et al., 1990, 2000; Fujimoto and Kita, 1992; Yoshida et al., 1993; Ryan and Sanders, 1994; Maurice et al., 1999). The early excitation is almost certainly mediated by a disynaptic pathway made up of the corticosubthalamic projection and the projection from STN to the output nuclei (Ryan and Sanders, 1994; Maurice et al., 1999; Nambu et al., 2000). The origin of the inhibitory response is controversial but the direct striatonigral/entopeduncular pathway, the feed-back loop to the STN from GP, and the feed-forward projection from GP to the output nuclei are all likely to contribute (Ryan and Sanders, 1994; Maurice et al., 1999; Nambu et al., 2000). The late excitation results from the activation of classical indirect pathway via a disinhibition of STN (Maurice et al., 1999; Nambu et al., 2000). Taken together, these data imply that the intrinsic and extrinsic connections of STN and GP neurons are organised in a way that permits the STN-GP network to exert a dynamic and powerful control over activity in the output nuclei following cortical activation and thus, over the planning, initiation, execution and termination of skeletomotor and oculomotor commands. Indeed, the focusing model of motor circuit function is founded on this premise and places a strong emphasis on the importance of the cortico-subthalamo-output nuclei disynaptic pathway (Mink and Thatch, 1993; Mink, 1996; Nambu et al., 2000). The pivotal role played by GABAergic input to the STN in motor function is epitomised by the observation that pharmacological manipulation of GABAergic systems in the STN with high doses of selective $GABA_A$ receptor agonists and antagonists leads to profound motor disturbances (Crossman et al., 1984; Jackson and Crossman, 1984; Murer and Pazo, 1993; Spooren et al., 1995; Dybdal and Gale, 2000; Nambu et al., 2000). Few studies have systematically examined the role of glutamatergic

neurotransmission in the GP. However, the importance of excitatory input to the GP is exemplified by the finding that blockade of excitatory amino acid receptors in the GP causes a hypokinetic syndrome (Kato and Kimura, 1992).

1.9.3 Functions of the network in disease

The importance of the STN-GP network to the function of the motor circuit of the basal ganglia is perhaps best brought to light by studying its component nuclei in disease. Indeed, it has long been recognised that damage to the STN in humans (Whittier, 1947) or lesion of the STN in monkeys (Carpenter et al., 1950; Hammond et al., 1979; Hamada and DeLong, 1992) results in a severe hyperkinetic movement disorder known as (hemi) ballismus, which is characterised by rapid, involuntary, and often violent movements of the contralateral limbs (Albin, 1995).

As discussed in section 1.8.1, the basal ganglia are intimately involved in Parkinson's disease. The development and refinement of the direct/indirect pathway concept of basal ganglia function and dysfunction has had a profound influence on research into the involvement of the basal ganglia in PD, providing a stimulus and rationale for anatomical, functional and clinical studies and indeed, has led to the development of new therapies and the resurgence of surgical approaches for the treatment of PD. The study of experimental parkinsonism has been greatly facilitated by the discovery that the neurotoxins 1-methyl-4-phenyl-1,2,3,6-tetrahydropyridine (MPTP) and 6-hydroxydopamine (6-OHDA) could be used in animals to induce a selective loss of catecholaminergic neurons in the midbrain and a "parkinsonian" syndrome (for reviews, see DeLong, 1990; Mink, 1996; Schwarting and Huston, 1996a, b). Since their introduction, these animal models of PD have been used extensively to study the pathophysiology of PD. In accordance with the predictions of the direct/indirect pathway model, the activity of neurons in the STN-GP network is dramatically altered by the depletion of dopamine; the discharge rates of GP neurons are

significantly reduced (Filion et al., 1988; Pan and Walters, 1988; Filion and Tremblay, 1991; Rothblat and Schneider, 1995; Boraud et al., 1998, 2000b; Raz et al., 2000), whilst, in contrast, STN neurons tend to be hyperactive (Hollerman and Grace, 1992; Bergman et al., 1994; Hassani et al., 1996; Kreiss et al., 1997; Vila et al., 2000). The abnormally high discharge rates of GABAergic neurons in the output nuclei in the parkinsonian state (Filion and Tremblay, 1991; Bergman et al., 1994; Burbaud et al., 1995; Rothblat and Schneider, 1995; Boraud et al., 1998, 2000b; Wichmann et al., 1999), which underlie, at least in part, the motor symptoms of PD (see section 1.8.1), are thought to arise as a consequence of increased drive from the overactive STN. In support of this, lesion of the STN (Bergman et al., 1990; Aziz et al., 1991, 1992; Wichmann et al., 1994b; Gill and Heywood, 1997) or high-frequency (> 130 Hz) stimulation of this structure (Benazzouz et al., 1993; Limousin et al., 1995; Pollak et al., 1996; Krack et al., 1998; Rodriguez et al., 1998), has been reported to significantly alleviate rigidity, akinesia and resting tremor in parkinsonian animals and in humans with intractable PD. Although the clinical benefits of high-frequency stimulation of the STN are clear, the underlying neurobiological mechanisms remain controversial. Indeed, output nuclei activity may be decreased by high-frequency stimulation of the STN because (1) STN neurons undergo a "depolarisation block", which is functionally equivalent to a lesion of the STN (Benazzouz et al., 1993; Beurrier et al., 2001); (2) GABAergic afferents to the STN are preferentially excited, thereby severely reducing excitatory output from the STN (Dostrovsky et al., 2000; Holsheimer et al., 2000); or, (3) in contrast, concomitant activation of the STN drives the GP to profoundly inhibit the output nuclei (Benazzouz et al., 1995; Windels et al., 2000).

Whilst changes in the firing rates of STN, GP and output nuclei neurons are likely of great significance in PD, alterations in the patterning and synchronisation of neuronal discharge in these structures may also be of importance (Wichmann and DeLong, 1996; Levy et al., 1997; Bergman et al., 1998; Obeso et al., 2000b). Indeed, the depletion of

dopamine is commonly associated with a shift in the predominant firing mode of neurons in the STN (Hollerman and Grace, 1992; Bergman et al., 1994; Hassani et al., 1996; Kreiss et al., 1997; Vila et al., 2000), the GP (Filion, 1979; Pan and Walters, 1988; Filion and Tremblay, 1991; Nini et al., 1995; Boraud et al., 1998, 2000b; Ni et al., 2000; Raz et al., 2000) and the output nuclei (Bergman et al., 1994; Burbaud et al., 1995; Nini et al., 1995; Murer et al., 1997; Wichmann et al., 1999; Raz et al., 2000; Tseng et al., 2000) from tonic, regular or irregular firing patterns to bursting activity. In MPTP-treated monkeys, a much larger proportion of neurons in the STN, GP and output nuclei discharge in low- (4-7 Hz) and moderately high- (10-17 Hz) frequency periodic bursts (Filion and Tremblay, 1991; Bergman et al., 1994; Nini et al., 1995; Wichmann et al., 1999; Raz et al., 2000). Furthermore, the low-frequency oscillatory activity of neurons in the STN and pallidum is often significantly correlated with the resting tremor that is sometimes displayed by these parkinsonian monkeys (Bergman et al., 1994; Nini et al., 1995; Wichmann et al., 1999; Raz et al., 2000). Similar findings have recently been described in humans with PD (Hutchison et al., 1997; Rodriguez et al., 1998; Hurtado et al., 1999; Levy et al., 2000; Magariños-Ascone et al., 2000; Magnin et al., 2000). Thus, both the rates and patterns of firing of single basal ganglia neurons are clearly altered following the depletion of dopamine.

Cross-correlation analysis has revealed that the discharge of STN and GP neurons within and between connected regions of the parent nuclei is rarely synchronised in normal monkeys (Bergman and DeLong, 1989; Wichmann et al., 1994; Nini et al., 1995; Bergman et al., 1998; Nambu et al., 2000; Raz et al., 2000). However, following the induction of experimental parkinsonism, the incidence of synchronised activity within the STN-GP network is dramatically increased (Nini et al., 1995; Bergman et al., 1998; Raz et al., 2000) and thus, it is likely that the functional relations between neurons are also altered in PD. Since the STN and GP are known to exert a powerful control over the activity of their target nuclei, it is probable that the abnormal synchronous activity of the STN-GP network is

propagated to other regions of the basal ganglia. Indeed, similar increases in correlated activity have been reported in the output nuclei following dopamine depletion (Nini et al., 1995; Bergman et al., 1998; Raz et al., 2000). Taken together, these data suggest that the STN-GP network is intimately involved in the pathophysiology of PD. In keeping with this suggestion, it has recently been shown that, in a tissue culture environment, the STN-GP network alone can generate low-frequency oscillatory activity and thus, could be responsible for driving the synchronised oscillatory discharge of neurons in the pathological basal ganglia (Plenz and Kitai, 1999). The mechanism supporting low-frequency neuronal oscillations within the STN-GP network is similar to that reported to underlie spindling activity in the thalamus, which contains similarly-coupled networks of glutamatergic and GABAergic neurons (for review see McCormick and Bal, 1997), and is discussed in more detail in Chapter 5.

The direct/indirect pathway model predicts that the development of parkinsonian akinesia and rigidity is caused by pathological changes in the tonic firing rates of neurons in the basal ganglia. However, the pathogenesis of tremor does not readily fit the model since tremor is an oscillatory phenomenon that seems to be unrelated to alterations in firing rate (for discussion of this issue, see DeLong, 1990; Bergman et al., 1998). Although the mechanisms underlying tremor are still under debate, these experimental data indicate that changes in the patterning of neuronal discharge and the emergence of synchronised oscillatory activity within the motor circuit may both be critical factors in the development of resting tremor and indeed, may also partly underlie the other cardinal symptoms of PD (Wichmann and DeLong, 1996; Levy et al., 1997; Bergman et al., 1998; Obeso et al., 2000b). A corollary hypothesis is that the rate, pattern, and synchronisation of neuronal discharge are all important for the processing of information by the normal basal ganglia.

1.10 Aims of thesis studies

It is clear that the STN-GP network plays a pivotal role in basal ganglia function and dysfunction. Yet, despite intensive studies of the anatomical and functional organisation of the basal ganglia and the large amount of data gathered about the pathophysiology of motor disorders, many of the mechanisms governing information processing within the STN-GP network remain obscure. The reciprocal connections between STN and GP neurons are probably crucial for information processing, but their functions remain largely undefined. Furthermore, little is known about the spatial and temporal integration of inputs within the STN-GP network. These important issues need to be addressed in order to gain a better understanding of the functions of the STN-GP network in health and disease.

The overall objective of this thesis was to elucidate the mechanisms that underlie activity in the STN-GP network. Three complimentary studies were performed, with the following specific aims in mind:

1) To characterise the relationship of activity in the normal STN-GP network to activity in the cerebral cortex (Chapter 3).

2) To determine whether the relationship between the STN-GP network and the cerebral cortex is altered by the chronic depletion of dopamine (Chapter 4).

3) To examine the dynamics of GABAergic inhibition in the STN and to test the hypothesis that input from the GP could contribute to the generation of low-frequency oscillatory activity in the STN-GP network (Chapter 5).

CHAPTER 2.

MATERIALS AND METHODS

2.1 Electrophysiological recordings *in vivo*

2.1.1 Animals

All experimental procedures were carried out on adult male Sprague-Dawley rats (Charles River, Margate, UK). Rats were housed in groups of 2 to 5 rats and maintained on a 12/12 hr light/dark cycle, with access to food and water *ad libitum*. Experiments were conducted in accordance with the Animals (Scientific Procedures) Act 1986.

2.1.2 Anaesthesia, analgesia and surgical procedures

All *in vivo* electrophysiological recordings were performed in animals that were deeply anaesthetised with standard general anaesthetics. Anaesthesia was induced with isoflurane (Isoflo, Schering-Plough Ltd., Welwyn Garden City, UK) in air by inhalation and maintained using one of the following two regimes: (1) ketamine (100 $mgkg^{-1}$, i.p.; Ketaset™, Willows Francis, Crawley, UK) and xylazine (10 $mgkg^{-1}$, i.p.; Rompun™, Bayer, Germany), plus supplemental doses as necessary; or (2) urethane (1.25 gkg^{-1} dissolved in H_20, i.p.; ethyl carbamate, Sigma, Poole, UK), plus supplemental doses of ketamine and xylazine (30 $mgkg^{-1}$ and 3 $mgkg^{-1}$, i.p., respectively). Hereafter, group (1) shall be referred to as "ketamine" anaesthetised and group (2) shall be referred to as "urethane" anaesthetised. All pressure points and wound margins were infiltrated with bupivacaine (0.75% w/v; Marcain™, Astra, Kings Langley, UK), or lignocaine (2% with adrenalin, C-Vet™, Leyland, UK), and corneal drying was prevented with frequent application of Hypromellose eye drops (Norton Pharmaceuticals Ltd., Harlow, UK). Animals were then placed in a stereotaxic frame (David Kopf Instruments, Tujunga, CA) and body temperature was maintained at 37 ± 0.5°C with the use of a homeothermic heating device (Harvard Apparatus Ltd., Edenbridge, UK). Anaesthesia levels were assessed by examination of the electroencephalogram (see 2.1.3 below) and by testing reflexes to a cutaneous pinch or to gentle corneal stimulation.

Electrocardiographic activity was recorded differentially via two silver wires inserted subcutaneously into a forelimb and a hindlimb and, together with respiration rate and depth, was also constantly monitored by visual inspection to ensure the animals' well-being. Small craniotomies (approx. 3 × 3 mm) were performed directly above the right STN and/or GP with a hand-held dental drill (Bracon Ltd., Hurst Green, UK) and the overlying dura mater was carefully removed. Mineral oil (Sigma) or saline solution (0.9% w/v NaCl) was applied to all areas of exposed cortex to prevent dehydration.

2.1.3 Electroencephalogram

Introduction

Prevailing cortical activity was assessed using the electroencephalogram (EEG). The EEG does not register unit activity *per se* but provides a gross measurement of fluxes in electrical field potentials as a function of time. While only a few of the neuronal substrates of EEG rhythms have been elucidated in detail, it is clear that each stage of the sleep-wake cycle is correspondingly reflected in the EEG as a stereotyped pattern of oscillations (for review, see Steriade, 2000). Thus, the EEG is also a good indicator of ongoing states of activity in descending corticofugal pathways to the basal ganglia. The EEG was recorded from frontal (motor) cortical areas since these regions are most relevant to the study of direct corticosubthalamic relationships and the somatomotor functions of the basal ganglia.

Procedure

A small burr hole was drilled in the skull and the EEG was recorded via a self-tapping steel screw juxtaposed to the dura mater above the ipsilateral or contralateral frontal cortex (3.0 mm anterior of bregma and 2.0 mm lateral to the midline) and referenced against an indifferent electrode placed adjacent to the temporal musculature. Raw EEG was band-pass filtered (0.1-100 Hz) and amplified (2000×) with a NL104 preamplifier (Digitimer Ltd.,

Welwyn Garden City, UK), collected on tape, and displayed simultaneously on a digital oscilloscope (DSO 610, Gould Instruments, Ilford, Essex, UK).

2.1.4 Extracellular recording of single and multiple units

Introduction

Activity of the STN-GP network *in vivo* was registered using extracellular recording techniques. Extracellular recordings of the action potential ("spike") trains of a single neuron ("unit"), or an ensemble of neurons, are technically undemanding to perform *in vivo* and provide precise measurements of the times of occurrence of neuronal activity.

Procedures

Electrodes for extracellular recordings were made from borosilicate glass capillary tubes (GC120F-10, 1.2 mm outside diameter (O.D.); Clarke Electromedical Instruments, Reading, UK) on a vertical puller unit (Model PE-2; Narashige, Tokyo, Japan). Electrodes were broken back under microscopic control to an external tip diameter of ~ 1.5 μm and filled with a 0.5 M NaCl solution containing 1.5% w/v of the tracer substance Neurobiotin™ (N-(2-aminoethyl) biotinamide; $C_{12}H_{23}N_4O_2S$; hydrochloride salt; Vector, Peterborough, UK). Electrodes with a resistance of 15-25 MΩ were selected and then advanced down into the basal ganglia with a piezoelectric motor unit (Burleigh Instruments Inc., New York, USA).

Extracellular action potential signals were isolated and amplified (10×) through the active bridge circuitry of an Axoprobe-1A amplifier (Axon Instruments, Foster City, CA), AC-coupled, and amplified a further 100× (AC-DC Amp, Digitimer), before being filtered between 0.3 and 5 kHz (NL125, Digitimer). Lastly, signals were passed through an input amplifier/DAT interface (EBU/DAT/5s; Department of Pharmacology, Oxford, UK), collected on tape (60ES DAT system, Sony, UK) for off-line analysis, and displayed simultaneously on a digital oscilloscope (Gould). This protocol was employed to perform single or double recordings of neurons. Spikes of single units were often several millivolts

in amplitude and always exhibited a biphasic waveform with an initial positive deflection (Fig. 2.1*A*). Recordings of spontaneous activity typically lasted for 4-25 min.

2.1.5 Juxtacellular labelling of single units

Introduction

The juxtacellular labelling method of Pinault (1994, 1996) was employed to unequivocally identify the location and morphology of recorded units following physiological characterisation since it allows single neurons to be selectively labelled with a neuronal tracer using extracellular microelectrodes. Following isolation and identification of a unit, the electrode tip is advanced into a "juxtamembranous" position and the tracer is ejected by microiontophoretic current pulses, under complete physiological control. Although the exact method by which the tracer enters the neuron is unknown, there is some evidence to suggest that neuronal filling could occur when small patches of somatic or dendritic membrane are transiently damaged by the juxtacellularly-applied electrical current (Pinault, 1996). The tracer substance Neurobiotin™, a biotin-containing compound of low molecular weight (Mr = 286), was utilised in these studies because it is easily dissolved in a variety of buffered or unbuffered electrode solutions and can be selectively iontophoresed into neurons with anodal current pulses (Kita and Armstrong, 1991). Once taken up by the neuron, Neurobiotin™ is rapidly and anterogradely transported into dendritic and axonal processes (Kita and Armstrong, 1991). The high affinity of biotin for the egg white protein, avidin, can be exploited to visualise Neurobiotin™-containing neurons with the use of sensitive, avidin-based detection techniques (Hsu and Raine, 1981; Hsu et al., 1981; Horikawa and Armstrong, 1988; Bolam, 1992; see section 2.3.1 for detailed histochemical procedures).

Procedure

The electrode was slowly advanced towards the neuron while a low-intensity microiontophoretic current was applied using the amplifier (1-10 nA anodal current, 200 ms

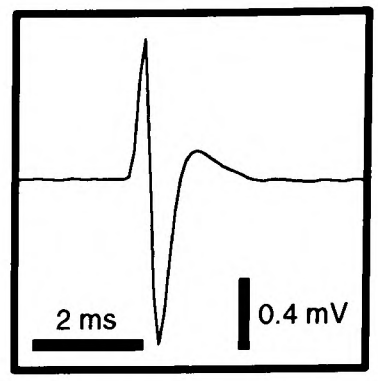
duration, 50% duty cycle). Microiontophoretic current pulse application was driven by an external pulse generator (Master-8; A.M.P.I., Jerusalem, Israel). The optimal position of the electrode for labelling (*i.e.* when electrode tip is juxtaposed to neuronal membrane) was identified when the firing pattern of the neuron was robustly modulated by current injection (Fig. 2.1*A*, *B*). Typically, neuronal firing was modulated by the microiontophoretic current for at least 5 min to obtain reliable, Golgi-like labelling (Fig. 2.1*C*). On the occasions when robust modulation could not be achieved or was not attempted, the position of the recorded unit was marked by a discrete extracellular deposit of neurobiotin (100 nA anodal current; 1 s (50%) duty cycle for 30-60 min; Pinault, 1996).

2.1.6 Survival time and perfusion fixation

Following microiontophoresis of Neurobiotin™, some time was allowed for the uptake and anterograde transportation of the tracer by neurons before perfusion fixation. Soma, proximal dendrites and local axons were labelled after 2 hr of transportation time and complete labelling of long axons was usually accomplished after 8-12 hr of survival time. When the survival time exceeded 4 hr, the animals received subcutaneous injections of sterile saline solution (1 ml, 0.9% w/v NaCl; Martindale Pharmaceuticals, Romford, UK) to prevent dehydration. At the end of experiment, animals were given a lethal dose of anaesthetic (ketamine and xylazine; 150 $mgkg^{-1}$ and 15 $mgkg^{-1}$, respectively, i.p.) and perfused via the ascending aorta with 100 ml of 0.1 M phosphate-buffered saline at pH 7.4 (PBS), followed by 300 ml of 0.1-0.3% w/v glutaraldehyde (TAAB, Aldermaston, UK) and 3-4% w/v paraformaldehyde (Sigma) in 0.1 M phosphate buffer (PB), pH 7.4, and then by 150 ml of the same solution without glutaraldehyde. Brains were then post-fixed in the latter solution at 4°C for at least 12 hr.

Figure 2.1. Experimental protocol for juxtacellular labelling of single basal ganglia neurons following electrophysiological characterisation. *A*, Unit recording of the spontaneous activity of a (STN) neuron in a urethane-anaesthetised rat. Note the good signal-to-noise ratio that was typically achieved with the extracellular electrodes used in these studies. *Inset* Average waveform taken from the 27 action potentials shown in *A*. Spikes were often over 1 mV in amplitude and less than 1.5 ms in duration, and always exhibited a biphasic/triphasic waveform with an initial positive deflection. *B*, After 20 min of recording, the electrode was advanced ventrally by 13 μm and the neuron was juxtalabelled under continuous electrophysiological monitoring by the systematic application of anodal current pulses (200 ms on/200 ms off; 2.5-3.0 nA positive current for 10 min). The optimal position for juxtacellular labelling was achieved when the activity of the neuron was robustly modulated by the current pulses. Note that spike amplitude and ambient noise both increased during juxtalabelling. Current pulse artefacts are truncated for clarity. Calibration bars in panel *A* apply to panel *B*. *C*, Following histochemical processing of the recovered brain for Neurobiotin™, a single, well-labelled neuron was observed near a large blood vessel (*) in the subthalamic nucleus (STN; borders delineated by *dashed line*). ZIV, ventral division of the zona incerta; CP, cerebral peduncle. Lateral is to the *left* and dorsal is to the *top* of the panel.

A **Spontaneous activity**



STN unit activity

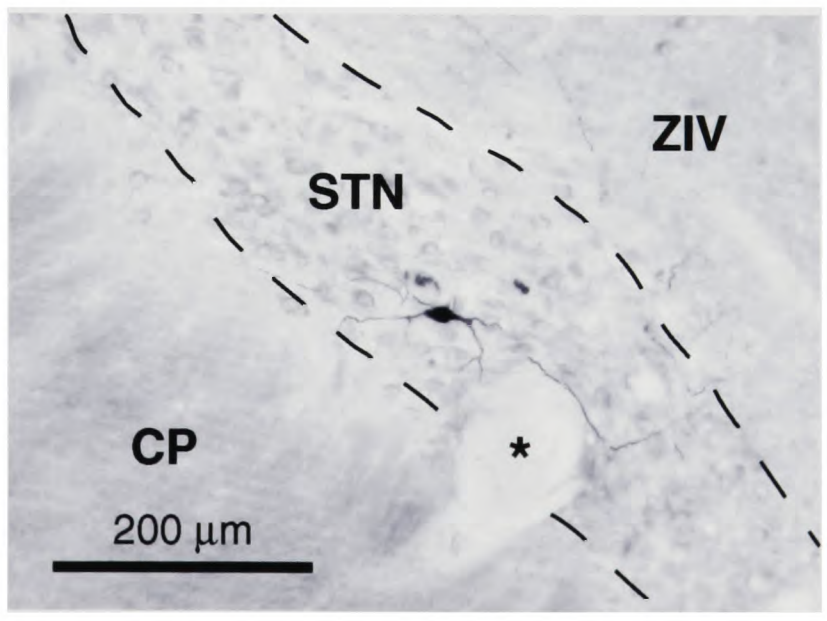
1 mV

0.5 s

B **Robust modulation during juxtalabelling**

STN unit activity

C **Single-neuron labelling**



2.2 Unilateral lesion of midbrain dopaminergic neurons with 6-hydroxydopamine

Introduction

To test whether STN-GP network interactions are altered after the chronic depletion of dopamine, which is a hallmark of PD, midbrain dopaminergic cell groups were lesioned by intracerebral injection of the neurotoxin 6-hydroxydopamine (6-OHDA). Subsequent to introduction into the brain, 6-OHDA, which has a chemical structure that is analogous to those of the catecholaminergic neurotransmitters, is sequestered by the membrane uptake systems of noradrenergic and dopaminergic neurons in a highly selective manner (Schwarting and Huston, 1996a, b). Once inside a neuron, 6-OHDA is rapidly oxidised, which results in the production of several highly cytotoxic compounds, including quinones, free radicals and hydrogen peroxide (Jonsson, 1980). The extensive damage caused by these agents quickly leads to neuron death. Mass destruction of neurons constituting the dopaminergic nigrostriatal pathway in rodents (Ungerstedt, 1968) leads to a syndrome that is similar in anatomy, neurochemistry, physiology and behaviour to idiopathic Parkinson's disease (for reviews, see Zigmond et al., 1990; Schwarting and Huston, 1996a, b). Since bilateral 6-OHDA lesions have a high postoperative risk of lethality, only the unilateral 6-OHDA-lesioned model of PD was utilised in these studies.

2.2.1 Animals

Unilateral 6-OHDA lesion experiments were carried out on adult male Sprague-Dawley rats (180-220 g).

2.2.2 Pretreatments, anaesthesia, analgesia and surgery

Since systemic administration of 6-hydroxydopamine (6-OHDA) can lead to widespread destruction of catecholaminergic neurons in the central and peripheral nervous systems, the compound must be injected directly into the midbrain in order to selectively destroy the catecholaminergic neurons located there.

Twenty five minutes before the injection of 6-OHDA, all animals received a bolus of desipramine (25 $mgkg^{-1}$, i.p.; Sigma) and pargyline (50 $mgkg^{-1}$, i.p.; Sigma) to minimise the uptake of 6-OHDA by noradrenergic neurons and to maximise the toxic effects on dopaminergic neurons, respectively (Breese and Taylor, 1971; Schwarting and Huston, 1996a). Anaesthesia for the lesioning procedure was induced with isoflurane in air by inhalation and maintained with ketamine (100 $mgkg^{-1}$, i.p.) and xylazine (10 $mgkg^{-1}$, i.p.). Animals were placed in a stereotaxic frame (Kopf Instruments) and body temperature was maintained at 37 ± 0.5°C with the use of a homeothermic heating device (Harvard Apparatus). Anaesthesia levels were assessed by testing reflexes to a cutaneous pinch or to gentle corneal stimulation. The rate and depth of respiration was also constantly monitored to ensure the animals' well-being. All wound margins were infiltrated with the local anaesthetic bupivacaine and corneal dehydration was prevented with application of Hypromellose eye drops. A small craniotomy (approx. 2 x 2 mm) was then performed directly above the right substantia nigra and the overlying dura mater was carefully removed.

The neurotoxin 6-OHDA (hydrochloride salt; Sigma) was dissolved immediately before use in ice-cold sterile 0.9% w/v NaCl solution containing 0.02% w/v ascorbate (Sigma) to a final concentration of 3 $\mu g\mu l^{-1}$. Under stereotaxic control, 4.5 µl of the 6-OHDA solution was slowly injected at a rate of 0.5 $\mu lmin^{-1}$ through a steel cannula (0.3 mm O.D.) attached to a 10 µl Hamilton™ microsyringe (Cole-Parmer, London, UK) into the region adjacent to the medial substantia nigra (4.5 mm posterior of bregma, 1.2 mm lateral to the midline, and 7.9 mm ventral to the dura, according to the atlas of Paxinos and Watson,

1986). The cannula was left in place for 5 min before being withdrawn to prevent reflux up the needle track.

Following injection of 6-OHDA, incision wounds were sutured (5/0 coated Vicryl, Ethicon™, Johnson and Johnson Intl., Brussels, Belgium) and bonded with a cyanoacrylate adhesive (Vetbond™; 3M Animal Care Products, St. Paul, USA), and the animal was then removed from the stereotaxic frame. A local anaesthetic gel (2% w/v lidocaine hydrochloride; Xylocaine™ gel, Astra) was applied to wound margins and inner ears. Animals also received a dose of long-lasting analgesic, buprenorphine (30 μgkg^{-1}, i.m.; Vetergesic™, Reckitt and Coleman Products Ltd., Hull, UK), before being returned to individual home cages for recovery and observation.

2.2.3 Postoperative care and recovery

Damage to ascending dopaminergic systems by injection of 6-OHDA has long been known to result in adipsia and aphagia (Fibiger et al., 1973; Baez et al., 1977). To combat potential dehydration and weight loss after surgery, the diet of lesioned animals was supplemented with orange segments, muesli, and a carbohydrate-rich, high-H_20 content gel (Transgel™; Charles River). Subcutaneous injections of sterile saline solution (1 ml) were given as necessary to prevent severe dehydration.

2.2.4 Testing for successful unilateral 6-OHDA lesions

The extent of the unilateral lesion of the SNpc was assessed initially by testing for apomorphine-induced turning behaviour, which is a reliable index of dopamine depletion in the basal ganglia (Hudson et al., 1993; Schwarting and Huston, 1996b). On the day of behavioural testing, apomorphine hydrochloride (hemihydrate salt; Sigma) was dissolved in sterile saline solution containing 0.02% w/v ascorbate to a final concentration of 0.1 $mgml^{-1}$, and stored in light-free conditions until used. The behavioural tests were performed 14 or 15

days after the injection procedure. Following a 15 min exploration and acclimation period in the observation chamber, animals received a single bolus of apomorphine (0.05 $mgkg^{-1}$, s.c.) and were returned to the chamber for behavioural observation. The number of turns made subsequently was counted. The lesioning procedure was considered a success in those animals that made at least 100 net contraversive rotations in 20 minutes (135 ± 26 rotations for all selected animals; $n = 7$). Rotational behaviour of this type and with this severity is indicative of a loss of greater than 90% of DA content from the ipsilateral striatum, with a concomitant depletion of greater than 50% of DA content in the corresponding SNpc (Hudson et al. 1993). Profound loss of dopaminergic neurons from the midbrain of animals that passed the rotation test was later confirmed using immunocytochemical methods (see 2.3.2 below).

2.3 Histochemistry and immunocytochemistry

2.3.1 Histochemical verification of recording sites and juxtacellularly-labelled neurons for light and electron microscopic analysis

Standard techniques were used to visualise the Neurobiotin™-filled cells for light microscopic (LM) analysis (Hsu et al., 1981; Horikawa and Armstrong 1988, 1991; Pinault, 1996; Bevan et al., 1998). Briefly, the fixed brain was sectioned (50-60 μm) in the sagittal or coronal plane on a vibrating microtome (Technical Products Intl., St. Louis, USA). The sections were then washed in PBS and incubated in an avidin-biotin peroxidase complex (ABC; 1:100, Vector) in PBS containing 0.3% v/v Triton™ X-100 (Sigma) overnight at room temperature (Hsu et al., 1981). After washes, the slices were incubated in Tris buffer (0.05 M, pH 8.0) containing hydrogen peroxide (0.002% w/v; Sigma), diaminobenzidine tetrahydrochloride (0.025% w/v; DAB; Sigma) and ammonium nickel sulphate ($(NH_4)_2SO_4.NiSO_4.6H_20$; 0.5% w/v; BDH, Poole, UK) for 15-30 min at room temperature.

Neurobiotin™-filled cells were intensely labelled with an insoluble, black/blue precipitate (Hsu and Soban, 1982). Sections were then mounted on gelatine-coated glass microscope slides and air-dried for 3 days. Lastly, sections were dehydrated in 100% v/v ethanol, cleared in xylene and preserved in neutral medium (XAM™; BDH) under coverslips for light microscopy, as described previously (Bolam, 1992).

Standard techniques were used to visualise the Neurobiotin™-filled cells for LM and subsequent electron microscopic (EM) analysis (see Bolam, 1992; Bevan et al., 1998 and references therein). The sections were made more permeable to the histochemical reagents by 2 or 3 freeze-thawing cycles in cryoprotectant (25% w/v sucrose and 10% v/v glycerol in 0.2 M PB, pH 7.4), cooled isopentane (Sigma) and liquid nitrogen. Sections were then washed in PBS and incubated in PBS containing ABC (1:100) for 48 hr at 4°C. After washes, the slices were incubated in Tris buffer (0.05 M, pH 8.0) containing hydrogen peroxide (0.002% w/v), DAB (0.025% w/v) and ammonium nickel sulphate (0.5% w/v) for 20-30 min at room temperature. Neurobiotin™-filled cells were intensely labelled with an insoluble, black/blue precipitate. Slices were then post-fixed in a buffered osmium solution (1% w/v osmium tetroxide; Oxkem Ltd., Oxford, UK; in 0.1 M PB) for 30 min, washed, and dehydrated in an ascending series of ethanol solutions (10 min in 50%, 70%, 90%, 100% and then 100% v/v ethanol, respectively). Following two 10 min washes in propylene oxide (99% v/v; Aldrich, Poole, UK), the slices were transferred to an electron microscopic resin (Durcupan® ACM; Fluka, Gillingham, UK) and left overnight at room temperature to equilibrate. The resin-impregnated sections were then transferred to glass microscope slides, a coverslip applied, and cured for 48 hr at 60°C.

2.3.2 Immunocytochemical verification of 6-OHDA lesions

The extent of the 6-OHDA-lesion was assessed by immunocytochemistry for tyrosine hydroxylase (TH), the rate-limiting enzyme in catecholamine synthesis, using standard

techniques (see Bolam, 1992 and references therein). The fixed brain was cut into two blocks at the level of the entopeduncular nucleus and sectioned in the coronal plane on a vibrating microtome. Rostral blocks that included the GP and caudal blocks that included the STN and SN were sectioned at 60 and 40 μm, respectively. Immunocytochemical incubations were carried out at room temperature. Sections were washed in PBS and then incubated in PBS containing mouse anti-TH monoclonal antibody (1:5000 dilution; Sigma), 0.2% v/v Triton X-100 and 1% w/v bovine serum albumin (Sigma) overnight. After washing, the slices were incubated in PBS containing biotinylated-horse anti-mouse IgG antibody (1:200; Vector) for 2 hr, washed, and incubated for a further 2 hr with ABC (1:100). The slices were then washed and incubated in hydrogen peroxide (0.01% w/v) and DAB (0.05% w/v) in Tris buffer (0.05 M, pH 7.4) for 10-20 min. Tyrosine hydroxylase-immunoreactive cell bodies, axons and dendritic processes were labelled intensely with an insoluble brown precipitate. Finally, sections were mounted, dehydrated, cleared, and preserved for LM analysis as described in section 2.3.1 above.

2.4 Acquisition and analysis of *in vivo* data

2.4.1 Data acquisition

Analogue tape records of unit activity and EEG were digitised off-line on an analogue-to-digital converter (1401plus; Cambridge Electronic Design, Cambridge, UK) and sampled at 12 kHz and 200 Hz, respectively, with Spike2™ acquisition and analysis software (Cambridge Electronic Design) running on a Windows™-based personal computer (Optiplex XMT590; Dell Computer Corp).

2.4.2 Data sampling

When performing the analysis protocols described below, it is important that the spike train is relatively stationary *i.e.* that the average rate or pattern of firing does not vary greatly over time (Perkel et al., 1967a). Neuronal activity *in vivo* is highly dynamic and thus, to ensure stationarity, relatively small segments of the entire recording session were isolated for analysis. Data from the entire recording session were visually inspected and epochs of robust cortical slow-wave activity were identified. A portion of the coincident spike train composed of 100 or 150 spikes (data in Chapters 3 and 4, respectively) was then isolated and the interspike intervals (ISIs) derived. The ISIs were then used for the statistical analysis of the pattern and rate of spike firing. Analysis was normalised with respect to firing rate because the number of spikes used for analysis was the same for each neuron.

2.4.3 Data analysis

Introduction

Standard and non-standard methods of analysis were employed to quantitatively characterise unit activity in the STN-GP network. Since spikes are indistinguishable, except for their times of occurrence, and spike discharge appears to be largely unpredictable, spike trains can be considered to be a random series of points in a contiguous time line or process. Indeed, spike trains have long been described as realisations of "stochastic point processes" (Perkel et al, 1967a). Two of the most popular methods used for describing point processes are the auto-correlation (or "renewal density") and the cross-correlation function (Perkel et al, 1967a, b; Abeles, 1982). These standard methods were used extensively to characterise the firing patterns of, and interactions between, single units recorded in the STN-GP network. The auto-correlogram was used to describe single spike trains and the cross-correlogram was used to define the relationship between the spike trains of two units. The temporal relationships of activity within and between the STN and GP were further elucidated by

determining the phase shifts in the spiking of pairs of neurons. In addition to auto-correlation and cross-correlation analyses, the coefficient of variation of the interspike intervals, a value used widely as an indicator of regularity in point processes (Johnson, 1996), was also calculated. As a final step in the analysis of spike trains, the statistical significance and frequency of any periodic discharge features (*e.g.* oscillations) were determined using the Lomb algorithm (Kaneoke and Vitek, 1996).

Activity in the EEG was quantified using standard spectral analysis methods. Subsequent comparisons of EEG spectra and characterised spike trains revealed the relationship of activity in the cerebral cortex to activity in the STN-GP network.

2.4.3.1 Power spectra, auto- and cross-correlograms, phase shifts, spike-triggered waveform averages, mean rates of firing, coefficients of variation

The frequencies and strengths of oscillations present in the coincident EEG recording were quantified using power spectra, which were obtained by tranforming the analogue voltage (waveform) data with the Fourier algorithm (Fast Fourier Transform function of Spike2™). The power spectrum of the EEG (pEEG) plots the "power" of an oscillation (*i.e.* oscillation strength) against respective frequency (0.1-100 Hz). The units of power are V^2Hz^{-1}. The amplitude of a peak in the power spectrum is a measure of the strength of an oscillation, whereas the location of a peak provides information as to the predominant frequency component of an oscillation. For display purposes in this thesis, power in V^2Hz^{-1} was converted into simple arbitrary units and was termed "relative power" (since this conversion was performed in an identical manner for all power spectra, the different spectra are relative to each other and power can be directly compared across data sets).

Auto- and cross-correlograms of action potentials were calculated for the 100 or 150 sampled spikes of data using Mathematica™ routines (Wolfram Research Inc., Long Hanborough, UK) based on standard methods and a bin size of 1, 5 or 10 ms (Perkel et al.,

1967a, b; Abeles, 1982; Stern et al., 1998): first- to nth-order ISIs were calculated, summated, and assigned density functions, which were subsequently plotted as a correlogram. Repetitive patterns or rhythmicity in a single spike train will lead to a prevalence of certain ISIs, which will be represented in the auto-correlogram as peaks and troughs (Perkel et al, 1967a, b). A flat cross-correlogram suggests that the two trains are independent, whilst peaks and troughs indicate some sort of relationship in time (Perkel et al, 1967a, b; Abeles, 1982). The quantification of correlograms to units of rate (spikes per second) ensured independence of bin size or total time of measurement (Abeles, 1982) and permitted the direct comparison of data from different sources. When paired with GP neurons (see section 3.3.5), the spike trains of STN neurons were used as the reference/template signals for cross-correlation analysis. For the cross-correlation analysis of pairs of STN neurons or pairs of GP neurons (see sections 3.3.6 and 3.3.7, respectively), one neuron from each pair was chosen at random to be the reference signal. To facilitate the approximation of phase shifts, correlograms were smoothed using a three-point moving average. Phase shifts were determined by calculating the time of the highest peak in the cross-correlogram (typically the peak closest to zero time) divided by the oscillation period of the reference neuron.

Spike-triggered averages of EEG waveform (AvWvs) across these samples were performed with Spike2™ and used to estimate phase relationships between the EEG and spike-firing. Mean firing rate was calculated from the reciprocal of the mean ISI.

The coefficient of variation of the interspike intervals (CV; Johnson, 1996) was calculated using the following equation:

$$CV = \sigma / \mu$$

where CV is the coefficient of variation, σ is the standard deviation of ISIs, and μ is the mean ISI.

The CV value does not depend on the mean firing rate of the neuron because ISI variability is normalised by the mean ISI. Furthermore, the more irregular the spike train, the larger the standard deviation of ISIs and thus, the larger the CV. A spike train with a CV = 0 is absolutely periodic and thus, has no variation in ISIs. A spike train with a CV ~ 0 can be considered to be "regular" (Johnson, 1996). A Poisson process, which is random because it does not have a history, has a CV = 1.0. The existence of a refractory period in action potential generation and other, more dynamic membrane properties (*e.g.* plasticity, input shunting, back-propagation of action potentials) in neurons means that discharge will always have a history and therefore, cannot be absolutely random. As such, point processes with a CV of ~ 1.0 are more often referred to as being "irregular" as they closely approximate the Poisson process (Johnson, 1996). Whilst it is possible for the CV of a spike train containing a wide range of ISIs (*e.g.* a spike train containing brief periods of high-frequency discharge that occur infrequently) to exceed 1.0, no term has been commonly ascribed to these CVs.

2.4.3.2 Lomb periodograms

The Lomb algorithm was used to determine the statistical significance and frequency of any periodic discharge features (*i.e.*, oscillations) present in the spike train within the 0.5-50 Hz range (Kaneoke and Vitek, 1996; Boraud et al., 1998; Ruskin et al., 1999). The auto-correlogram of the sampled spike train was constructed, smoothed and then transformed to give a power spectrum of unit activity in the frequency domain (Kaneoke and Vitek, 1996). Frequency spectra of spiking are displayed as "Lomb periodograms". The significance of each frequency peak in the Lomb periodogram was then tested against the null hypothesis that spectrum data are independent Gaussian random values. The relative power of a frequency peak in the Lomb periodogram is indicated by the clearance of the peak from the significance level of $p = 0.05$ (represented by a dashed line in the periodograms).

2.4.3.3 Determination of firing pattern

Neurons that displayed significant oscillations at frequencies less than 2.0 Hz in their spike trains were termed "low-frequency oscillatory" (LFO) neurons. Neurons that did not display significant, low-frequency oscillations were further subdivided into "regular" (CV ≤ 0.35) and "irregular" (CV > 0.35) firing units. As described previously, neurons that discharge in a regular manner often display a significant frequency of oscillation that is similar to the mean firing rate (Kaneoke and Vitek, 1996).

2.4.4 Statistical analysis

The software package GB-STAT™ 5.0 was used for all statistical tests. Statistical comparisons of firing rates and oscillation frequencies were conducted using the Mann-Whitney U-test. The Wilcoxon Signed Rank test was employed in the determination of significance for paired data (*e.g.* pinch effects). The significance level for all tests was taken to be $p < 0.05$. All data are expressed as mean ± standard deviation (SD).

2.5 Electrophysiological recordings *in vitro*

2.5.1 Animals

Brain slices for *in vitro* experiments were obtained from young male Sprague-Dawley rats aged between 16 and 23 days.

2.5.2 Anaesthesia and preparation of brain slices

Anaesthesia was induced with isoflurane in air by inhalation and maintained at very deep levels with ketamine (150 $mgkg^{-1}$, i.p.) and xylazine (15 $mgkg^{-1}$, i.p.). When reflexes to a strong cutaneous pinch or to gentle corneal stimulation were abolished, animals were

perfused via the ascending aorta with 20-30 ml of ice-cold, modified artificial cerebrospinal fluid (mACSF; contained (in mM): sucrose, 230; KCl, 2.5; $NaHCO_3$, 26; $Na_2HPO_4.H_2O$, 1.25; $CaCl_2.2H_2O$, 0.5; $MgSO_4.7H_2O$, 10; and glucose, 10; pH 7.4; osmolarity, 300-310 mosmol) that had been oxygenated by bubbling with a mixture of 95/5% v/v O_2/CO_2. The substitution of NaCl by sucrose in mACSF improves slice viability by minimising the deleterious effects of passive chloride entry into neurons during slicing (Aghajanian and Rasmussen, 1989).

The forebrain was then rapidly removed, blocked in either the coronal or sagittal plane, glued to the stage of a vibrating microtome (VT1000S; Leica Microsystems, Nussloch, Germany), and immersed in ice-cold mACSF. Slices containing the STN were cut at a thickness of 300 μm and were then transferred to a holding chamber that contained oxygenated standard artificial cerebrospinal fluid (ACSF; contained (in mM): NaCl, 126; KCl, 2.5; $NaHCO_3$, 26; Na_2HPO_4, 1.25; $CaCl_2.2H_2O$, 2; $MgSO_4.7H_2O$, 2; and glucose, 10; pH 7.4; 300-310 mosmol) at room temperature. Slices were held in the chamber for at least 1 hr prior to recording to allow for equilibration with the ACSF to take place and to allow neurons to recover from the trauma associated with the slicing procedure.

2.5.3 Perforated patch-clamp recordings

Introduction

Disruption of plasmalemmal ionic gradients profoundly alters the responses of neurons to excitatory and inhibitory synaptic neurotransmission. To avoid the perturbation and dialysis of the cytosolic contents of neurons that occurs during conventional sharp microelectrode or whole-cell patch-clamp recording, the perforated patch-clamp technique was instead employed in all *in vitro* experiments. Perforation of the membrane patch was achieved by the inclusion of the pore-forming, antimicrobial substance gramicidin to the solution in the recording electrode (Ebihara et al., 1995; Ulrich and Huguenard, 1997a). Gramicidin is a 15

residue polypeptide that forms monovalent cation-selective channels in phospholipid membranes following dimerisation (Hladsky and Haydon 1984). Importantly, the cation ionophores formed by gramicidin are largely voltage-insensitive and allow uninterrupted passage of water molecules across the cell membrane. Since recording with the gramicidin perforated patch-clamp method maintains natural intracellular concentrations of anions and large, charged molecules, it is ideal for the determination of the equilibrium potentials of chloride-mediated post-synaptic currents and potentials (Fig. 2.2*A*; Ebihara et al., 1995; Ulrich and Huguenard, 1997a; see sections 2.6.2.1and 2.6.2.2).

Procedures

Gramicidin stock solution was made daily as follows: gramicidin (from *Bacillus brevis* (gramicidin D); Sigma) was dissolved in dimethyl sulphoxide (Sigma) to a final concentration of 5 $mgml^{-1}$ and sonicated (Nusonics ultrasonicator; Fisher, Milton Keynes, UK) at 42 kHz for 1 min.

Somatic recordings of STN neurons were made using patch electrodes prepared from borosilicate glass capillary tubes (GC120F-10, 1.2 mm O.D.; Clarke) on a horizontal laser puller unit (Model P-2000; Sutter Instrument Co., Novato, USA) to give an external tip diameter of 2-2.5 μm. The tips of patch electrodes were front-filled with a filtered patch electrode solution (contained (in mM): $KMeSO_4$, 106; KCl, 25; $MgCl_2.6H_2O$, 1; $CaCl_2.2H_2O$, 0.1; HEPES, 10; EGTA, 1; pH 7.3; 290-300 mosmol) and then back-filled with the same solution containing gramicidin (5 μgml^{-1} final concentration; sonicated at 42 kHz for 30 s). Rupture of the cell membrane (*i.e.* establishing whole-cell configuration) and subsequent diffusion of chloride ions from the "high-chloride" electrode solution into the cytosol resulted in a positive shift in the equilibrium potential of chloride (E_{Cl}) towards –42 mV (at 35-37°C), as predicted by the Nernst equation (Fig. 2.2*C*). Resistance of the gramicidin-filled electrodes before recording ranged from 3 to 6 MΩ.

Individual slices were transferred to a submersion-type recording chamber, secured under a nylon mesh, and continuously perfused (2-3 $mlmin^{-1}$) with oxygenated ACSF at 30-32°C or 35-37°C. Slices were examined by infrared-differential interference contrast (IR-DIC) video microscopy using a 60× water-immersion objective (Zeiss, Oberkochen, Germany) mounted on an upright light microscope (Axioscop; Zeiss) equipped with a video camera (Newvicon C2400; Hamamatsu, Hamamatsu City, Japan). Optimal positioning of slices and electrodes was achieved with a motor-driven microscope stage and micromanipulator, respectively (Infrapatch™; Luigs and Neumann GmBH, Ratingen, Germany). Minimal positive pressure was applied to the electrode before cell contact. A tight seal (resistance of >0.9 GΩ) between the electrode tip and somatic membrane was obtained by application of slight negative pressure to the electrode, thus leading to the cell-attached configuration of recording. Complete perforation of the membrane patch (as indicted by a stable series resistance of 25-75 MΩ) typically occurred 40-60 min after establishing the cell-attached configuration. Recordings were carried out in current- and voltage-clamp modes using an EPC-9 double patch-clamp amplifier (HEKA Electronik, Lambrecht, Germany) that was controlled from a personal computer (PowerMac G3, Macintosh) running the PULSE™ data acquisition and analysis programme (HEKA). Signals were amplified, low-pass filtered (1.7-33.3 kHz) and digitised (5-100 kHz; > 3× the frequency of filtering) on-line. Fast capacitive transients of the electrode, but not slow capacitive transients of the cell membrane, were nulled on-line at the cell-attached stage of recording. Series resistance and associated voltage errors were compensated off-line. Correction of liquid junction potentials is most appropriate when there is a free exchange of ions between the electrode solution and cell interior (Neher, 1992). This free exchange does not occur in the perforated patch-clamp configuration and thus, junction potentials were left uncorrected.

2.5.4 Pharmacological manipulations

Gamma-aminobutyric acid (Tocris Cookson Ltd., Bristol, UK) was applied to the somatic regions of neurons by pressure pulse (Fig. 2.2*B*; 10-30 ms, 10-30 psi; Picospritzer® II, General Valve Corp., Fairfield, NJ, USA). "Spritzer pipettes" were prepared from borosilicate glass capillary tubes (GC120F-10, 1.2 mm O.D.; Clarke) on a horizontal laser puller unit (Sutter) to give an external tip diameter of 8-10 μm. Stock solutions of GABA (100 mM in H_2O) were made daily and were diluted in ACSF to give a final concentration of 100 μM in the spritzer pipette.

Other drugs were dissolved in oxygenated ACSF and bath-applied at the following concentrations, in μM: 4-aminopyridine (4-AP; Sigma), 100; D(-)-2-amino-5-phosphonovaleric acid (APV; Tocris), 50; (+)-bicuculline (free base; Tocris), 30; [3-[[1-(S)-(3,4-dichlorophenyl) ethyl]amino]-2-(S)-hydroxypropyl] (phenyl-methyl)-phosphinic acid hydrochloride (CGP 55845A; gift from Novartis Pharma AG, Basel, Switzerland), 10; 6,7-dinitroquinoxaline-2,3-dione (DNQX; Tocris), 40; ethoxyzolamide (Sigma), 50.

2.5.5 Verification of recording sites

After recording sessions, the position of the neuron and the patch electrode were verified at low magnification (2.5× objective; Zeiss). The STN was identified as a darkly shaded discoid area immediately dorsal to the lightly shaded fibre tracts of the cerebral peduncle. Recorded neurons were located throughout the STN, with the exception of the extreme rostral and caudal poles of the nucleus.

2.6 Acquisition and analysis of *in vitro* data

2.6.1 Data acquisition

Electrophysiological signals were amplified, filtered and digitised on-line (PULSE™ programme, HEKA; see 2.5.3 above).

2.6.2 Data analysis

The programmes PulseTools™ (HEKA) and Origin™ 5.0 (Microcal Software Inc., Northampton, USA) were used to analyse data off-line.

Series resistance (R_{series}) and associated voltage errors were compensated off-line. Series resistance was determined by analysing instantaneous membrane responses to cathodal current injections (–5 to –80 pA; 30 ms) and voltage-clamp steps (± 5 mV; 30 ms). For example, in current-clamp mode, R_{series} was calculated by applying Ohm's law as follows:

$$R_{series} = V / I$$

where V is the instantaneous voltage deflection, I is the injected current, and R_{series} is the series resistance.

In current-clamp mode, the instantaneous voltage error associated with injection of current across the series resistance was calculated using Ohm's law and subtracted accordingly.

In voltage-clamp mode, series resistance produces an error in recordings of membrane potential such that the actual membrane potential will differ from the holding (clamp) potential by the voltage drop across the series resistance *i.e.* holding potential is more hyperpolarised than actual potential. Any such voltage errors were corrected according to the following equation (Johnston and Wu, 1995; Ulrich and Huguenard, 1997a):

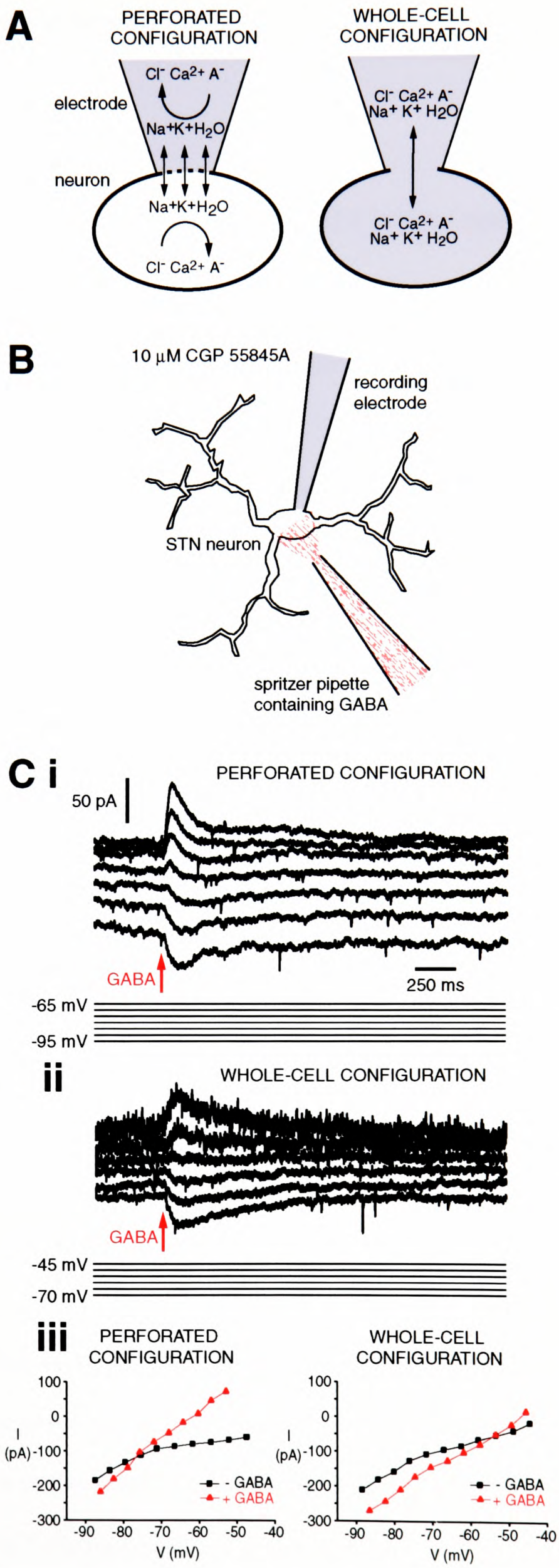
$$V_{corrected} = V_{hold} - (I_{clamp} \times R_{series})$$

where $V_{corrected}$ is the corrected (actual) membrane potential, V_{hold} is the holding potential recorded, I_{clamp} is the clamp current, and R_{series} is the series resistance.

2.6.2.1 Determination of the equilibrium potential of $GABA_A$ receptor-mediated current

Recordings were performed in coronal or parasagittal slices of STN. Responses of STN neurons to pressure-pulse application of GABA were recorded at various holding potentials in current-clamp and voltage-clamp modes (Fig. 2.2*B*, *C*). Gamma-aminobutyric acid was pressure-pluse applied once every 10 s and was directed at the soma of neurons since membrane responses can be most accurately determined and controlled in somatic and proximal dendritic compartments. The amount of GABA applied was usually just above threshold for evoking a detectable response. Holding potentials were between –40 mV and –100 mV, which is well within the voltage range that gramicidin pores show no voltage dependency (Ebihara et al., 1995). Changes in holding potential were made 1 s before the application of GABA to allow the membrane potential to approximate its steady-state value. The GABA-evoked current always fully decayed within < 1 s and was only mediated by $GABA_A$ receptors since $GABA_B$ receptors were selectively blocked with CGP 55845A (see section 5.2.1). In current-clamp, the equilibrium potential of the $GABA_A$ receptor-mediated current ("$GABA_A$ current"; $E_{GABA\text{-}A}$) was measured as the potential at which the GABA application evoked no response, or as the mean of the two voltages at which the smallest depolarising and hyperpolarising responses were evoked. In voltage-clamp, $E_{GABA\text{-}A}$ was taken as the intersection of peak GABA current and "baseline" current plotted against voltage (see figure 2.2*C* for I-V curves). Baseline current was measured as the current

Figure 2.2. Measurement of the equilibrium potential of $GABA_A$ receptor-mediated current in STN neurons. *A*, The perforated patch-clamp recording configuration allows the regulation of intracellular anions (A^-) and divalent cations by the recorded neuron. In contrast, the intracellular concentration of all ions and neutral molecules is dominated by the electrode solution when the whole-cell patch-clamp configuration is established. *B*, During recording, GABA was directed towards the soma of neurons by brief, pressure-pulse application. $GABA_B$ receptor-mediated responses were selectively blocked with 10 μM CGP 55845A in all experiments. *C*, Voltage-clamp recordings of the responses of an STN neuron held at various membrane potentials to the pressure-pulse application of GABA (20 ms duration; 19 psi; *red arrow*) in the perforated patch-clamp configuration (*Ci*) and subsequently, in the whole-cell patch-clamp configuration (*Cii*). Since the electrode solution contained a high concentration of chloride ions, a depolarising shift in $E_{GABA\text{-}A}$ occurred after the whole-cell configuration was achieved. This shift is evident from the size and direction of the peak current evoked by the application of GABA at various holding potentials in the two configurations: the inward $GABA_A$ current reversed and became an outward $GABA_A$ current when the membrane potential at the soma was between –85 and –75 mV in the perforated patch-clamp recording, and between –60 and –50 mV in the whole-cell patch-clamp recording. The exact value for $E_{GABA\text{-}A}$ was taken as the intersection of peak GABA current (+GABA) and baseline current (–GABA) plotted against voltage (*Ciii*; perforated $E_{GABA\text{-}A}$ = –77 mV; whole-cell $E_{GABA\text{-}A}$ = –54 mV). Calibration bars in *Ci* apply to *Cii*.


A
PERFORATED CONFIGURATION
WHOLE-CELL CONFIGURATION
electrode
neuron
Cl⁻ Ca2+ A⁻
Na+K+H2O
Cl⁻ Ca2+ A⁻
Na+ K+ H2O
B
10 μM CGP 55845A
recording electrode
STN neuron
spritzer pipette containing GABA
C i
PERFORATED CONFIGURATION
50 pA
GABA
250 ms
-65 mV
-95 mV
ii
WHOLE-CELL CONFIGURATION
GABA
-45 mV
-70 mV
iii
PERFORATED CONFIGURATION
WHOLE-CELL CONFIGURATION
I (pA)
100
0
-100
-200
-300
-90 -80 -70 -60 -50 -40
V (mV)
- GABA
+ GABA

flowing at the same time as the peak GABA response by repeating the voltage-step protocol in the absence of GABA.

2.6.2.2 Determination of the reversal potential of $GABA_A$ receptor-mediated IPSPs

Inhibitory post-synaptic potentials were evoked in STN neurons by extracellular application of constant current pulses (50-750 μA; 50-100 μs; at 0.1 Hz) between two poles of a 20-pole matrix microelectrode (MX54CBW; FHC Inc., Bowdoinham, USA). The matrix microelectrode was placed in the internal capsule at a position rostral to the STN, or in rostral STN itself, and was triggered by a multichannel pulse generator (Master-8; A.M.P.I). Stimulation conditions were considered to be supramaximal. Inhibitory post-synaptic potentials were considered to be monosynaptic when the change in latency of the evoked event was very small (< 3 ms) and graded upon increasing the stimulus intensity.

Methods for the determination of the reversal potential of $GABA_A$ receptor-mediated IPSPs ($E_{IPSP\text{-}A}$) were as described above for determination of $E_{GABA\text{-}A}$ (section 2.6.2.1), with the exceptions that: 1) recordings were performed in parasagittal slices of STN maintained at 35-37°C; and 2) peak IPSPs were measured instead of peak GABA voltage/current responses.

2.6.2.3 Determination of the level of membrane hyperpolarisation required for rebound burst-firing

Injections of varying amounts of hyperpolarising current were made through the electrode for 500 ms in current-clamp mode and the maximum level of membrane hyperpolarisation achieved during the pulses was measured. The frequency of firing that followed the current pulse was then analysed: A "rebound burst" of action potential firing was defined as an

epoch of firing that contained one or more ISIs that were at least three times shorter in duration than the ISIs associated with spontaneous activity (during zero current application). The threshold for rebound burst-firing was defined as the minimum value of peak hyperpolarisation required to evoke a rebound burst after the current pulse.

2.6.3 Statistical analysis

The software package GB-STAT™ 5.0 was used for all statistical tests. Statistical comparisons were conducted using the Mann-Whitney U-test. The significance level for all tests was taken to be $p < 0.05$. All data are expressed as mean ± SD.

CHAPTER 3.

RELATIONSHIP OF ACTIVITY IN THE NORMAL SUBTHALAMIC NUCLEUS – GLOBUS PALLIDUS NETWORK TO ACTIVITY IN THE CEREBRAL CORTEX *IN VIVO*.

3.1 Introduction

The glutamatergic subthalamic nucleus is a key integrative structure in the circuitry of the basal ganglia. It receives and relays excitatory signals from the cortex and thalamus to basal ganglia output nuclei (Rouzaire-Dubois and Scarnati, 1987; Canteras et al., 1990; Nambu et al., 1990; Robledo and Féger, 1990; Fujimoto and Kita, 1992, 1993; Ryan and Sanders, 1993, 1994; Mouroux et al., 1995; Maurice et al., 1999). GABAergic neurons of the GP shape the response of STN neurons and their targets to cortical stimulation by two mechanisms. First, by feed-back inhibition via their reciprocal connections with the STN (Rouzaire-Dubois et al., 1980; Kita et al., 1983b; Smith et al., 1990; Ryan and Clark, 1991; Fujimoto and Kita, 1993; Bevan et al., 1995, 1997; Maurice et al., 1998a,b) and secondly, by a disinhibitory mechanism involving corticostriatal and striatopallidal pathways (Ryan and Clark, 1991; Ryan et al., 1992; Ryan and Sanders, 1994; Maurice et al., 1998a; Smith et al., 1998). Thus, the complex spatiotemporal patterns of facilitation and inhibition of basal ganglia structures that follow cortical excitation during movement are likely to be supported, in part, by the STN-GP network (Nambu et al., 1990). The functional properties of this network are, in turn, likely to be dependent on cortical activity (Hammond et al., 1978b; Aldridge et al., 1990; Aldridge and Gilman, 1991).

The responses of the STN and GP to brief cortical stimulation have been described in detail (Levine et al., 1974; Kitai and Deniau, 1981; Rouzaire-Dubois and Scarnati, 1985; Toan and Schultz, 1985; Nambu et al., 1990; Ryan and Clark, 1991; Kita, 1992; Fujimoto and Kita, 1993; Yoshida et al., 1993; Maurice et al., 1998a), but activity of the STN-GP network in relation to natural patterns of cortical activity remains to be established. In order to test the hypothesis that the activity of the STN-GP network is dependent on the pattern of cortical input, network behaviour was studied during various states of cortical activation. In natural slow-wave sleep and anaesthesia, cortical activity is characterised by regularly

alternating periods of synchronous spike discharge ("active component" of slow-wave) and neuronal silence ("inactive" component) in projection neurons (Evarts, 1964; Armstrong-James and Fox, 1983; Buzsáki et al., 1988; Steriade et al., 1993c,d; Stern et al., 1997; Steriade and Amzica, 1998; Destexhe et al., 1999). Furthermore, brief periods of cortical activation that occur due to capricious fluctuations in slow-wave activity (SWA), or that result from sensory stimulation, are analogous to global arousal (Buzsáki et al., 1988; Metherate et al., 1992; Steriade et al., 1990; 1993a; Contreras and Steriade, 1997b; Maloney et al., 1997). Thus, the anaesthetised preparation is a good model for establishing the impact of extremes of cortical activity on the STN-GP network. The spike discharge of single and paired STN and GP neurons and coincident cortical EEG were, therefore, recorded during various stereotyped modes of cortical activity (Fig. 3.1).

The discharge of STN and GP neurons within and between connected regions of the parent nuclei during wakefulness displays little or no correlation (Bergman and DeLong, 1989; Cheruel et al., 1994, 1996; Wichmann et al., 1994; Nini et al., 1995; Bergman et al., 1998; Nambu et al., 2000; Raz et al., 2000). Uncorrelated activity in the STN-GP network might arise from asynchronous afferent input or may result from a pattern of hardwiring that ensures that individual neurons receive few common inputs (Bergman and DeLong, 1989; Bevan et al., 1997). These hypotheses were tested by intra- and inter-nuclear STN and GP recordings during periods of synchronous cortical input that were associated with SWA (Fig. 3.1). A low incidence of correlated discharge during the synchronous cortical activity present in sleep and anaesthesia would favour the hypothesis that uncorrelated activity within the STN-GP network is due to a low degree of input sharing.

Subthalamic and GP neuronal discharge changes from asynchronous and irregular firing in health to a pattern of synchronous, rhythmic burst-firing in idiopathic or animal models of Parkinson's disease (Filion, 1979; Filion et al., 1988; Pan and Walters, 1988; Filion and Tremblay, 1991; Hollerman and Grace, 1992; Bergman et al., 1994, 1998;

Rothblat and Schneider, 1995; Wichmann et al., 1994; Nini et al., 1995; Hassani et al., 1996; Kreiss et al., 1997; Boraud et al., 1998). This rhythmic activity is phase-related to resting tremor in PD (Bergman et al., 1994, 1998; Rodriguez et al., 1998; Levy et al., 2000; Raz et al., 2000). Futhermore, recent investigations of STN-GP network activity in organotypic co-cultures suggest that the network alone can support this pattern of activity and act as a generator of physiological and pathophysiological activity in the basal ganglia (Plenz and Kitai, 1999). In order to determine whether the STN-GP network in isolation from the cortex can support synchronous low-frequency, oscillatory activity *in vivo*, cortical input was transiently suppressed using a spreading depression paradigm (Fig 3.1; Leão, 1944; Albe-Fessard et al., 1983; Contreras et al., 1997; see section 3.2.2).

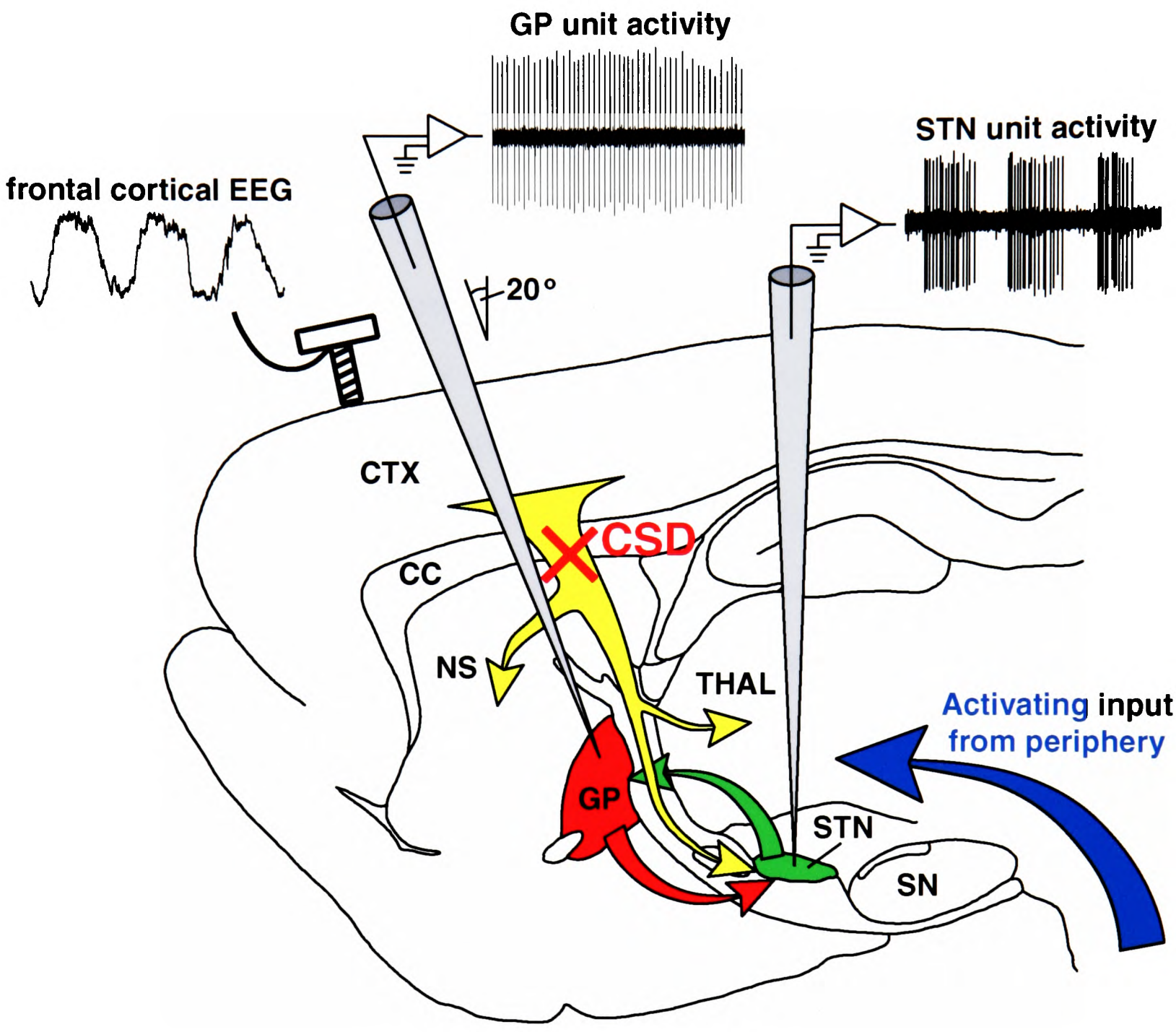
3.2 Experimental procedures

3.2.1 Electrophysiological recording and labelling of neurons in the STN-GP network of anaesthetised rats.

Experiments were carried out on male Sprague-Dawley rats (180-280 g). Anaesthesia was induced with isoflurane in air by inhalation and maintained using one of the following two regimes: (1) ketamine (100 $mgkg^{-1}$, i.p.) and xylazine (10 $mgkg^{-1}$, i.p.), plus supplemental doses as necessary; or (2) urethane (1.25 gkg^{-1}, i.p.), plus supplemental doses of ketamine and xylazine (30 $mgkg^{-1}$ and 3 $mgkg^{-1}$, i.p., respectively). Hereafter, group (1) shall be referred to as "ketamine" anaesthetised and group (2) shall be referred to as "urethane" anaesthetised.

Intra- and inter-nuclear recording techniques were employed to determine the incidence of correlated discharge in the STN-GP network across the sleep-wake cycle. Two separate electrodes were advanced into the STN and GP to record activity across the

Figure 3.1. Experimental design and set-up. Figure shows a parasagittal section of the rat brain at the level of the basal ganglia (adapted from section 2.4 mm lateral of Paxinos and Watson, 1986). Activity in the subthalamic nucleus (STN; *green*) is intimately related to activity in the reciprocally-connected globus pallidus (GP; *red*). Furthermore, direct (corticosubthalamic) and/or indirect (via the neostriatum (NS) and thalamus (THAL)) cortical inputs (both in *yellow*) are likely to influence interactions in the STN-GP network. Experiments were carried out to (1) characterise the relationship between activity in the STN and GP across the sleep-wake cycle; and (2) elucidate the role of descending corticofugal projections in orchestrating activity within the STN-GP network. Activity in the STN and/or GP was assessed from extracellular unit recordings in anaesthetised animals. Frontal cortical activity was simultaneously determined from the electroencephalogram (EEG), which was registered through a screw juxtaposed to the dura mater. Network activity was studied "at rest" and during cortical inactivation (by spreading depression (CSD); *red cross*) or activation (by somatosensory input from the periphery; *blue arrow*). CC, corpus callosum; CTX, cortex; SN, substantia nigra. Rostral is to the *left* and dorsal is to the *top* of the figure.


GP unit activity
STN unit activity
frontal cortical EEG
20°
CTX
CSD
CC
NS
THAL
Activating input
from periphery
GP
STN
SN

network; the STN electrode was set at vertical and the GP electrode was set at 20° to vertical (Fig. 3.1). Since neurons are distributed at a relatively high density in the STN (Oorschot, 1996), direct investigations of local neuronal synchrony were carried out using multiunit recordings from a single extracellular electrode. In contrast to the STN, neurons in the GP are relatively sparsely distributed (Oorschot, 1996). Since multiple GP units were never registered with the type of electrode that was used in this study, it was necessary to use two separate electrodes (set at vertical and 20° to vertical, respectively) when investigating intranuclear synchrony.

To identify the location and morphology of recorded units following physiological characterisation with extracellular electrodes, neurons were selectively labelled with Neurobiotin™ by the juxtacellular method (Pinault, 1994, 1996). Indeed, the majority (93%) of STN and GP neurons recorded in this study were juxtalabelled following physiological characterisation. However, on five occasions (two STN and three GP neurons), when robust modulation could not be achieved, the position of the recorded unit was marked by a discrete extracellular deposit of neurobiotin (100 nA anodal current; 1 s (50%) duty cycle for 30-60 min). The precise locations of all recorded neurons were verified under the light microscope.

Detailed descriptions of the procedures for simultaneous recording of the EEG and unit activity, juxtalabelling, perfusion fixation, histochemical visualisation of recording sites, and data analysis are noted in sections 2.1, 2.1, 2.3 and 2.4, respectively.

3.2.2 Cortical spreading depression

Introduction

The evocation of cortical spreading depression by focal application of a highly concentrated potassium solution has been used extensively to study the effects of reversible functional elimination of the cerebral cortex on the activity of subcortical structures (Weiss and

Fifková, 1961; Bures et al., 1963; Albe-Fessard et al., 1983; Contreras et al., 1997). Cortical spreading depression is attributed to the paroxysmal depolarisation of large numbers of cortical neurons in unison (Leão, 1944, 1947; Albe-Fessard et al., 1983). Prolonged exposure to the depolarising environment temporarily overwhelms the plasmalemmal mechanisms that maintain K^+ and Na^+ gradients across the neuronal membrane, which in turn, results in a loss of resting membrane potential, inactivation of voltage-dependent action potential conductances, and neuronal silence (Weiss and Fifková, 1961; Albe-Fessard et al., 1983). A major advantage of the K^+-evoked spreading depression paradigm is that stable unit recordings of subcortical neurons can be maintained during disruption of cortical input. Thus, this paradigm was used to assess directly the effects of cortical inactivation on unit activity in the STN-GP network.

Procedure

Cortical spreading depression was elicited by the focal application of a 3 M potassium acetate solution to the surface of the frontal cortex that was ipsilateral to the recording site. Recovery of cortical activity was facilitated by irrigation of the cortical surface with saline solution.

3.2.3 Activation of the forebrain by somatosensory stimulation

Introduction

During waking, the low-frequency oscillations present during slow-wave sleep are replaced by faster rhythms with lower amplitudes. This change in electrical activity pattern, termed "activation", is largely controlled by the midbrain reticular activating system (for review, see Steriade, 2000). In anaesthetised animals, this activating system can be recruited by intense somatosensory input to briefly activate the forebrain and produce patterns of neuronal activity that are similar to those seen in naturally aroused animals (for more details, see results and discussion sections).

Procedure

Somatosensory stimulation was elicited by pinching the contralateral hindpaw at the level of the palm for 7 s using pneumatically-driven, serrated forceps. The forceps exerted a standard pressure of ~ 183 gmm^{-2} when closed, which was above the threshold of pain in behaving rats (Cahusac et al., 1990). For multiple recordings, a long interstimulus interval (> 15 min) was used to allow recovery and minimise augmentation of responses.

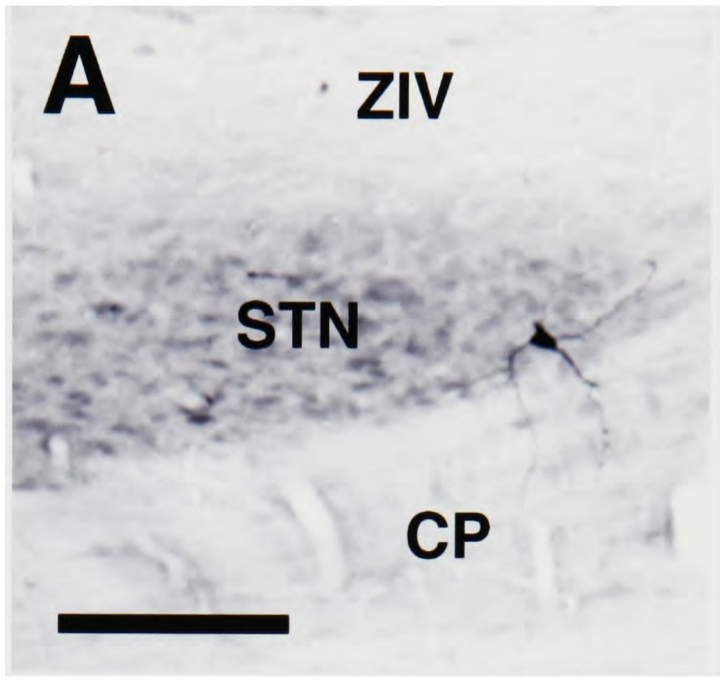
3.3 Results

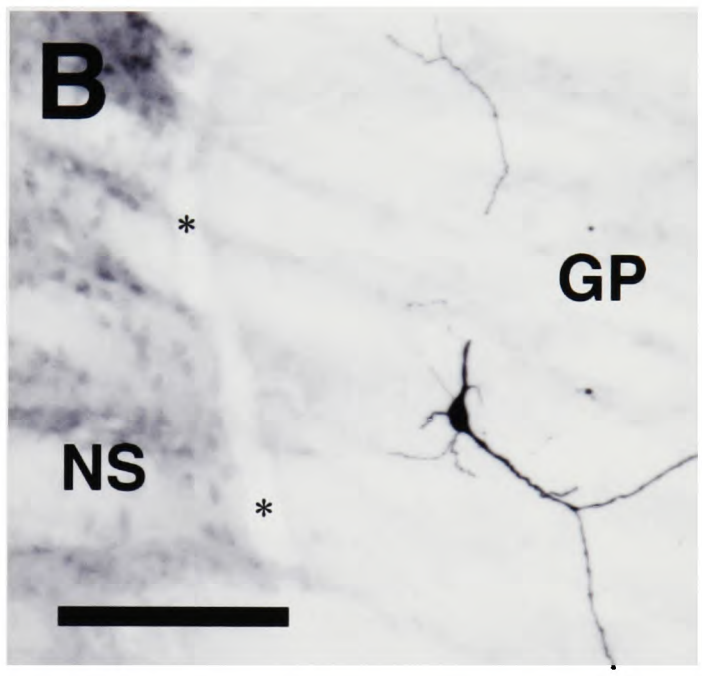
3.3.1 Juxtacellularly-labelled STN and GP neurons

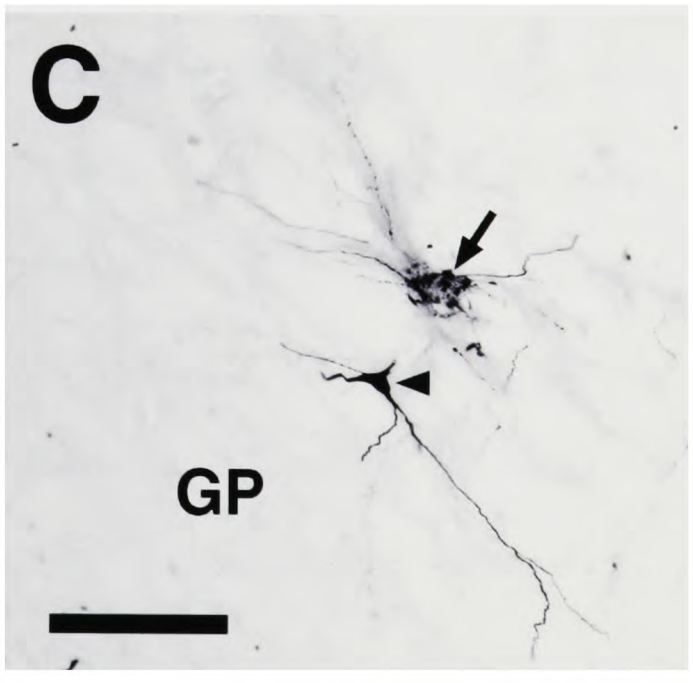
Following physiological characterisation of single or multiple units, robust modulation of the firing of a single unit with juxtacellular microiontophoresis always led to a single neuron being well labelled (n = 71; Fig. 3.2). Juxtacellularly-labelled STN neurons were situated throughout the nucleus (Fig. 3.2*A*). Most of the GP neurons were located throughout the medial half of GP (Fig. 3.2*B*). Discrete extracellular deposits of Neurobiotin™ marked the positions of the five recorded units that could not be juxtacellularly-labelled (Fig. 3.2*C*). Occasionally, the Neurobiotin™ was taken up by neurons surrounding the site of the extracellular deposit (Fig. 3.2*C*).

Preliminary anatomical analyses at the LM level suggested that a subpopulation of GP neurons (at least 7 of 44 well-labelled neurons) projected to the neostriatum (Staines et al., 1981; Beckstead, 1983a; Walker et al., 1989; Kita and Kitai, 1994; Spooren et al., 1996; Nambu and Llinás, 1997; Bevan et al., 1998; Kita et al., 1999; Sato et al., 2000a). The physiological characteristics of these pallidostriatal neurons were indistinguishable from the GP neurons that did not project to the NS. Three VP neurons were recorded and labelled during the course of this study and were subsequently excluded from further analysis.

Figure 3.2. Histochemical verification of recording sites. *A*, *B*, Light micrographs of subthalamic nucleus (STN) and globus pallidus (GP) neurons that were juxtacellularly-labelled with Neurobiotin™. *A*, The STN neuron was located in the caudal portion of the more darkly stained STN. Note that the dendrites of neurons located in the peripheral parts of the STN were occasionally observed to cross the nuclear boundary and extend into the cerebral peduncle (CP) or ventral division of the zona incerta (ZIV). *B*, The GP neuron was situated in the rostral aspect of the GP. A blood vessel (*) lies on the border between the GP and the more darkly stained neostriatum (NS). *C*, When juxtalabelling was not possible, the position of the recorded unit was marked by a discrete deposit of Neurobiotin™ (*arrow*). Occasionally, the tracer was taken up by neighbouring neurons (*arrowhead*). Rostral is to the *left* and dorsal is to the *top* of each panel. Scale bars = 200 μm.


A
ZIV
STN
CP


B
*
GP
NS
*


C
GP

3.3.2 Characterisation of EEG activity

Regardless of anaesthetic protocol, surgical anaesthesia was accompanied by regularly occurring slow-waves of large amplitude (>500 μV) in the frontal EEG (Figs. 3.3, 3.4). Slow-wave activity in the ketamine-anaesthetised group had a significantly faster frequency of oscillation than that recorded in animals under urethane anaesthesia (Tables 3.1, 3.2). Higher-frequency (> 2 Hz) activity, which was of a smaller amplitude (< 200 μV), was commonly superimposed on specific portions of the large slow-waves (Fig. 3.3*B, C*). These portions of the slow-wave (or "slow oscillation") are associated with synchronous spike discharge in cortical projection neurons (Steriade and Amzica, 1998) and will be referred to as the "active components". The frequency range of the smaller amplitude waves varied widely, but spindle activity in the 7-14 Hz range was often predominant (Fig. 3.3*B*; Steriade et al., 1990, 1993d; McCormick and Bal, 1997; Amzica and Steriade, 1998; Steriade and Amzica, 1998).

3.3.3 Physiological characteristics of STN neurons

Extracellular unit recordings revealed that 97% of STN neurons (n = 29) exhibited low-frequency (≤ 2.0 Hz) oscillatory (LFO) firing patterns at variable firing rates under both anaesthetic regimes (Table 3.1). However, mean spontaneous firing rate and CVs of STN neurons recorded under ketamine were significantly higher than the mean rate and CVs of neurons recorded under urethane (Table 3.1). Thus, the burst-like discharges of STN neurons were proportionally more intense in ketamine anaesthesia than in urethane-based anaesthesia. One STN neuron recorded in urethane fired in an irregular manner. Taken together, these data suggest that rhythmic activity is expressed to a greater extent in the STN during ketamine anaesthesia than during urethane anaesthesia.

Table 3.1. Firing properties of STN neurons.

	Type of Anaesthesia	
	Urethane	**Ketamine**
No. of observations	10	19
Low-frequency oscillatory neurons [a]	9	19
Irregular neurons	1	0
Regular neurons	0	0
Mean Firing rate (Hz)		
All neurons	10.6 ± 6.2	21.2 ± 11.4
Low-frequency oscillatory neurons	10.2 ± 6.4	21.2 ± 11.4
Irregular neurons	14.4	-
Regular neurons	-	-
Coefficient of Variation		
Low-frequency oscillatory neurons	1.68 ± 0.64	2.07 ± 0.58
Irregular neurons	1.38	-
Regular neurons	-	-
No. of oscillating neurons	9	19
Low-frequency oscillatory neurons	9	19
Irregular neurons	0	0
Regular neurons	0	0
Frequency of spike train oscillation (Hz)		
Low-frequency oscillatory neurons	0.81 ± 0.29	1.33 ± 0.19
Irregular neurons	-	-
Regular neurons	-	-
Frequency of cortical SWA (Hz)	0.81 ± 0.15	1.34 ± 0.19

a Neurons were defined as displaying a significant, low-frequency oscillation in their spike trains (frequency of ≤ 2.0 Hz; $p < 0.05$).
Data are expressed as mean ± SD.

During episodes of robust SWA, the rhythmic cortical oscillation was mirrored in the spontaneous firing patterns of STN neurons (Figs. 3.3*A*, *B*, 3.4*A; n* = 28). Indeed, burst-like firing of STN neurons was correspondingly periodic (see auto-correlograms in Figs. 3.3*A*, *B*, 3.4*A*) and was precisely phase-locked with SWA (see spike-triggered waveform averages in Figs. 3.3*A*, *B*, 3.4*A*). Spike firing of STN neurons was predominantly restricted to the active component of the slow oscillation (Fig. 3.3*B*). In addition, STN burst-like discharges could be sub-divided into "miniature bursts" (two to four spikes) that were phase-locked to the spindle sequences superimposed on the SWA (Fig. 3.3*B*, *C*). A statistical comparison of Lomb periodograms, which are measures of significant oscillations in the spike train, with the power spectra of the EEG demonstrated a similar periodicity (Figs. 3.3*A*, *B*, 3.4*A*; Table 3.1).

Spontaneous, short-lived losses of EEG power (*i.e.* rhythmicity and amplitude) in the slow-wave and spindle frequency-range, a process hereafter referred to as "activation", were always reflected as changes in firing patterns of STN neurons. They rapidly adopted an irregular, single-spike firing pattern during episodes of activated cortical patterns (Fig. 3.3*A;* see also Figs. 3.4*B*, 3.6*B, C*). Activation mechanisms originating in the brain stem and/or forebrain can be recruited by somatosensory input from the periphery to activate the cortex and obliterate SWA in the EEG (Moruzzi and Mougoun, 1949; Détári and Vanderwolf, 1987; Buzsáki et al., 1988; Steriade et al., 1990, 1993a; Nuñez, 1996). Sensory stimulation by hindpaw pinching was rarely effective in fully activating the frontal EEG in animals anaesthetised with ketamine (see also Svoboda et al., 1999). However, a small decrease in SWA amplitude and periodicity was observed in 9 of 14 cases. This was closely linked with a significant decrease in firing rate of STN neurons (54 ± 18% of control levels; mean firing rates before and during pinch were 25.4 ± 11.1 Hz and 14.5 ± 8.9 Hz, respectively), but was usually not associated with a change in gross firing pattern. Under urethane anaesthesia, somatosensory and nociceptive responses are left relatively intact (Angel and Gratton, 1982;

Maggi and Meli, 1986, Nuñez, 1996), and indeed, paw pinch was more effective in activating the frontal cortex in urethane-anaesthetised animals compared to ketamine-anaesthetised animals. Activation of the EEG was commensurate with a loss of LFO activity and a change in firing to an irregular, single-spike pattern, together with a significant increase in firing rate (136 ± 43% of control; mean firing rates before and during pinch were 10.7 ± 3.7 Hz and 14.4 ± 5.5 Hz, respectively; n = 5; Figs. 3.4, 3.8*B*). It should be noted, however, that a profound change in firing pattern can occur with a relatively minor change in firing rate (Fig. 3.4; pinch caused firing rate to increase to only 110 % of control, but LFO activity was completely lost). Fluctuations in firing rate and firing pattern of STN neurons in response to pawa pinch were only observed when changes in cortical activity occurred. Taken together, these findings suggest that there is a tight relationship between cortical activity and somatosensory responses in the STN during both types of anaesthesia.

The relationship between cortical and STN activity was further analysed by testing neuronal responses to transient cortical inactivation induced by spreading depression (Leão, 1944; Albe-Fessard et al., 1983; Contreras et al., 1997). Spreading depression resulted in a graded loss of coherent, rhythmic activity in the cortex (SWA reduced to 5-25% of original power; Fig. 3.3*D*), which was associated with a loss of LFO activity, a change to irregular firing, and a significant drop in firing rate in the ipsilateral STN (28 ± 26% of control; one neuron became quiescent; n = 5). Although the effects of the depression on firing rate were highly variable, this switch in firing mode was robust. In most cases, the depression of cortical activity was fully reversible and LFO activity only resumed when SWA reappeared (Fig. 3.3*D*). These data suggest that the cortex directly or indirectly exerts an excitatory influence on the neurons of the STN and that oscillatory activity in the STN is not maintained in the absence of rhythmic cortical input.

Figure 3.3. Spike-firing patterns of STN neurons are related to coincident cortical activity during ketamine anaesthesia. *A*, Spike-firing of the STN neuron (CV = 2.14) was dominated by a robust, low-frequency oscillation such that the neuron tended to fire on the rising phase of the cortical slow-wave. Note that during periods of prolonged cortical activation (under *white bar*), the duration of the burst-like discharge was increased. Rhythmic spike-firing was manifest as peaks in the auto-correlogram (AC). Comparison of the Lomb periodogram (Lomb) with the power spectrum of the EEG (pEEG) shows a similar frequency of rhythmic activity in the STN spike train and cortex. Dashed line in this and subsequent Lomb periodograms denotes the significance level of $p = 0.05$. The phase relationship between spiking and the EEG waves is shown on the spike-triggered average of the EEG waveform (AvWv). *B*, The firing of another LFO neuron (CV = 3.20) was phase-locked to the crest of the cortical slow-wave. Note the smaller amplitude, spindle-like events (frequency ~10 Hz) superimposed on the peaks of the slow-wave in the EEG trace. The large bursts occurred at a frequency ~1 Hz and were composed of a number of "miniature bursts", which are shown as small peaks riding on the top of the three larger peaks in the auto-correlogram. The main Lomb periodogram shows significant oscillatory activity at a frequency very similar to that of the large slow-wave. The inset Lomb periodogram is filtered between 4-25 Hz and shows a significant oscillation in the spike train at ~ 10 Hz frequency. *C*, The boxed area in *B* (1 second of data) on an expanded time scale. The firing of miniature bursts was phase-locked with the generation of the spindle-like wavelets. *D*, Low-frequency oscillatory activity in the same neuron was replaced with irregular, single-spike activity during episodes of cortical spreading depression (*white bar*). The four graphs to the right of the trace in *D* were constructed from the period under the *white bar*; note that a significant oscillation in the Lomb periodogram was no longer present and that the auto-correlogram did not have peaks when power in the EEG was severely attenuated. Partial recovery of cortical SWA was accompanied by a partial restoration of LFO activity (*black bar*). Calibration bars apply to all panels except *C*. In this and following figures, AC designates auto-correlograms of spiking activity (bin size 10 ms), Lomb designates Lomb periodograms of spiking activity, pEEG designates power spectra of the coincident EEG, and AvWv designates spike-triggered averages of EEG.

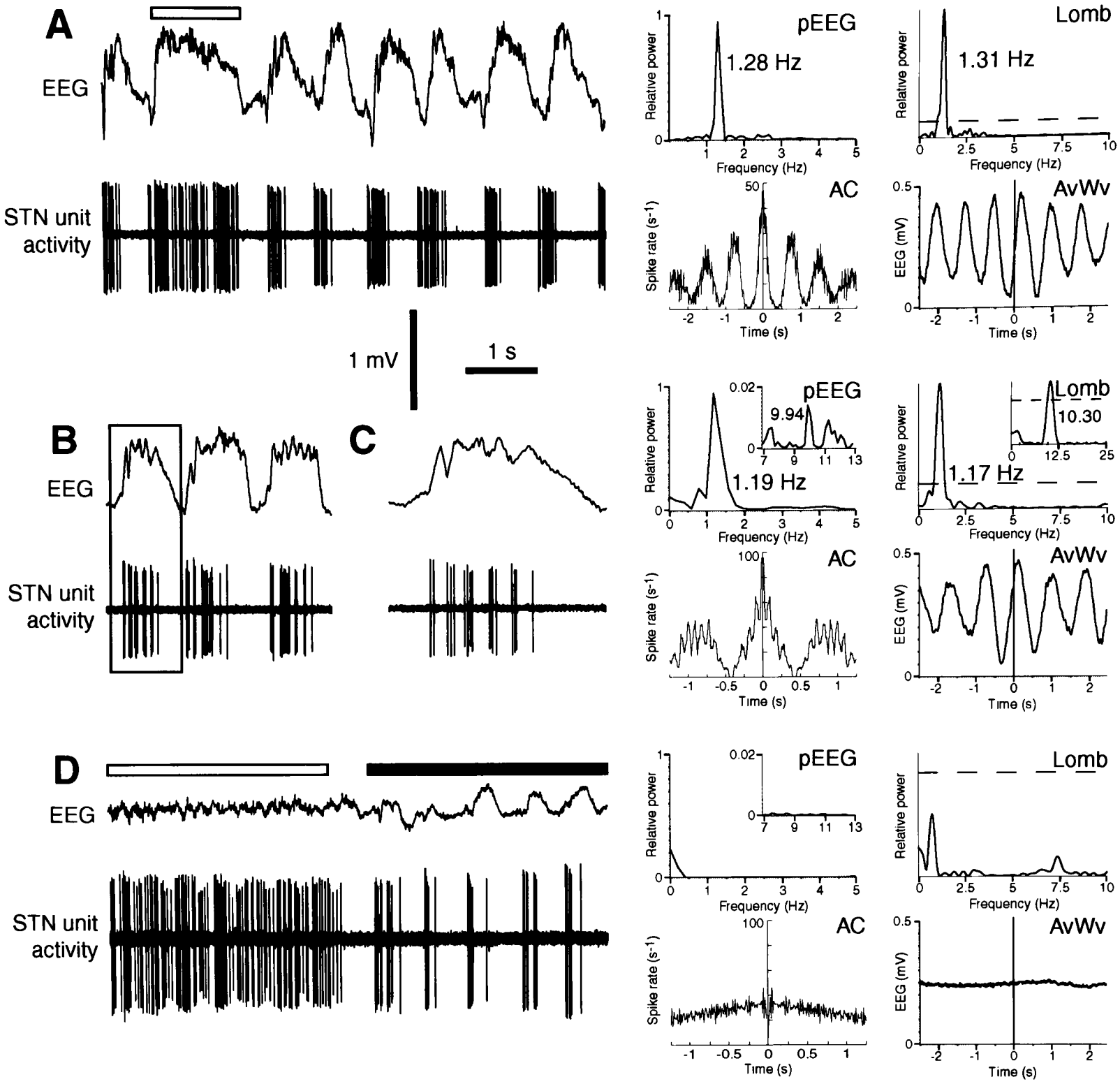
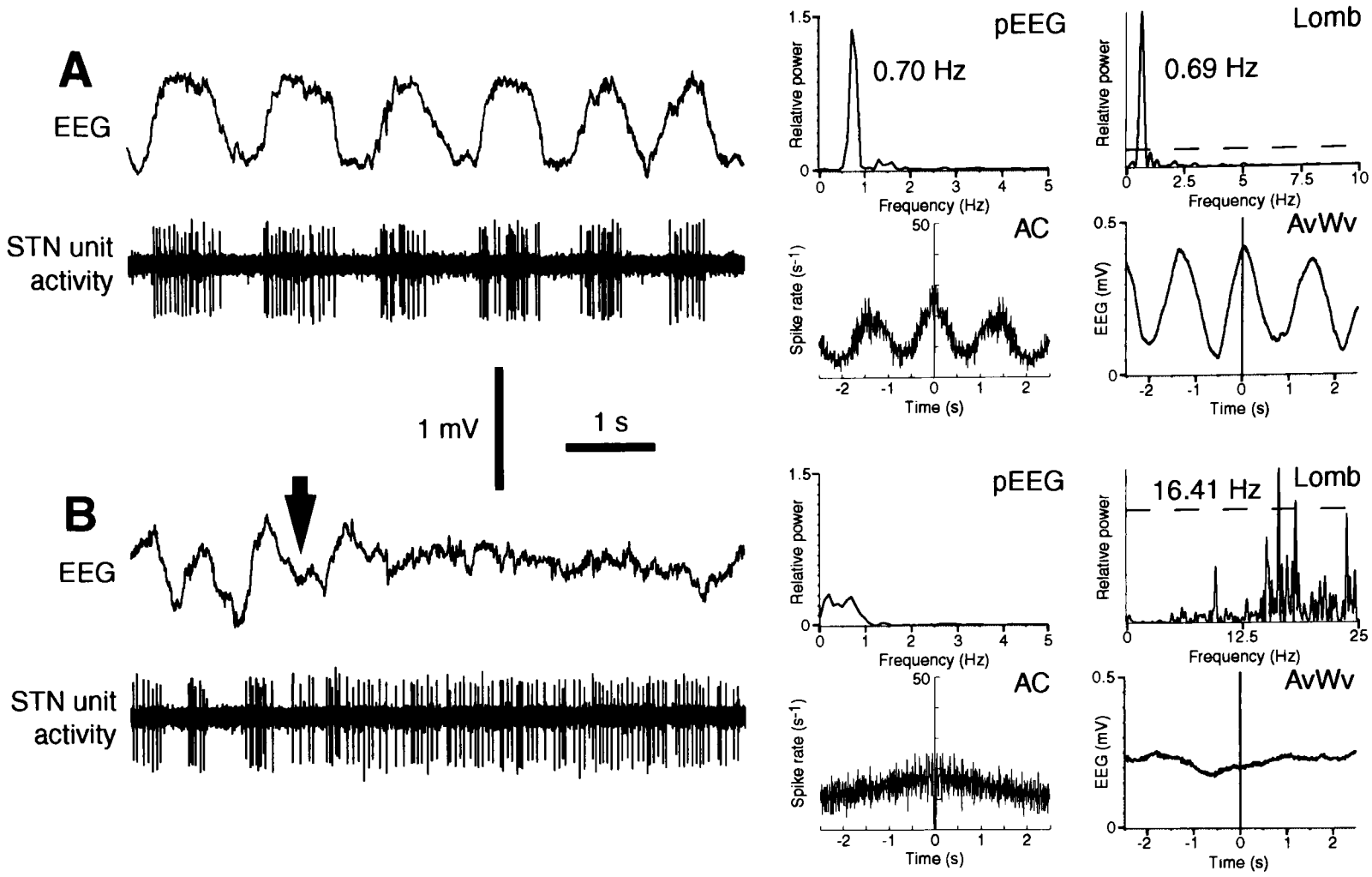

A
EEG
STN unit activity
1 mV
1 s
B
EEG
STN unit activity
C
D
EEG
STN unit activity
pEEG
1.28 Hz
Relative power
Frequency (Hz)
Lomb
1.31 Hz
AC
Spike rate (s-1)
Time (s)
AvWv
EEG (mV)
9.94
1.19 Hz
10.30
1.17 Hz

Figure 3.4. Spike-firing patterns of STN neurons are related to coincident cortical activity in urethane anaesthesia. *A*, Low-frequency oscillatory STN neuron (CV = 1.47), the firing of which was phase-locked to cortical SWA. Note the significantly lower frequency of SWA and periodic, burst-like discharge as compared to activity during ketamine anaesthesia. *B*, Disruption of SWA by sensory stimulation (hindpaw pinch of 10 s duration; starts at *arrow*) was concomitant with a loss of LFO activity in the same neuron. Auto-correlogram, Lomb periodogram, pEEG and AvWv in *B* were determined during the pinch. Calibration bars apply to both panels.


A
EEG
STN unit activity
1 mV
1 s
B
EEG
STN unit activity
pEEG
0.70 Hz
Relative power
Frequency (Hz)
Lomb
0.69 Hz
Relative power
Frequency (Hz)
AC
Spike rate (s-1)
Time (s)
AvWv
EEG (mV)
Time (s)
pEEG
Relative power
Frequency (Hz)
Lomb
16.41 Hz
Relative power
Frequency (Hz)
AC
Spike rate (s-1)
Time (s)
AvWv
EEG (mV)
Time (s)

3.3.4 Physiological characteristics of GP neurons

Similar to the observations in the STN under ketamine anaesthesia, GP neurons (n = 32) exhibited both LFO and irregular firing patterns at variable firing rates (Fig. 3.5*A*, *B*; Table 3.2). In contrast, under urethane anaesthesia, GP neurons (n = 15) discharged single spikes in a regular manner even when SWA simultaneously occurred in the cortex (Fig. 3.5*D*, Table 3.2). Furthermore, GP neurons recorded during urethane anaesthesia were significantly more active than those recorded in ketamine anaesthesia.

Cortical oscillations were reflected in the spontaneous firing patterns of the majority of GP neurons recorded under ketamine anaesthesia. Indeed, 91% of GP neurons recorded expressed a significant, low-frequency oscillation in their spike train with a frequency that was similar to the concurrent slow oscillation in the frontal cortex (Table 3.2). In contrast to STN neurons, the firing of GP neurons oscillated in time with either the active or inactive components of the slow oscillation (22% and 78% of recorded neurons, respectively; Figs. 3.5*A*, 3.9*A*). In common with activity in the STN, the large, burst-like discharges of LFO pallidal neurons were occasionally divided into miniature bursts in time with the coincident spindles (Figs. 3.5*A*, 3.6*A*). Three GP neurons (9%) fired in an irregular fashion during robust cortical SWA (Fig. 3.5*B*). Although the CVs of irregular GP neurons were significantly smaller than the CVs of LFO neurons, the mean firing rates of the two groups were similar (Table 3.2).

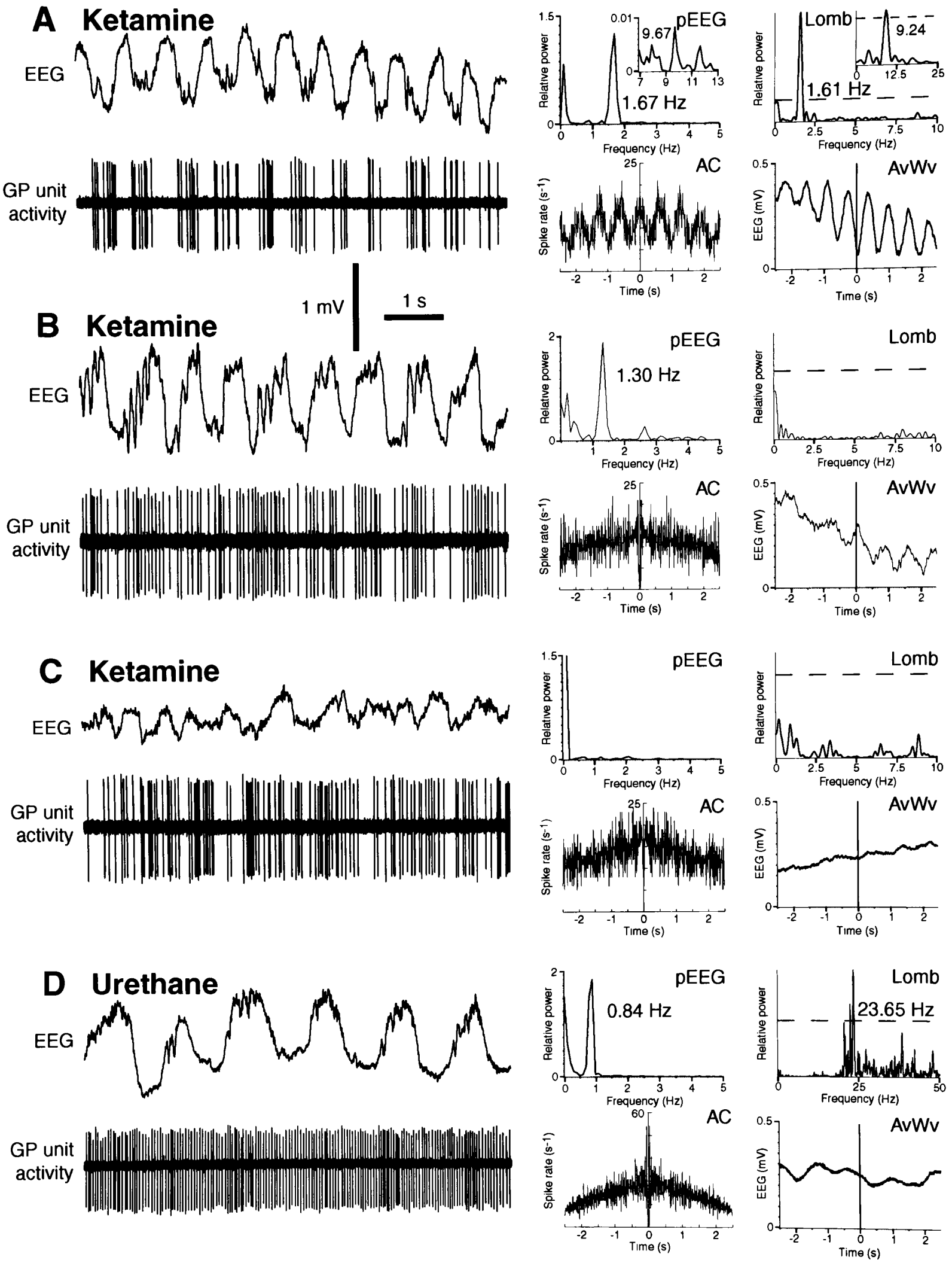
Spontaneous or hindpaw pinch-evoked activation of cortex in ketamine anaesthesia typically resulted in a loss of LFO activity of GP neurons with either a decrease (65.7 ± 18.1% of control; mean firing rates before and during pinch were 14.1 ± 9.9 Hz and 9.9 ± 5.5 Hz, respectively; 8 of 30 neurons tested) or an increase (231 ± 116% of control; mean firing rates before and during pinch were 11.4 ± 8.0 Hz and 26.1 ± 31.4 Hz, respectively; 6 of 30 neurons) in firing rate (Figs. 3.6*B*, *C*, 3.7*C*). In 10 cases, the pinch caused no change in the EEG or spike discharge. Cortical inactivation by spreading depression resulted in a decrease

Table 3.2. Firing properties of GP neurons.

	Type of Anaesthesia	
	Urethane	**Ketamine**
No. of observations	15	32
Low-frequency oscillatory neurons [a]	0	29
Irregular neurons	0	3
Regular neurons	15	0
Mean Firing rate (Hz)		
All neurons	21.7 ± 7.9	13.4 ± 7.5
Low-frequency oscillatory neurons	-	13.3 ± 7.6
Irregular neurons	-	15.2 ± 8.6
Regular neurons	21.7 ± 7.9	-
Coefficient of Variation		
Low-frequency oscillatory neurons	-	1.19 ± 0.23
Irregular neurons	-	0.57 ± 0.06
Regular neurons	0.22 ± 0.04	-
No. of oscillating neurons	15	29
Low-frequency oscillatory neurons	0	29
Irregular neurons	0	0
Regular neurons	15	0
Frequency of spike train oscillation (Hz)		
Low-frequency oscillatory neurons	-	1.26 ± 0.25
Irregular neurons	-	-
Regular neurons	24.54 ± 7.60	-
Frequency of cortical SWA (Hz)	0.83 ± 0.15	1.24 ± 0.22

a Neurons were defined as displaying a significant, low-frequency oscillation in their spike trains (frequency of ≤ 2.0 Hz; $p < 0.05$).
Data are expressed as mean ± SD.

Figure 3.5. Spike-firing patterns of GP neurons are related to coincident cortical activity in ketmine anaesthesia, but not in urethane anaesthesia. *A*, Low-frequency oscillatory pallidostriatal GP neuron (CV = 1.16) firing burst-like discharges of spikes during the troughs of the cortical slow-wave in ketamine anaesthesia. Comparison of the Lomb periodogram with the power spectrum shows very similar frequencies of rhythmic activity in the spike train and EEG. The main Lomb periodogram shows significant oscillatory behaviour at a frequency similar to that of the large slow-wave; the inset Lomb periodogram is filtered between 4-25 Hz and shows a significant oscillation in the spike train at ~ 10 Hz frequency, which is similar to the spindle frequency. *B*, Irregular-firing GP neuron (CV = 0.58) during robust SWA. Note that the spike train of the neuron did not display any significant oscillations and that large peaks were not present in the auto-correlogram and AvWv. *C*, Same neuron as in *A*. During cortical spreading depression, the amplitude of the SWA was attenuated and LFO activity in the neuron was replaced with irregular, single-spike activity. The neuron eventually became quiescent following prolonged depression of cortical activity. The neuron did not oscillate again until cortical SWA had recovered. *D*, During urethane anaesthesia, GP neurons displayed a highly regular, single-spike firing pattern that persisted during episodes of robust SWA. The GP neuron in *D* (CV = 0.20) had a mean firing rate of 23.7 Hz, which is similar to the dominant frequency of activity in the Lomb periodogram, thus confirming the regular, tonic nature of spiking. Calibration bars apply to all panels.


A Ketamine
EEG
GP unit activity
1 mV
1 s
B Ketamine
EEG
GP unit activity
C Ketamine
EEG
GP unit activity
D Urethane
EEG
GP unit activity
pEEG
1.67 Hz
9.67
Lomb
1.61 Hz
9.24
AC
AvWv
Relative power
Frequency (Hz)
Spike rate (s-1)
EEG (mV)
Time (s)
1.30 Hz
0.84 Hz
23.65 Hz

in SWA and a profound and significant reduction in spike-firing rate (27 ± 36% of pre-depression spike rates; n = 5; Fig. 3.5*C*). In three neurons, cortical inactivation resulted in total quiescence, which persisted for the duration of the spreading depression. These data suggest that the cortex indirectly or directly exerts an excitatory influence on the neurons of the GP and that low-frequency oscillatory activity in the GP in ketamine anaesthesia is not maintained in the absence of rhythmic cortical activity.

A neuron with a regular discharge pattern is likely to have a significant peak in the Lomb periodogram that is similar to the mean rate of spiking. The highly-regular nature of firing in the GP under urethane anaesthesia was demonstrated by the facts that (1) these two values did not differ significantly for GP neurons (Fig. 3.5*C*, Table 3.2); and (2) CVs were relatively small (significantly smaller than CVs of GP neurons in ketamine). Neuronal firing rate and pattern were relatively insensitive to minor fluctuations in SWA. However, the hindpaw pinch, which typically caused a robust activation of the EEG, was associated with a significant increase in firing rate (136 ± 31% of control; mean firing rates before and during pinch were 21.4 ± 8.4 Hz and 28.1 ± 9.4 Hz, respectively; n = 7). In one case, the pinch failed to activate the cortex or change the firing rate of the GP neuron. As was the case for STN neurons, fluctuations in firing rate and pattern of GP neurons during the pinch, under either anaesthetic regime, were only observed when there were changes in cortical SWA. These data suggest that the cortex plays a fundamental role in mediating the responses of GP neurons to innocuous and noxious tactile stimuli.

3.3.5 Simultaneously-recorded STN and GP neurons

All seven pairs of neurons recorded simultaneously in ketamine anaesthesia discharged spikes in a highly-correlated manner that was phase-locked to the coincident cortical SWA (Fig. 3.6*A*). Correlated firing occurred on the time scale of tens and hundreds of milliseconds (see broad peaks of cross-correlogram in Fig. 3.6*A*), possibly reflecting input

synchrony (Perkel et al., 1967b). Correlations on the low millisecond (< 20 ms) time scale were not observed. The cross-correlation procedure was replicated for different epochs along the spike train and phase relationships did not vary significantly when robust SWA was present. All 14 neurons displayed a significant, low-frequency oscillation in their spike trains. The mean frequency of this oscillation (1.41 ± 0.24 Hz) was not statistically different from the mean frequency of the slow oscillation in the EEG (1.39 ± 0.24 Hz). The frequency of oscillations in the spike trains of simultaneously-recorded neurons were tightly coupled (mean difference in the frequency of paired LFO activity was 0.07 ± 0.08 Hz for the seven pairs). However, the phase relationships between the firing of STN and GP neurons varied between 5 and 330 ms (phase lag in GP firing compared to STN firing of approximately 2°-135°; Table 3.3; see section 2.4.3.1 for determination of phase shifts). It cannot be ascertained from the present study if the pairs of neurons were recorded from functionally-equivalent and/or reciprocally-connected areas of the STN and GP. Thus, these data imply that, although the temporal aspects of oscillatory activity in the STN-GP network are strictly related to cortical activity, the phase differences in firing may be dictated by the spatial constraints of the network.

Correlated firing of STN and GP neurons was transiently lost during capricious, or paw pinch-evoked, fluctuations in SWA (Fig. 3.6*B*; also compare cross-correlograms in Fig. 3.6*A* and 3.6*C*). Indeed, episodes of cortical activation were immediately accompanied by a switch from correlated LFO activity to uncorrelated, irregular activity in both types of neuron (Fig. 3.6*B*, *C*). Taken together with the results from singularly-recorded neurons, these data suggest that correlated bursting at 0.5-2 Hz is unlikely to be generated within the STN-GP network itself and is most probably not a self-perpetuating oscillation in the absence of rhythmic cortical input.

Figure 3.6. Simultaneous recordings of a STN neuron and a GP neuron during ketamine anaesthesia. *A*, This pair of LFO neurons displayed near-synchronous oscillatory activity during robust SWA. The CVs of the STN and GP neurons were 1.87 and 1.37, respectively. Burst-like firing of both neurons was phase-locked to the slow cortical oscillation. The cross-correlogram (CC) possessed several broad peaks: on average, the STN neuron fired approximately 30 ms before the GP neuron (18° phase difference). Narrow peaks on the millisecond time scale were not observed, which implies that the pair were not monosynaptically connected. The GP neuron was anatomically identified at the LM level as being of the pallidostriatal subtype. *B*, Spontaneous, brief periods of reduction of slow-wave amplitude and rhythmicity were associated with a loss of correlated activity in the same neurons (under *white bar*). Correlated LFO activity swiftly resumed when robust SWA was restored. *C*, Later in the same recording session, SWA effectively collapsed for approximately 40 s, and periodic and correlated activity were lost in the pair. Note that the GP neuron fired faster during the prolonged loss of SWA in *C* as compared to the short-lived loss of SWA in *B*. In this and following figures, CC designates cross-correlograms of spiking activity between pairs of neurons (bin size 10 ms). Calibration bars apply to all panels.

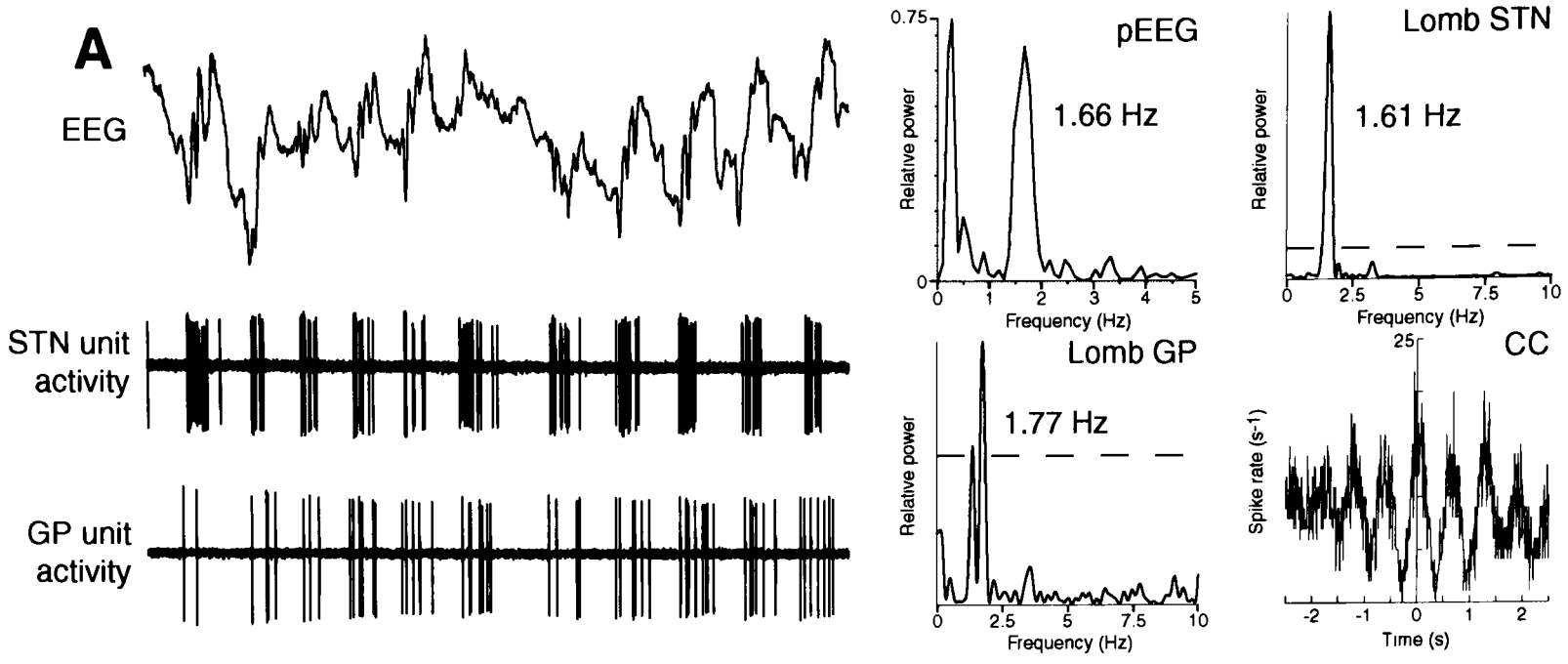

A
EEG
STN unit activity
GP unit activity
pEEG
1.66 Hz
Relative power
Frequency (Hz)
Lomb STN
1.61 Hz
Lomb GP
1.77 Hz
CC
Spike rate (s-1)
Time (s)
B
EEG
1 mV
1 s
STN unit activity
GP unit activity
C
EEG
STN unit activity
GP unit activity
pEEG
0.28 Hz
Lomb STN
0.28 Hz
Lomb GP
14.27 Hz
CC

Table 3.3. The phase lags, but not the frequency, of oscillations in the STN-GP network vary widely in ketamine anaesthesia.

Type of simultaneous recording	Number of pairs recorded	Mean difference in frequency of oscillatory firing across each pair (Hz)	Range of phase lags across pairs
STN-GP	7	0.07 ± 0.08	2°-153°
STN-STN	4	0.10 ± 0.03	1°-13°
GP-GP	6	0.07 ± 0.09	9°-177°

Data are expressed as mean ± SD.

Seven pairs of STN and GP neurons recorded simultaneously during urethane anaesthesia did not exhibit any correlation in spike-firing (Fig. 3.7). The lack of synchrony between the two nuclei was manifest as regular-firing in GP neurons concomitant with LFO firing in STN neurons that was phase-locked to cortical SWA. Uncoordinated activity in the STN-GP network was not due to atypical SWA because there was no significant difference in the amplitude or frequency of the SWA in the paired- or single-neuron recording sessions.

3.3.6 Simultaneously-recorded pairs of STN neurons

The variation in phase relationships between LFO activity in STN and GP neurons recorded simultaneously may be due, in part, to asynchronous firing within the STN and/or GP. To address this, multiunit recordings from single electrodes were made in the STN under ketamine or urethane anaesthesia. In good agreement with single unit recordings, spike-firing in pairs of neurons was phase-locked to cortical activity (Fig. 3.8). The oscillation in the spike trains of four pairs of STN neurons (1.25 ± 0.14 Hz) was not significantly different from that of the slow cortical oscillation (1.29 ± 0.18 Hz) during ketamine anaesthesia. Furthermore, the discharge of neighbouring STN cells was tightly correlated and occurred only during the active component of the SWA (Fig. 3.8*A*), which resulted in a small

Figure 3.7. Simultaneous recordings of a STN neuron and a GP neuron during urethane anaesthesia. *A*, Typical example of uncorrelated firing in the STN-GP network. Although STN neurons fired bursts of spikes in a discrete, phase-locked manner, all GP neurons maintained a regular firing mode under this anaesthetic regime. The CVs of the STN and GP neurons were 1.22 and 0.23, respectively.

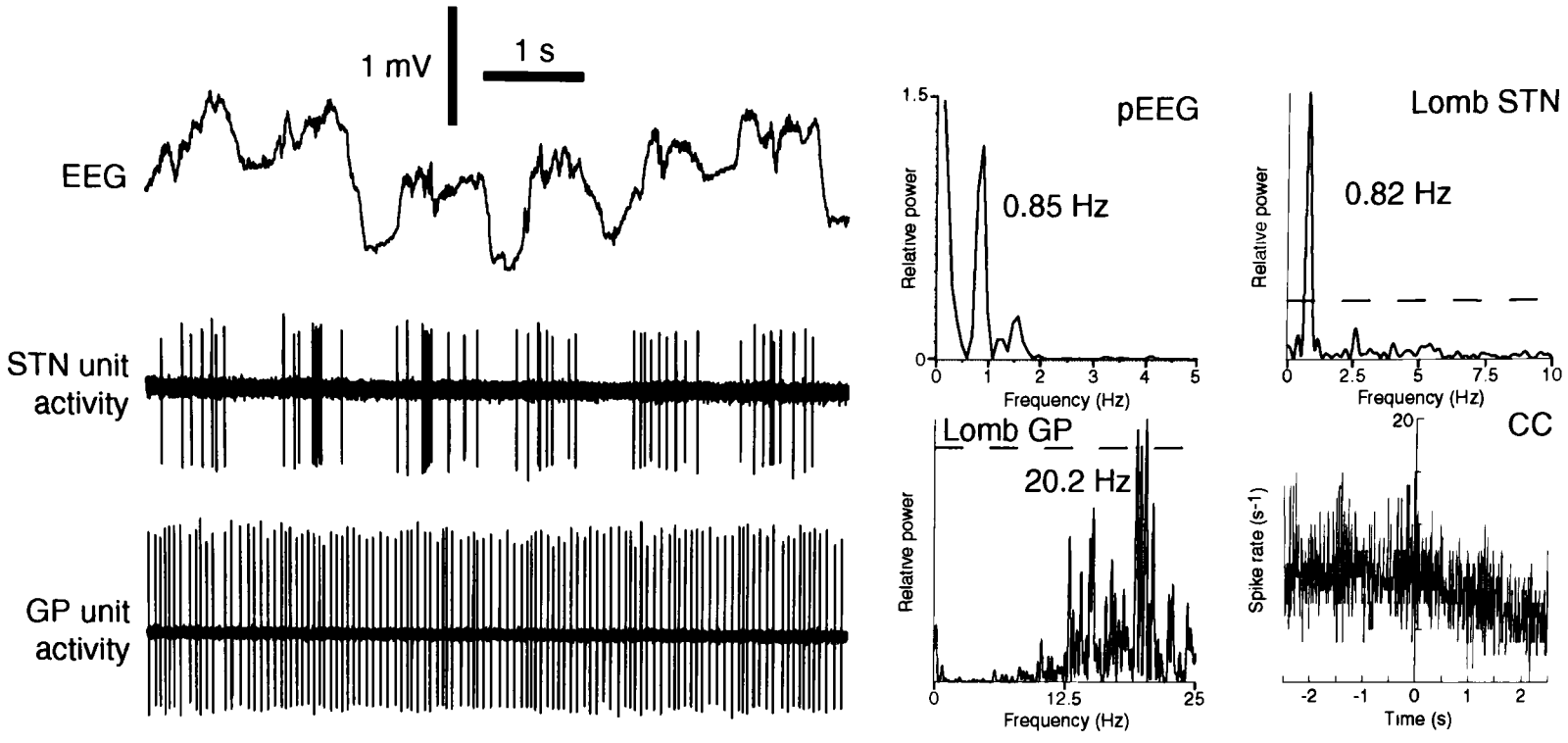
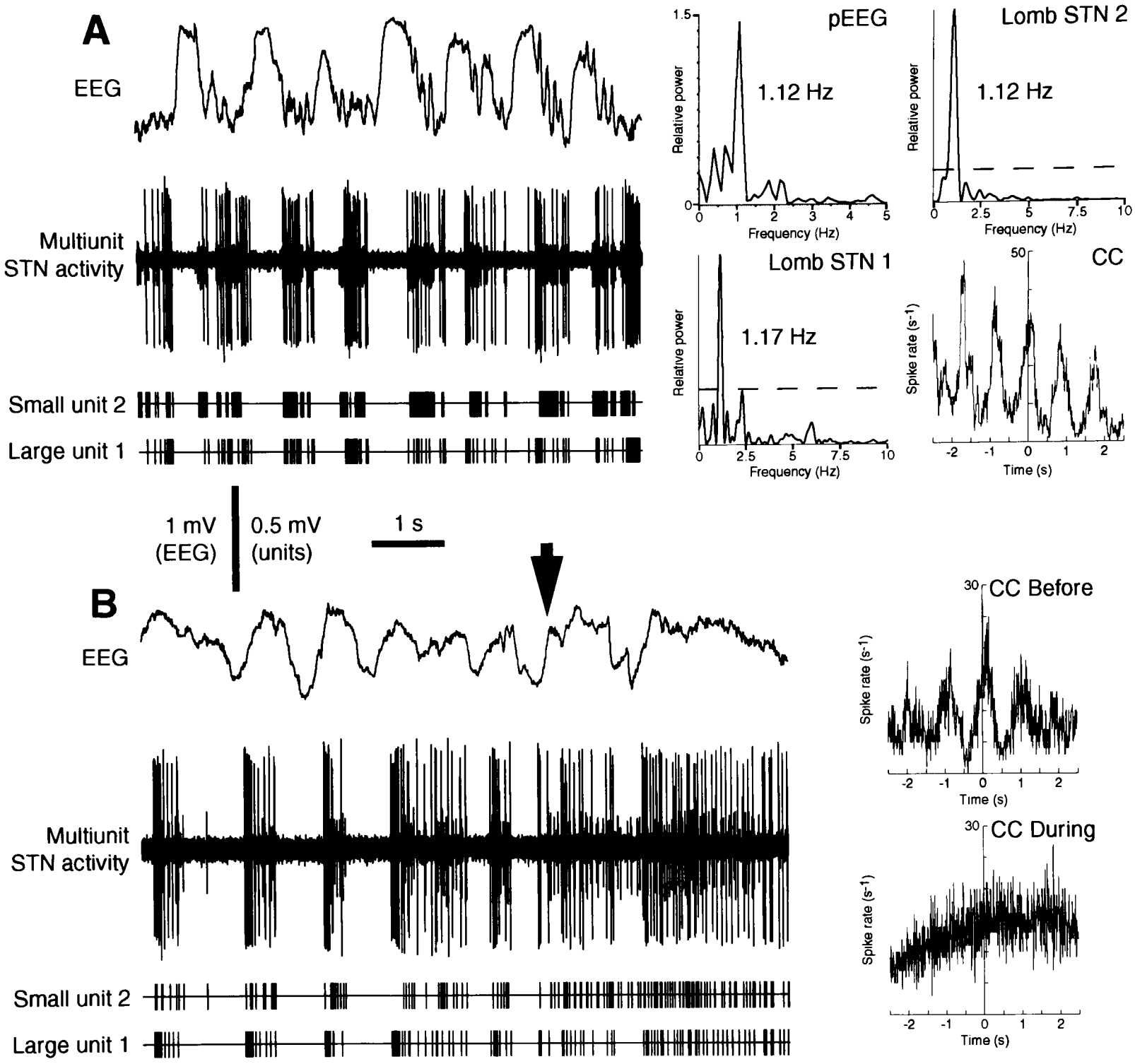

1 mV
1 s
EEG
STN unit activity
GP unit activity
pEEG
0.85 Hz
Relative power
Frequency (Hz)
Lomb STN
0.82 Hz
Lomb GP
20.2 Hz
CC
Spike rate (s-1)
Time (s)

Figure 3.8. Near neighbours in the STN exhibit synchronous, phase-locked firing during robust SWA. *A*, Multiunit recording from a single electrode during ketamine anaesthesia demonstrated that the firing of STN neurons in close proximity was tightly correlated. This pair of neurons (CVs of 1.80 and 3.03 for larger and smaller unit, respectively) showed a small phase lag of ~ 30 ms (12°). Bottom two traces are spike-triggered digital-pulse trains dissected from the unit recordings and show more clearly the individual patterns of spike-firing of the two neurons. *B*, Multiunit recordings of near synchronous firing of neighbouring STN neurons during urethane anaesthesia (phase difference of ~ 60 ms (19°); both units had a CV of 1.58). Disruption of the robust SWA by pinching (*arrow*) was associated with transitions to irregular single-spike firing by the two neurons and a loss of correlated activity. Calibration bars apply to both panels.

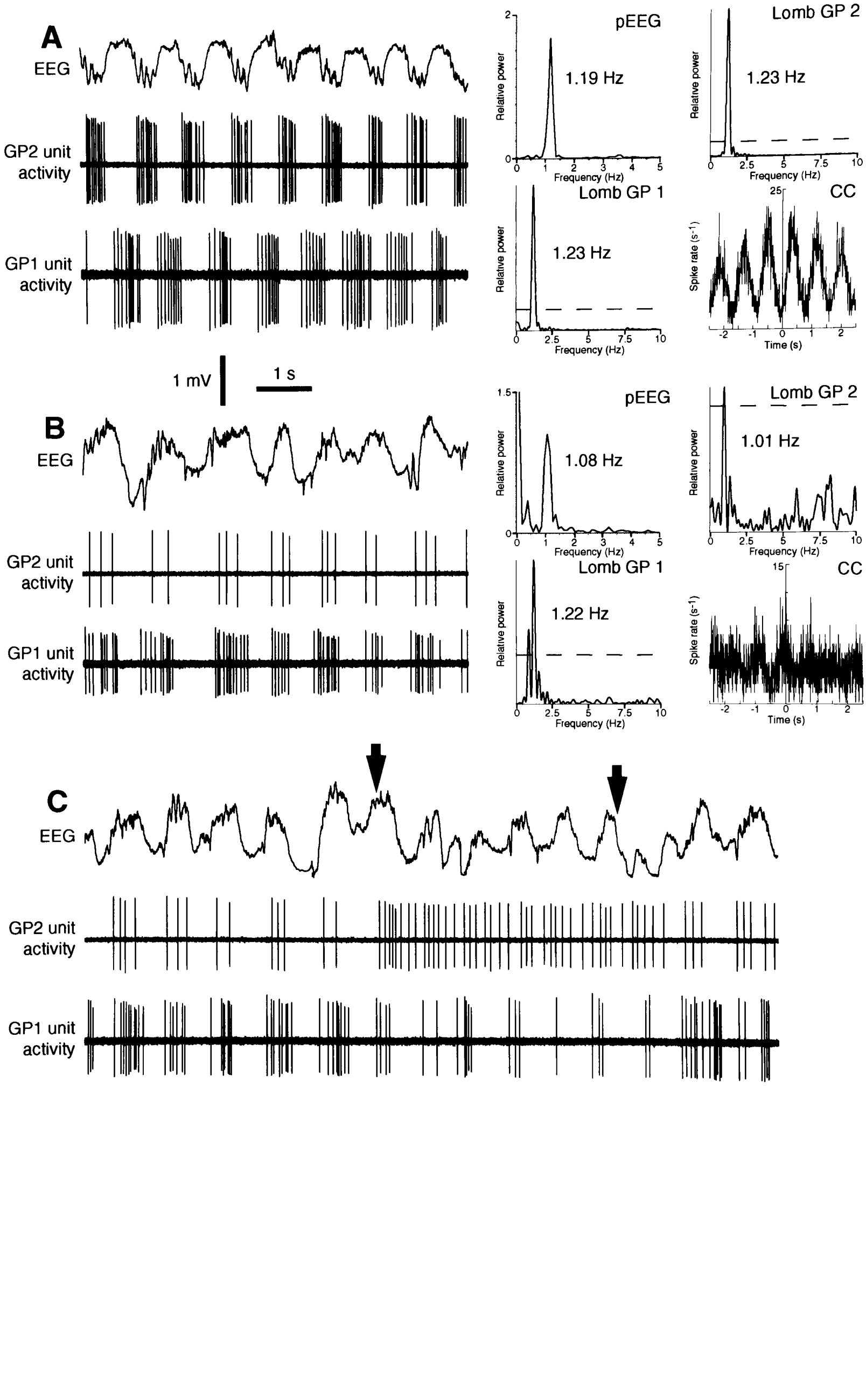

A
EEG
Multiunit
STN activity
Small unit 2
Large unit 1
1 mV
(EEG)
0.5 mV
(units)
1 s
B
EEG
Multiunit
STN activity
Small unit 2
Large unit 1
pEEG
1.12 Hz
Relative power
Frequency (Hz)
Lomb STN 2
1.12 Hz
Relative power
Frequency (Hz)
Lomb STN 1
1.17 Hz
Relative power
Frequency (Hz)
CC
Spike rate (s-1)
Time (s)
CC Before
Spike rate (s-1)
Time (s)
CC During
Spike rate (s-1)
Time (s)

difference in the frequency of oscillatory firing between paired neurons (mean difference of 0.10 ± 0.03 Hz for the four pairs). However, the phase relationships of firing in pairs were inconsistent, falling in the range of 5-65 ms (approximately 1°-13° phase shift; Table 3.3). Broad, symmetrical peaks spanning hundreds of milliseconds in the cross-correlograms of neighbouring STN neurons suggests that correlated firing was a possible consequence of input synchrony (Fig. 3.8*A*, *B*; see also Ryan et al., 1992 and Wichmann et al., 1994). Correlated firing on the low millisecond time scale was not observed. A loss of SWA during pinching was associated with a suppression of correlated firing (Fig. 3.8*B*). These results suggest that local synchrony in the STN is directly or indirectly dependent on synchronous rhythmic input descending from the cortex to the basal ganglia.

3.3.7 Simultaneously-recorded pairs of GP neurons

To elucidate the potential contribution of the GP to the varied phase relationships seen in the STN-GP network, single unit recordings were made from pairs of electrodes in the GP during ketamine anaesthesia. In good agreement with single electrode recordings, spike discharge was intimately related to the coincident SWA (Fig. 3.9). Indeed, the frequencies of the slow oscillation present in the spike trains of six pairs of GP neurons (1.23 ± 0.19 Hz) and the cortex (1.19 ± 0.14 Hz) were very similar. The oscillatory discharge of pairs of GP cells was tightly coupled (mean difference in the frequency of simultaneously-recorded LFO activity of 0.07 ± 0.09 Hz for the six pairs), but burst-like firing was phase-locked to the active or inactive components of the SWA (Fig. 3.9*A*). Thus, the phase relationships of firing between pairs of GP neurons were highly variable, with differences in neuronal spike timing of between 50-330 ms (approximately 9°-177° phase shifts; Table 3.3). Correlated firing of pairs of GP neurons was evident as broad peaks in the cross-correlograms; discharge was almost inversely-correlated in four pairs (Fig. 3.9*A*) and tended towards synchrony in two pairs (Fig. 3.9*B*).

Figure 3.9. Simultaneous recordings of pairs of GP neurons during ketamine anaesthesia. *A*, Phase-locked LFO activity in a pair of GP neurons. The neurons had an identical frequency of oscillation in their spike trains, which was similar in frequency to the cortical slow oscillation. Unit 1 (CV = 1.20) was anatomically identified as being of the pallidostriatal subtype of GP neuron and predominantly fired during the inactive component of the SWA. Unit 2 (CV = 1.51) did not project to the neostriatum and predominantly fired during the active component. Thus, their firing was inversely-correlated with a phase lag of ~ 400 ms (176°). *B*, The LFO activity of another pair of GP neurons was much more closely synchronised with a phase difference of ~ 60 ms (24°). Unit 1 had a CV of 1.22 and unit 2 had a CV of 0.81. *C*, Heterogeneous response of neurons in *B* to a 5 s hindpaw pinch (between *arrows*): Unit 2 adopted a regular-firing mode with a small increase in firing rate; in contrast, unit 1 maintained a LFO mode, but with a decreased mean firing rate. This diverse response resulted in uncorrelated firing between the two neurons. Calibration bars apply to all panels.


A
EEG
GP2 unit activity
GP1 unit activity
1 mV
1 s
pEEG
1.19 Hz
Relative power
Frequency (Hz)
Lomb GP 2
1.23 Hz
Lomb GP 1
1.23 Hz
CC
Spike rate (s-1)
Time (s)
B
EEG
GP2 unit activity
GP1 unit activity
pEEG
1.08 Hz
Lomb GP 2
1.01 Hz
Lomb GP 1
1.22 Hz
CC
C
EEG
GP2 unit activity
GP1 unit activity

In order to investigate the spatial aspects of network activity in the GP, the separation of pairs of GP neurons along the mediolateral axis was measured. The four inversely-correlated pairs of neurons were separated by approximately 30, 60, 120 and 240 μm. The two pairs that tended to fire synchronously were separated by ~ 300 and 350 μm in the mediolateral axis. Although these data imply that neurons tending towards synchronous firing are more distantly placed and that more closely placed cells are inversely correlated, this sample is not large enough to allow firm conclusions to be made about the possible association between the position and firing relationships of GP neuron pairs.

Attenuation of SWA was associated with a loss of correlated firing (Fig. 3.9*C*). Thus, correlated activity in the GP under ketamine anaesthesia depended on the direct and/or indirect influences of the cortex.

3.4 Discussion

The results of this study demonstrate directly that the spike discharge properties of neurons in the STN-GP network are strictly related to coincidental cortical activity and hence, the sleep-wake cycle. Simultaneous recordings of STN and GP neurons in ketamine anaesthesia revealed that low-frequency oscillatory activity was correlated with ongoing cortical SWA and with each other. Correlated oscillatory activity was lost during cortical activation or depression, implying that rhythmic, synchronous inputs are required for the expression of this activity in the STN-GP network. Paired intranuclear recordings suggest that the continuum of phase relationships between STN and GP neurons is due, in part, to asynchronous activity within each parent nucleus. In contrast to the data obtained during ketamine anaesthesia, the discharge of STN neurons, but not GP neurons, was phase-locked to cortical SWA in urethane anaesthesia.

Rhythmic oscillatory activity of the cerebral cortex is transmitted to the STN-GP network

The EEGs of rats anaesthetised with ketamine were dominated by a slow, rhythmic oscillation with a frequency of approximately 1 Hz that was similar in form to that previously described in naturally sleeping or anaesthetised rats, cats and humans (Steriade et al., 1993c; Achermann and Borbély, 1997; Amzica and Steriade, 1998; Steriade and Amzica, 1998; Duque et al., 2000; Urbain et al., 2000). In accordance with previous observations, this slow oscillation triggered and grouped delta (1-4 Hz) and spindle (7-14 Hz) oscillations (Contreras and Steriade, 1995, 1997a; Amzica and Steriade, 1998; Steriade and Amzica, 1998). During the slow oscillation, neuronal discharge is highly synchronised across large areas of the cortex (Adrian and Matthews, 1934; Amzica and Steriade, 1995; Destexhe et al., 1999) and is associated with rhythmic depolarising (active component) and hyperpolarising (inactive component) shifts in the membrane potential of principal neurons (Contreras and Steriade, 1995, 1997a). Since corticosubthalamic neurons are likely to be entrained during SWA (Evarts, 1964; Féger et al., 1994; Stern et al., 1997) and brief electrical stimulation of the cortex drives burst-firing in subthalamic neurons (Kitai and Deniau, 1981; Rouzaire-Dubois and Scarnati, 1985; Fujimoto and Kita, 1993), it is likely that rhythmic cortical activity is transmitted directly to the STN. Indeed, the data indicate that diverse oscillatory cortical activity may be simultaneously and faithfully represented in the spike trains of subthalamic neurons. Thus, STN neurons fired large burst-like discharges of spikes (of several hundred milliseconds duration) during the active components with a periodicity that closely matched the coincident cortical slow oscillation. Furthermore, these large, burst-like discharges were occasionally sub-divided into miniature bursts of activity (less than 100 ms duration), the frequency of which was similar to the frequency of coincident faster activity (*i.e.* spindle-like events) in the EEG.

Slow and spindle oscillatory frequencies of the EEG were also reflected in the spike trains of GP neurons. The major routes of transmission of cortical information to the GP are via indirect pathways involving the STN and the NS (for review see Smith et al., 1998). It seems unlikely that the direct corticopallidal pathway (Naito and Kita, 1994b; Lévesque et al., 1996; Lévesque and Parent, 1998) contributes substantially to oscillatory activity in the GP as it has been demonstrated that it is the STN that mediates the fast excitatory responses of GP neurons to brief electrical stimulation of the cortex (Nambu et al., 1990; Ryan and Clark, 1991; Kita, 1992; Yoshida et al., 1993; Maurice et al., 1998a; Nambu et al., 2000). Thus, the oscillatory firing of GP neurons observed in this and other studies is probably a consequence of periodic excitation of the STN and subsequent feed-forward input to the GP (Morison and Bassett, 1945; Buchwald et al., 1961; Détári et al., 1987; Buzsáki, 1991; Ryan and Sanders, 1993; Nuñez, 1996; Ruskin et al., 1999). Further evidence for this is provided by simultaneous recordings of GP and STN units during SWA, which demonstrated that oscillations in the spike trains of neurons in the two nuclei possessed very similar frequencies. In contrast to STN neurons however, the burst-like firing of GP neurons was sometimes phase-locked to inactive components of the slow-wave. Complex responses like this are difficult to interpret because of the possible involvement of trans-striatal and trans-thalamic routes of cortical information flow in shaping oscillatory activity in the STN-GP network (Ryan and Clark, 1992; Ryan et al., 1992; Maurice et al., 1998a). Indeed, the activity of striatal and thalamic inputs may also be phase-locked to cortical SWA (Steriade et al., 1990, 1993b; Cowan and Wilson, 1994; Stern et al., 1997,1998).

In accordance with studies in other species, the frequency of the slow cortical oscillation was significantly slower during urethane anaesthesia than during ketamine anaesthesia and STN neurons discharged in bursts of less intensity (Steriade et al., 1993c). Nevertheless, LFO activity was again tightly correlated with the coincident slow cortical oscillation. In contrast, all GP neurons adopted a regular firing pattern, which was unrelated

to cortical SWA. A possible explanation for this is that the weaker STN activity under this anaesthetic regime is insufficient to relay the slow cortical oscillation to the GP and drive LFO activity. Indeed, simultaneous recordings of STN and GP neurons showed that weaker burst-like firing of STN neurons was coincident with the regular activity of GP neurons. Although the pairs may not have been recorded in connected regions of the network, this observation challenges the view that the STN is a driving force of neuronal activity in the basal ganglia in resting animals and is not in keeping with the widely-held direct/indirect pathway model, which predicts that activity should be correlated across the network (Albin et al., 1989b; DeLong, 1990). Furthermore, the independent, highly-regular discharge of GP neurons in this preparation implies that intrinsic pacemaker properties, which have been observed *in vitro* (Nambu and Llinás, 1994; Stanford and Cooper, 1999; Cooper and Stanford, 2000), may also underlie the discharge of GP neurons *in vivo*. One additional inference that can be made from paired STN-GP recordings in urethane anaesthesia is that rhythmic activity in the corticosubthalamic pathway, rather than activity in the indirect pathway, underlies oscillatory activity in the STN because cortical SWA had little effect on the firing patterns of GP neurons.

Activity of the STN-GP network is related to the sleep-wake cycle

The amplitude of the EEG is closely related to the spatial and temporal coherence of activity in cortical and thalamic neuronal networks (Contreras and Steriade, 1997a, b). Spontaneous decreases in the amplitude of SWA are the result of reductions in the synchrony of cortical principal cell firing and arise from fluctuations in the depth of anaesthesia or sleep-wake state (Contreras and Steriade, 1997b). Changes of this nature in the cortex were always reflected in the activity of the STN-GP network. Moreover, sensory stimulation by hindpaw pinch resulted in a similar disruption of rhythmic activity in the STN-GP network. The effects of paw pinch on the EEG were similar to those that have been reported following

electrical stimulation of the midbrain reticular activating system (Moruzzi and Magoun, 1949), which suppresses the periods of hyperpolarization associated with the slow oscillation and leads to increased cortical activity and a reduction in long-range cortical synchrony (Steriade et al., 1993a). Thus, the increase in GP neuronal activity during pinch may have resulted from increased cortical drive that was relayed to the GP by the STN (Ryan and Clark, 1991; Ryan and Sanders, 1993). This is in agreement with previous studies that have reported increased GP activity during the transition from sleep to waking (Détári and Vanderwolf, 1987; Détári et al., 1987; Nuñez, 1996; Chernyshev and Weinberger, 1998; Duque et al., 2000). The changes in firing pattern and rate during the paw pinch may also have been driven by the intralaminar thalamic nuclei. These nuclei are major targets of the midbrain reticular activating system (Steriade et al., 1990), send excitatory projections to the STN-GP network (Kincaid et al., 1991b; Mouroux and Féger, 1993; Bevan et al., 1995; Mouroux et al., 1995, 1997; Deschênes et al., 1996) and increase their activity during noxious somatosensory stimuli (Peschanski et al., 1981; Yen et al., 1989; Dafny et al., 1990). Monosynaptic inputs to the STN-GP network from the DRN (Mori et al., 1985; Canteras et al., 1990; Flores et al., 1995), MTg (Hammond et al., 1983; Bevan and Bolam, 1995) and/or SNpc (Lindvall and Björklund, 1979; Schultz and Romo, 1987; Flores et al., 1993; Hassani et al., 1997) may also shape activity in the STN-GP network during global activation. Taken together, these data illustrate that, at least in this preparation, activity in the STN-GP network is intimately related to the state of activity in the cortex, and hence the sleep-wake cycle, and that LFO unit activity is dependent on coincident cortical oscillations.

Temporal and spatial relationships of STN-GP network activity

Rhythmic neuronal activity in the STN-GP network was correlated during SWA, with a similar periodicity to the slow oscillation in the cortex during ketamine anaesthesia. However, the phase relationships of firing of neurons within the STN or GP and between the

nuclei were variable. The phase-differences of intranuclear GP recordings were greater than those from within the STN. The intranuclear recordings from the STN and GP are incongruous with observations made in the cortex and the NS during SWA, in which it has been shown that activity is relatively synchronous across wide areas (Buzsáki et al., 1988; Amzica and Steriade, 1995; Contreras and Steriade, 1997a; Stern et al., 1997, 1998; Destexhe et al., 1999). It is likely that the disparate phase relationships within the STN and GP contributed to the variable phase relationships between the nuclei. These phase differences might also be generated within the STN-GP network by open and closed subthalamopallidal loops (Smith et al., 1990; Ryan and Clark, 1991; Shink et al., 1996; Bevan et al., 1997; Joel and Winer, 1997) and/or by local intranuclear connectivity (Kita et al., 1983a; Kita and Kitai, 1994; Bevan et al., 1998; Huntsman et al., 1999; Stanford and Cooper, 1999; Ogura and Kita, 2000). Even when pairs of neurons displayed synchronous LFO activity, correlations on the low millisecond time scale, which might indicate shared synaptic input or monosynaptic relationships (Perkel et al., 1967b; Abeles, 1982), were not observed (see also Bergman and DeLong, 1989; Ryan et al., 1992; Wichmann et al., 1994). During SWA, cortical regions may oscillate with small phase lags (Buzsáki et al., 1988; Contreras and Steriade, 1995). Lags in cortical afferent activity are, therefore, also likely to contribute to the continuum of phase relationships seen in the network. Taken together, these data indicate that the firing pattern and periodicity of STN and GP neurons is dependent on coincident cortical activity, but the phase-relationship of activities in these structures may be regulated in a complex manner in space by a pattern of connectivity that ensures a low degree of input-sharing.

The cortex is an important pattern generator of the STN-GP network

The effective removal of cortical influence on the STN-GP network by spreading depression caused an immediate loss of LFO activity and a reduction in firing rates. Low-frequency,

oscillatory activity only resumed after recovery of SWA. Thus, the STN-GP network did not support oscillatory activity after the removal of oscillatory cortical input. This finding is in contrast to the thalamus, which contains similar ensembles of reciprocally-connected excitatory and inhibitory neurons that can generate and sustain spindle oscillations in the absence of cortical influence (Morison and Bassett, 1945; Contreras et al., 1996, 1997; McCormick and Bal, 1997). It is thus likely that the cortex is primarily responsible for spindle-related bursting in the STN-GP network because, if thalamic inputs were dominant, then the bursting would be evident even when the cortex was inactivated.

Functional considerations

Recent EEG studies have suggested a role for low-frequency oscillations (< 3Hz) in the preparation and execution of motor commands (Gevins et al., 1989; Bringmann, 1995; McAuley et al., 1999; Feige et al., 2000). The function of low-frequency oscillatory activity in cortical-basal ganglia-thalamocortical loops during sleep is unknown, but it may help to consolidate motor programs established during wakefulness (Steriade, 1999). The shift in the activity of the STN-GP network during the transition from sleep to waking is similar to that reported in other forebrain regions and is likely to reflect more efficient information processing (Détári and Vanderwolf, 1987; Buzsáki et al., 1988; Steriade et al., 1990, 1993a; Nuñez, 1996). The failure of the STN-GP network to support low-frequency oscillations when isolated from the cortex suggests that pathological oscillatory activity observed in this network and its' targets in Parkinson's disease are derived from aberrant, rhythmic activity of corticofugal systems. However, the possibility that the STN-GP network itself can develop rhythmogenic activity when dopaminergic tone is reduced cannot be excluded (Hassani et al., 1996; Kreiss et al., 1997; Plenz and Kitai, 1999; Bergman et al., 1998; Rodriguez et al., 1998; Magariños-Ascone et al., 2000; Raz et al., 2000). Nevertheless, any emergent

oscillatory activity in the STN-GP network is still likely to be influenced by descending cortical input (Contreras and Steriade, 1997a; Contreras et al., 1996, 1997).

The role of dopamine in modulating the relationship of activity in the STN-GP network to activity in the cortex is addressed in Chapter 4.

CHAPTER 4.

RELATIONSHIP OF ACTIVITY IN THE DOPAMINE-DEPLETED SUBTHALAMIC NUCLEUS – GLOBUS PALLIDUS NETWORK TO ACTIVITY IN THE CEREBRAL CORTEX *IN VIVO*.

4.1 Introduction

Normal information processing within the STN-GP network is characterised by complex spatiotemporal patterns of activity (Georgopoulos et al., 1983; DeLong et al., 1985; Nambu et al., 1990; Aldridge and Gilman, 1991; Anderson and Turner, 1991; Bergman et al., 1994; Cheruel et al., 1994, 1996; Wichmann et al., 1994a; Jaeger et al., 1995). Alterations in the rate and/or pattern of activity in the STN-GP network have been reported in idiopathic and animal models of PD (Filion, 1979; Filion et al., 1988; Pan and Walters, 1988; Filion and Tremblay, 1991; Hollerman and Grace, 1992; Bergman et al., 1994, 1998; Rothblat and Schneider, 1995; Hassani et al., 1996; Kreiss et al., 1997; Boraud et al., 1998, 2000b; Levy et al., 2000; Magnin et al., 2000; Raz et al., 2000; Vila et al., 2000). Abnormal overactivity of the indirect pathway is believed to underlie pathological increases in the firing rate of STN neurons and GABAergic output neurons (Albin et al., 1989b; DeLong, 1990). The resultant excessive inhibition of basal ganglia targets has been suggested to underlie the symptoms of PD (Albin et al., 1989b; DeLong, 1990). It has been proposed more recently that changes in the firing pattern of neurons in the STN-GP network, with or without changes in their overall firing rates, are also of importance (Chesselet and Delfs, 1996; Wichmann and DeLong, 1996; Levy et al., 1997; Bergman et al., 1998; Obeso et al., 2000b; Raz et al., 2000). Indeed, STN and GP neurons display more synchronous, bursting patterns of activity, which may be a reflection of emergent, oscillatory activity within the network (Bergman et al., 1994, 1998; Nini et al., 1995; Raz et al., 2000). Pathological oscillatory activity in the STN-GP network is associated with resting tremor and may also contribute to other symptoms of PD (Benazzouz et al., 1993; Bergman et al., 1994; Chesselet and Delfs, 1996; Limousin et al., 1995; Nini et al., 1995; Volkmann et al., 1996; Wichmann and DeLong, 1996; Levy et al., 1997, 2000; Krack et al., 1998; Rodriguez et al., 1998; Magariños-Ascone et al., 2000; Magnin et al., 2000, Obeso et al., 2000b; Raz et al., 2000).

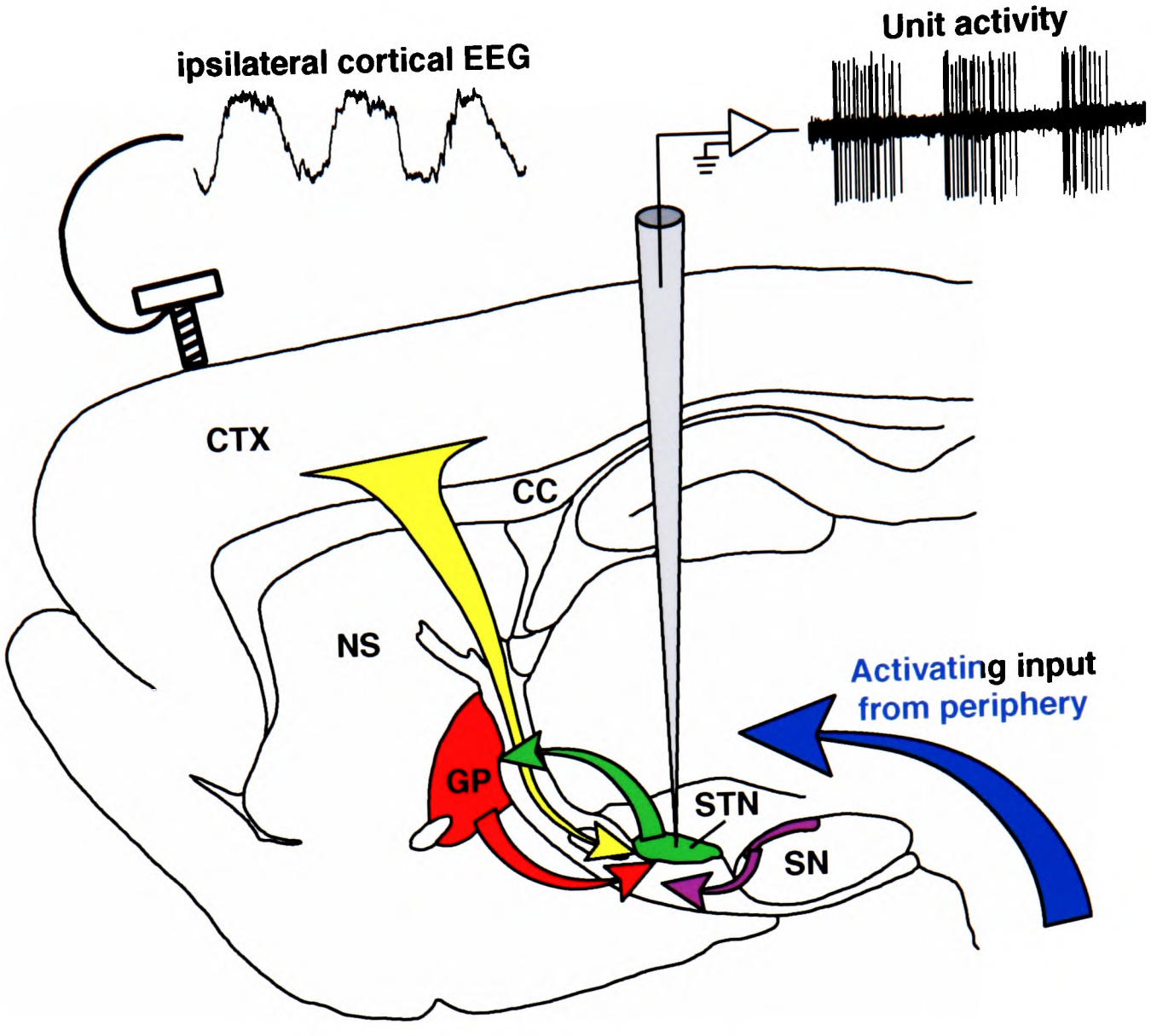
The overall objective of this study was to further characterise activity in the STN-GP network in relation to cortical activity in the normal and dopamine-depleted brain. As discussed in Chapter 3, anaesthetised rats were utilised in this study because the STN-GP network may be easily studied in the context of global activity, as determined from the EEG. Urethane anaesthesia was used exclusively because STN-GP network activity under this anaesthetic regimen closely resembles that observed in the unanaesthetised preparation (see Chapter 3; Pan and Walters, 1988; Urbain et al., 2000).

As detailed in Chapter 3, low-frequency oscillations in the STN-GP network are abolished by transient cortical inactivation. In contrast, in organotypic co-cultures, oscillatory activity in the STN-GP network persists when cortical input is physically removed, leading to the proposal that this network acts as a pattern generator of physiological and pathophysiological activity in the basal ganglia (Plenz and Kitai, 1999). Furthermore, neurons in the isolated STN *in vitro* can fire spontaneously in a rhythmic, bursting manner (Beurrier et al., 1999). To test the hypothesis that oscillatory activity in the STN-GP network in anaesthetised rats requires an intact cortical input, single unit activity in this network was recorded before and after ipsilateral cortical ablation (Fig. 4.1). The results from the previous study suggest that the corticosubthalamic projection may directly drive LFO activity in the STN during urethane anaesthesia (see section 3.3.5). Thus, this experimental paradigm is particularly useful for elucidating the functions of this enigmatic projection.

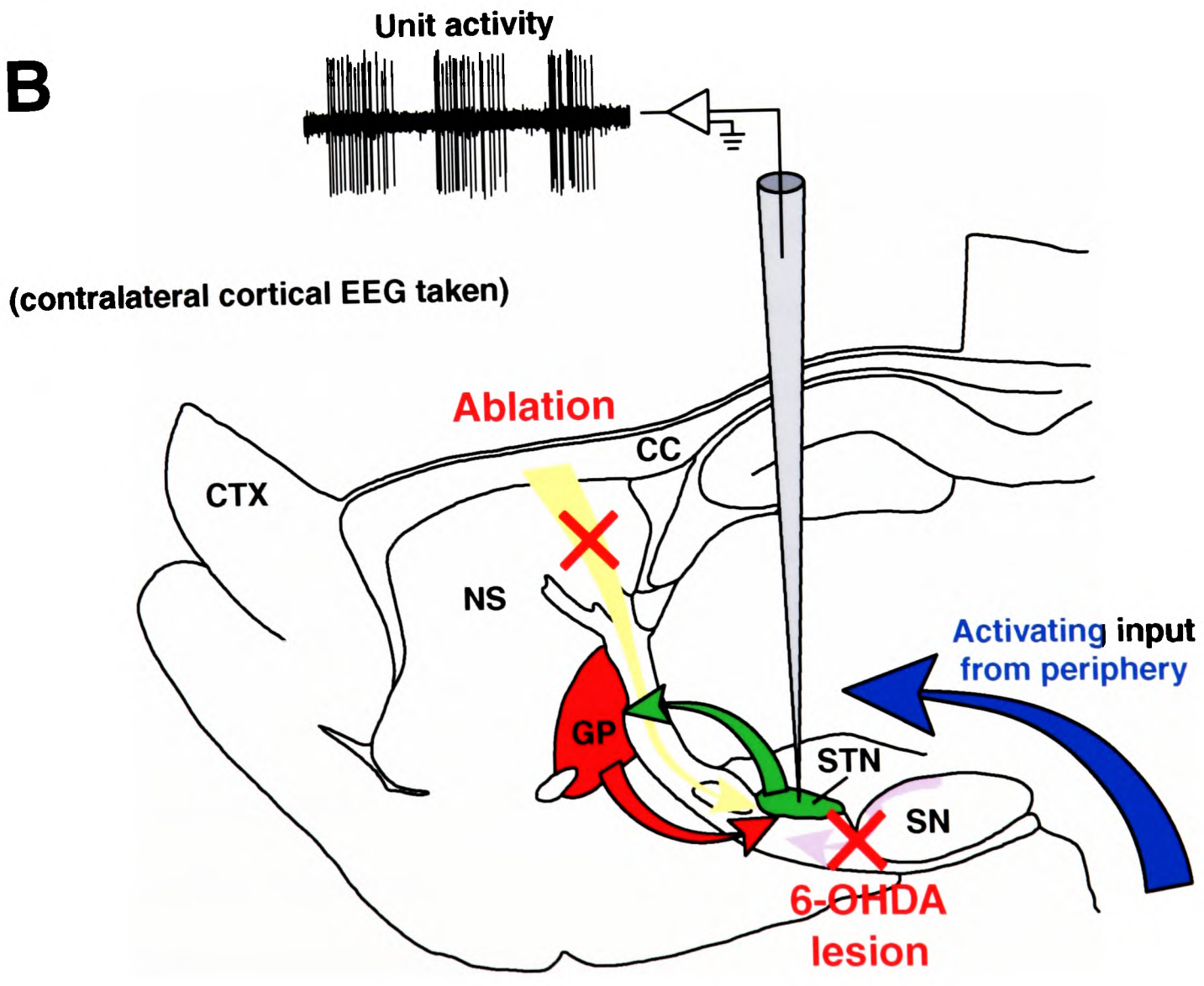
One explanation for the discrepancy between observations *in vivo* and in culture is that the absence of dopamine in the cultures perturbs the dynamics of the STN-GP network, permitting oscillatory activity to arise independently of the cortex. To test this hypothesis, activity in the STN-GP network in normal and unilateral 6-OHDA-lesioned animals (Ungerstedt, 1968; see section 2.2) was recorded in the presence or absence of cortical influence (Fig. 4.1).

Figure 4.1. Experimental design and set-up. Panels shows parasagittal sections of the rat brain at the level of the basal ganglia (adapted from section 2.4 mm lateral of Paxinos and Watson, 1986). *A*, As reported in Chapter 3, activity in the normal subthalamic nucleus (STN; *green*) and globus pallidus (GP; *red*) is dependent on activity in the cortex. This strict relationship is supported, at least in part, by cortical input via the direct corticosubthalamic projection (*yellow*). Furthermore, it is highly likely that dopaminergic projections from the substantia nigra (SN; *purple*) modify activity in the STN-GP network. Experiments were carried out to characterise activity within the STN-GP network in the presence (*A*) or absence (*B*) of inputs from the cortex and/or SN. Activity in the STN or GP was assessed from extracellular unit recordings in anaesthetised animals. Cortical activity was simultaneously determined from the frontal electroencephalogram (EEG). *B*, Dopaminergic projection neurons in the SN were destroyed (*pale purple*) by injection of 6-hydroxydopamine (6-OHDA lesion). Corticosubthalamic input was removed (*pale yellow*) by ablation of ipsilateral frontal and parietal cortices. The effects of forebrain activation by input from the periphery (*blue arrow*) were studied in each paradigm. CC, corpus callosum; CTX; cortex; NS, neostriatum. Rostral is to the *left* and dorsal is to the *top* of each panel.

A


Unit activity
ipsilateral cortical EEG
CTX
CC
NS
GP
STN
SN
Activating input
from periphery

B


Unit activity
(contralateral cortical EEG taken)
Ablation
CTX
CC
NS
GP
STN
SN
Activating input
from periphery
6-OHDA
lesion

The symptoms of PD vary according to states of arousal *e.g.* parkinsonian tremor is associated with quiet wakefulness but disappears during sleep and movement (see review by Elble and Koller, 1990; Rodriguez et al., 1998; Magariños-Ascone et al., 2000). Therefore, oscillatory activity in the STN-GP network may emerge only during certain states of global activity. To test this hypothesis, activity in the STN-GP network in normal and 6-OHDA-lesioned animals during extremes of global activation was compared, in the presence and absence of cortical influence (Fig. 4.1).

4.2 Experimental procedures

4.2.1 Electrophysiological recording and labelling of neurons in the normal and dopamine-depleted STN-GP network of anaesthetised rats.

Animals were rendered hemi-parkinsonian by unilateral 6-OHDA lesion of midbrain dopamine neurons as detailed in section 2.2. Animals with intact dopaminergic systems are hereafter referred to as "control" animals.

Electrophysiological recordings were made in 13 male Sprague-Dawley rats (280-510 g), 6 of which had received successful 6-OHDA lesions. Recordings were made in 6-OHDA-lesioned animals 7 to 25 days after behavioural testing with apomorphine. Anaesthesia was induced with isoflurane and maintained with urethane (1.25 gkg^{-1}, i.p.), and supplemental doses of ketamine and xylazine (30 $mgkg^{-1}$ and 3 $mgkg^{-1}$, i.p., respectively). Thus, all animals in this study shall be referred to as being "urethane" anaesthetised.

The EEG was recorded from the ipsilateral frontal cortex before ablation and from the contralateral frontal cortex after ablation (3.0 mm anterior of bregma and 2.0 or 4.0 mm lateral to the midline, respectively). Contralateral EEG was recorded from a more medial position to avoid the path of the callosal transection (see section 4.2.2).

To identify the location of recorded units following physiological characterisation with extracellular electrodes, neurons were selectively labelled with Neurobiotin™ by the juxtacellular method (Pinault, 1994, 1996).

Detailed descriptions of the procedures for simultaneous recording of the EEG and unit activity, juxtalabelling, perfusion fixation, histochemical and immunocytochemical verification of recording sites and lesions, and data analysis are described in sections 2.1, 2.1, 2.1, 2.3 and 2.4, respectively.

4.2.2 Transection of the corpus callosum

Introduction

The popularity of the unilateral 6-OHDA lesion model of PD is due, in part, to the common conception that this paradigm includes a convenient internal control *i.e.* the unlesioned, contralateral hemisphere. However, it has long been known that the flow of information through the basal ganglia is subject to interhemispheric regulation (Nieoullon et al., 1977, 1979). Furthermore, cross-talk between the two hemispheres still occurs after unilateral lesion of nigrofugal pathways, leading to lesion-induced alterations in the contralateral basal ganglia (see Lawler et al., 1995 and references therein). Indeed, it has recently been established that the activity of the two subthalamic nuclei and the substantia nigrae *pars reticulata* are altered in a reciprocal fashion following a unilateral 6-OHDA lesion (Rohlfs et al., 1997; Perier et al., 2000). It is also known that chronic, contralateral influences on the unlesioned hemisphere can be attenuated by transection of the corpus callosum shortly after the lesion procedure (Lawler et al., 1995). Given that communication between the hemispheres is two-way, it is also likely that the 6-OHDA-lesioned side of the brain is acutely and chronically affected by input from the unlesioned side. Thus, to minimise the acute influences of the unlesioned hemisphere on activity in the dopamine-depleted

hemisphere, at least via crossed corticocortical and corticostriatal projections, the corpus callosum was transected in all animals 1-2 hr before recording commenced.

Procedure

Following a craniotomy (3 x 12 mm), the corpus callosum was transected under stereotaxic control with a razor blade, set at an angle of 30° to vertical, along the length of the left (contralateral) hemisphere; from 5.0 mm anterior of bregma to 6.5 mm posterior of bregma and along a course that ran 2.0 mm lateral to the midline (Paxinos and Watson, 1986). Histological verification of the extent and path of the callosal transection was performed for each animal.

4.2.3 Acute cortical ablation

Introduction

The data reported in Chapter 3 demonstrate that oscillatory activity in the STN-GP network in anaesthetised rats is phase-locked to rhythmic cortical activity and is abolished during episodes of cortical spreading depression. A major advantage of the spreading depression paradigm is that stable unit recordings can be maintained during disruption of cortical activity. Therefore, the effects of cortical inactivation on the STN-GP network can be easily assessed in a direct way by comparing activity during depression to activity before depression. However, one disadvantage of the spreading depression paradigm is that it is transient and it is possible, therefore, that while corticofugal neurons at the front of the depressing wave are being inactivated, neurons well behind the wave-front are recovering from inactivation. As such, simultaneous and full depression of all cortical inputs to the STN-GP network cannot be guaranteed and the inherent variability of the spreading depression paradigm is likely to underlie, at least in part, the inconsistent responses of STN and GP neurons to cortical inactivation (see sections 3.3.3 and 3.3.4, respectively). Physical removal of cortex by ablation has the potential to permanently and completely isolate the

STN-GP network from cortical influences or, at least, allows the investigator to negate the influence of the same area of cortex in different animals. Furthermore, it is possible to confirm the consistency of the ablation by histological means. Thus, the cortical ablation model is a useful adjunct to cortical spreading depression for investigating the role of the cortex in orchestrating activity in the STN-GP network.

Procedure

Cortical ablation procedures were carried out on the day of electrophysiological recording (ablation was typically performed after a small number of units had been isolated and recorded under conditions of an intact cortical input). Following extensive craniotomy, large areas of ipsilateral frontal and parietal cortex (see Fig. 4.2*D*, *E*) were ablated by suction generated by a polished Pasteur pipette connected to a rubber bulb, with minimal disturbance of underlying white matter. The ablative cavity was filled with warm (35-37°C) mineral oil to prevent dehydration. Histological verification of the location and extent of the acute ablation was performed for each animal.

4.2.4 Activation of the forebrain by somatosensory stimulation

Somatosensory stimulation was elicited by pinching the contralateral hindpaw at the level of the palm for 7 s using pneumatically-driven serrated forceps (for further details, see section 3.2.3). For multiple recordings, a long interstimulus interval (> 15 min) was used to allow recovery and minimise augmentation of responses.

4.2.5 Local field potential recordings

Introduction

To investigate further the expression of rhythmic cortical activity in the STN-GP network at the local population level, local field potentials (LFPs) were simultaneously recorded with unit activity using the same extracellular electrode. The LFPs produced by a group of

neurons indirectly reflect the membrane potential changes *i.e.*, the synaptic and action potentials, that the neurons undergo in unison (Hubbard et al., 1969). A study of such potentials gives, therefore, valuable information regarding the gross activity of synaptic terminals and neurons surrounding the tip of the microelectrode.

Procedures

Extracellular electrodes for simultaneous unit and LFP recordings were fabricated as detailed in section 2.1.4 above. However, electrodes with slightly larger tips than usual (1.5-2 μm) were selected because LFPs were most easily registered using electrodes with resistances of < 20 MΩ. Local field potential signals were isolated and amplified (10×) through the active bridge circuitry of an Axoprobe-1A amplifier (Axon) and amplified a further 100× (AC-DC Amp, Digitimer), before being band-pass filtered between 0 (d.c.) and 100 Hz (NL125, Digitimer). Lastly, signals were passed through an input amplifier/DAT interface (EBU/DAT/5s; Department of Pharmacology), collected on tape (60ES DAT system, Sony) for off-line analysis, and displayed simultaneously on a digital oscilloscope (Gould). Analogue tape records of LFPs were digitised off-line on an analogue-to-digital converter (1401plus; Cambridge Electronic Design) and sampled at 200 Hz with Spike2™ acquisition and analysis software (Cambridge Electronic Design). Power spectra and spike-triggered averages of LFPs were calculated using Spike2™ as described for the EEG (section 2.4.3.1). Cross-correlations of LFP and EEG waves were calculated using the waveform correlation function of Spike2™; the results of the correlation function range from values of 1.0 through 0.0 to -1.0 and indicate that the two waves are identical in phase and frequency, uncorrelated, and correlated but phase inverted, respectively.

4.3 Results

4.3.1 Histochemical, immunocytochemical and histological observations

4.3.1.1 Location of recorded neurons

After physiological characterisation, juxtacellular microiontophoresis of Neurobiotin™ led in each case to a single neuron being well labelled (Fig. 4.2*A*, *B*): 46 of 181 recorded neurons were labelled using this technique. The locations of the remainder were determined directly from extracellular deposits of Neurobiotin™ (see Fig. 3.1*C* for example), or inferred from the stereotaxic position of the recorded unit relative to deposits or juxtacellularly-labelled neurons. All regions of the STN and the rostral half of the GP were sampled in control and 6-OHDA-lesioned animals.

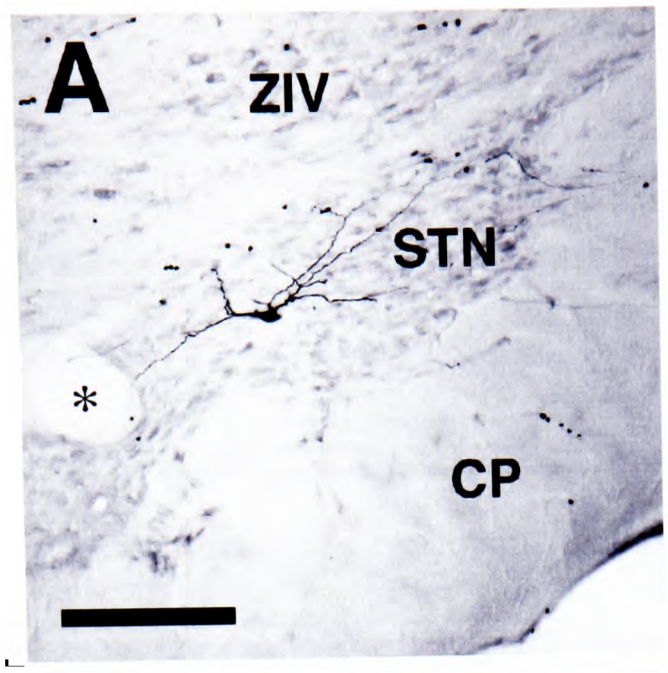
4.3.1.2 Extent of unilateral 6-OHDA lesions

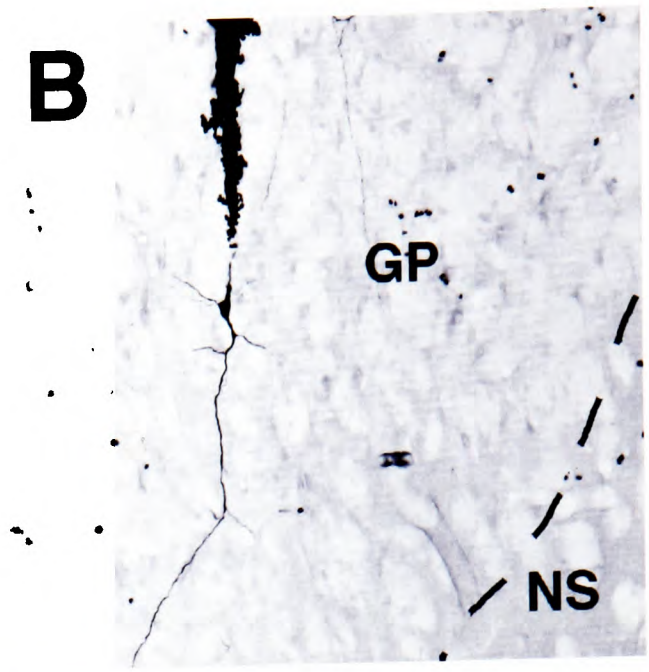
A successful nigral lesion, as inferred from behavioural testing, was confirmed in each animal by a near complete loss of TH-immunoreactive neurons from the substantia nigra of the right hemisphere (Fig. 4.2*C*). The dopaminergic neurons of the ventral tegmental area (VTA) were also affected in all animals, but to differing extents.

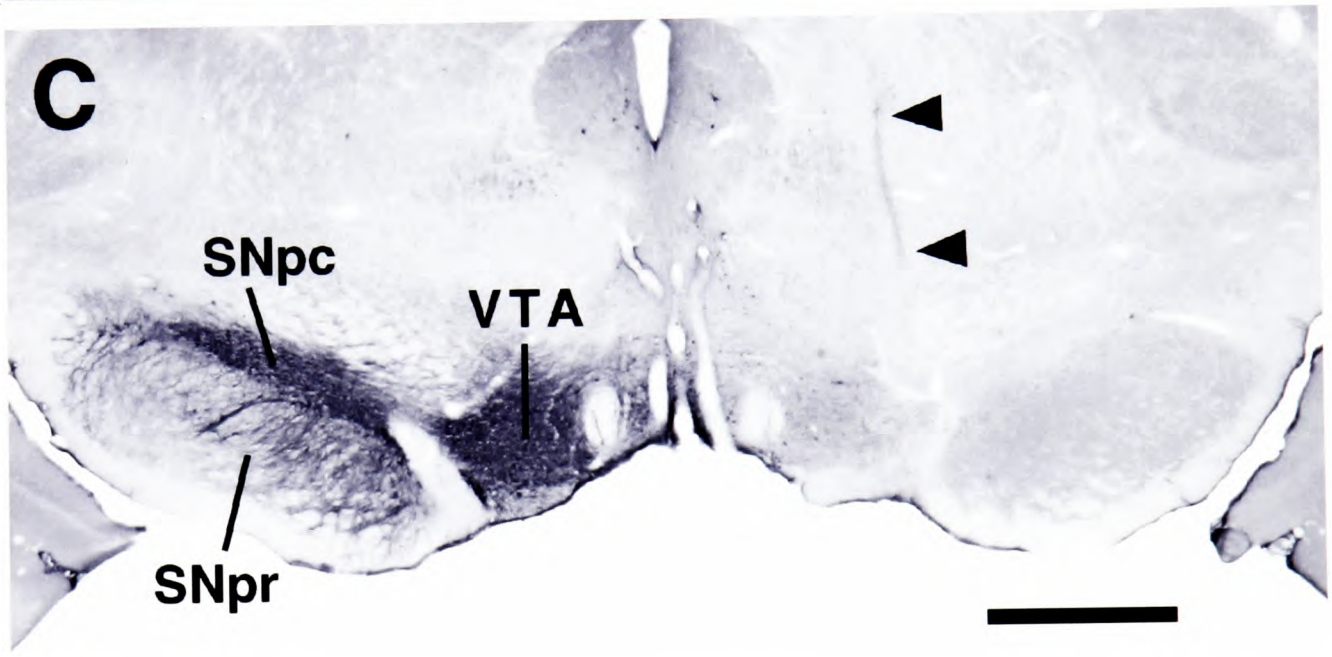
4.3.1.3 Verification of callosal transections and cortical ablations

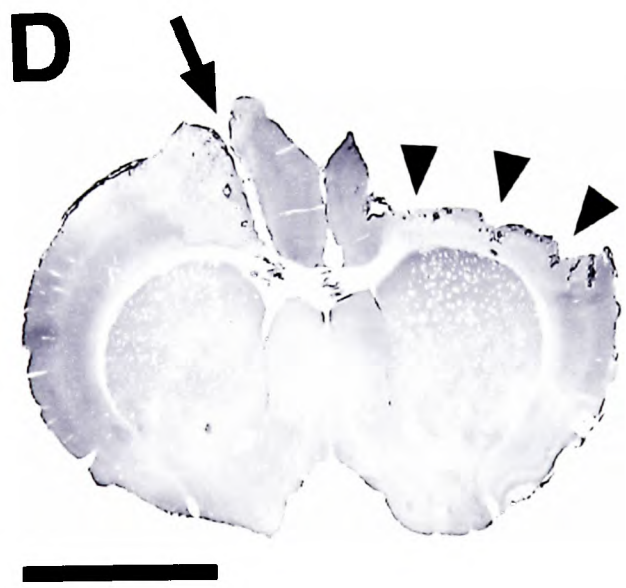
In each animal, the corpus callosum was transected near the midline and along the rostral-caudal extent of the forebrain of the left hemisphere (Fig. 4.2*D*, *E*). Thus, transection largely isolated the recorded hemisphere from the contralateral cortex. Large areas of the right frontal and parietal cortices were also ablated in each animal (Fig. 4.2*D*, *E*). Ablation of neighbouring medial cortical areas (infralimbic, prelimbic, cingulate, retrosplenial) was not attempted due to the proximity of the superior sagittal sinus. Ventral and lateral cortical

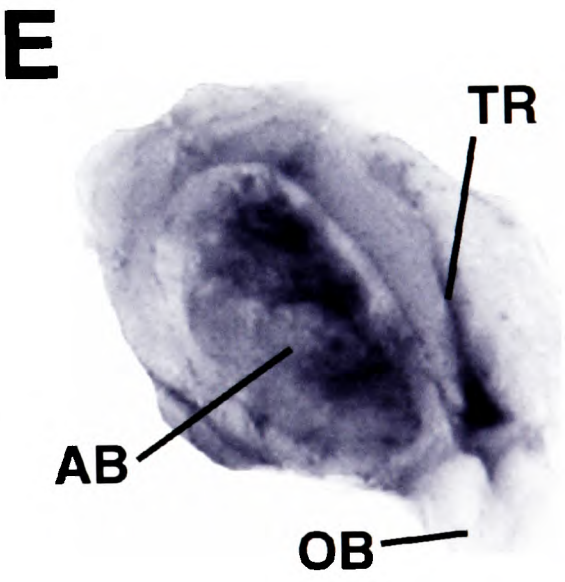
Figure 4.2. Anatomical verification of recording sites, unilateral nigral lesions and surgical manipulations. *A,B,* Light micrographs of STN and GP neurons that were juxtacellularly labelled with Neurobiotin™. *A*, The STN neuron was located near the centre of the nucleus. The STN lies dorsal to the cerebral peduncle (CP) and is characterised by a higher density of neurons compared to the overlying ventral division of the zona incerta (ZIV). A large blood vessel (*) lies on the border between medial STN and ZIV. *B*, The GP neuron was situated near the centre of the rostral half of the GP. Note the track of the electrode above the labelled neuron. The border (*dashed line*) between the GP and the neostriatum (NS) is also indicated. Scale bar in *A* also applies to *B* = 200 μm. *C*, Light micrograph of a coronal section though the midbrain of a 6-OHDA-lesioned rat, which was stained to reveal tyrosine hydroxylase (TH). Intense TH immunoreactivity was observed in the left substantia nigra *pars compacta* (SNpc) and ventral tegmental area (VTA) and lighter labelling was observed in the substantia nigra *pars reticulata* (SNpr). Staining for TH was virtually absent in the right hemisphere. Note also the trajectory of the injection cannula (between *arrowheads*). Scale bar = 1 mm. *D*, Photomicrograph of a coronal section from a transected and ablated control rat, at the level of the NS. The majority of the right frontal and parietal cortices were ablated (*arrowheads*) and the corpus callosum was transected close to the midline in the left hemisphere (*arrow*). Scale bar = 4 mm. *E*, Digital image of a rat brain after callosal transection and cortical ablation. The callosal transection (TR) extended along the length of the left hemisphere. The ablative cavity (AB) encompassed the frontal and parietal cortical areas of the right hemisphere. OB, olfactory bulbs.


A
ZIV
STN
*
CP


B
GP
NS


C
SNpc
VTA
SNpr


D


E
TR
AB
OB

regions (orbital, agranular, insular, piriform, parietal area 2) were also left intact. Thus, cortical ablation removed a large proportion of the cortical afferents to the basal ganglia of the right hemisphere.

The rat STN only receives monosynaptic cortical input from ipsilateral prefrontal, frontal and parietal cortical areas (Afsharpour, 1985b; Canteras, 1990, Fujimoto and Kita, 1993). In contrast, the corticostriatial projection is derived from almost the entire ipsilateral cortical mantle (Gerfen and Wilson, 1996). It follows that whilst the ablative surgery was likely to eliminate the majority of the corticosubthalamic projection, a larger proportion of the corticostriatal projection was probably left intact.

4.3.2 Characterisation of EEG activity

Prevailing cortical activity was assessed from EEG recordings. As described previously (Steriade et al., 1993c; see Chapter 3), surgical anaesthesia was accompanied by regularly-occurring slow-waves of large amplitude (>400 μV) in the frontal EEG (Figs. 4.3 to 4.14). Higher frequency (> 2 Hz) activity, which was of smaller amplitude (<200 μV), was often superimposed on specific portions of the slow-wave (*e.g.* Fig. 4.3). These parts of the slow-wave are associated with synchronous spike discharges in cortical projection neurons and will be referred to as the "active component" (Amzica and Steriade, 1995; Steriade et al., 1996). The frequency range of the smaller amplitude waves varied widely but spindle activity in the range of 7-14 Hz was often observed (Steriade et al., 1993d; McCormick and Bal, 1997). Characterisation of the EEG recordings and the cellular mechanisms underlying EEG phenomena are discussed in greater detail in section 3.3.

4.3.3 Firing properties of STN and GP neurons in control animals before and after cortical ablation

The relationship between activity in the cortex and the STN-GP network was examined by simultaneous recording of the EEG and unit activity during urethane anaesthesia. During periods of robust SWA in the ipsilateral cortex, extracellular unit recordings revealed that STN neurons exhibited low-frequency oscillatory firing patterns (Fig. 4.3*A*, Table 4.1). When the active component of the slow-wave was clearly observed, the discharge of STN neurons was predominantly restricted to this component. Spectral and correlation analyses revealed that the frequency at which these envelopes of activity occurred closely matched the predominant frequency of the coincident slow-wave (Fig. 4.3*A*, Table 4.1). Following cortical ablation, low-frequency oscillatory firing in STN neurons was abolished (Fig. 4.3*B*, *C*, Table 4.1). During periods of robust SWA in the contralateral cortex, STN neurons discharged in an irregular or regular manner throughout the entire cycle of the cortical slow-wave and the activity of STN neurons no longer matched the frequency of the coincident slow oscillation (Fig. 4.3*B*, *C*, Table 4.1). CVs were significantly reduced after ablation. Neurons that discharged in a regular manner displayed a significant peak in the Lomb periodogram at a frequency that matched closely the mean rate of firing (Fig. 4.3*C*, Table 4.1). These data indicate that the pattern and frequency of firing of STN neurons was correlated tightly with coincident activity in the ipsilateral cortex.

All GP neurons exhibited a tonic, regular firing pattern during robust SWA under urethane anaesthesia (Fig. 4.4*A*). The highly regular discharge of GP neurons was confirmed by the observation that the mean peak frequency in Lomb periodograms was not significantly different from mean firing rates (Table 4.2). Neuronal firing rate and pattern were relatively insensitive to minor fluctuations in SWA, such as the occurrence of spindles (Fig. 4.4*A*). Following cortical ablation, GP neurons discharged in a similar, regular manner

Figure 4.3. Neuronal activity in the STN of control rats under urethane anaesthesia is closely related to coincident cortical activity. *A*, Low-frequency oscillatory STN neuron (CV = 0.99; mean rate = 6.0 Hz). The neuron fired predominantly during the active component of the cortical slow-wave; the active component was seen in the ipsilateral cortical EEG trace as periods of superimposition of small-amplitude, high-frequency events on the peaks of the large-amplitude slow-wave. Rhythmic spike-firing was apparent from the broad peaks in the auto-correlogram (AC). Comparison of the Lomb periodogram (Lomb) with the power spectrum of the EEG (pEEG) indicated a similar frequency of rhythmic activity in the STN spike train and cortex. The dashed line in this and subsequent Lomb periodograms denotes a significance level of $p = 0.05$. The phase relationship between spiking and the EEG is shown on the spike-triggered average of EEG waveform (AvWv). *B*, Irregular firing STN neuron (CV = 0.65; mean rate = 5.9 Hz) recorded after ipsilateral cortical ablation. The discharge was not correlated with contralateral cortical EEG and did not display a significant oscillatory component. *C*, Regular firing STN neuron (CV = 0.26; mean rate = 5.0 Hz) recorded after cortical ablation. Activity was not related to coincident SWA. The neuron exhibited a mean firing rate that was similar to the dominant frequency of activity in the Lomb periodogram. Note that the CV values of each neuron reflected the differences in firing pattern observed. Neurons were recorded in the same animal. Calibration bars apply to all left hand panels. In this and subsequent figures, AC designates auto-correlograms of spiking activity (bin size 10 ms), Lomb designates Lomb periodograms of spiking activity, pEEG designates power spectra of the coincident EEG, and AvWv designates spike-triggered averages of EEG.

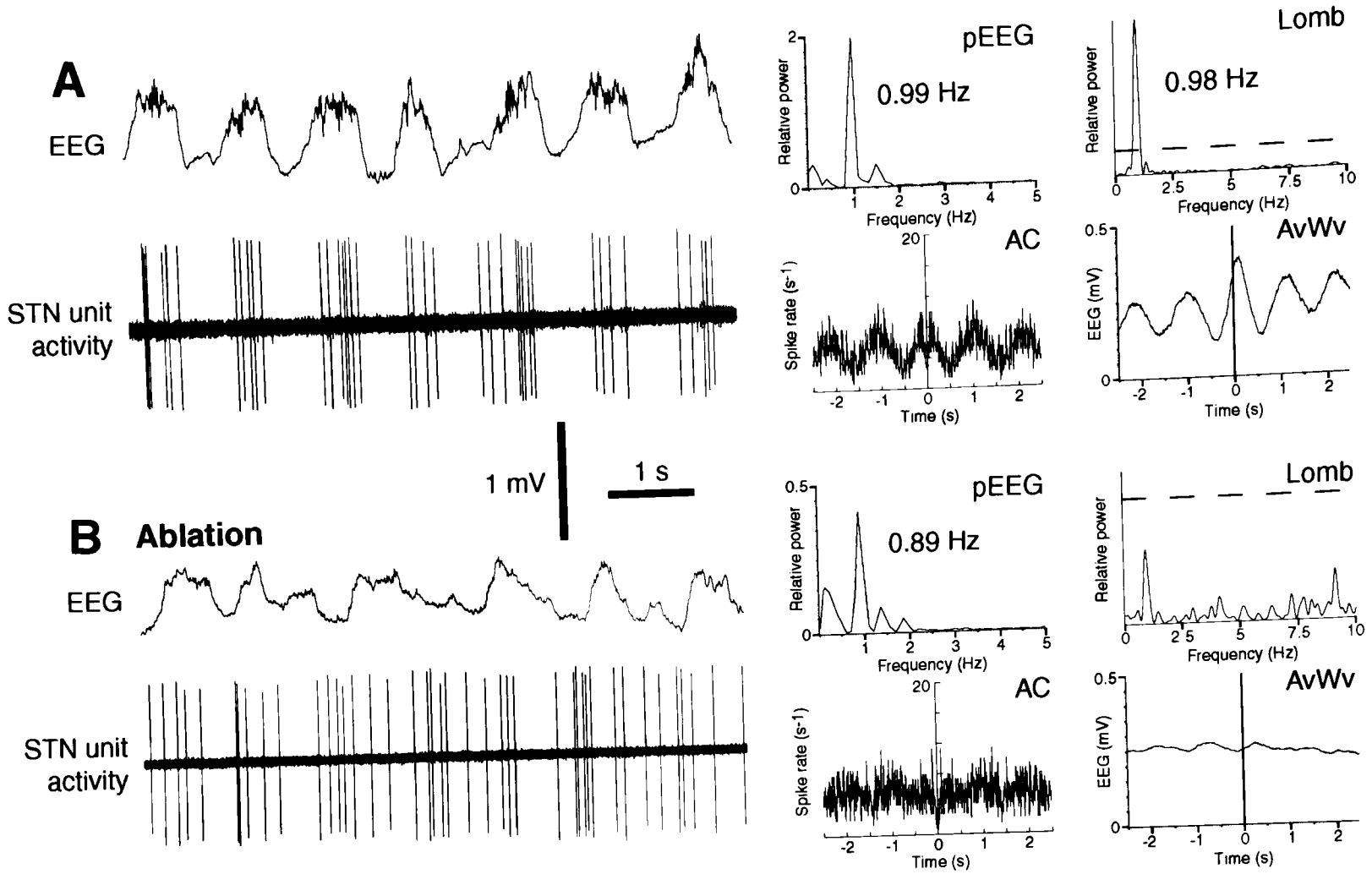

A
EEG
STN unit activity
1 mV
1 s
pEEG
0.99 Hz
Relative power
Frequency (Hz)
Lomb
0.98 Hz
Relative power
Frequency (Hz)
AC
Spike rate (s-1)
Time (s)
AvWv
EEG (mV)
Time (s)
B Ablation
EEG
STN unit activity
pEEG
0.89 Hz
Relative power
Frequency (Hz)
Lomb
Relative power
Frequency (Hz)
AC
Spike rate (s-1)
Time (s)
AvWv
EEG (mV)
Time (s)
C Ablation
EEG
STN unit activity
pEEG
0.89 Hz
Relative power
Frequency (Hz)
Lomb
4.87 Hz
Relative power
Frequency (Hz)
AC
Spike rate (s-1)
Time (s)
AvWv
EEG (mV)
Time (s)

Table 4.1. Firing properties of STN neurons in control animals under urethane anaesthesia.

	CONTROL	
	Intact cortex	**Ablated cortex**
No. of observations	28	10
Low-frequency oscillatory neurons [a]	28	0
Irregular neurons	0	8
Regular neurons	0	2
Mean Firing rate (Hz)		
All neurons	8.1 ± 2.9	5.7 ± 4.3
Low-frequency oscillatory neurons	8.1 ± 2.9	-
Irregular neurons	-	5.1 ± 4.5
Regular neurons	-	7.9 ± 4.0
Coefficient of Variation		
Low-frequency oscillatory neurons	1.30 ± 0.36	-
Irregular neurons	-	0.66 ± 0.25
Regular neurons	-	0.26 ± 0.01
No. of oscillating neurons	28	2
Low-frequency oscillatory neurons	28	0
Irregular neurons	0	0
Regular neurons	0	2
Frequency of spike train oscillation (Hz)		
Low-frequency oscillatory neurons	0.84 ± 0.10	-
Irregular neurons	-	-
Regular neurons	-	8.06 ± 4.57
Frequency of cortical SWA (Hz) [b]	0.83 ± 0.09	0.84 ± 0.09

a Neurons were defined as displaying a significant, low-frequency oscillation in their spike trains (frequency of ≤ 2.0 Hz; $p < 0.05$);

b Cortical SWA was determined from contralateral frontal EEG in the case of neurons recorded after ablation of ipsilateral cortex.

Data are expressed as mean ± SD.

Figure 4.4. Neuronal activity in the GP of control rats under urethane anaesthesia is not closely related to coincident cortical activity. *A*, Regular firing GP neuron (CV = 0.15; mean rate = 12.5 Hz). The GP neuron displayed a highly regular, single-spike firing pattern that was maintained during episodes of robust SWA. Thus, the pEEG and Lomb periodogram were dissimilar, broad peaks were not observed in the auto-correlogram, and the AvWvs were almost flat. The occurrence of spindle sequences (*) in the EEG had no detectable effect on firing rate or pattern. *B*, Regular firing GP neuron (CV = 0.22; mean rate = 14.9 Hz) recorded in the same animal after cortical ablation. The rate and pattern of firing of GP neurons was not altered by ablation. Calibration bars apply to both left hand panels.

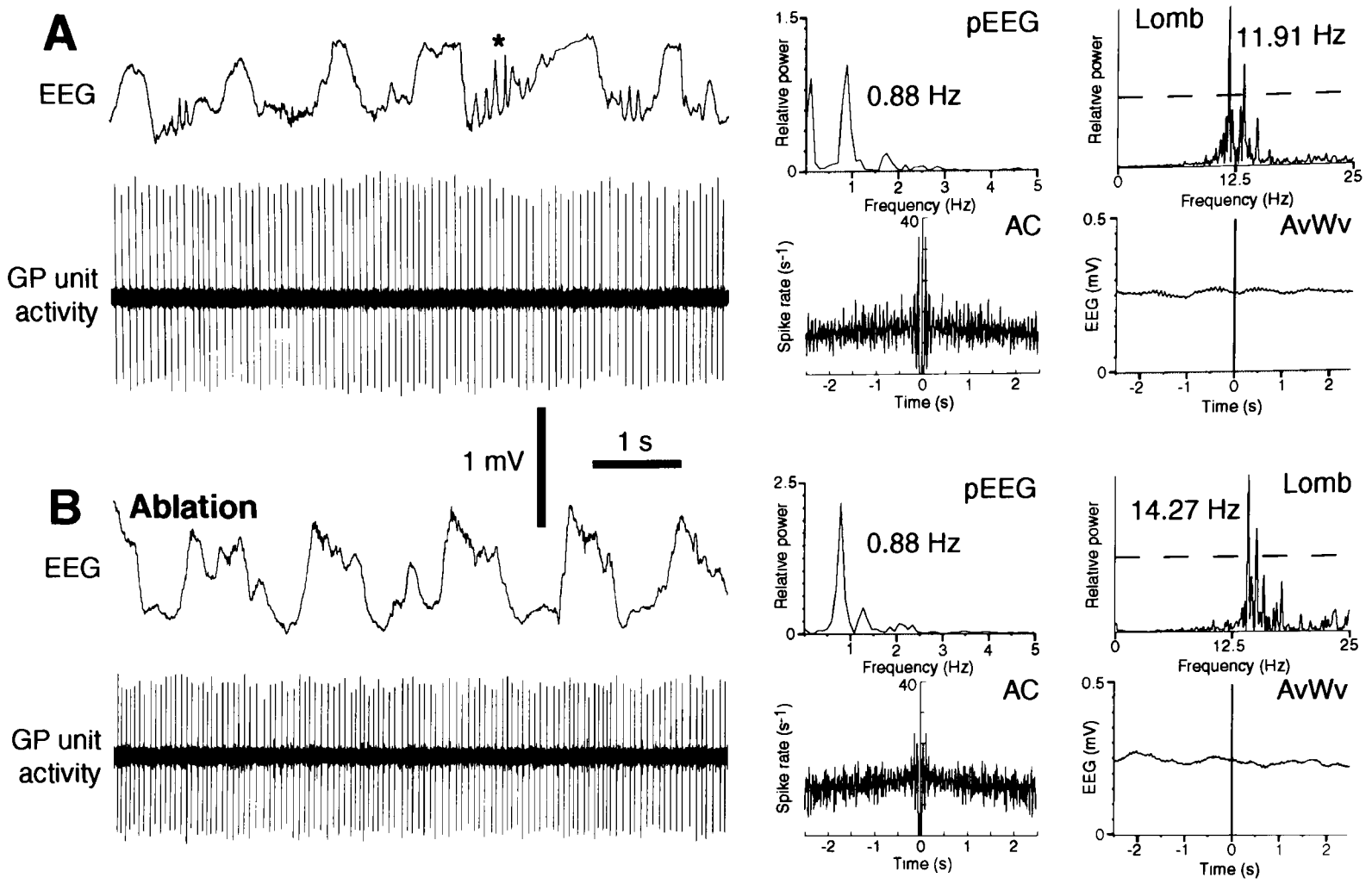

A
EEG
GP unit activity
1 mV
1 s
B
Ablation
EEG
GP unit activity
pEEG
0.88 Hz
Relative power
Frequency (Hz)
AC
Spike rate (s-1)
Time (s)
Lomb
11.91 Hz
AvWv
EEG (mV)
14.27 Hz

Table 4.2. Firing properties of GP neurons in control animals under urethane anaesthesia.

	CONTROL	
	Intact cortex	**Ablated cortex**
No. of observations	18	29
Low-frequency oscillatory neurons [a]	0	0
Irregular neurons	0	0
Regular neurons	18	29
Mean Firing rate (Hz)		
All neurons	18.0 ± 6.3	17.0 ± 8.3
Low-frequency oscillatory neurons	-	-
Irregular neurons	-	-
Regular neurons	18.0 ± 6.3	17.0 ± 8.3
Coefficient of Variation		
Low-frequency oscillatory neurons	-	-
Irregular neurons	-	-
Regular neurons	0.23 ± 0.05	0.17 ± 0.04
No. of oscillating neurons	18	29
Low-frequency oscillatory neurons	0	0
Irregular neurons	0	0
Regular neurons	18	29
Frequency of spike train oscillation (Hz)		
Low-frequency oscillatory neurons	-	-
Irregular neurons	-	-
Regular neurons	18.63 ± 5.96	17.07 ± 8.41
Frequency of cortical SWA (Hz) [b]	0.89 ± 0.10	0.89 ± 0.21

a Neurons were defined as displaying a significant, low-frequency oscillation in their spike trains (frequency of ≤ 2.0 Hz; $p < 0.05$);

b Cortical SWA was determined from contralateral frontal EEG in the case of neurons recorded after ablation of ipsilateral cortex.

Data are expressed as mean ± SD.

at a mean rate that was not significantly different from the firing frequency of units recorded with an intact ipsilateral cortex (Fig. 4.4*B*). These data suggest that the pattern and frequency of firing of GP neurons in control animals under urethane anaesthesia is not strongly influenced by coincident, rhythmic cortical activity.

4.3.4 Firing properties of STN and GP neurons in 6-OHDA-lesioned animals before and after cortical ablation

To examine the impact of the cortex on the STN-GP network in the dopamine-depleted brain, the EEG and coincident unit activity were recorded in 6-OHDA-lesioned rats under urethane anaesthesia. As in control animals, unit recordings in 6-OHDA-lesioned animals revealed that STN neurons displayed low-frequency oscillatory firing patterns during periods of robust SWA in the ipsilateral cortex (Fig. 4.5*A*, Table 4.3). Furthermore, STN neurons discharged predominantly during the active component of the slow-wave. The frequencies at which these epochs of activity occurred closely matched the frequencies of the coincident slow-wave and were not significantly different from control animals (Fig. 4.5*A*, Table 4.3). The mean rate of firing and CVs were, however, significantly higher in 6-OHDA-lesioned animals compared to control animals.

Following cortical ablation, low-frequency oscillatory firing was not recorded in the majority (80%) of STN neurons (Fig. 4.5*B-D*, Table 4.3). During periods of robust SWA in the contralateral cortex, most STN neurons discharged in a regular or irregular, single-spike manner during both the inactive and active components of the slow-wave (Fig. 4.5*B-D*, Table 4.3). The frequency of SWA in the contralateral (unlesioned) cortex was similar to the frequency of SWA in the 6-OHDA-lesioned hemisphere. The mean discharge rate and CVs of STN neurons following ablation was significantly lower than before ablation. However, the mean firing rate of STN neurons in 6-OHDA-lesioned animals after ablation was similar to that of STN neurons recorded in control animals after cortical ablation. These

observations indicate that the impact of the cortex on STN neuronal activity is greater in the dopamine-depleted brain and that rhythmic activity in the STN is driven largely by the cortex in this preparation.

In contrast to recordings in control animals, GP neurons in the 6-OHDA-lesioned rats exhibited low-frequency oscillatory firing patterns during robust SWA (Fig. 4.6*A*, *B*, Table 4.4). During periods of robust SWA in the ipsilateral cortex, when the active component of the slow-wave was most clearly seen, oscillatory GP neurons discharged predominantly during the active or inactive components of the slow-wave (Fig. 4.6*A*, *B*, respectively). Neurons discharging predominantly during the active (18% of population) or inactive (82%) components were similarly distributed throughout the GP (data not shown). The majority (89%) of neurons displayed a significant peak oscillation in their Lomb periodogram that was similar to the frequency of the coincident slow-wave (Fig. 4.6*A*, *B*, Table 4.4). The mean firing rates of GP neurons in 6-OHDA-lesioned and control animals were not significantly different. However, CVs were significantly higher in the 6-OHDA-lesioned animals. In cortical ablated animals, 85% of GP neurons did not display significant low-frequency oscillations and thus, firing was not correlated with the contralateral cortical oscillation (Fig. 4.6*C*, Table 4.4). Furthermore, the firing rates of regularly discharging GP neurons in 6-OHDA-lesioned animals after ablation were not significantly different from those recorded in control animals before or after cortical ablation. The frequency of SWA in the contralateral (unlesioned) cortex was similar to the frequency of SWA in the lesioned hemisphere. These results show that in the 6-OHDA-lesioned hemisphere, rhythmic cortical activity is propagated to the GP and underlies rhythmic bouts of high-frequency firing in the majority of GP neurons.

In contrast to the recordings in control animals, a small proportion of STN (20%) and GP (15%) neurons recorded in 6-OHDA-lesioned animals displayed low-frequency oscillatory firing after ablation of the cortex. The frequency of neuronal oscillation was

Figure 4.5. Neuronal activity in the STN of 6-OHDA-lesioned rats under urethane anaesthesia is closely related to coincident cortical activity. *A*, Low-frequency oscillatory STN neuron (CV = 2.35; mean rate = 15.8 Hz) recorded in a 6-OHDA-lesioned animal. The neuron discharged powerfully during the active component of the slow-wave. Comparison of the Lomb periodogram with the power spectrum showed identical frequencies of rhythmic activity in the spike train and EEG. In 6-OHDA-lesioned animals, the mean rate of firing of STN neurons was significantly higher than that in control animals. Cortical ablation in 6-OHDA-lesioned animals abolished low-frequency oscillatory activity and reduced the mean rates of firing in the majority of STN neurons. *B*, Regular firing STN neuron (CV = 0.32; mean rate = 9.8 Hz) recorded after cortical ablation. *C*, Irregular firing STN neuron (CV = 0.44; mean rate = 4.1 Hz) recorded after cortical ablation. *D*, Low-frequency oscillatory neuron (CV = 2.12; mean rate = 12.5 Hz) recorded after cortical ablation. Twenty percent of STN neurons continued to oscillate at low frequencies after ablation and discharge was correlated weakly with SWA in the contralateral cortex. Neurons in *A*, *B* and *C* were recorded in the same animal. Calibration bars apply to all left hand panels.

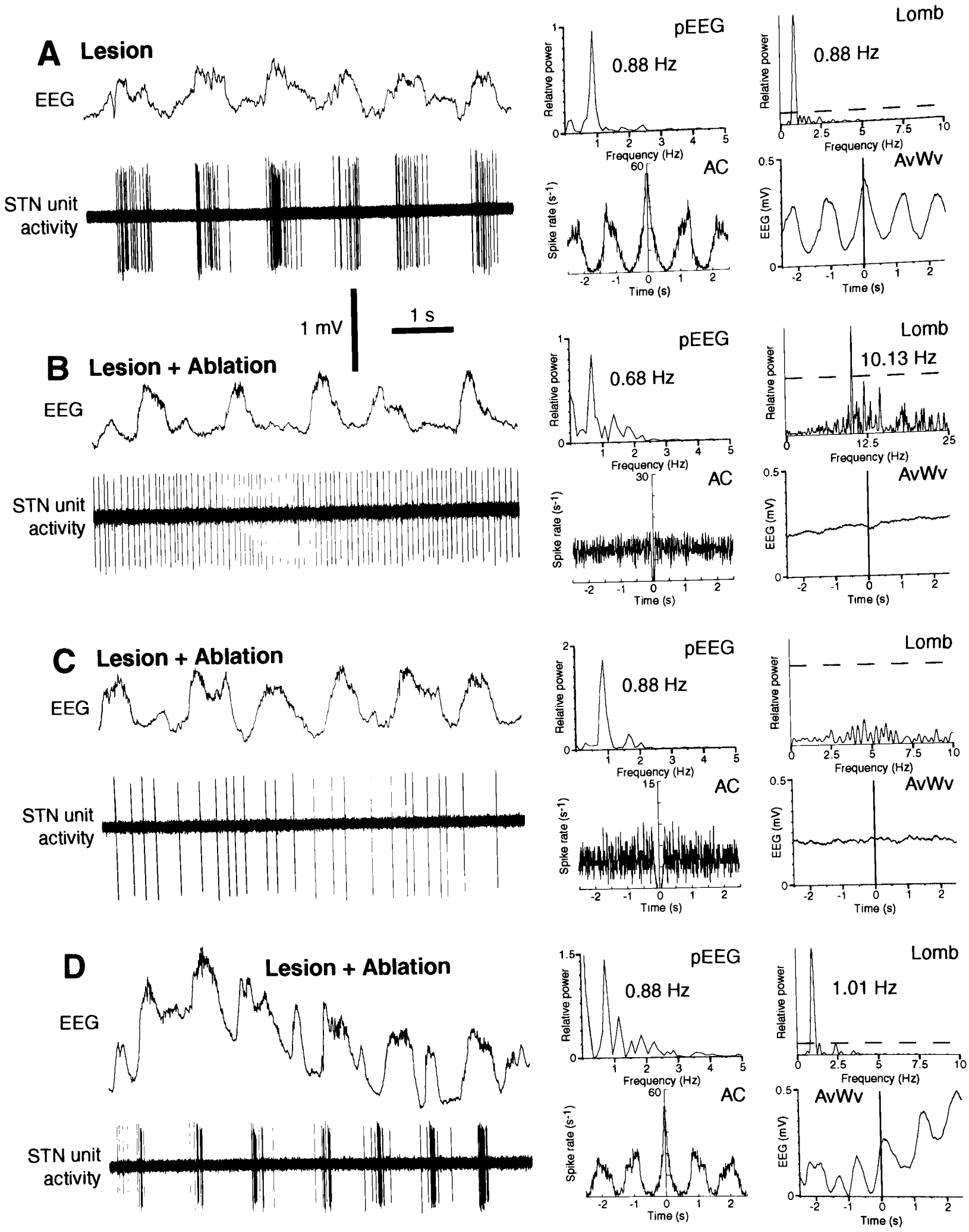

A Lesion
EEG
STN unit activity
1 mV
1 s
pEEG
0.88 Hz
Relative power
Frequency (Hz)
Lomb
0.88 Hz
Relative power
Frequency (Hz)
AC
Spike rate (s-1)
Time (s)
AvWv
EEG (mV)
Time (s)
B Lesion + Ablation
EEG
STN unit activity
pEEG
0.68 Hz
Relative power
Frequency (Hz)
Lomb
10.13 Hz
Relative power
Frequency (Hz)
AC
Spike rate (s-1)
Time (s)
AvWv
EEG (mV)
Time (s)
C Lesion + Ablation
EEG
STN unit activity
pEEG
0.88 Hz
Relative power
Frequency (Hz)
Lomb
Relative power
Frequency (Hz)
AC
Spike rate (s-1)
Time (s)
AvWv
EEG (mV)
Time (s)
D
Lesion + Ablation
EEG
STN unit activity
pEEG
0.88 Hz
Relative power
Frequency (Hz)
Lomb
1.01 Hz
Relative power
Frequency (Hz)
AC
Spike rate (s-1)
Time (s)
AvWv
EEG (mV)
Time (s)

Table 4.3. Firing properties of STN neurons in 6-OHDA-lesioned animals under urethane anaesthesia.

	6-OHDA-LESIONED	
	Intact cortex	**Ablated cortex**
No. of observations	33	15
Low-frequency oscillatory neurons [a]	33	3
Irregular neurons	0	7
Regular neurons	0	5
Mean Firing rate (Hz)		
All neurons	18.9 ± 12.2	5.8 ± 4.2
Low-frequency oscillatory neurons	18.9 ± 12.2	7.2 ± 4.8
Irregular neurons	-	2.7 ± 1.7
Regular neurons	-	9.4 ± 3.4
Coefficient of Variation		
Low-frequency oscillatory neurons	2.27 ± 0.82	1.75 ± 0.39
Irregular neurons	-	0.91 ± 0.47
Regular neurons	-	0.30 ± 0.08
No. of oscillating neurons	33	8
Low-frequency oscillatory neurons	33	3
Irregular neurons	0	0
Regular neurons	0	5
Frequency of spike train oscillation (Hz)		
Low-frequency oscillatory neurons	0.88 ± 0.20	0.89 ± 0.14
Irregular neurons	-	-
Regular neurons	-	9.41 ± 3.24
Frequency of cortical SWA (Hz) [b]	0.88 ± 0.18	0.91 ± 0.21

a Neurons were defined as displaying a significant, low-frequency oscillation in their spike trains (frequency of ≤ 2.0 Hz; $p < 0.05$);

b Cortical SWA was determined from contralateral frontal EEG in the case of neurons recorded after ablation of ipsilateral cortex.

Data are expressed as mean ± SD.

Figure 4.6. Neuronal activity in the GP of 6-OHDA-lesioned rats under urethane anaesthesia is tightly correlated with coincident cortical activity. *A*, Low-frequency oscillatory GP neuron (CV = 1.48; mean rate = 9.5 Hz) that fired predominantly during the active component of the cortical slow-wave. Rhythmic spike-firing was manifest clearly as broad peaks in the auto-correlogram. *B*, Low-frequency oscillatory GP neuron (CV = 0.75; mean rate = 19.0 Hz) that discharged predominantly during the trough (inactive component) of the cortical slow wave. The dramatic alteration in firing pattern that was observed in lesioned animals (cf. GP neuron in Fig. 4.4*A*) was not associated with a change in mean firing rate. *C*, Regular firing GP neuron (CV = 0.19; mean rate = 23.1 Hz) recorded after ipsilateral cortical ablation. Most of the GP neurons recorded after ablation fired in a tonic, regular manner that was not statistically different to the regular firing patterns observed in control animals and was not related to coincident contralateral EEG. *D*, Low-frequency oscillatory GP neuron (CV = 2.03; mean rate = 12.4 Hz) recorded after cortical ablation. This form of activity was observed in 15% of GP neurons after ablation. The activity of this neuron was correlated weakly with contralateral cortical SWA. Neurons in *A*, *C* and *D* were recorded in the same animal. Calibration bars apply to all left hand panels.

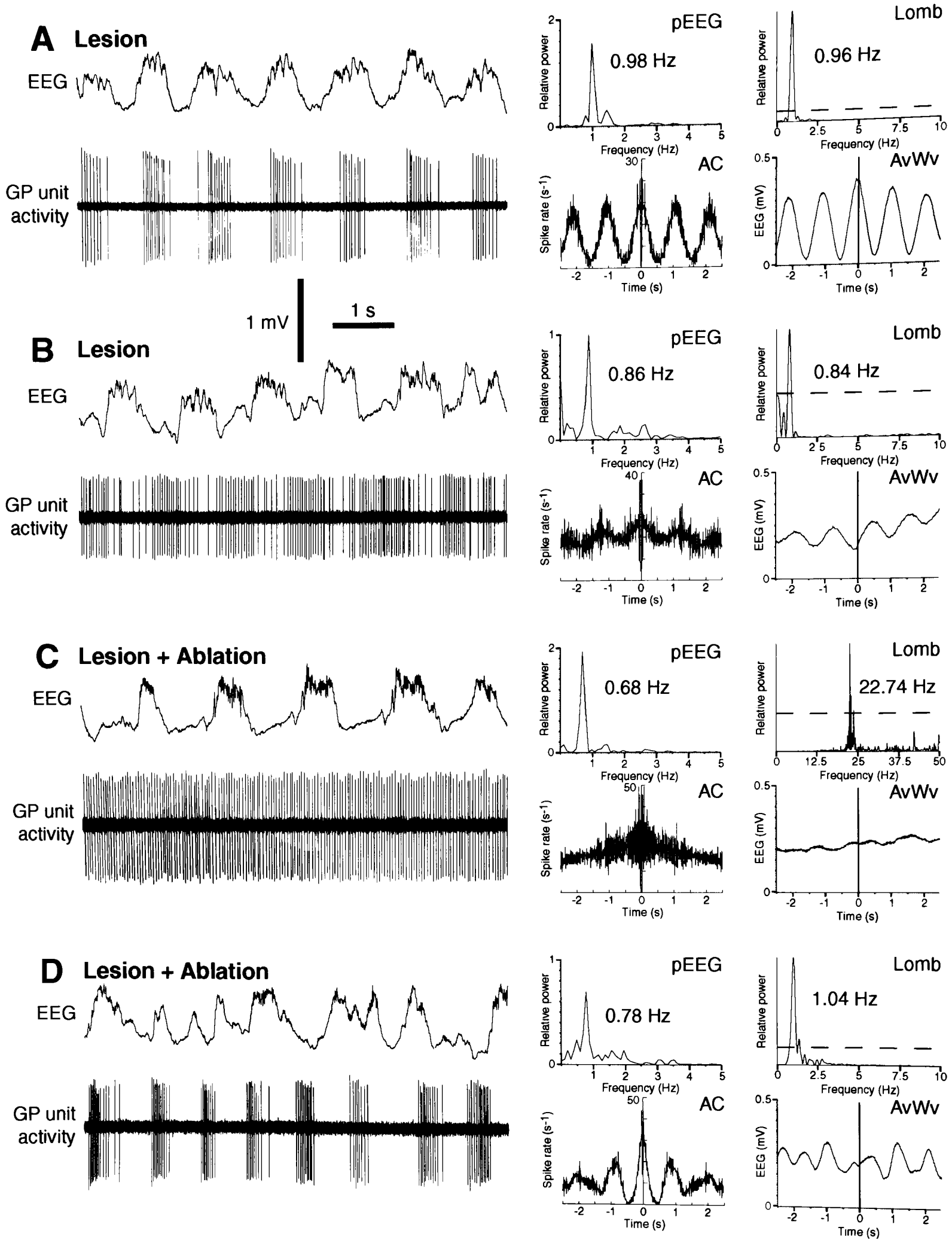

A Lesion
EEG
GP unit activity
1 mV
1 s
pEEG
0.98 Hz
Relative power
Frequency (Hz)
Lomb
0.96 Hz
AC
Spike rate (s-1)
Time (s)
AvWv
EEG (mV)
B Lesion
0.86 Hz
0.84 Hz
C Lesion + Ablation
0.68 Hz
22.74 Hz
D Lesion + Ablation
0.78 Hz
1.04 Hz

Table 4.4. Firing properties of GP neurons in 6-OHDA-lesioned animals under urethane anaesthesia.

	6-OHDA-LESIONED	
	Intact cortex	**Ablated cortex**
No. of observations	28	20
Low-frequency oscillatory neurons [a]	25	3
Irregular neurons	3	1
Regular neurons	0	16
Mean Firing rate (Hz)		
All neurons	21.7 ± 8.6	18.7 ± 7.3
Low-frequency oscillatory neurons	22.2 ± 8.5	14.6 ± 2.8
Irregular neurons	17.3 ± 9.0	5.3
Regular neurons	-	20.31 ± 7.0
Coefficient of Variation		
Low-frequency oscillatory neurons	1.11 ± 0.39	1.53 ± 0.44
Irregular neurons	0.67 ± 0.18	0.45
Regular neurons	-	0.16 ± 0.04
No. of oscillating neurons	25	19
Low-frequency oscillatory neurons	25	3
Irregular neurons	0	0
Regular neurons	0	16
Frequency of spike train oscillation (Hz)		
Low-frequency oscillatory neurons	0.92 ± 0.22	0.88 ± 0.16
Irregular neurons	-	-
Regular neurons	-	19.87 ± 6.96
Frequency of cortical SWA (Hz) [b]	0.92 ± 0.21	0.92 ± 0.19

a Neurons were defined as displaying a significant, low-frequency oscillation in their spike trains (frequency of ≤ 2.0 Hz; $p < 0.05$);

b Cortical SWA was determined from contralateral frontal EEG in the case of neurons recorded after ablation of ipsilateral cortex.

Data are expressed as mean ± SD.

similar to coincident SWA in the contralateral cortex and the spike-triggered waveform average displayed small peaks, which suggested that there was a weak correlation in activity (Figs. 4.5*D*, 4.6*D*).

4.3.5 Responses of STN and GP neurons to global activation in control animals before and after cortical ablation

To investigate the effects of global activation on the STN-GP network, the responses of the EEG and coincident unit activity to hindpaw pinch were recorded under urethane anaesthesia. During hindpaw pinch-evoked sensory stimulation, the slow oscillation in the cortex was obliterated and was replaced by smaller-amplitude (< 100 μV), higher-frequency (> 10 Hz) activity. Changes in the EEG of this type were always reflected as changes in the rate and pattern of firing of STN and GP neurons (Figs. 4.7, 4.8). Indeed, hindpaw pinch led to ipsilateral cortical activation and abolished significant, low-frequency oscillations in the spike trains of STN neurons. Furthermore, during cortical activation, STN and GP neurons adopted a tonic, regular or irregular firing pattern with a significantly increased mean rate of activity (Figs. 4.7*A*, 4.8*A*, Table 4.5; STN neurons increased rates of firing to 146 ± 32% of control firing rates; mean firing rates before and during pinch were 7.5 ± 3.4 Hz and 10.5 ± 4.4 Hz, respectively, $n = 17$; GP neurons increased their rates to 142 ± 19% of control; mean firing rates before and during pinch were 16.6 ± 5.9 Hz and 23.7 ± 9.9 Hz, respectively, $n = 16$). Low-frequency oscillatory activity in the STN only resumed when SWA reappeared in the EEG (data not shown).

After ablation of the ipsilateral cortex, sensory stimulation, as measured from the contralateral cortex, was also accompanied by changes in the rate and pattern of firing of STN and GP neurons (Figs. 4.7, 4.8). During activation, STN and GP neurons adopted a tonic, regular or irregular firing pattern with a significantly increased mean rate (Figs 4.7*B*, 4.8*B*, Table 4.5; STN neurons increased rates of firing to 132 ± 29% of control rates; mean

firing rates before and during pinch were 7.0 ± 4.2 Hz and 8.5 ± 4.2 Hz, respectively, $n = 7$; GP neurons increased their rates to 121 ± 11%; mean firing rates before and during pinch were 15.8 ± 6.6 Hz and 18.9 ± 8.1 Hz, respectively, $n = 9$). These observations indicate that global activation results in a profound alteration of activity in the STN-GP network and that subcortical structures play a major role in this effect.

Table 4.5. Responses of neurons in the STN-GP network to global activation in control animals under urethane anaesthesia.

		CONTROL	
		Intact cortex	**Ablated cortex**
STN	No. of neurons tested	17	7
	% of neurons that INCREASED firing	100	100
	% INCREASE in firing rate	146 ± 32	132 ± 29
GP	No. of neurons tested	16	9
	% of neurons that INCREASED firing	100	100
	% INCREASE in firing rate	142 ± 19	121 ± 11

4.3.6 Response of STN and GP neurons to global activation in 6-OHDA-lesioned animals before and after cortical ablation

To characterise the effects of global activation on the STN-GP network in the 6-OHDA-lesioned hemisphere, the responses of the EEG and coincident unit activity to hindpaw pinch were recorded under urethane anaesthesia. Sensory stimulation by paw pinch in 6-OHDA-lesioned animals obliterated the slow oscillation in the cortex and also produced changes in the rate and pattern of firing of STN and GP neurons (Figs. 4.9, 4.10). During ipsilateral cortical activation, significant low-frequency oscillations in STN firing were lost. Indeed,

Figure 4.7. Cortical activation alters the firing patterns and increases the firing rates of STN neurons in control rats under urethane anaesthesia. *A*, Sensory stimulation by hindpaw pinch obliterated cortical SWA (7 s duration; starts at *arrow*), which resulted in a loss of LFO activity and increased the mean firing rate of the STN neuron (CV = 1.07 mean = 7.0 Hz, before pinch; CV = 0.45, mean = 10.5 Hz, during pinch). The pEEGs and Lomb periodograms in the left and right hand columns in this and following figures were determined before and during the pinch, respectively. Low-frequency oscillatory unit activity swiftly resumed when robust SWA was restored to the EEG (data not shown). *B*, Irregular firing STN neuron recorded after ablation (CV = 0.50; mean = 9.4 Hz, before pinch). Sensory stimulation (starts at *arrow*) obliterated contralateral SWA and led to an increase in firing frequency (CV = 0.42; mean = 11.9 Hz, during pinch). Calibration bars apply to both left hand panels.

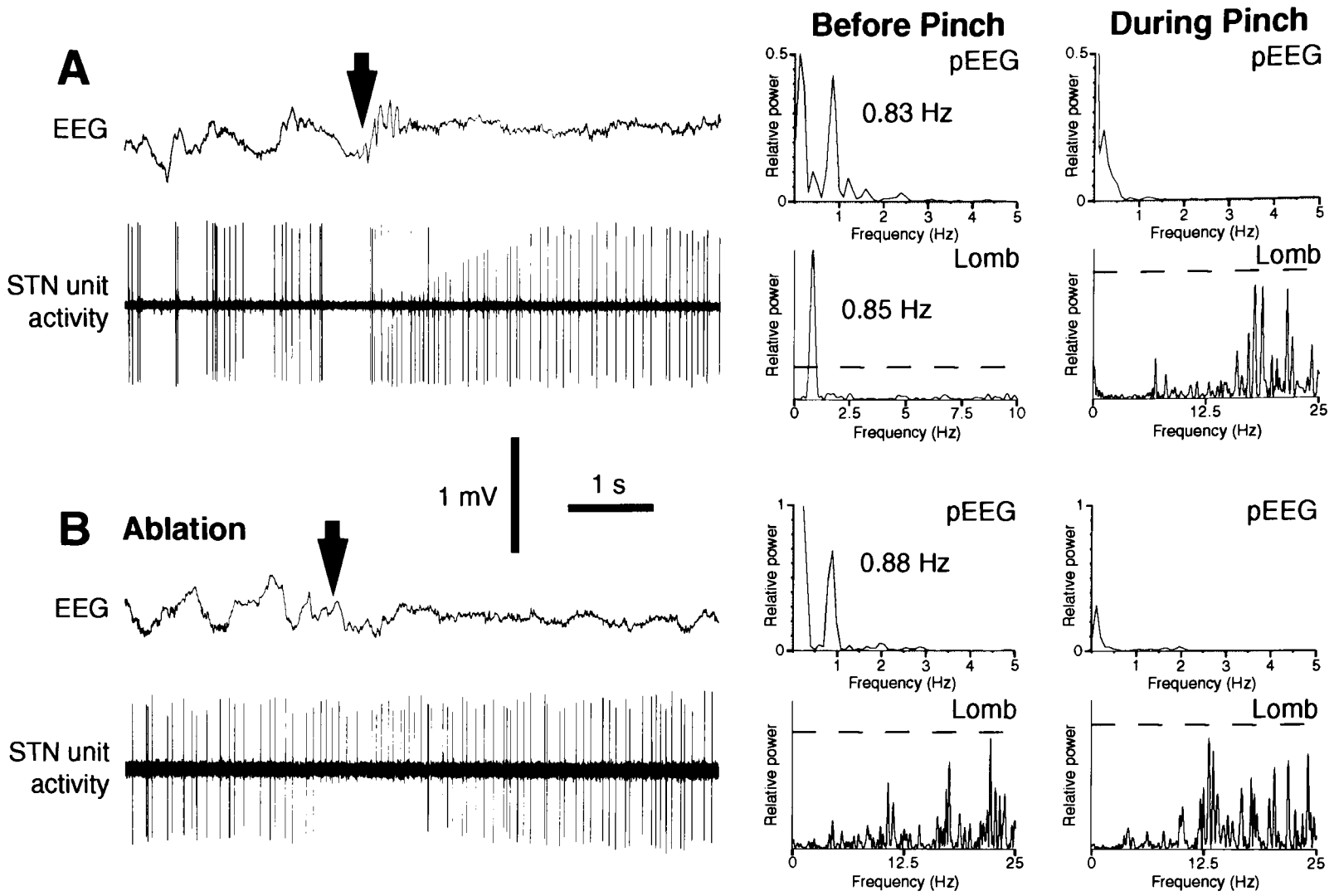
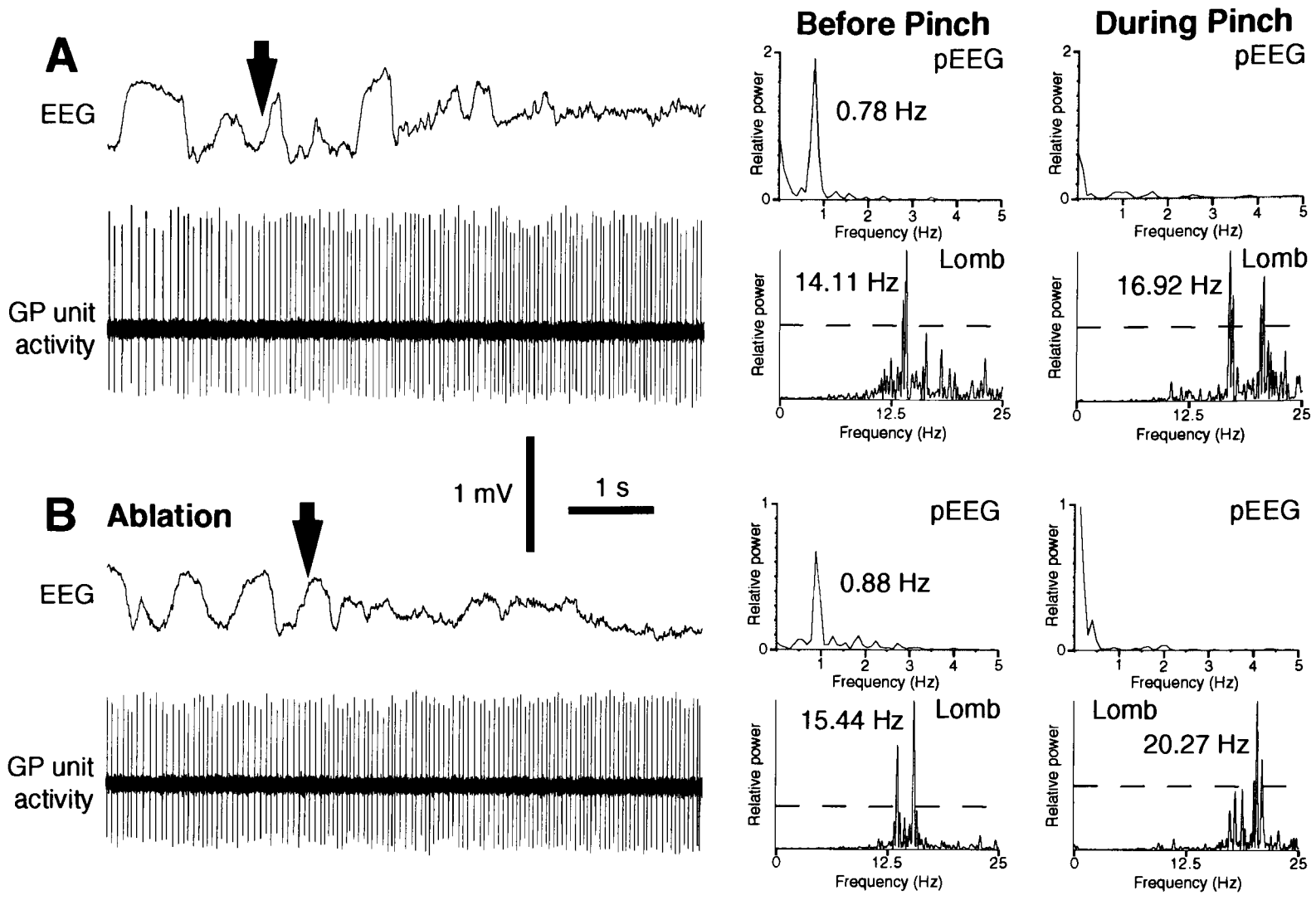

A
EEG
STN unit activity
1 mV
1 s
B
Ablation
EEG
STN unit activity
Before Pinch
During Pinch
pEEG
0.83 Hz
Lomb
0.85 Hz
pEEG
0.88 Hz
Lomb
Relative power
Frequency (Hz)

Figure 4.8. Cortical activation increases the firing rates of GP neurons in control rats under urethane anaesthesia. *A*, Regular firing GP neuron (CV = 0.21; mean = 14.2 Hz, before pinch). Typical response to cortical activation (evoked by a 7 s hindpaw pinch; starts at *arrow*). The loss of SWA resulted in slightly more irregular firing and an increase in the mean firing rate (CV = 0.24; mean = 18.9 Hz, during pinch). *B*, Regular firing GP neuron recorded after ablation (CV = 0.17; mean = 14.4 Hz, before pinch). Disruption of contralateral SWA by pinching (*arrow*) increased the mean rate and irregularity of firing of the GP neuron (CV = 0.19; mean = 20.2 Hz, during pinch). Neurons in *A* and *B* were recorded in the same animal. Calibration bars apply to both left hand panels.


A
EEG
GP unit activity
1 mV
1 s
B
Ablation
EEG
GP unit activity
Before Pinch
During Pinch
pEEG
0.78 Hz
Relative power
Frequency (Hz)
Lomb
14.11 Hz
16.92 Hz
pEEG
0.88 Hz
Lomb
15.44 Hz
Lomb
20.27 Hz

STN neurons adopted a tonic, regular or irregular firing pattern and the mean rate of discharge was significantly increased (Fig. 4.9*A*, Table 4.6; 229 ± 100% of control firing rate; mean firing rates before and during pinch were 17.8 ± 8.3 Hz and 35.0 ± 11.6 Hz, respectively; n = 16). The sensory stimulation-evoked increases in STN activity were significantly higher in 6-OHDA-lesioned animals compared to control animals. During cortical activation, GP neurons adopted tonic, regular or irregular firing patterns and significant low-frequency oscillations in firing were abolished. In marked contrast to the responses of GP neurons to sensory stimulation in control animals, a large proportion of GP neurons (61%) in 6-OHDA-lesioned animals significantly decreased their rates of activity during coincident cortical activation (Fig. 4.10*B*, Table 4.6; 58 ± 24% of control; mean firing rates before and during pinch were 22.2 ± 11.4 Hz and 11.8 ± 6.6 Hz, respectively; n = 14 [3 of 14 fired predominantly during the active component before pinch]). The firing rates of the remaining GP neurons significantly increased during cortical activation (Fig. 4.10*A*; 134 ± 23%; mean firing rates before and during pinch were 20.4 ± 6.9 Hz and 27.0 ± 8.8 Hz, respectively; n = 9 [2 of 9 fired predominantly during the active component before pinch]). Neurons that decreased or increased activity during global activation displayed similar mean firing rates prior to hindpaw pinch and were similarly distributed throughout the GP (data not shown). In congruence with activity in control animals, low-frequency oscillations in the STN-GP network did not emerge until SWA reappeared in the EEG (data not shown).

Subsequent to ipsilateral cortical ablation, sensory stimulation by paw pinch was accompanied by changes in the rate and pattern of firing of STN and GP neurons (Figs. 4.9, 4.10). Indeed, STN and GP neurons uniformly adopted a tonic, regular or irregular firing pattern with a significantly increased mean rate (Figs. 4.9*B*, 4.10*C*, respectively, Table 4.6; firing rates of STN neurons increased to 151 ± 62% of control rates before pinch; mean firing rates before and during pinch were 6.2 ± 4.1 Hz and 9.2 ± 5.8 Hz, respectively, n = 9; firing rates of GP neurons increased to 121 ± 20% of controls; mean firing rates before and

during pinch were 18.8 ± 8.0 Hz and 21.8 ± 7.6 Hz, respectively, n = 12). Taken together, these observations show that the response of the STN-GP network to sensory stimulation is altered dramatically in the dopamine-depleted brain and that corticofugal pathways are involved in these changes.

Table 4.6. Responses of neurons in the STN-GP network to global activation in dopamine-depleted animals under urethane anaesthesia.

		6-OHDA-LESIONED	
		Intact cortex	**Ablated cortex**
STN	No. of neurons tested	16	9
	% of neurons that INCREASED firing	100	100
	% INCREASE in firing rate	229 ± 100	151 ± 62
GP	No. of neurons tested	23	12
	% of neurons that INCREASED firing	39	100
	% INCREASE in firing rate	134 ± 23	121 ± 20
	% of neurons that DECREASED firing	61	0
	% DECREASE in firing rate	58 ± 24	-

4.3.7 Characterisation of local field potentials in the STN and GP

To determine directly the expression of cortical SWA at a local level in the STN-GP network, unit activity and the LFP were simultaneously recorded from single extracellular electrodes in three control animals. During periods of robust SWA in the cortex, STN neurons (n = 13) exhibited low-frequency oscillatory firing patterns (0.89 ± 0.10 Hz; n = 13), and LFPs were dominated by slow oscillations with a predominant frequency component that was similar to that observed in coincidental EEG (Fig. 4.11*A*; 0.89 ± 0.07 Hz and 0.88 ± 0.06 Hz for slow-waves in EEGs and LFPs, respectively). The gross morphology

Figure 4.9. Cortical activation alters the firing patterns and increases the firing rates of STN neurons in 6-OHDA-lesioned rats under urethane anaesthesia. *A*, Low-frequency oscillatory STN neuron (CV = 1.54; mean = 9.1 Hz, before pinch). Obliteration of cortical SWA by hindpaw pinch (starts at *arrow*) altered STN unit activity; LFO activity was lost and there was a dramatic increase in the mean firing rate (CV = 0.28; mean = 22.7 Hz, during pinch). Low-frequency oscillatory unit activity resumed when robust SWA recovered (data not shown). *B*, Regular firing STN neuron (CV = 0.23; mean = 7.0 Hz, before pinch) recorded after ablation. Activation of contralateral cortex by hindpaw pinch (*arrow*) was associated with a modest increase in the mean firing rate of the STN neuron (CV = 0.20; mean = 11.8 Hz, during pinch). Neurons in *A* and *B* were recorded in the same animal. Calibration bars apply to both left hand panels.

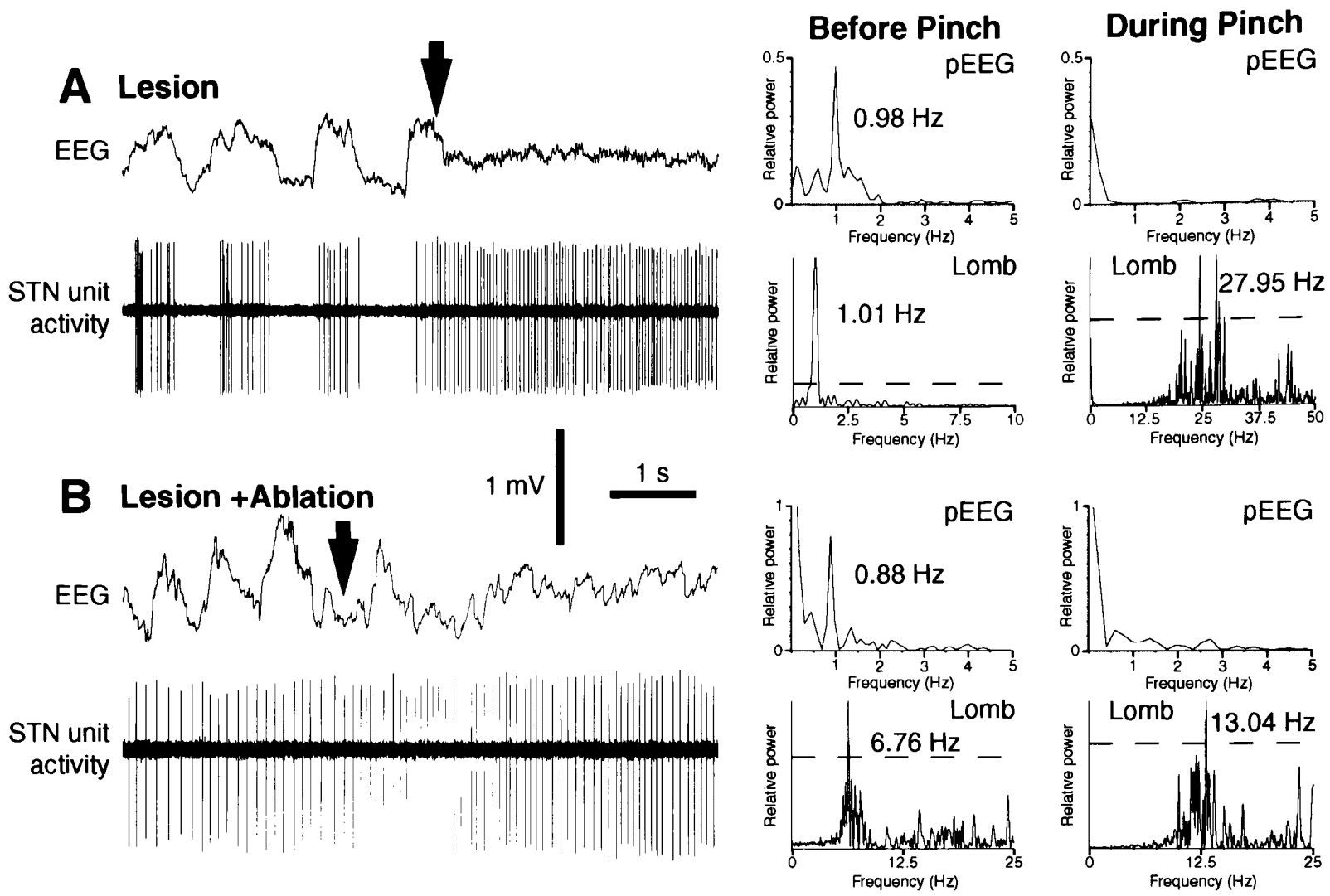
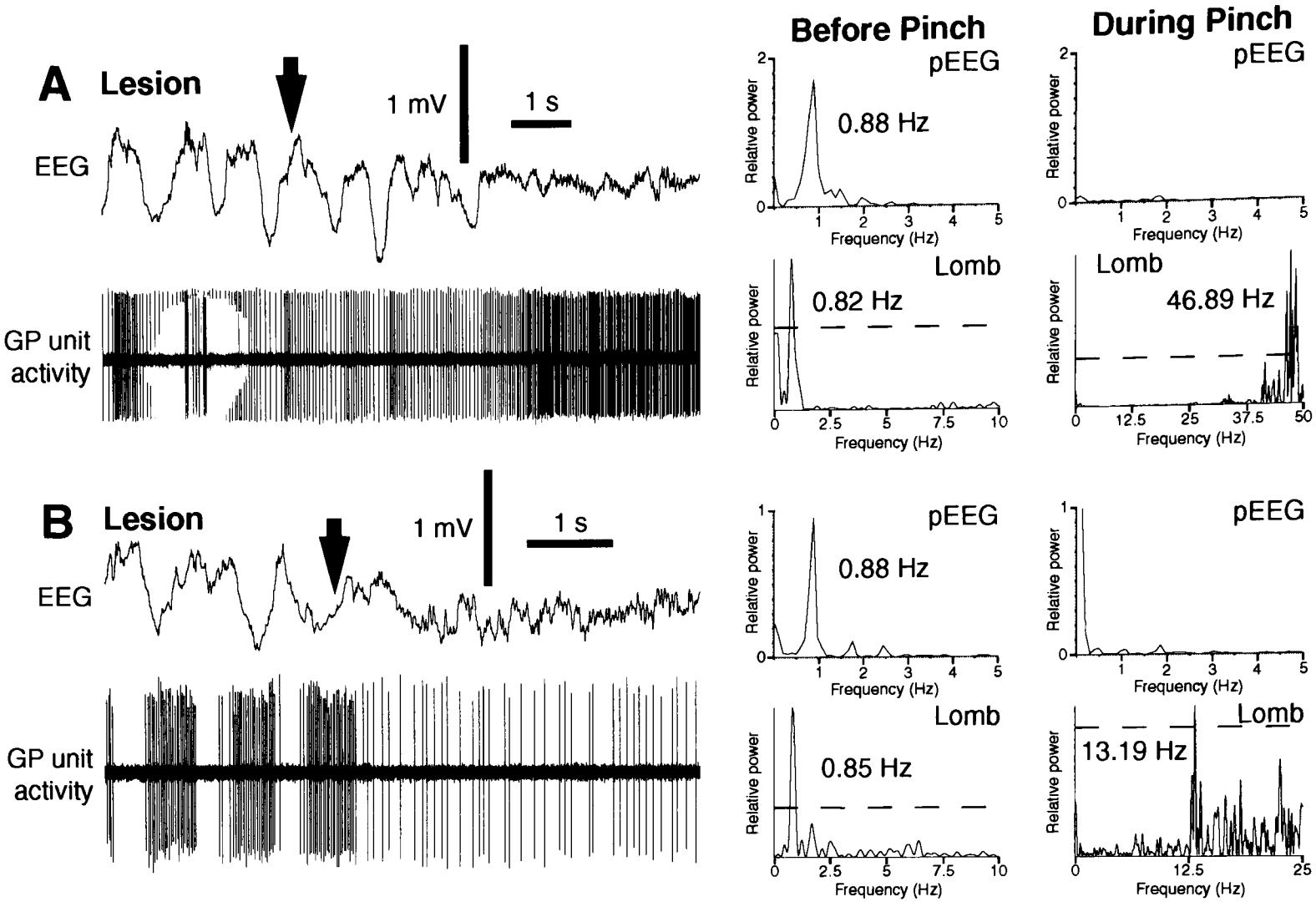

A Lesion
EEG
STN unit activity
1 mV
1 s
B Lesion +Ablation
EEG
STN unit activity
Before Pinch
During Pinch
pEEG
0.98 Hz
Lomb
1.01 Hz
pEEG
Lomb
27.95 Hz
pEEG
0.88 Hz
Lomb
6.76 Hz
pEEG
Lomb
13.04 Hz
Relative power
Frequency (Hz)

Figure 4.10. The heterogeneity in the responses of GP neurons in 6-OHDA-lesioned animals to global activation is abolished by ipsilateral cortical ablation. *A*, Low-frequency oscillatory GP neuron (CV = 0.60, mean = 23.1 Hz, before pinch). Obliteration of cortical SWA by sensory stimulation (pinch starts at *arrow*) produced an alteration in the firing pattern, from LFO firing patterns to irregular firing, and increased the mean firing rate of the GP neuron (CV = 0.12; mean = 43.6 Hz, during pinch). *B*, Low-frequency oscillatory GP neuron (CV = 0.96, mean = 36.5 Hz, before pinch). Obliteration of cortical SWA by sensory stimulation (starts at *arrow*) was associated with an alteration in the firing pattern, from LFO firing to irregular firing, and decreased the mean firing rate of the GP neuron (CV = 0.55; mean = 10.9 Hz, during pinch). Decreased activity of GP neurons in response to global activation was only observed in 6-OHDA-lesioned animals. Low-frequency oscillatory unit activity in *A* and *B* did not resume until robust SWA reappeared in the EEG (data not shown). *C*, Regular firing GP neuron (CV = 0.17; mean = 15.5 Hz, before pinch) recorded after ablation. Activation of contralateral cortex (*arrow*) was accompanied by a modest increase in the mean firing rate of the GP neuron (CV = 0.18; mean = 16.4 Hz, during pinch). All GP neurons recorded after cortical ablation increased their mean firing rates in response to the hindpaw pinch. Neurons in *A* and *B* were recorded in the same animal. Calibration bars in *B* apply to *C*.


A
Lesion
1 mV
1 s
EEG
GP unit activity
Before Pinch
During Pinch
pEEG
0.88 Hz
Relative power
Frequency (Hz)
Lomb
0.82 Hz
46.89 Hz
B
Lesion
1 mV
1 s
EEG
GP unit activity
pEEG
0.88 Hz
Lomb
0.85 Hz
13.19 Hz
C
Lesion +Ablation
EEG
GP unit activity
pEEG
0.78 Hz
Lomb
15.34 Hz
16.01 Hz

of SWA in the LFP was similar to that of SWA in the corresponding EEG, but the polarity of the LFP was reversed compared to the EEG (Fig. 4.11*A*; see cross-correlograms of the EEG and LFP waveforms [WvCC]). Consequently, unit activity was more pronounced during the negative and positive portions of slow-waves in the LFP and EEG, respectively (Fig. 4.11*A*; see spike-triggered waveform averages).

As in the previous experiments, the low-frequency oscillatory firing of STN neurons was abolished by cortical ablation. During periods of robust SWA in the contralateral cortex, STN neurons (n = 7) discharged in an irregular (n = 5) or regular (n = 2) manner throughout the entire cycle of the cortical slow-wave and the activity of STN neurons no longer matched the frequency of the coincident SWA (Fig. 4.11*B*). Although SWA was present in the contralateral cortex, similar slow oscillations were almost absent from the ipsilateral LFP (Fig. 4.11*B*).

Sensory stimulation resulted in the obliteration of low-frequency oscillations in unit activity and SWA in the EEG and LFP (Fig. 4.11*C*). Moreover, in congruence with EEG recordings, LFPs were dominated by small-amplitude (< 100 μV), high-frequency (> 10 Hz) oscillations for the duration of the pinch (Fig. 4.11*C*). Slow-wave activity did not appear in the LFP until SWA was restored to the EEG (data not shown).

In contrast to the STN, unit activity in the GP was not phase-locked to the LFP under urethane anaesthesia. Indeed, GP neurons (n = 6) exhibited regular firing patterns when SWA was prevalent in the simultaneously-recorded LFP and EEG (Fig. 4.12*A*). In good agreement with STN recordings, the LFP polarity tended towards the inverse of the EEG polarity (Fig. 4.12*A*, *B*). Furthermore, a statistical comparison between power spectra of EEGs and LFPs demonstrated a similar periodicity (0.96 ± 0.10 Hz and 0.95 ± 0.10 Hz for EEG and LFP, respectively; n = 6).

Sensory stimulation by hindpaw pinch was accompanied by marked decreases in the power of SWA in the EEG and LFP (Fig. 4.12*B*). These reductions in SWA were typically

Figure 4.11. Neuronal activity in the STN of control rats under urethane anaesthesia is closely related to the coincident local field potential. *A*, Low-frequency oscillatory STN neuron (CV = 0.99; mean rate = 6.0 Hz) recorded during robust cortical SWA. Slow-wave activity in the cortex was reflected in the LFP. Oscillations in the LFP were similar in morphology to cortical SWA, but the polarity of the LFP was reversed compared to cortical EEG. Cross-correlations of the LFP and EEG (WvCC) confirmed the reciprocal phase relationship of the two waveforms. The neuron fired predominantly during the positive part (active component) of the cortical slow-wave and thus, during the negative portion of the LFP oscillation. The phase relationships of spiking to the EEG and LFP are shown on the spike-triggered waveform averages (AvWv and AvLFP, respectively). Comparison of the Lomb periodogram with the power spectra of the EEG and the LFP (pLFP) indicated similar frequencies of rhythmic activity in the STN spike train, cortex, and local STN milieu. *B*, Irregular firing STN neuron (CV = 0.64; mean rate = 2.2 Hz) recorded after ipsilateral cortical ablation. The discharge of the neuron was not correlated with contralateral cortical EEG or ipsilateral LFP and did not display a significant oscillatory component. Activity in the EEG and LFP was not correlated; although SWA was present in the contralateral cortex, similar large-amplitude, low-frequency oscillations were not present in the LFP. *C*, Hindpaw pinch (7 s duration; starts at *arrow*) obliterated SWA in the intact cortex and LFP with a similar latency, which was accompanied by a loss of LFO activity and increased the mean firing rate of another STN neuron (CV = 2.17 mean = 15.0 Hz, before pinch; CV = 0.53, mean = 18.9 Hz, during pinch). Low-frequency oscillatory unit activity swiftly resumed when robust SWA was restored to the EEG and LFP (data not shown). Neurons were recorded in the same animal. Calibration bars apply to all left hand panels. In this and the following figure, WvCC designates cross-correlograms of LFP and EEG waves, pLFP designates power spectra of the coincident LFP, AvLFP designates spike-triggered averages of LFP.

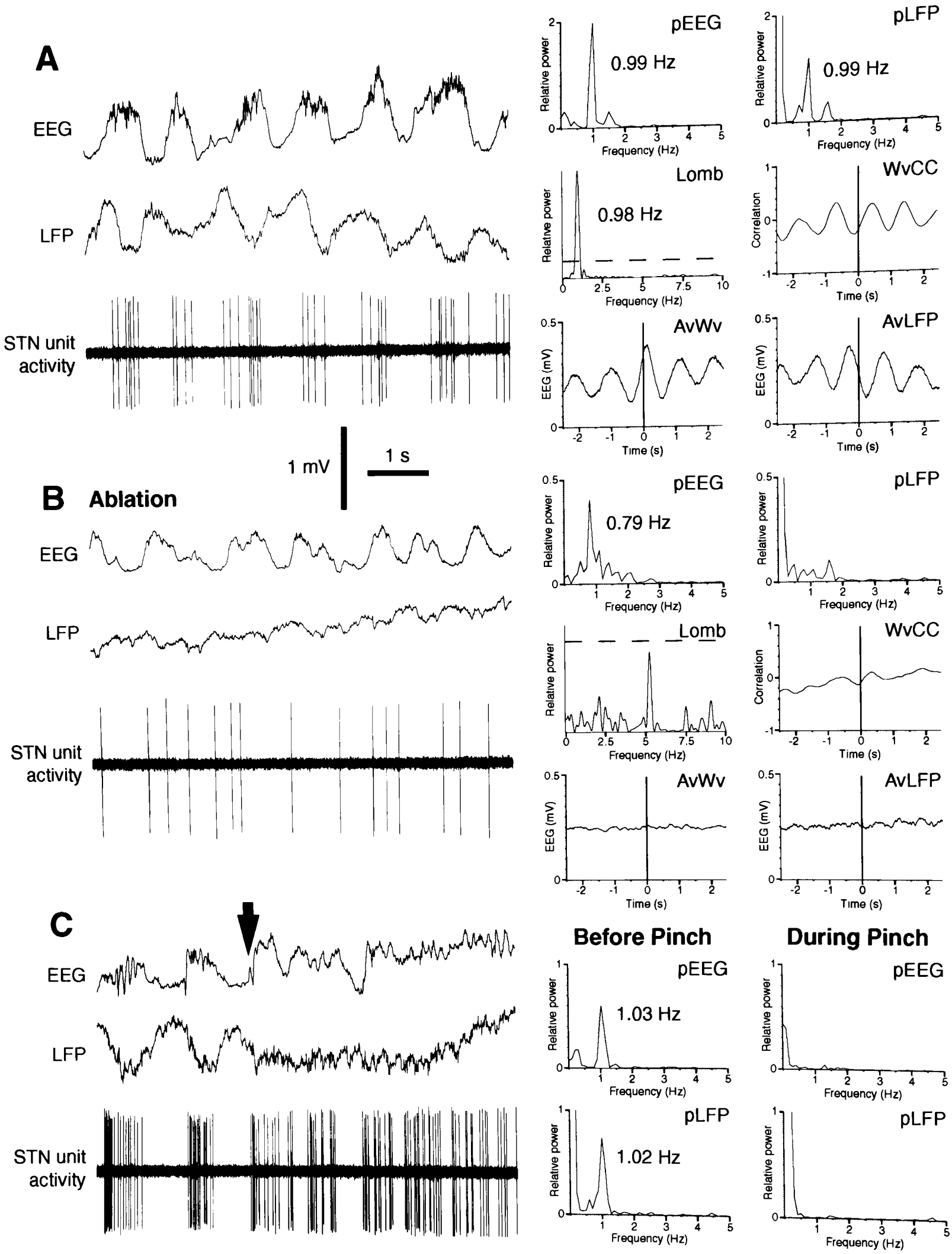
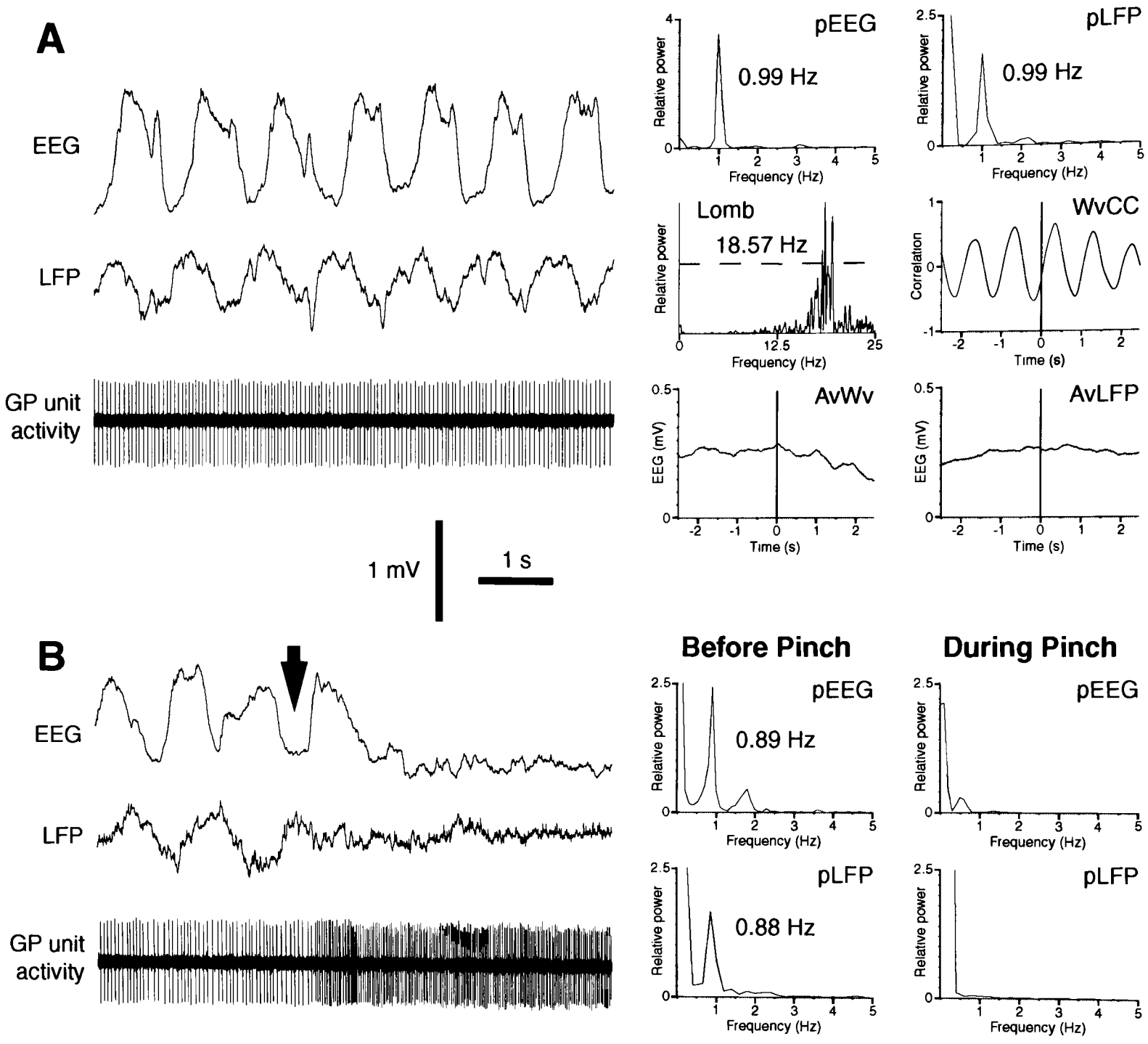

A
EEG
LFP
STN unit activity
1 mV
1 s
B Ablation
EEG
LFP
STN unit activity
C
EEG
LFP
STN unit activity
pEEG
0.99 Hz
Relative power
Frequency (Hz)
pLFP
0.99 Hz
Relative power
Frequency (Hz)
Lomb
0.98 Hz
Relative power
Frequency (Hz)
WvCC
Correlation
Time (s)
AvWv
EEG (mV)
Time (s)
AvLFP
EEG (mV)
Time (s)
pEEG
0.79 Hz
Relative power
Frequency (Hz)
pLFP
Relative power
Frequency (Hz)
Lomb
Relative power
Frequency (Hz)
WvCC
Correlation
Time (s)
AvWv
EEG (mV)
Time (s)
AvLFP
EEG (mV)
Time (s)
Before Pinch
During Pinch
pEEG
1.03 Hz
Relative power
Frequency (Hz)
pEEG
Relative power
Frequency (Hz)
pLFP
1.02 Hz
Relative power
Frequency (Hz)
pLFP
Relative power
Frequency (Hz)

Figure 4.12. Neuronal activity in the GP of control rats under urethane anaesthesia is not closely related to the coincident local field potential. *A*, Regular firing GP neuron (CV = 0.21 ; mean rate = 19.0 Hz). The neuron displayed a highly regular, single-spike firing pattern that was maintained during episodes of cortical SWA. Note that robust SWA in the cortex was mirrored in the LFP. Thus, the pLFP and Lomb periodogram were dissimilar and the AvLFP was almost flat. Oscillations in the LFP were similar in morphology to cortical SWA, but the polarity of the LFP was reversed compared to cortical SWA. Comparison of the power spectra of the EEG and the LFP demonstrated identical frequencies of oscillatory activity in the cortex and in the local vicinity of the GP neuron. Cross-correlation analysis of the LFP and EEG (WvCC) confirmed the near-reciprocal phase relationship of the two waveforms. *B*, Hindpaw pinch (7 s duration; starts at *arrow*) obliterated SWA in the intact cortex and LFP, and evoked an increase in the mean firing rate of another GP neuron (CV = 0.26 mean = 24.1 Hz, before pinch; CV = 0.28, mean = 44.4 Hz, during pinch). Neurons were recorded in the same animal. Calibration bars apply to all left hand panels.


A
EEG
LFP
GP unit activity
1 mV
1 s
pEEG
0.99 Hz
Relative power
Frequency (Hz)
pLFP
0.99 Hz
Lomb
18.57 Hz
WvCC
Correlation
Time (s)
AvWv
EEG (mV)
AvLFP
B
Before Pinch
During Pinch
0.89 Hz
0.88 Hz

mirrored by increases in the rate of firing of GP neurons as discussed in section 4.3.5 above (Fig. 4.12*B*). Slow-wave activity was not observed in the LFP before the resumption of SWA in the EEG (data not shown).

These preliminary data suggest that cortical SWA propagates to the STN and is expressed at a local level as low-frequency oscillations in the field potential and unit activity. Furthermore, the absence of LFO firing in the normal GP during urethane anaesthesia is probably not due to a breakdown in the propagation of oscillations to the GP, but may be the result of the failure of rhythmic input (as evidenced by oscillations in LFP) to reach firing threshold.

4.3.8 Firing properties and response profiles of substantia nigra *pars reticulata* neurons in a 6-OHDA-lesioned animal before and after cortical ablation

Histochemical analysis of recording sites in one 6-OHDA-lesioned animal revealed that the recorded units were located in the rostral portion of the substantia nigra *pars reticulata*. The physiological data from this experiment are pertinent to this thesis and have been included within since it is important to establish how the outcome of information processing in the STN-GP network is integrated by the output nuclei of the basal ganglia to influence behaviour.

During periods of robust SWA in the ipsilateral cortex, extracellular unit recordings revealed that SNpr neurons (n = 6) in the 6-OHDA-lesioned animal exhibited LFO firing patterns and that the discharge of these neurons was most closely associated with the active component of the cortical slow-wave (Fig. 4.13*A*, Table 4.7). Moreover, the frequency of LFO unit activity was not statistically different from the frequency of the coincident slow oscillation in the frontal cortex (Table 4.7).

Following cortical ablation, LFO firing in SNpr neurons was abolished (Fig. 4.13*B*). During periods of robust SWA in the contralateral cortex, SNpr neurons (n = 6) discharged

Figure 4.13. Neuronal activity in the SNpr of 6-OHDA-lesioned rats under urethane anaesthesia is closely related to coincident cortical activity. *A*, Low-frequency oscillatory SNpr neuron (CV = 0.77; mean rate = 36.2 Hz). The neuron fired predominantly during the active component of the cortical slow-wave (also see AvWv). Rhythmic spike-firing was apparent from the broad peaks in the auto-correlogram. Comparison of the Lomb periodogram with the pEEG indicated a similar frequency of rhythmic activity in the SNpr spike train and cortex. *B*, Regular firing SNpr neuron (CV = 0.23; mean rate = 20.6 Hz) recorded after cortical ablation. The SNpr neuron displayed a highly regular, single-spike firing pattern that was maintained during episodes of robust SWA in the contralateral cortex. Thus, the pEEG and Lomb periodogram were dissimilar, broad peaks were not observed in the auto-correlogram, and the AvWvs were almost flat. The neuron exhibited a mean firing rate that was similar to the dominant frequency of activity in the Lomb periodogram. Note that the CV values of each neuron reflected the differences in firing pattern observed. Neurons were recorded in the same animal. Calibration bars apply to both left hand panels.

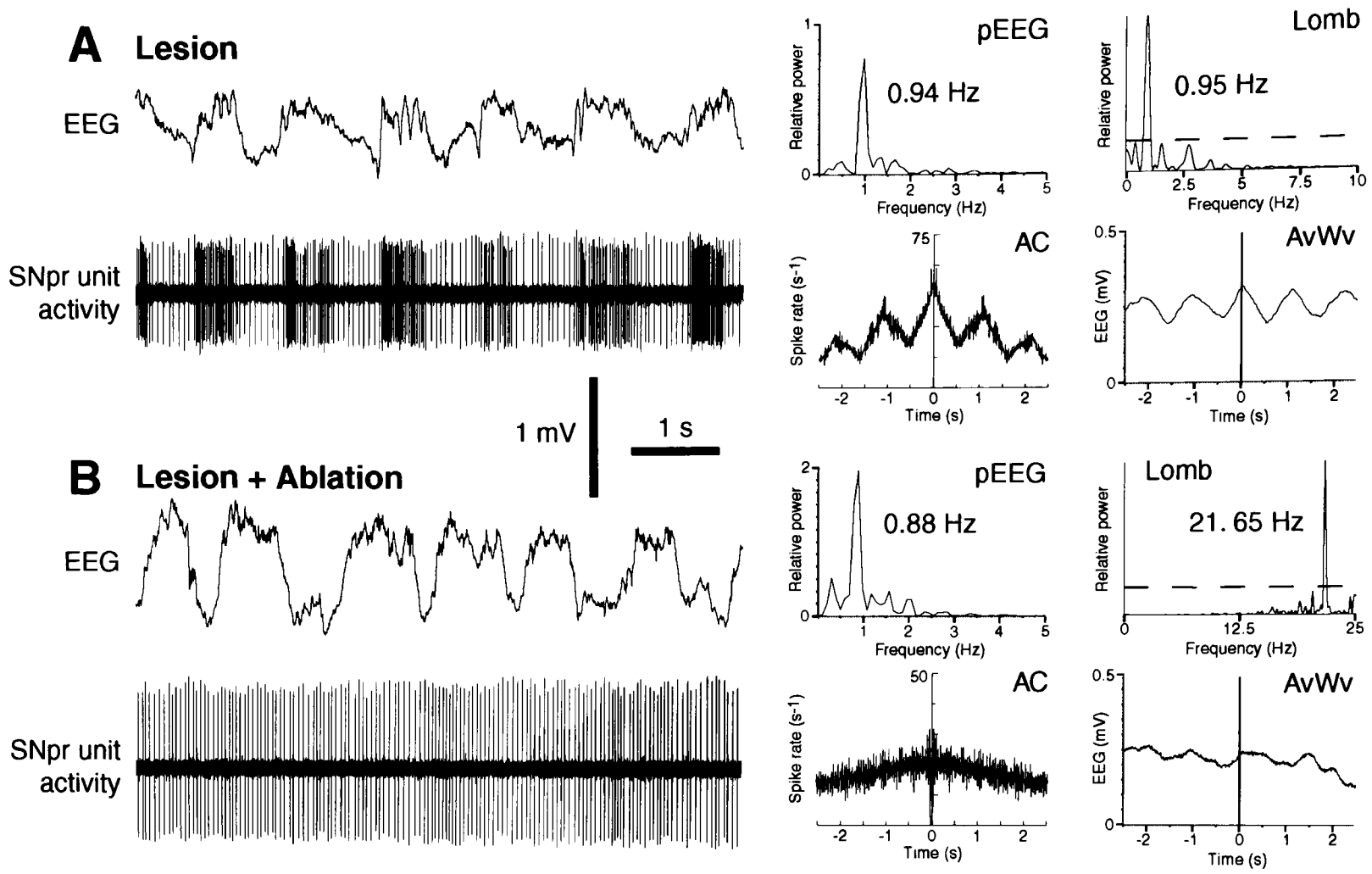

A
Lesion
EEG
SNpr unit activity
1 mV
1 s
B
Lesion + Ablation
EEG
SNpr unit activity
pEEG
0.94 Hz
Relative power
Frequency (Hz)
Lomb
0.95 Hz
Relative power
Frequency (Hz)
AC
Spike rate (s-1)
Time (s)
AvWv
EEG (mV)
Time (s)
pEEG
0.88 Hz
Relative power
Frequency (Hz)
Lomb
21.65 Hz
Relative power
Frequency (Hz)
AC
Spike rate (s-1)
Time (s)
AvWv
EEG (mV)
Time (s)

Table 4.7. Firing properties of SNpr neurons in a 6-OHDA-lesioned animal under urethane anaesthesia.

	6-OHDA-LESIONED	
	Intact cortex	**Ablated cortex**
No. of observations	6	6
Low-frequency oscillatory neurons [a]	6	0
Irregular neurons	0	0
Regular neurons	0	6
Mean Firing rate (Hz)		
All neurons	34.5 ± 10.2	14.3 ± 5.2
Low-frequency oscillatory neurons	34.5 ± 10.2	-
Irregular neurons	-	-
Regular neurons	-	14.3 ± 5.2
Coefficient of Variation		
Low-frequency oscillatory neurons	0.73 ± 0.27	-
Irregular neurons	-	-
Regular neurons	-	0.19 ± 0.05
No. of oscillating neurons	6	6
Low-frequency oscillatory neurons	6	0
Irregular neurons	0	0
Regular neurons	0	6
Frequency of spike train oscillation (Hz)		
Low-frequency oscillatory neurons	0.79 ± 0.13	-
Irregular neurons	-	-
Regular neurons	-	14.54 ± 4.45
Frequency of cortical SWA (Hz) [b]	0.82 ± 0.14	0.82 ± 0.10

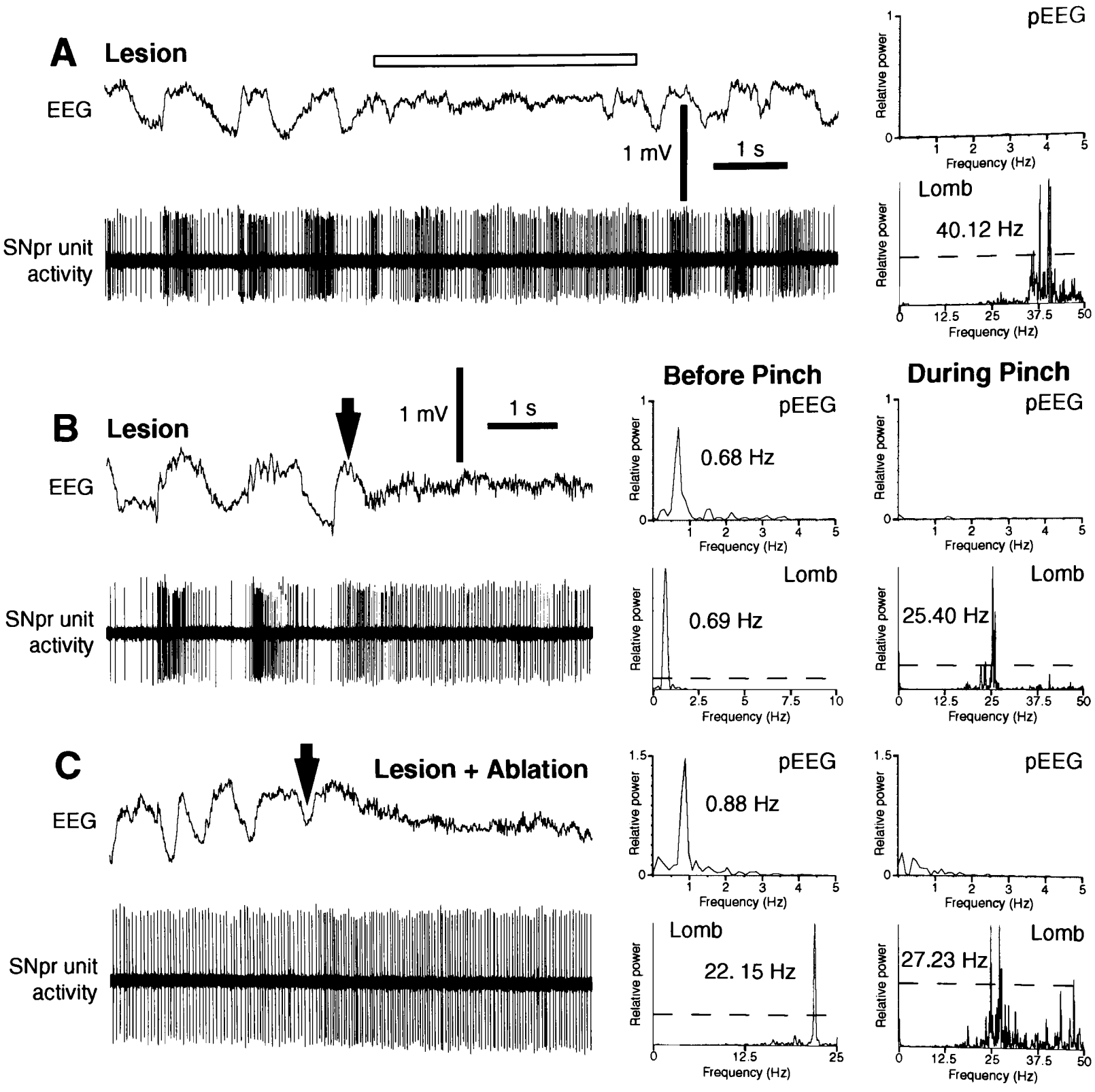
a Neurons were defined as displaying a significant, low-frequency oscillation in their spike trains (frequency of ≤ 2.0 Hz; $p < 0.05$);
b Cortical SWA was determined from contralateral frontal EEG in the case of neurons recorded after ablation of ipsilateral cortex.
Data are expressed as mean ± SD.

in a regular manner throughout the entire cycle of the cortical slow-wave; these neurons displayed a significant peak in the Lomb periodogram at a frequency that closely matched the mean rate of firing (Fig. 4.13*B*, Table 4.7). Furthermore, the mean discharge rate of SNpr neurons after ablation was significantly lower than before ablation. These data indicate that the pattern and rate of firing of SNpr neurons was tightly correlated with coincident activity in the ipsilateral cortex of the 6-OHDA-lesioned animal in urethane anaesthesia.

Hindpaw pinch-evoked or spontaneous decreases in the power of cortical SWA were always associated with changes in the rate and/or pattern of firing of SNpr neurons (Fig. 4.14). During ipsilateral cortical activation, significant low-frequency oscillations in SNpr firing were abolished and neurons adopted tonic, regular or irregular firing patterns (Fig. 4.14*A*, *B*). Furthermore, the firing rates of SNpr neurons either increased (Fig. 4.14*A*; 113 ± 7% of control rates; n =2 [1 pinch]) or decreased (Fig. 4.14*B*; 89 ± 1%; n = 2 [1 pinch]) in response to cortical activation.

Subsequent to ipsilateral cortical ablation, sensory stimulation by hindpaw pinch was accompanied by changes in the rate and pattern of firing of SNpr neurons (Fig. 4.14*C*). In contrast to responses observed with an intact cortical input, SNpr neurons uniformly adopted a tonic firing pattern and slightly increased their mean rate of firing (Fig. 4.14*C*; 125 ± 11%; mean firing rates before and during pinch were 13.2 ± 6.2 Hz and 16.2 ± 7.3 Hz, respectively (not significantly different); n = 4). Taken together, these preliminary observations suggest that the responses of SNpr neurons to global activation are heterogeneous in dopamine-depleted animals under urethane anaesthesia and that corticofugal pathways are involved in these complex responses.

Figure 4.14. Global activation alters the patterns and rates of firing of SNpr neurons in 6-OHDA-lesioned rats under urethane anaesthesia. *A*, Low-frequency oscillatory SNpr neuron. Spontaneous, brief reductions in cortical SWA (under *white bar*) were associated with a loss of LFO activity and an increase in the mean firing rate of the SNpr neuron (same neuron as in Fig. 4.13*A*; CV = 0.77; mean = 36.2 Hz, before spontaneous cortical activation; CV = 0.43; mean = 39.1 Hz, during activation). The pEEG and Lomb periodogram to the *right* were determined during a prolonged period of spontaneous activation that occurred later in the same recording session since the reduction in SWA shown was too short-lived to analyse accurately. Low-frequency oscillatory activity swiftly resumed when robust SWA was restored to the EEG (data not shown). *B*, Sensory stimulation (pinch starts at *arrow*) obliterated cortical SWA and led to a loss of LFO activity, with a concomitant decrease in firing rate, of another SNpr neuron (CV = 1.20; mean = 27.0 Hz, before pinch; CV = 0.25; mean = 22.0 Hz, during pinch). *C*, Regular firing SNpr neuron recorded after ablation (CV = 0.20; mean = 21.6 Hz, before pinch). Disruption of contralateral SWA by the pinch (*arrow*) was associated with an increase in the mean firing rate of the SNpr neuron (CV = 0.22; mean = 26.2 Hz, during pinch). Neurons were recorded in the same animal. Calibration bars in left hand panel of *B* apply to *C*.


A
Lesion
EEG
1 mV
1 s
SNpr unit activity
pEEG
Relative power
Frequency (Hz)
Lomb
40.12 Hz
B
Lesion
Before Pinch
During Pinch
0.68 Hz
0.69 Hz
25.40 Hz
C
Lesion + Ablation
0.88 Hz
22. 15 Hz
27.23 Hz

4.4 Discussion

The results of this study extend the findings of the previous study and demonstrate that the spike discharge properties of neurons in the normal and dopamine-depleted STN-GP network are strictly related to coincidental cortical or global activity. In control animals, the spike trains of STN neurons displayed low-frequency oscillations and firing was predominantly correlated with the active component of the slow-wave in the cortex and LFP. In contrast, GP neurons fired in a tonic, regular manner that was not correlated with activity in the STN, cortex or LFP. In the absence of dopamine, STN neurons also discharged in time with SWA, but over 2 fold more intensely, and GP neurons developed SWA-related, LFO firing patterns without a change in mean rate. Low-frequency oscillatory firing patterns in the control and dopamine-depleted network were largely abolished by ipsilateral cortical ablation. Obliteration of SWA by sensory stimulation reduced oscillatory firing and increased activity in the control STN-GP network. Following the depletion of dopamine, the response of the STN-GP network to global activation was altered profoundly; STN activity was greatly increased and a population of GP neurons was inhibited.

The cerebral cortex dictates the rate and pattern of activity in the STN, but not in the GP, of normal animals under urethane anaesthesia

The EEGs of rats anaesthetised with urethane were dominated by a low-frequency oscillation (~1 Hz) that was similar in form to that described previously in naturally sleeping or anaesthetised rats, cats and humans (Steriade et al., 1993c, 1996; Achermann and Borbély, 1997; Amzica and Steriade, 1998; Steriade and Amzica, 1998; Duque et al., 2000; Urbain et al., 2000). As such, EEG activity was essentially identical to that described in Chapter 3. The slow oscillation is generated by synchronous, rhythmic depolarising (active component) and hyperpolarising (inactive component) transitions in the membrane potential

of principal cortical neurons (Steriade et al., 1993c; Cowan and Wilson, 1994; Amzica and Steriade, 1995; Contreras and Steriade, 1995; Destexhe et al., 1999). This activity leads to synchronous discharges in corticofugal pathways, which in turn, entrains the basal ganglia, thalamus and other subcortical structures to the slow oscillation (Steriade et al., 1993b; Stern et al., 1997). Indeed, in the present study, activity in STN neurons was tightly correlated with coincident SWA in the EEG and LFP. Subthalamic nucleus neurons tended to discharge more intensely during the positive and negative portions of the EEG and LFP slow-waves, respectively. Although, the non-laminar distribution of perikarya and dendrites in the STN (Hammond and Yelnik, 1983, Kita et al., 1983a; Afsharpour, 1985a) complicates the extrapolation of LFPs at the cellular and synaptic levels (Hubbard et al., 1969; Johnston and Wu, 1995), it is likely that negative voltage deflections in the LFP reflect periodic synaptic excitation and (net) depolarising potentials within the somata and/or dendrites of STN neurons (Frost, 1968; Hubbard et al., 1969; Steriade et al., 1993c, d; Johnston and Wu, 1995). The contribution of periodic synaptic inhibition to the LFP oscillations was probably minor since GP neurons only fired in a tonic, regular manner.

The removal of the ipsilateral cortex abolished LFO activity in STN neurons and SWA in the LFP. This change in activity was not due to shifts in states of global activation because SWA persisted in the contralateral hemisphere. The removal of cortical synaptic input by ablation resulted in slower, tonic firing of STN neurons, which was similar to the discharge pattern of STN neurons in deafferented, brain slice preparations (Nakanishi et al., 1987a; Flores et al., 1995; Overton and Greenfield, 1995; Abbott et al., 1997; Beurrier et al., 1999, 2000; Bevan and Wilson, 1999; Wigmore and Lacey, 2000; also see Chapter 5) and suggests that the cortex acts as a potent driving force of neuronal activity in the STN. It is likely that SWA in neurons of the corticosubthalamic pathway, rather than activity in the indirect pathway, underlies oscillatory activity in the STN because the cortical ablation had little effect on the activity of GP neurons.

In contrast to the STN, the GP was not entrained by coincident cortical SWA, suggesting that monosynaptic (Naito and Kita, 1994b; Lévesque et al., 1996; Lévesque and Parent, 1998) and polysynaptic pathways (Smith et al., 1998) from the cortex to the GP have minimal impact on neuronal activity (Urbain et al., 2000). Furthermore, cortical ablation had no effect on the rate or pattern of firing of GP neurons. Indeed, the activity of GP neurons in this preparation mimicked the spontaneous, autorhythmic discharge observed *in vitro* (Nakanishi et al., 1985; Nambu and Llinás, 1994; Stanford and Cooper, 1999; Cooper and Stanford, 2000). Thus, activity of neurons in the STN-GP network display little correlation in normal, urethane anaesthetised or unanaesthetised animals during sleep (Urbain et al., 2000). Given that the GP may actually receive rhythmic excitatory synaptic input from the STN, as indicated by the negative deflections in the LFPs (Hubbard et al., 1969), the fact that this input is not reflected at the soma as oscillatory spiking activity suggests that a powerful synaptic drive is needed to overcome the mechanisms underlying the tonic, regular firing of these neurons. These observations confirm and extend the findings detailed in Chapter 3 and, taken together, indicate that in this preparation, the normal STN-GP network does not support emergent oscillatory activity in isolation from the cerebral cortex.

Rhythmic cortical activity is transmitted more effectively to the STN-GP network following the depletion of dopamine

The profile of SWA and the frequency of coincident, oscillatory activity in STN neurons in 6-OHDA-lesioned animals were similar to those observed in control animals. However, the intensity of oscillatory discharge was greater in 6-OHDA-lesioned animals. This effect was mostly abolished by cortical ablation, implying that the impact of cortical SWA on the STN is greater in the absence of dopamine. As in control rats, this change in activity was not due to shifts in states of global activation because SWA persisted in the contralateral hemisphere.

In marked contrast to observations in control animals under urethane anaesthesia, GP neurons in 6-OHDA-lesioned animals displayed LFO firing patterns with a frequency that closely matched the frequency of coincident SWA. However, the firing rate was not significantly different from that observed in control animals. The oscillatory firing patterns of GP neurons were likely to have been generated by more intense activity in subthalamopallidal projections because ablation of the STN in parkinsonian animals has been shown to regularise activity in GP and basal ganglia output nuclei (Wichmann et al., 1994b; Burbaud et al., 1995; Murer et al., 1997; Ni et al., 2000; Tseng et al., 2000). In support of this, destruction of the cortex, which results in the abolition of LFO activity in the STN, led to more regular activity in the GP. The increased rate of STN activity following 6-OHDA-lesions, or the decreased rate of STN activity following cortical ablation, were not associated with an alteration in the rate of firing of GP neurons. The poor correlations in the relative rates of activity in the STN and GP observed in this part of the study are not in keeping with the widely held direct/indirect pathway model (Albin et al., 1989b; DeLong, 1990). Furthermore, these findings indicate that the majority of the STN-GP network in this preparation does not support emergent oscillatory activity in isolation from the cerebral cortex. It should be stressed however, that a subpopulation of neurons (20% in STN, 15% in GP) continued to display LFO activity following ipsilateral cortical ablation. It is possible that (1) these neurons were driven by remaining parts of the cortex (Canteras et al., 1988, 1990); (2) the STN-GP network does in fact support oscillatory activity, but this activity is only expressed in a minority of neurons (Plenz and Kitai, 1999); or (3) oscillatory activity was driven by intrinsic membrane properties (Nambu and Llinás, 1994; Beurrier et al., 1999).

Dopamine has multiple pre- and post-synaptic actions in each nucleus of the basal ganglia (see recent reviews by Greengard et al., 1999; Nicola et al., 2000; Smith and Kieval, 2000 and references therein). Loss of dopaminergic tone will have profound effects on the

manner in which basal ganglia neurons communicate with each other and, as a consequence, the interaction of basal ganglia networks with the rest of the brain. Although cortical EEG was not altered by dopamine depletion, the possibility that pathological STN-GP network activity reverberated throughout the cortical-basal ganglia-thalamocortical loop and led to abnormal input from other afferents, which further exacerbated pathological activity, cannot be excluded.

Rhythmic cortical activity is expressed in the substantia nigra *pars reticulata* in the dopamine-depleted brain

All SNpr neurons in 6-OHDA-lesioned animals displayed low-frequency oscillatory firing patterns that matched the frequency of coincident SWA. Although a direct comparison between activity in the normal and dopamine-depleted SNpr cannot be made from these preliminary findings, it is noteworthy that a transition from regular or slightly irregular patterns of activity to rhythmic, bursting activity in the SNpr is almost exclusively associated with the parkinsonian disease state (Sanderson et al., 1986; MacLeod et al., 1990; Burbaud et al., 1995; Murer et al., 1997; Rohlfs et al., 1997; Wichmann et al., 1999; Tseng et al., 2000). It is likely that the LFO firing of SNpr neurons was driven by powerful, rhythmic activity in the subthalamonigral projection. Indeed, it has been shown that ablation of the STN in parkinsonian animals regularises activity in the SNpr (Burbaud et al., 1995; Murer et al., 1997; Tseng et al., 2000). In further support of this, destruction of the cortex, which resulted in the abolition of LFO activity in the STN, led to regular activity in the SNpr. It is also interesting to note that ketamine anaesthesia, in which spike-firing in the normal STN approximates the rate and pattern of firing observed in the STN of 6-OHDA-lesioned, urethane-anaesthetised animals (see Chapter 3), appears to promote burst-firing in SNpr neurons (Villa and Bajo Lorenzana, 1997). Although output from the hyperactive STN is probably critical, rhythmic input from the GP, which projects heavily to the SNpr (Totterdell

et al., 1984; Smith and Bolam, 1989, 1990b; Bevan et al., 1998), may also play a part in sculpting the burst-like activity of nigral output neurons (Fujimoto and Kita, 1992; Celada et al., 1999; Maurice et al., 1999). In addition, it is also possible that inhibitory input from other SNpr neurons (Deniau et al., 1982; Grofová et al., 1982) contributed to the LFO activity.

The removal of the cortical synaptic input by ablation resulted in the abolition of LFO activity and the subsequent adoption of slower, regular firing in SNpr neurons. This change in activity was not due to shifts in states of global activation because SWA persisted in the contralateral hemisphere. The regular pattern of firing observed *in vivo* following ablation was similar to the discharge pattern exhibited by GABAergic SNpr neurons in the *in vitro* slice preparation (Nakanishi et al., 1987b; Richards et al., 1997) and suggests that the cortex indirectly (*i.e.* through the STN) or directly (Bunney and Aghajanian, 1976; Kornhuber et al., 1984; Naito and Kita, 1994a) acts as a potent driving force of neuronal activity in the SNpr following the depletion of dopamine.

The depletion of dopamine profoundly alters the response of the STN-GP network to cortical activation

Sensory stimulation by hindpaw pinch was associated with the obliteration of large-amplitude, low-frequency oscillations and the appearance of smaller-amplitude, higher-frequency waves in the EEG. In control animals, such cortical activation was associated with increases in the mean firing rates of all neurons that were tested. Low-frequency oscillatory activity in STN neurons was abolished during cortical activation, whereas the firing patterns of GP neurons were unaltered. The effects of sensory stimulation on the EEG were similar to those that have been observed after electrical stimulation of the midbrain reticular activating system (Moruzzi and Magoun, 1949; Steriade et al., 1993a, 1996). This activating system suppresses the episodes of hyperpolarisation in cortical neurons during

SWA, resulting in an increase in corticofugal activity and a reduction in global synchrony (Steriade et al., 1993a, 1996). Thus, the increased activity observed in the STN-GP network is probably driven, at least in part, by the cortex. Excitatory subcortical afferents to the STN-GP network, including those from the intralaminar thalamic nuclei (Sugimoto et al., 1983; Kincaid et al., 1991b; Mouroux and Féger, 1993; Mouroux et al., 1995, 1997), PPN (Hammond et al., 1983a; Garcia-Rill, 1991; Lee et al., 1988; Canteras et al., 1990; Bevan and Bolam, 1995; Flores et al., 1996) and DRN (Mori et al., 1985a, b; Canteras et al., 1990; Flores et al., 1995) may have been activated by sensory stimulation since increases in network activity were also observed following cortical ablation.

Sensory stimulation in 6-OHDA-lesioned animals led to cortical activation, which was similar in profile to that observed in control animals. Cortical activation increased the activity of STN neurons to a greater degree than in control animals. In clear distinction to the responses of GP neurons in control animals, both inhibition and facilitation of firing accompanied global activation in 6-OHDA-lesioned animals. Decreased activity in the GP, together with significantly increased activity in the STN, suggests that the indirect pathway is overactive in the parkinsonian brain, as predicted by the direct/indirect pathway model of basal ganglia pathophysiology (Albin et al., 1989b; DeLong, 1990). Thus, in this preparation, evidence for overactivity of the indirect pathway was observed during states of global activation and not during spontaneous, resting activity. This observation may help to reconcile conflicting reports of the effects of dopamine deficiency on the firing rates of GP neurons in awake animals (significant decrease in firing rate: Filion et al., 1988; Pan and Walters, 1988; Filion and Tremblay, 1991; Boraud et al., 1998, 2000b; Raz et al., 2000) and urethane-anaesthetised animals (little or no change in firing rate: Pan and Walters, 1988; Hassani et al., 1996; Ni et al., 2000). The increases in activity in the GP that were also observed during cortical activation in 6-OHDA-lesioned animals however, suggest that the relationship between the STN and GP cannot be accounted for simply in terms of firing rate.

In 6-OHDA-lesioned animals with cortical ablations, increased activity in the STN-GP network was the only response to sensory stimulation. The activity of GP neurons is largely governed by inputs from the STN and the NS (Robledo and Féger, 1990; Ryan and Clark, 1991; Kita and Kitai, 1991; Kita, 1992; Yoshida et al., 1993; Soltis et al., 1994; Smith et al., 1998; Nambu et al., 2000), as well as intrinsic membrane properties (Nambu and Llinás, 1994; Stanford and Cooper, 1999; Cooper and Stanford, 2000). Since STN neurons were excited during global activation in 6-OHDA-lesioned rats with intact cortices, the inhibition of GP activity was probably the result of cortical activation of the neostriatum and, hence, the indirect pathway. However, the possibility that other inputs to GP neurons (see section 1.3) are important cannot be ruled out. Finally, these data demonstrate that in 6-OHDA-lesioned animals, LFO activity in the STN-GP network is not a feature associated with global activation.

Implications for information processing in the STN-GP network in health and Parkinson's disease

The principal findings of this study are that oscillatory cortical activity is expressed more powerfully by the STN-GP network in the dopamine-depleted brain and that the manner in which cortical information is processed by the network is altered profoundly by the chronic loss of dopaminergic tone. Furthermore, oscillatory activity in the network is largely abolished by removal of rhythmic cortical input. These data imply that resting tremor in PD may be caused by the inappropriate amplification, transformation and propagation by the basal ganglia of cortical rhythms associated with quiet wakefulness (Alberts et al., 1969; Elble and Koller, 1990; Volkmann et al., 1996; Llinás et al., 1999; Hellwig et al., 2000). By inference, the loss of resting tremor during voluntary movement may be due to the adoption of higher frequency cortical rhythms during global activation (Hari and Selenius, 1999; Feige et al., 2000; Kilner et al., 2000). However, a component of the STN-GP network

continued to oscillate independently of the cortex in the 6-OHDA-lesioned hemisphere, implying that intrinsic properties of this network may also pattern oscillatory activity in PD (Nambu and Llinás, 1994; Beurrier et al., 1999; Plenz and Kitai, 1999). As low-frequency oscillatory activity in the brain is associated with long term changes in synaptic efficacy, abnormally intense oscillatory activity in the parkinsonian brain may be consolidated during sleep and/or wakefulness, and further exacerbate the symptoms of PD (Kavanau, 1997; Charpier et al., 1999; Steriade, 1999).

The augmentation of the indirect pathway during global activation indicates that inputs from the activated cortex are processed differently in the parkinsonian brain. Indeed, incorrect integration of cortical information has been proposed to underlie, in part, the symptoms of PD (Filion et al., 1988; DeLong, 1990; Bergman et al., 1994; Rothblat and Schneider, 1995; Calabresi et al., 1996; Boraud et al., 2000a).

Taken together, the results of this and other studies demonstrate that both the rate and pattern of activity of basal ganglia neurons are altered profoundly in PD. Furthermore, the relative contribution of rate and pattern to aberrant information coding is related to the state of activation of the cerebral cortex.

The relative contributions of inhibitory and excitatory synaptic inputs to shaping activity in the STN-GP network cannot be directly determined from extracellular unit recordings. As detailed in Chapter 5, an *in vitro* brain slice preparation was utilised to better elucidate the dynamics of inhibitory (GABAergic) synaptic input to the STN.

CHAPTER 5.

$GABA_A$ RECEPTOR-MEDIATED INPUT TO SUBTHALAMIC NUCLEUS NEURONS *IN VITRO*

5.1 Introduction

Inhibitory, GABAergic inputs to the STN predominantly arise from the GP (Fonnum et al., 1978; van der Kooy et al., 1981; Smith et al., 1990), the VP (Groenewegen and Berendse, 1990, Bell et al., 1995; Bevan et al., 1997) and, to a lesser extent, the MTg (Bevan and Bolam, 1995). The boutons of pallidosubthalamic fibres establish synaptic contact with all parts of STN neurons and are often grouped to ensheath the perikarya and dendrites of STN neurons in a basket-like fashion, such that single GP axons may give rise to several varicosities apposed to a single STN neuron (Smith et al., 1990; Bevan et al, 1997). Furthermore, pallidosubthalamic synaptic terminals converge with cortical or thalamic terminals on the dendrites of STN neurons (Bevan et al., 1995). Taken together, these anatomical data suggest that the pallidosubthalamic projection is well suited to tempering and shaping activity in the STN.

The GP has long been regarded as having an important inhibitory influence over the spontaneous activity of STN neurons *in vivo* (Tsubokawa and Sutin, 1972; Ohye et al., 1976; Rouzaire-Dubois et al., 1980). Pharmacological blockade of GABAergic neurotransmission with the selective $GABA_A$ receptor antagonist, bicuculline (Rouzaire-Dubois et al., 1980; Robledo and Féger, 1990; Féger and Robledo, 1991; Rouzaire-Dubois and Scarnati, 1987), or excitotoxic lesion of the GP (Ryan and Clark, 1992; Ryan et al., 1992) both result in substantially increased rates and altered patterns of unit activity in the STN. Activation of $GABA_A$ receptors in the STN predictably decreases unit activity (Rouzaire-Dubois et al., 1980; Rouzaire-Dubois and Scarnati, 1987; Féger and Robledo, 1991; Nambu et al., 2000). Intracellular recordings have shown that electrical stimulation of the GP or internal capsule evokes Cl^--dependent, monosynaptic IPSPs in STN neurons (Kita et al., 1983b; Nakanishi et al., 1987a; Shen and Johnson, 2000). Furthermore, these evoked IPSPs are bicuculline-sensitive (Nakanishi et al., 1987a; Shen and Johnson, 2000). Taken together with the results

of studies of unit activity *in vivo*, the intracellular data suggest that the inhibitory input to the STN from the GP is largely mediated by $GABA_A$ receptors, which are fast-acting, ligand-gated Cl^- channels (see Kaila, 1994; Stephenson, 1995 and references therein).

The pivotal role of $GABA_A$ receptor-mediated neurotransmission in the STN in normal, motor-related functions of the basal ganglia is exemplified by studies in awake, behaving rats, cats and monkeys that have demonstrated that pharmacological manipulation of GABAergic input with high doses of selective $GABA_A$ receptor agonists or antagonists leads to profound motor disturbances (Crossman et al., 1984; Jackson and Crossman, 1984; Murer and Pazo, 1993; Spooren et al., 1995; Dybdal and Gale, 2000; Nambu et al., 2000). Furthermore, inactivation of the STN with very low doses of $GABA_A$ receptor agonists may still produce attentional and motivational deficits without inducing stereotypy or hypermotility (Baunez and Robbins, 1999). The $GABA_A$ receptor-mediated inhibition of STN neurons is also critical for non-motor functions of the basal ganglia. Indeed, the role of the SNpr in the modulation of generalised epileptic seizures is a direct reflection of activity in the epileptogenic subthalamonigral pathway (Deransart et al., 1996, 1998a, b; Velísková et al., 1996; Dybdal and Gale, 2000).

The termination of synaptic inhibition or a similar hyperpolarising potential can result in a paradoxical "rebound burst response" in many types of central neuron (Andersen et al., 1964; Llinás and Yarom, 1981; Deschênes et al., 1982; Jahnsen and Llinás, 1984a, b). The rebound burst response is composed of two distinct parts: (1) a voltage- and Ca^{2+}-dependent low-threshold spike (LTS; for review see Huguenard, 1996); and (2) a rapid succession of fast, Na^+-dependent action potentials that are superimposed on the LTS (Jahnsen and Llinás, 1984b). Removal of hyperpolarising current in STN neurons can also produce a rebound depolarisation that is accompanied by a high-frequency burst of spikes (Nakanishi et al., 1987a; Bevan and Wilson, 1999; Plenz and Kitai, 1999; Beurrier et al., 2000; Song et al., 2000). Thus, the effects of GABAergic inhibition on the STN are

potentially complex and may subserve other functions in addition to simply suppressing spiking activity. On the basis of whole-cell patch-clamp recordings of cultured STN and GP neurons, Plenz and Kitai (1999) have recently proposed that the phenomenon of rebound burst-firing in the STN is crucial for the generation of the pathological oscillatory activity that is commonly observed in the STN-GP network and its target nuclei in idiopathic and animal models of PD (Bergman et al., 1994; Nini et al., 1995; Rodriguez et al., 1998; Wichmann et al., 1999; Levy et al., 2000; Magariños-Ascone et al., 2000; Magnin et al., 2000, Raz et al., 2000). Rebound burst-firing is thought to arise through the interactions of STN neurons with reciprocally-connected GABAergic neurons of the GP via a mechanism that is similar to that reported to underlie spindling activity in the thalamus (for review see McCormick and Bal, 1997; Plenz and Kitai 1999). Low-frequency oscillatory activity is also present in the STN under normal resting conditions (see Chapters 3 and 4) and may also be supported, at least in part, by rebound burst responses to inhibition from the GP.

The first aim of this study was to test whether $GABA_A$ receptor-mediated inhibition could theoretically generate sufficient membrane hyperpolarisation in STN neurons with intact Cl^- gradients to produce rebound burst-firing. Thus, the equilibrium potential of $GABA_A$ receptor-mediated current ($E_{GABA\text{-}A}$) and the hyperpolarisation required for rebound burst-firing were determined in STN neurons using perforated patch-clamp recording techniques. The cation-selective, pore-forming substance gramicidin was used to maintain a natural intracellular concentration of Cl^- (Ebihara et al., 1995; Ulrich and Huguenard, 1997a), the major permeant ion of the $GABA_A$ receptor (Kaila, 1994). The second objective was to test whether IPSPs could evoke rebound burst responses in STN neurons. Thus, the reversal potential of monosynaptic $GABA_A$ receptor-mediated IPSPs ($E_{IPSP\text{-}A}$) was determined and the responses of STN neurons to electrically-evoked IPSPs were then characterised.

It should be noted that the research described in this chapter was performed in close collaboration with Dr. Mark Bevan. Approximately half of all neurons were recorded by Dr. Bevan. The two data samples were pooled together in order to better communicate this research. All of the following figures were derived from neurons that I recorded.

5.2 Experimental procedures

Methods for the preparation of brain slices and the recording of visualised STN neurons using the perforated patch-clamp technique are described in section 2.5.

5.2.1 Determination of $E_{GABA\text{-}A}$ and $E_{IPSP\text{-}A}$

Detailed descriptions of the methods employed for the measurement of these parameters are noted in section 2.6.

Recent physiological studies suggest that inhibition of the STN by GABAergic, pallidosubthalamic afferents may also be mediated by a second class of GABA receptor, the $GABA_B$ receptor (Booth et al., 1999). In contrast to $GABA_A$ receptors, the metabotropic $GABA_B$ receptors are functionally coupled to post-synaptic K^+ conductances and pre-synaptic Ca^{2+} conductances via G-proteins and second messenger systems and are typically slow-acting (for review see Deisz, 1997). To avoid possible confounding effects of $GABA_B$ receptor activation during pressure-pulse application of GABA or electrical stimulation of GABAergic axons, the selective $GABA_B$ receptor antagonist CGP 55845A was bath applied in all experiments at a concentration that saturated $GABA_B$ receptors (10 μM, IC_{50} = 7 nM; Froestl et al., 1992; Deisz, 1999). During the measurement of $E_{IPSP\text{-}A}$ and the subsequent characterisation of responses to inhibitory synaptic input, excitatory synaptic transmission was selectively blocked by bath application of the ionotropic excitatory amino acid receptor

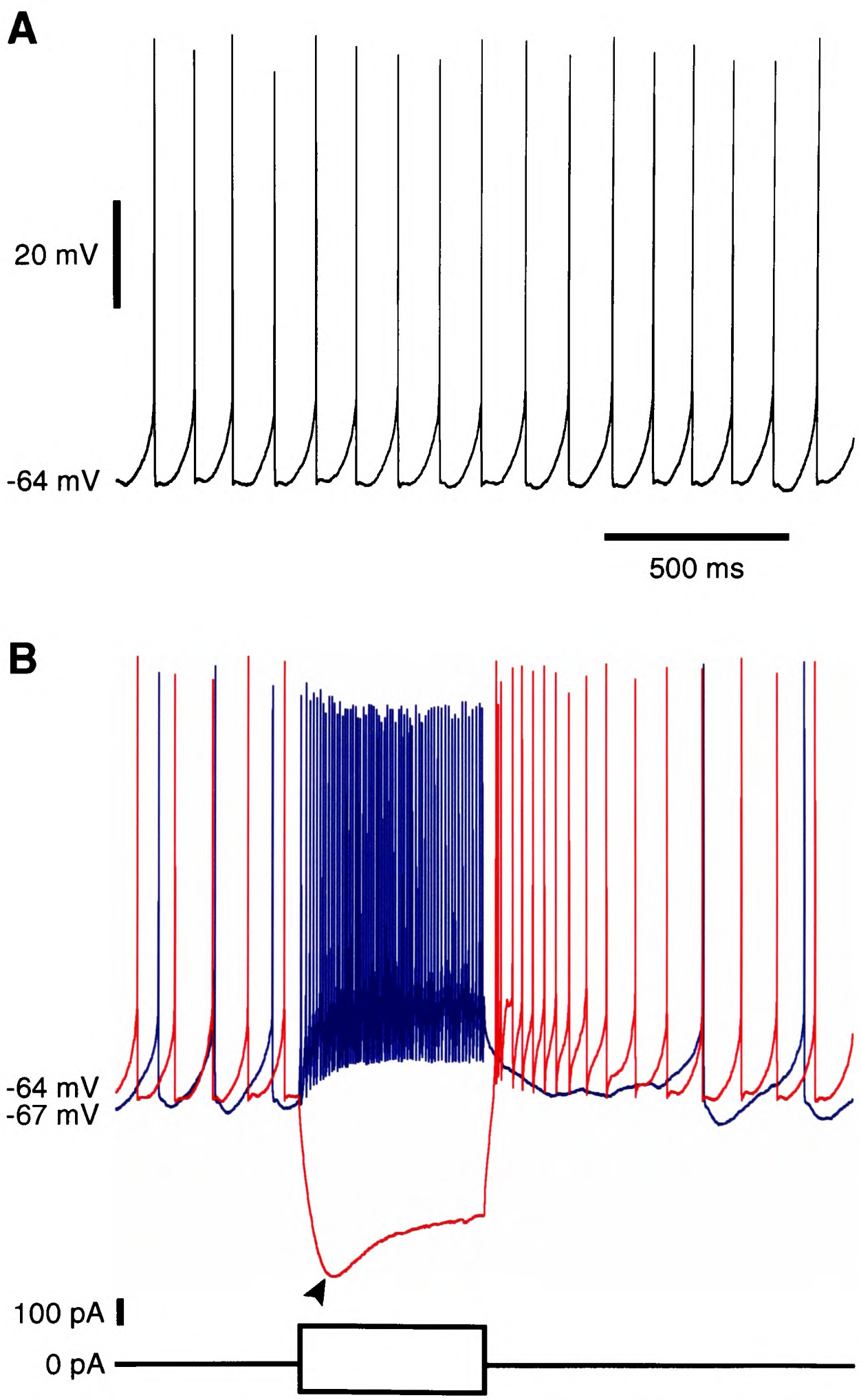
antagonists DNQX and APV (40 and 50 μM, respectively). For further details on acquisition and analysis of *in vitro* data, see section 2.6.

5.3 Results

5.3.1 Electrophysiological characteristics of STN neurons *in vitro*

In congruence with recordings made using the conventional whole-cell patch-clamp technique (Bevan and Wilson, 1999; Beurrier et al., 2000), most STN neurons (96%) recorded with the perforated patch-clamp method displayed slow and highly regular spontaneous spiking activity (Fig. 5.1*A*; mean firing rate of 10.3 ± 3.6 Hz; CV of 0.13 ± 0.05; n = 51). Spontaneous burst-firing activity (Beurrrier et al, 1999) was very rarely observed (4%; 2 of 51 recorded neurons). Spontaneous activity of STN neurons was stable for long periods (up to 3 hr) at physiological temperatures and was not dependent on the degree of membrane perforation or the series resistance (data not shown). The driven activity of STN neurons in perforated recordings was very similar to that reported for STN neurons recorded with the whole-cell patch-clamp technique (Fig. 5.1*B*; cf. Bevan and Wilson, 1999; Beurrier et al., 2000). Subthalamic nucleus neurons showed prominent time- and voltage-dependent inward rectification at very hyperpolarised membrane potentials (–75 mV and below; Figs. 5.1*B*, 5.2). Rebound burst responses were often seen at the break of hyperpolarising current pulses (Fig. 5.1*B*; see section 5.3.3 below). Furthermore, STN neurons were capable of firing at very high rates (300-500 Hz) with little frequency adaptation or spike accommodation in response to large depolarising current injections (Fig. 5.1*B*).

Figure 5.1. Spontaneous and driven firing of STN neurons recorded using the perforated patch-clamp technique. *A*, Current-clamp recording of spontaneously firing STN neuron in the absence of any current application. Note the highly regular nature of the single-spike discharge (mean firing rate = 9.6 Hz; CV = 0.12). *B*, Responses of the same STN neuron to large hyperpolarising (–100 pA; *red trace*) and depolarising (+140 pA; *blue trace*) current pulses of 500 ms duration. *Red trace*, The STN neuron responded to the hyperpolarising current pulse with a characteristic "sag" in membrane potential (*arrowhead*), which was attributable to the activation of a hyperpolarisation-activated mixed-cation current (I_h) at potentials below –70-75 mV (Bevan and Wilson, 1999). Note also the rebound burst response at the break of the hyperpolarising current pulse. *Blue trace*, The STN neuron was driven to fire at a high rate (~ 130 Hz), with only weak frequency adaptation and little spike accommodation, by the depolarising current injection. Note the long-duration AHP that followed the high-frequency firing. Voltages to the left of the traces refer to the membrane potential at the first point of the trace. Calibration bars in *A* apply to *B*.


A
20 mV
-64 mV
500 ms
B
-64 mV
-67 mV
100 pA
0 pA

5.3.2 Equilibrium potential of $GABA_A$ current in STN neurons

$E_{GABA\text{-}A}$ was determined using the current-clamp recording mode (–78 ± 5 mV, n = 20) and, in most cases, also using voltage-clamp mode (–78 ± 4 mV, n = 15). Note that similar estimations of $E_{GABA\text{-}A}$ were obtained with the two techniques and the difference in $E_{GABA\text{-}A}$ in individual STN neurons was small (2 ± 1 mV, n = 15). To ascertain whether the estimates of $E_{GABA\text{-}A}$ were influenced by damage of the patch membrane, the whole-cell configuration was established following perforated recording by rupturing the patch membrane with a negative pressure pulse (see sections 2.5, 2.6 and Fig. 2.2*C*; n = 6). In these cases, $E_{GABA\text{-}A}$ significantly shifted towards more positive values (–77 ± 6 mV, perforated; –52 mV ± 6 mV, whole-cell), as predicted by the Nernst equation (Cl^- equilibrium potential = –42 mV). Different recording temperatures did not significantly alter $E_{GABA\text{-}A}$ (–77 ± 5 mV at 30-32°C, n = 11; and –80 ± 4 mV at 35-37°C, n = 9). The responses of STN neurons to GABA were solely due to actions at $GABA_A$ receptors because the selective antagonist bicuculline (30 μM) abolished responses (n = 4).

Prolonged Cl^- influx leads to intracellular accumulation of the anion, which in turn, results in a decrease in the Cl^- driving force and a positive shift in $E_{GABA\text{-}A}$ (Huguenard and Alger, 1986; Thompson and Gähwiler, 1989). Since $GABA_A$ receptor-mediated currents are carried by both Cl^- and bicarbonate (HCO_3^-) ions, which travel in opposite directions through the receptor channel (Kaila, 1994), chloride loading of the cytosol is accompanied by an extracelluar accumulation of HCO_3^- (Kaila, 1994). The resultant shift in the HCO_3^- gradient is rapidly compensated by the regeneration of HCO_3^- by the intraneuronal enzyme, carbonic anhydrase (Staley et al., 1995). To test whether chloride-loading of neurons by pressure application of GABA altered $E_{GABA\text{-}A}$, the membrane-permeable carbonic anhydrase inhibitor, ethoxyzolamide, was applied during the $E_{GABA\text{-}A}$ determination protocol for 6 neurons. $E_{GABA\text{-}A}$ did not significantly change in the presence of the inhibitor (–77 ± 6 mV for control; –79 ± 5 mV for ethoxyzolamide), which suggests that (1) there was no shift in

the HCO_3^- gradient; and (2) neurons were not chloride-loaded, and thus, $E_{GABA\text{-}A}$ was dominated by the chloride gradient (Staley et al., 1995). Since the pore of the gramicidin ionophore does not allow the free passage of divalent cations (Hladsky and Haydon, 1984), neurons recorded using the perforated patch-clamp technique can be considered to have intact Ca^{2+} handling. Thus, the potential modulatory effects of intracellular Ca^{2+} on $GABA_A$ receptor function (Kaila, 1994) were probably limited by natural buffering mechanisms.

5.3.3 Rebound burst-firing of STN neurons

Rebound burst-firing was observed at the break of a hyperpolarising current pulse of 500 ms duration in 17 of 20 neurons tested in the $E_{GABA\text{-}A}$ study (Figs. 5.2, 5.3). The appearance of the rebound burst varied dramatically and neurons fired either short- (Fig. 5.2*A*, *C*, n = 12) or long-duration bursts (Fig. 5.2*B*, n = 5). Three neurons did not fire rebound bursts when membrane potentials of ~ −100 mV and less were tested under the standard experimental conditions (Fig. 5.2*D*).

The mean hyperpolarisation threshold required for rebound burst-firing was −78 ± 3 mV (n = 17). Burst thresholds were not significantly different at the two recording temperatures (−78 ± 3 mV at 30-32°C, n = 11; and −77 ± 3 mV at 35-37°C, n = 6). $E_{GABA\text{-}A}$ was equal to, or more hyperpolarised than, the threshold for rebound burst-firing in 14 of the 17 neurons that fired rebound bursts (Fig. 5.3). These data suggest that $GABA_A$ receptor-mediated current could theoretically generate rebound burst-firing in STN neurons that are capable of generating this type of response.

5.3.4 Reversal potential of $GABA_A$ receptor-mediated IPSPs in STN neurons

Subsequent to the $E_{GABA\text{-}A}$ study, a second series of experiments were carried to test whether inhibitory post-synaptic potentials could evoke rebound burst responses in STN neurons. The reversal potential of $GABA_A$ receptor-mediated IPSPs was determined and the

Figure 5.2. Heterogeneity of rebound burst-firing in STN neurons following the removal of hyperpolarising current. *A-D*, Rebound burst responses were of two types. The most common was of short duration (less than 100 ms; *A, C*) and was followed immediately by spontaneous firing (*A*) or by a deep AHP (*C*), which was sometimes followed by a second, weaker rebound (*C*). The less common type had long-duration rebound bursts (several hundred ms; *B*). Some neurons did not display rebound bursts (*D*). Rebound firing is shown at a larger time scale in the *insets* to the right of each panel. The peak levels of membrane hyperpolarisation that were reached during the current pulse are represented by *red dashed lines*. Voltages to the left of the traces refer to the membrane potential at the first point of the trace. Calibration bars in *A* apply to all panels.

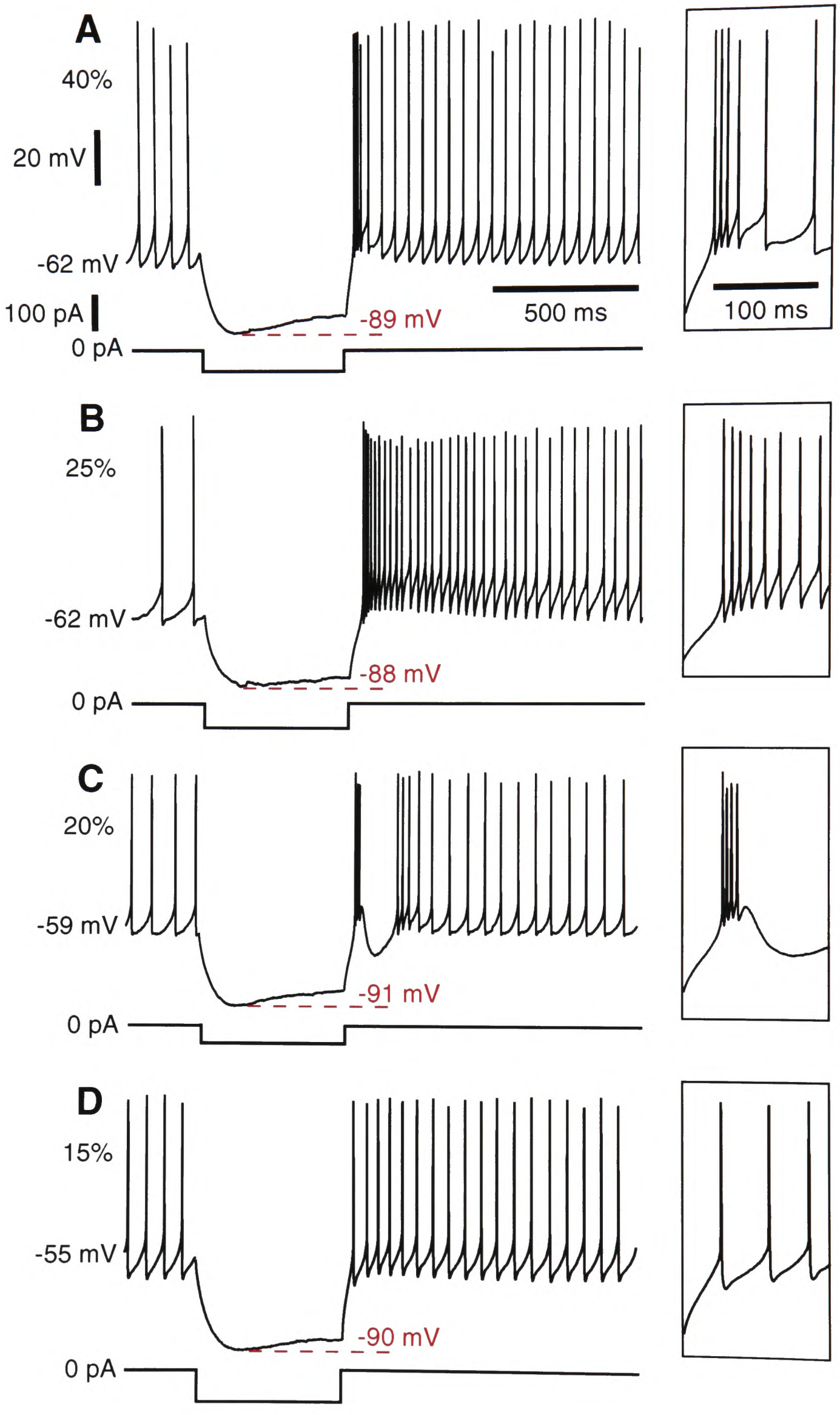
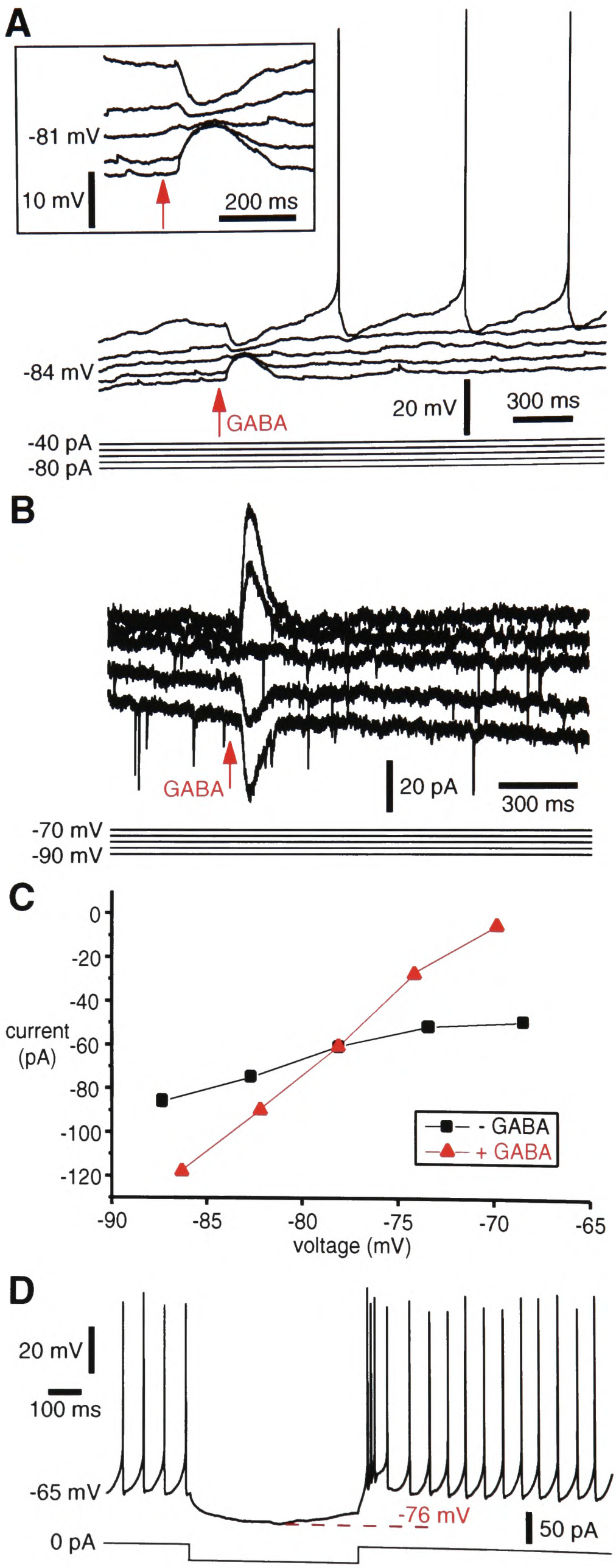

A
40%
20 mV
-62 mV
100 pA
0 pA
-89 mV
500 ms
100 ms
B
25%
-62 mV
0 pA
-88 mV
C
20%
-59 mV
0 pA
-91 mV
D
15%
-55 mV
0 pA
-90 mV

Figure 5.3. $E_{GABA\text{-}A}$ is more hyperpolarised than the threshold for rebound bursting in most STN neurons. *A*, Current-clamp recordings demonstrating the depolarising and hyperpolarising responses of a STN neuron to the pressure-pulse application of GABA (25 ms; 25 psi; *red arrow*). *Inset*, reversal of the GABA-evoked potential shown at larger time and voltage scales. $E_{GABA\text{-}A}$ was measured as –79 mV from the current-clamp recordings. *B*, Voltage-clamp recordings of the same STN neuron demonstrating the reversal of the $GABA_A$ current. Spontaneous fast inward currents were observed at all membrane potentials. Note the slowly-increasing inward baseline current, which is due to the activation of I_h at potentials below –70 mV (Bevan and Wilson, 1999). *C*, Plots of peak $GABA_A$ current (+GABA; *red*) and baseline current that flowed in the absence of GABA application (-GABA; *black*) against voltage (point of intersection of I-V curves: –78 mV). *D*, Removal of a 500 ms hyperpolarising current pulse, which held the membrane potential close to $E_{GABA\text{-}A}$ (peak hyperpolarisation at –76 mV; *red dashed line*), elicited a rebound burst of short duration in the same STN neuron.


A
-81 mV
10 mV
200 ms
-84 mV
GABA
20 mV
300 ms
-40 pA
-80 pA
B
GABA
20 pA
300 ms
-70 mV
-90 mV
C
current (pA)
0
-20
-40
-60
-80
-100
-120
-90
-85
-80
-75
-70
-65
voltage (mV)
- GABA
+ GABA
D
20 mV
100 ms
-65 mV
-76 mV
50 pA
0 pA

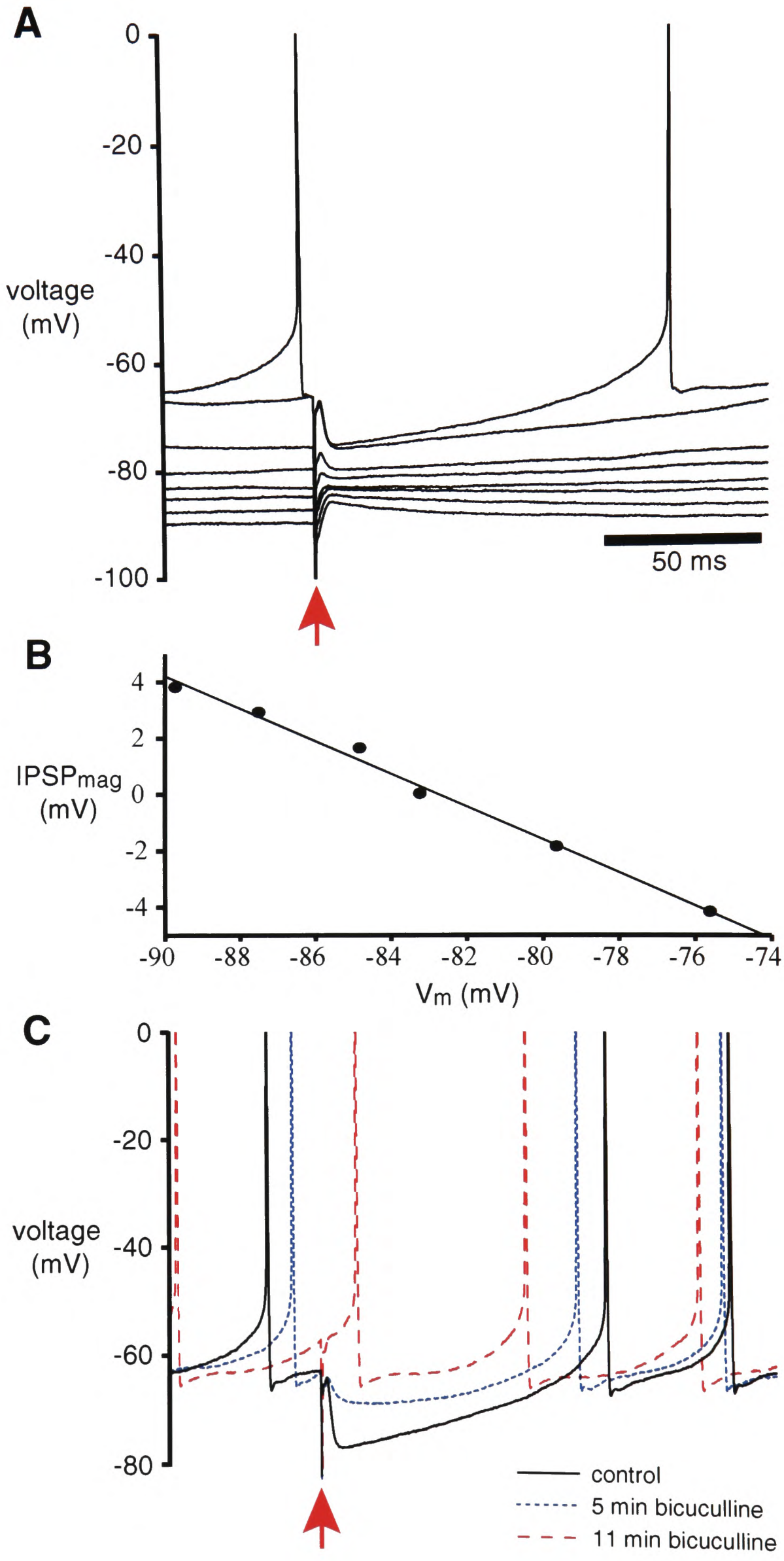
responses of STN neurons to evoked IPSPs were then characterised. During selective blockade of fast excitatory neurotransmission, supramaximal electrical stimulation of fibre tracts in the internal capsule or rostral STN evoked fast, monosynaptic IPSPs in all STN neurons tested (Fig. 5.4*A*; $n = 31$). The magnitude and polarity of IPSPs were dependent on somatic membrane potential (Fig 5.4*B*). $E_{IPSP\text{-}A}$ was determined to be -79 ± 7 mV ($n = 31$) and was not significantly different from $E_{GABA\text{-}A}$, which further supports the argument that neurons were not chloride loaded by the pressure-pulse application of GABA. Single IPSPs did not generate rebound burst-firing in STN neurons at any membrane potential or at any stage of the oscillatory cycle of spontaneous firing. However, the degree of hyperpolarisation achieved had profound effects on the timing of action potential generation (Fig. 5.4*A*, *C*). Evoked IPSPs were abolished by bicuculline, suggesting that these events were exclusively mediated by $GABA_A$ receptors (Fig. 5.4*C*; $n = 15$).

Rebound burst-firing was observed at the break of a hyperpolarising current pulse in 29 of 31 neurons tested in the $E_{IPSP\text{-}A}$ study. The appearance of the rebound burst varied dramatically and neurons fired either short- (Fig. 5.2*A*, *C*, $n = 19$) or long-duration bursts (Fig. 5.2*B*, $n = 10$). The mean hyperpolarisation threshold required for rebound burst-firing was -78 ± 5 mV ($n = 29$). $E_{IPSP\text{-}A}$ was equal to, or more hyperpolarised than, the threshold for rebound burst-firing in 18 of the 29 neurons that fired rebound bursts.

5.3.5 Responses of STN neurons to irregular synaptic barrage and bursts of IPSPs

Single electrically-evoked IPSPs did not hyperpolarise STN neurons to threshold levels for rebound burst-firing (Fig. 5.4*A*). However, it is possible that asynchronous and irregular sequences of IPSPs could lead to the generation of rebound burst-firing in STN neurons. To test this hypothesis, frequent and stochastic release of neurotransmitter was induced by the bath application of 4-AP (100 μM), which facilitates large-scale transmitter release in brain

Figure 5.4. Electrical stimulation of internal capsule evokes $GABA_A$ receptor-mediated post-synaptic potentials in STN neurons. *A*, Current-clamp recordings demonstrating the depolarising and hyperpolarising post-synaptic potentials evoked in a STN neuron by supramaximal electrical stimulation of the internal capsule (50 μs duration, 300 μA; *red arrow*). Although single IPSPs did not evoke rebound burst-firing in the neuron, the degree of hyperpolarisation achieved had profound effects on the timing of action potential generation. *B*, Plot of relationship between IPSP magnitude ($IPSP_{mag}$) and somatic membrane potential (V_m) for neuron in *A* (data from six most hyperpolarised membrane potentials only). $E_{IPSP\text{-}A}$ was taken as the potential at which IPSP magnitude was zero (–82.8 mV). *C*, Bath application of bicuculline (30 μM) abolished the IPSP response in the same neuron (cf. *black* and *red* traces) and thus, confirmed that evoked IPSPs were mediated by $GABA_A$ receptors. Calibration bar in *A* applies to *C*. Stimulation artefacts in *C* are truncated for clarity. Experiments in were conducted in the presence of 40 μM DNQX, 50 μM APV and 10 μM CGP 55845A.


A
0
-20
-40
-60
-80
-100
voltage
(mV)
50 ms
B
4
2
0
-2
-4
IPSPmag
(mV)
-90
-88
-86
-84
-82
-80
-78
-76
-74
Vm (mV)
C
0
-20
-40
-60
-80
voltage
(mV)
control
5 min bicuculline
11 min bicuculline

slices by blocking K^+ conductances at or near the nerve terminals of cut extrinsic afferents (Thesleff, 1980; Flores-Hernández et al., 1994).

Following the application of 4-AP in the presence of DNQX plus APV, the asynchronous barrage of STN neurons with IPSPs reduced the frequency and rhythmicity of spontaneous firing (Fig. 5.5*A*, *B*; mean rate of 12.3 ± 4.2 Hz and CV of 0.11 ± 0.04 for controls; mean rate of 8.1 ± 3.2 Hz and CV of 0.25 ± 0.10 for 4-AP; $n = 6$). Regardless of the membrane potential or the stage of the oscillatory cycle of firing, 4-AP-induced IPSPs did not provoke rebound burst-firing in STN neurons (Fig. 5.5*B*). Regular spontaneous activity patterns were restored following the antagonism of $GABA_A$ receptors with bicuculline (Fig. 5.5*C*; $n = 5$).

To investigate whether bursts of IPSPs could temporally summate to produce the necessary degree of hyperpolarisation for rebound burst-firing, trains of IPSPs (2-20 events) were evoked by repetitive stimulation of the internal capsule (at 10-100 Hz) and the responses of STN neurons recorded ($n = 15$). In general, small trains of IPSPs (< 5 events at 10-100 Hz) were not sufficient to evoke rebound burst-firing in STN neurons at any membrane potential or at any stage of the oscillatory cycle of spontaneous firing (Fig. 5.6*A*). However, stimulus trains of longer duration (10 or 20 events at 20-100 Hz) generated rebound burst-firing after the decay of the IPSPs (Fig. 5.6*B*, *C*; 12 of 15 neurons tested). Furthermore, the rebound burst response was often augmented by increasing the duration of the train from 10 to 20 events (Fig. 5.6*B*, *C*). The abolition of the rebound burst-firing by bicuculline confirmed that IPSPs were mediated by $GABA_A$ receptors (Fig. 5*D*; $n = 7$). Taken together, these data suggest that large bursts of $GABA_A$ receptor-mediated IPSPs, but not irregular sequences of IPSPs, may summate and produce the membrane hyperpolarisation required to evoke rebound burst-firing in STN neurons.

Figure 5.5. Asynchronous $GABA_A$ receptor-mediated input reduces the frequency and rhythmicity of the spontaneous action potential discharge of STN neurons. *A*, Current-clamp recording demonstrating regular spontaneous activity of a STN neuron (mean rate = 17.1 Hz; CV = 0.11). *B*, Application of 4-AP (100 μM) induced an asynchronous barrage of large IPSPs (*red arrowheads*) on the same STN neuron, which reduced the rate and rhythmicity of spontaneous firing (mean rate = 13.9 Hz; CV = 0.24). Note that IPSPs did not hyperpolarise the neuron sufficiently to generate rebound burst-firing. *C*, The neuron resumed more regular spontaneous activity (mean rate = 23.1 Hz; CV = 0.13) following the abolition of 4-AP-induced IPSPs by the $GABA_A$ receptor antagonist, bicuculline (30 μM). Calibration bar in *A* applies to all panels. Action potentials are truncated for clarity. All experiments were conducted in the presence of 40 μM DNQX, 50 μM APV and 10 μM CGP 55845A.

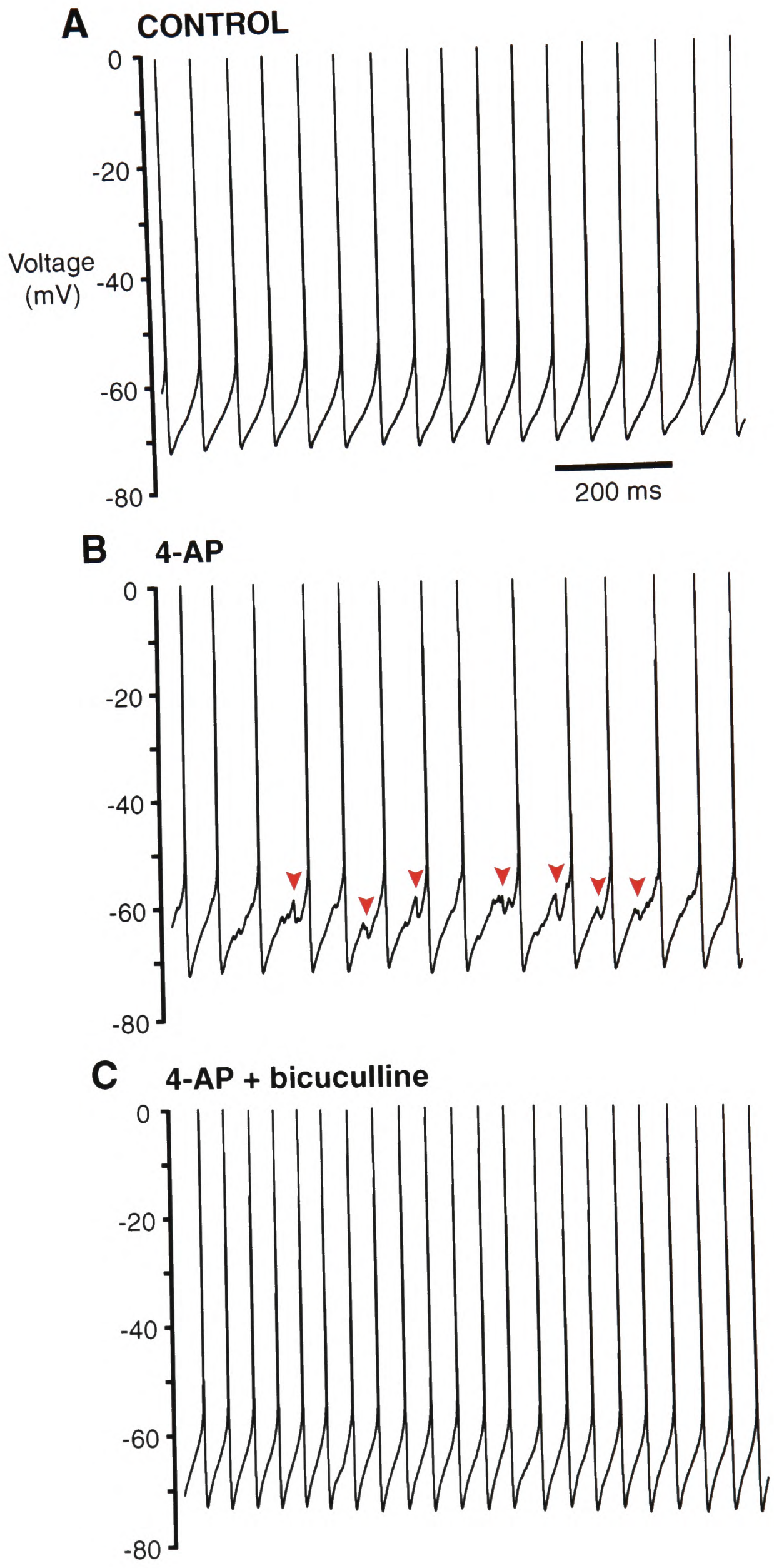
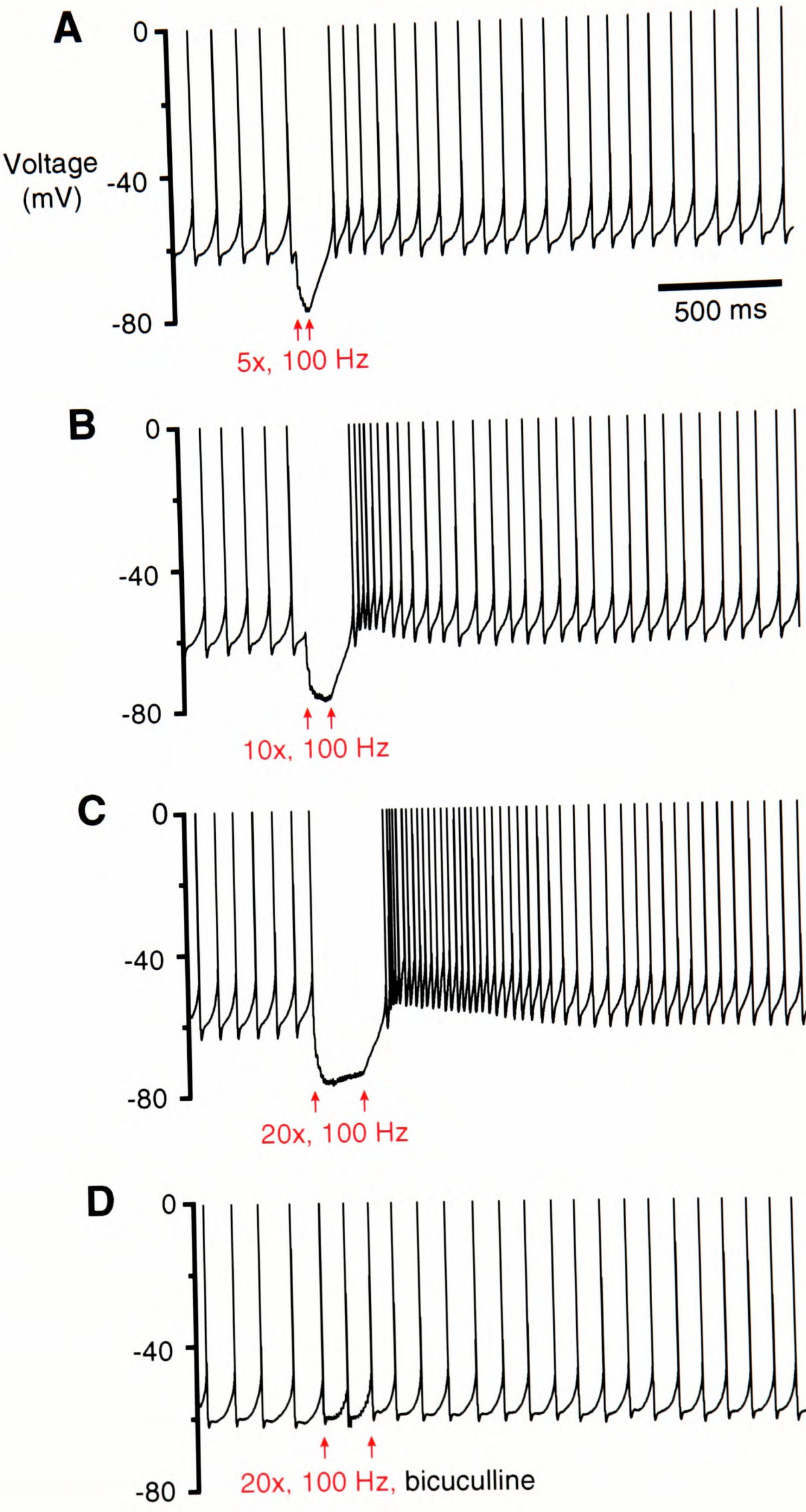

A
CONTROL
0
-20
-40
-60
-80
Voltage
(mV)
200 ms
B
4-AP
0
-20
-40
-60
-80
C
4-AP + bicuculline
0
-20
-40
-60
-80

Figure 5.6. Bursts of $GABA_A$ receptor-mediated IPSPs generate rebound burst-firing in STN neurons. *A*, Current-clamp recording of the response of a spontaneously firing STN neuron to a small train of high-frequency stimuli delivered to the internal capsule (5 stimuli, each of 100 μs duration, at 100 Hz; 350 μA; between *red arrows*). Although the IPSPs were temporally summated to form a compound hyperpolarising potential, the neuron did not display a rebound burst response after stimulation ceased. *B*, *C*, Increasing the number of pulses in the train to 10 (*B*) or 20 (*C*) enhanced the duration of the compound hyperpolarising potential in the same neuron and threshold for rebound burst-firing was reached as indicated by the generation of a long-duration rebound burst response after termination of the stimulus train. Note that the train of 20 IPSPs evoked a greater rebound burst response compared to the train of 10 IPSPs. *D*, The stimulus train used in *C* failed to evoke rebound burst-firing in the same neuron after IPSPs had been abolished by bicuculline (30 μM). Calibration bar in *A* applies to all panels. Action potentials are truncated and stimulation artefacts are deleted for clarity. All experiments were conducted in the presence of 40 μM DNQX, 50 μM APV and 10 μM CGP 55845A.


A
0
Voltage
(mV)
-40
-80
500 ms
5x, 100 Hz
B
0
-40
-80
10x, 100 Hz
C
0
-40
-80
20x, 100 Hz
D
0
-40
-80
20x, 100 Hz, bicuculline

5.4 Discussion

To determine whether $GABA_A$ receptor-mediated synaptic potentials could theoretically generate rebound burst-firing in STN neurons, $E_{GABA\text{-}A}$ and the degree of hyperpolarisation required for rebound firing were determined using perforated patch-clamp recordings. The rebound burst-firing of STN neurons in response to hyperpolarising input was found to be heterogeneous. In the majority of neurons that fired rebounds, $E_{GABA\text{-}A}$ were equal to or more hyperpolarised than the level of membrane hyperpolarisation required for rebound burst-firing, suggesting that $GABA_A$ receptor-mediated inputs from the pallidum could potentially produce rebound burst-firing of STN neurons. Subsequent experiments on $GABA_A$ receptor-mediated post-synaptic inhibition showed that $E_{IPSP\text{-}A} = E_{GABA\text{-}A}$ and that $E_{IPSP\text{-}A}$ was equal to or more hyperpolarised than the level of membrane hyperpolarisation required to evoke rebound excitations in most neurons. A single electrically-evoked IPSP, or an asynchronous barrage of IPSPs, exerted powerful effects on the timing of action potential generation but did not provoke rebound burst-firing. However, bursts of IPSPs (> 5 events at 20-100 Hz) hyperpolarised STN neurons to an extent that provoked rebound burst-firing after the stimulus train. Taken together, these results suggest that the levels of hyperpolarisation required for rebound burst-firing in STN neurons could only be generated by synchronous, high-frequency bursts of GABAergic synaptic inputs.

The chloride equilibrium potential is more hyperpolarised than resting membrane potential in STN neurons

The estimates of $E_{GABA\text{-}A}$ and $E_{IPSP\text{-}A}$ at ~ -79 mV in STN neurons are in good agreement with the values measured in neurons of rat thalamic relay nucleus (Ulrich and Huguenard, 1997a), a brain region in which synaptic inhibition is known to have a profound effect on neuronal activity (Ulrich and Huguenard, 1997b; McCormick and Bal, 1997). Although

E_{GABA-A} can theoretically have any value between the relatively negative Cl^- equilibrium potential (E_{Cl}) and relatively positive HCO_3^- equilibrium potential (E_{HCO3}), resting E_{GABA-A} is usually determined by E_{Cl} because the permeability of the $GABA_A$ receptor channel to Cl^- is five times that of HCO_3^- (Bormann et al., 1987; Kaila, 1994; Ulrich and Huguenard, 1997a). The approximation of $E_{GABA-A} = E_{IPSP-A} \approx E_{Cl}$ is further justified in the case of STN neurons because pharmacological inhibition of carbonic anhydrase, which acts to set E_{HCO3}, did not affect E_{GABA-A}. It should be noted however, that whilst the value of E_{GABA-A} that was derived from the somatic pressure-pulse application of GABA probably holds true for E_{Cl} in somatic and proximal dendritic compartments, more distal dendrites may maintain very different Cl^- distributions (Hara et al., 1992; Staley et al., 1995; Jarolimek et al., 1999).

The finding that E_{GABA-A}/E_{IPSP-A} are maintained well below the "resting" membrane potential indicates that that STN neurons possess a battery of active Cl^- extrusion mechanisms, including primary (Cl^- ATPase) and secondary (K^+/Cl^- co-transporter, Na^+-dependent Cl^--HCO_3^- exchange) active transporters (Kaila, 1994). Although the exact combination of active transporters present in STN neurons is unknown, the best candidate for the regulation of Cl^- homeostasis for fast hyperpolarising post-synaptic inhibition is the recently cloned K^+/Cl^- co-transporter, KCC2 (Rivera et al., 1999).

Subthalamic nucleus neurons possess heterogeneous rebound burst-firing properties

The STN is generally believed to contain a physiologically homogeneous population of projection neurons (Nakanishi et al., 1987a; Yung et al., 1991; Overton and Greenfield, 1995; Bevan et al., 1999). However, it was found that the rebound burst responses of STN neurons were heterogeneous. Whilst the functions supported by response heterogeneity in the STN are not clear, these results may account for the fact that less then 50% of STN neurons exhibit a spontaneous burst-firing mode of activity (Beurrier et al., 1999), which is known to be dependent on the rebound burst response to membrane hyperpolarisation. It is

now well established that a specialised type of Ca^{2+} current, the low-threshold Ca^{2+} current or T (for tiny or transient) current (I_T), is responsible for generating the LTS component of the rebound burst response in most central neurons (for review, see Huguenard, 1996). T-type Ca^{2+} channels (T-channels) are thought to be derived from a subfamily of genes that encode the novel Ca^{2+} channel subunits α1G, α1H and α1I (Perez-Reyes et al., 1998; Lee et al., 1999). The finding that rebound burst-firing of STN neurons was heterogeneous suggests that the expression of T-channels in the STN may vary from neuron to neuron. *In situ* hybridisation studies of the distribution of T-channel subunit transcripts support this hypothesis since the STN was found to contain high levels of α1I, moderate levels of α1H, and a low levels of α1G (Talley et al., 1999). When expressed in the same cell type (HEK 293 cells), α1I currents have slower kinetics and depolarised voltage dependency of activation compared with the other two channels (Lee et al., 1999). Thus, preferential expression of α1I or α1H channels by STN neurons may result in rebound responses of long- or short-duration, respectively. Electrophysiological studies have suggested that T-channels are preferentially distributed on the dendritic processes of STN neurons (Song et al., 2000). Thus, differential and spatially segregated expression of T-channel subunits within the dendritic arbors of STN neurons could also underlie the variation in rebound burst-firing.

Functional implications for the role of $GABA_A$ receptor-mediated inhibition in the normal STN

Activation of $GABA_A$ receptors on the soma and proximal dendrites of STN neurons will probably have an hyperpolarising, inhibitory effect due to E_{Cl} being more hyperpolarised than the local membrane potential in resting conditions. In general, the membrane potential of an STN neuron oscillates between ~ –45 mV (threshold for spike firing) and ~ –65 mV (peak of AHP) during spontaneous activity under resting conditions. Thus, at any time in the

oscillatory cycle of activity, there exists a substantial driving force of at least –14 mV for Cl^- in the soma and proximal dendrites of STN neurons. This suggests that $GABA_A$ receptor-mediated inhibitory input from pallidosubthalamic terminals, which are predominantly located on the perikarya and proximal dendrites of neurons (Smith et al., 1990), is likely to have a powerful influence over ongoing neuronal activity in the STN (Kita et al., 1983b). Indeed, it was found that even a single IPSP could substantially delay action potential generation. Thus, during rest, the largely asynchronous and regular/irregular, single-spiking activity of GP neurons (Georgopoulos et al., 1983; Aldridge and Gilman, 1991; Anderson and Turner, 1991; Cheruel et al., 1994; Urbain et al., 2000; see Chapters 3 and 4) may effectively set an "inhibitory tone" in the STN. Furthermore, tonic inhibition may be subsequently modulated during normal movement to limit or time cortically-driven activity in the STN (DeLong et al., 1985; Nambu et al., 1990; Ryan and Clark, 1991, 1992; Ryan et al., 1992; Fujimoto and Kita, 1993; Yoshida et al., 1993; Maurice et al., 1998a, b). The fact that GABAergic pallidal terminals are juxtaposed with glutamatergic cortical and thalamic terminals along the dendrites of STN neurons (Smith et al., 1990; Bevan et al., 1995) indicates that inhibitory inputs are well suited to shunt or even cancel excitatory synaptic inputs. In addition, the non-inactivating (persistent) Na^+ current in STN neurons (Bevan and Wilson, 1999; Beurrier et al., 2000) may serve to amplify IPSPs of dendritic origin, thereby increasing the efficacy of inhibition during episodes of spontaneous firing (Stuart, 1999).

Although the driving force for Cl^- is large in STN neurons, asynchronous feed-back inhibition from the normal GP is unlikely to cause sufficient hyperpolarisation to evoke a rebound burst response. Indeed, STN neurons did not fire rebound bursts when exposed to an asynchronous barrage of IPSPs in the presence of 4-AP. Similarly, small trains of evoked IPSPs (< 5 events at 10-100 Hz) were not sufficient to cause rebound burst-firing at any membrane potential or at any stage of the oscillatory cycle of spontaneous firing. Taken together with the results from Chapters 3 and 4, these data suggest that rhythmic burst-firing

activity of STN neurons in the normal STN-GP network is probably generated by powerful excitatory drive from the cortex.

Functional implications for the role of $GABA_A$ receptor-mediated inhibition in the parkinsonian STN

Neurons in the STN are hyperactive and display more bursting activity patterns in idiopathic or animal models of PD (Hollerman and Grace, 1992; Bergman et al., 1994; Hassani et al., 1996; Kreiss et al., 1997; Levy et al., 2000; Magnin et al., 2000; Vila et al., 2000). The direct/indirect pathway model of hypokinetic movement disorders predicts that increased activity in the STN arises as a consequence of decreased inhibition from the GP (Albin et al., 1989b; DeLong, 1990). However, the synaptic mechanisms underlying the increased incidence of bursting activity in the STN *in vivo* are unknown. Studies of co-cultured basal ganglia neurons *in vitro* have led to the proposal that recruitment of the rebound excitatory response of STN neurons by inhibitory input from the GP may be responsible for the pathological alterations in firing pattern observed in PD (Plenz and Kitai, 1999; also see Bergman et al., 1994). The values of $E_{GABA\text{-}A}/E_{IPSP\text{-}A}$ and the magnitude and duration of membrane hyperpolarisation required for rebound burst-firing suggest that sufficient hyperpolarisation could only be generated by a synchronous barrage of GABAergic synaptic inputs. Previous studies in rats, cats and primates have shown that GP neurons fire in a more synchronous and bursting manner in PD compared to the normal state (Filion, 1979; Filion et al., 1988; Pan and Walters, 1988; Filion and Tremblay, 1991; Rothblat and Schneider, 1995; Bergman et al., 1998, Boraud et al., 1998, 2000b; Levy et al., 2000; Magnin et al., 2000; Ni et al., 2000; Raz et al., 2000; also see Chapter 4). Thus, synchronised input from bursting pallidosubthalamic neurons in PD could produce sufficient hyperpolarisation in STN neurons to generate rebound burst-firing. The finding that only burst-like, high-frequency trains of IPSPs ($\geq$ 5 events at 20-100 Hz) led to rebound burst-firing of STN neurons

indirectly supports this hypothesis and suggests that the emergence of rebound bursting may underlie some of the alterations in firing pattern seen in the parkinsonian STN. To date, the presence of rebound burst discharges in the parkinsonian STN has only been systematically investigated in one study (Magnin et al., 2000). Using standard extracellular criteria for the identification of "LTS discharges" (*i.e.* a progressive increase in ISI duration and a logarithmic relationship of the duration of the first ISI to the number of progressive spikes in the burst, which are based on classic LTS discharges of thalamic relay neurons; see Domich et al., 1986), the authors concluded that primate STN neurons do not exhibit rebound burst-firing activity *in vivo* (Magnin et al., 2000). However, the functional heterogeneity in rebound bursting displayed by rat STN neurons, coupled with the clear qualitative differences in the structure of rebound burst discharges in thalamic and STN neurons (Huguenard and Prince, 1992), suggests that this interpretation needs to be re-evaluated.

The assumption that $GABA_A$ receptor-mediated pallidal input to the STN is hyperpolarising is only correct when E_{Cl} is more hyperpolarised than the local membrane potential. Pallidosubthalamic inputs from GP neurons with normal, uncorrelated activity states are unlikely to effectively summate in STN neurons and therefore, would not perturb Cl^- homeostasis to any great degree. However, when GP neurons are engaged in synchronous bursting activity, as in PD, temporal summation of IPSPs in STN neurons is more likely to occur. Prolonged summation of $GABA_A$ receptor-mediated input could eventually lead to the collapse of somatic and dendritic Cl^- gradients, which would render subsequent GABAergic inputs depolarising. In support of this hypothesis, it has been shown that depolarising "inhibitory" post-synaptic potentials can be brought about in pyramidal cells by high-frequency (100-200 Hz), tetanic stimulation of interneurons in area CA1 of adult rat hippocampal slices (Grover et al, 1993; Staley et al., 1995; Taira et al., 1997). The excitatory actions of GABA are not yet fully understood, although a breakdown in the transmembrane Cl^- gradient, as well as sustained outflux of HCO_3^- anions though $GABA_A$

receptors, seem to be involved (Kaila, 1994; Staley et al., 1995; Taira et al., 1997). Thus, abnormal patterns of activity in the parkinsonian GP may lead to $GABA_A$ receptor-mediated excitation of STN neurons, thereby exacerbating STN hyperactivity in the hypokinetic disease state.

CHAPTER 6.

GENERAL DISCUSSION

6.1 Summary and concluding remarks

The overall objective of the research in this thesis was to elucidate the mechanisms underlying activity in the STN-GP network in health and disease. To achieve this objective, both *in vivo* and *in vitro* electrophysiological approaches were taken. Specifically, *in vivo* studies were designed to define the relationship of activity in the cerebral cortex, the principal excitatory afferent of the basal ganglia, to activity in the normal and dopamine-depleted STN-GP network (Chapters 3 and 4). Furthermore, a series of complementary *in vitro* studies were carried out to characterise the role of inhibitory synaptic input to the STN, which predominantly arises from the GP (Chapter 5). A precis of the data obtained in each study can be found at the beginning of the discussion sections of Chapters 3, 4 and 5.

To characterise the relationship of activity in the normal STN-GP network to activity in the cerebral cortex, single and multiple unit activity in STN and/or GP were recorded together with frontal cortical EEG in ketamine- and urethane-anaesthetised rats during various stereotypical states of cortical activation. The role of the cerebral cortex in shaping activity in the STN-GP network was further investigated with a spreading depression paradigm. The data obtained in this study indicate that: (1) the rate and pattern of firing of neurons in the STN-GP network is intimately related to coincidental cortical activity and hence, the sleep-wake cycle; (2) oscillatory activity in the STN-GP network is disrupted by inactivation of the cortex and thus, may be driven by the cortex in health and disease; and (3) neuronal activity in the STN-GP network is regulated in space and time in a complex manner.

To provide insight as to whether the relationship between the STN-GP network and the cerebral cortex is altered in Parkinson's disease, unit activity in the STN-GP network was recorded together with cortical EEG in urethane-anaesthetised normal and 6-OHDA-lesioned rats. This relationship was characterised during stereotypical states of cortical

activation and was further tested by cortical ablation. The results of this study suggest that: (1) activity in the STN-GP network is dramatically altered by the chronic loss of dopamine from the forebrain; (2) the impact of the cortex on the network is increased following dopamine depletion and thus, pathological oscillatory activity in the basal ganglia in PD may be caused by the inappropriate processing of rhythmic cortical input; (3) the classical indirect pathway through the NS is abnormally augmented during activation of the parkinsonian brain; (4) the relative contribution of firing rate and pattern to information coding in the STN-GP network and the basal ganglia is related to the state of cortical activation.

To test whether $GABA_A$ receptor-mediated synaptic input from the GP could generate rebound burst-firing in STN neurons, a phenomenon that may contribute to normal and abnormal activity in the STN-GP network *in vivo*, $E_{GABA\text{-}A}$, $E_{IPSP\text{-}A}$ and the degree of hyperpolarisation required for rebound burst-firing were determined using perforated patch-clamp recordings *in vitro*. An extension of this study investigated the responses of STN neurons to different patterns of inhibitory synaptic input. The findings of this study imply that: (1) active chloride homeostasis ensures a large net driving force for $GABA_A$ receptor-mediated events in STN neurons; (2) asynchronous and irregular inhibitory input from the GP has a profound influence on activity in the STN; and (3) synchronous, bursting activity in the parkinsonian GP could contribute to pathological oscillatory activity in the basal ganglia by generating rebound burst-firing in STN neurons.

In conclusion, the three studies have identified a number of key mechanisms underlying the activity of the STN-GP network. The two *in vivo* studies have established that the corticosubthalamic projection plays an important role in driving the activity of the STN-GP network and further suggest that the output of midbrain dopaminergic neurons directly or indirectly modulates the impact of this powerful excitatory input on the STN. As such, these findings add further weight to the argument that the STN can no longer be

viewed as a simple relay station along the classical indirect pathway, but rather as a second important entry point for cortical inputs into the basal ganglia. Taken together, the results of these three studies have further clarified the functions subserved by the reciprocal connections between the STN and GP. In the absence of strong cortical drive under resting conditions, the discharge of STN neurons may be insufficient to strongly influence the pattern and/or rate of firing of GP neurons. As such, the tonically active GP neurons may effectively set a GABAergic tone in the STN that would subdue the firing of STN neurons and temper the influence of excitatory inputs on the STN. During movement, increases in cortical drive would likely lead to a widespread excitation of STN neurons via the corticosubthalamic pathway. The synchronised discharge of STN neurons may then be sufficient to reach the excitation threshold in the GP, so that GP neurons phasically discharge and provide dynamic feed-back inhibition to the activated STN neurons. Whilst the pallidosubthalamic input may simply reduce the frequency and rhythmicity of firing of STN neurons, it could also generate rebound burst responses in STN neurons, which in turn, may lead to an oscillatory cycle of activity in the STN-GP network. In PD, an increase in the efficacy of the corticosubthalamic projection may lead to an excessive excitation of STN neurons and hence, GP neurons, so that pathological oscillations are generated in the STN-GP network in the absence of movement.

6.2 Technical considerations

The experimental observations and resultant interpretations in this thesis should be considered in light of a number of technical issues arising from the methods employed.

6.2.1 *In vivo* studies

All *in vivo* electrophysiological recordings were performed in animals that were deeply anaesthetised with standard general anaesthetics. Although general anaesthesia may interfere with a number of neurophysiological variables (Nicoll and Madison, 1982; Franks and Lieb, 1994), the major impact of anaesthetics on CNS physiology is on activity produced by cortical structures, with lesser degrees of effect on subcortical structures (for review, see Sloan, 1998). Urethane is highly lipophilic and is thought to induce a depression of the CNS by disrupting the structure or dynamic properties of the lipid portions of nerve membranes (Franks and Lieb, 1994), which may lead, in the case of some central neurons, to hyperpolarisation and reduced activity (Nicoll and Madison, 1982). Nevertheless, it has been well established that urethane has barely detectable effects on neurotransmission in subcortical areas (for review, see Maggi and Meli, 1986). In good agreement with this, activity in the STN-GP network and cortex of urethane-anaesthetised animals closely resembled that observed in the unanaesthetised preparation (Urbain et al., 2000). However, the activity of the STN-GP network in ketamine anaesthesia was markedly different from that in urethane anaesthesia. Ketamine produces analgesia and sedation ("dissociative" anaesthesia; Sloan, 1998), by primarily antagonising the effects of excitatory amino acids on NMDA receptors (Anis et al., 1983; Franks and Lieb, 1994). In contrast to urethane, the surgical anaesthetic state induced by ketamine is marked by a paradoxical excitation of CNS structures and is reflected in the cerebral cortex as "hypersynchronous" slow-wave activity (Winters and Ferrar-Allado, 1972). This finding suggests that hypersynchronicity in the corticosubthalamic pathway may underlie, in part, the increased LFO activity in the STN-GP network of ketamine-anaesthetised animals compared to activity in urethane-anaesthetised or unanaesthetised animals. Thus, urethane is potentially the more useful anaesthetic for investigating the activity of the STN-GP network. The major benefits associated with anaesthetic use include increased stability for neuronal recording and a steady

metabolic/physiological state that is ideal for surgical and pharmacological manipulations of the CNS. In particular, these data suggest that the anaesthetised animal is a good model for establishing the impact of extremes of cortical activity on the STN-GP network. However, it should not be forgotten that the extrapolation of data gathered from anaesthetised animals to the awake, behaving animal is based only on the *assumption* that motor-related activity in the cortex falls somewhere between these extremes of activity. In conclusion, these studies in anaesthetised animals have provided a valuable insight into the mechanisms underlying activity in the STN-GP network, but they should be further validated in freely-moving animals.

To gain some insight into the functions of the STN-GP network in idiopathic PD, network activity was studied using a well established model of experimental PD, the unilateral 6-OHDA-lesioned rat. This model of experimental PD has been intensively studied since its introduction and subsequently, it has been firmly established that the syndrome that develops as a consequence of unilateral dopamine depletion is similar in many respects to PD (for reviews, see Zigmond et al., 1990; Schwarting and Huston, 1996a, b). Indeed, many of the pathophysiological hallmarks of idiopathic or primate models of PD, including alterations in the rates and patterns of firing of STN and GP neurons, have been reproduced using the 6-OHDA lesion model in these and other studies. However, in the present studies, the 6-OHDA lesions were unilaterally placed and usually included the VTA, and thus, *in these respects*, did not closely mimic the pathology of PD. The unilateral placement of the 6-OHDA lesion means that cross-talk between the unlesioned and 6-OHDA-lesioned sides of the brain before the time of recording may have adversely affected the development of pathophysiological activity in the STN-GP network (Lawler et al., 1995; Rohlfs et al., 1997; Perier et al., 2000). This hypothesis has never been directly tested. To address this issue, these experiments should be replicated in animals that have received callosal transections shortly after the injection of the neurotoxin into their midbrains.

Interhemispheric communication is significantly reduced in unilaterally 6-OHDA-lesioned rats following chronic callosotomy (Lawler et al., 1995) and thus, this procedure will permit any pathophysiological activity to develop undisturbed in the 6-OHDA-lesioned side of the brain. Since the dopaminergic neurons of the VTA, and to a lesser extent, the medial SNpc, project to prefrontal cortical areas (see Berger et al., 1991 and references therein), the 6-OHDA-induced degeneration of these neurons may have had an adverse effect on cortical activity in the lesioned hemisphere. Although this possibility cannot be ruled out, it does seem unlikely because the frequency of cortical SWA in the 6-OHDA-lesioned hemisphere was not significantly different from that of SWA in the contralateral hemisphere or from that of SWA in either hemisphere of normal animals. The neurons of the VTA also send their axons to ventromedial regions of the NS (see Joel and Weiner, 2000) and thus, the destruction of this projection may have exacerbated pathophysiological activity in the basal ganglia. Degeneration of the VTA could be minimised by injecting the 6-OHDA into more lateral sites in the midbrain, *i.e.* not in medial forebrain bundle, or by injecting the neurotoxin into the dorsolateral aspects of the NS (Kirik et al., 1998). The electrophysiological recordings in this thesis were performed at a time (21 to 39 days) when the pathophysiological state had most likely stabilised at a maximum level after the injection of 6-OHDA into the midbrain (Pan and Walters, 1988; Vila et al., 2000). The use of a single time point does not therefore, allow for many of the compensatory processes that are in place in PD (Zigmond et al., 1990; Lang and Lozano, 1998a, b). Thus, it would be of interest to perform similar experiments along a series of time points to determine the time-dependent changes in the relationship of the STN-GP network to the cerebral cortex. Quantification of the 6-OHDA-induced loss of dopamine in the STN and GP was not performed in these studies and thus, it is possible that a reduction in the direct dopaminergic input to the STN-GP network (in addition to a reduction in dopaminergic input to the NS) greatly contributed to the development of pathophysiological activity. Studies in parkinsonian monkeys have

shown that the density of dopaminergic fibres in the STN-GP network is significantly reduced following treatment with MPTP (Bergman et al., 1994; Jan et al., 2000). Thus, it would be of interest to quantify the loss of dopamine in the STN-GP network in order to test for any correlation between the extent of dopaminergic denervation and the expression of pathophysiological activity. In conclusion, the unilateral 6-OHDA lesion model does not parallel some of the pathological features of PD but the model has been, and continues to be, hugely important for the betterment of our understanding of PD.

Taken together, the data from the two *in vivo* studies suggest that the cerebral cortex acts as a potent driving force for neuronal activity in the STN. Furthermore, data obtained from urethane-anaesthetised animals indicate that the excitatory corticosubthalamic projection is critical for the expression of cortical rhythms in the STN-GP network. Given that both the STN and GP receive an additional excitatory input from the Cm-Pf of the thalamus (see sections 1.4 and 1.3, respectively), and that Cm-Pf neurons are likely to be entrained by the cortical slow oscillation (Steriade et al., 1993b, c, d), it is possible that rhythmic input from these thalamic structures significantly contributed to the LFO activity in the STN in normal animals and the LFO activity in both the STN and GP in 6-OHDA-lesioned animals. The corticosubthalamic and thalamosubthalamic projections are glutamatergic and both exert their effects via the activation of AMPA and NMDA receptors (Rouzaire-Dubois and Scarnati, 1987; Mouroux and Féger, 1993; Maurice et al., 1999; Nambu et al., 2000). As such, it would be technically difficult to pharmacologically dissect out their respective influences on STN neurons by local drug application. Thus, to determine the relative contribution of these two excitatory pathways to LFO activity in the STN-GP network, the Cm-Pf could be discretely lesioned by injection of a fibre-sparing excitotoxin, such as ibotenic acid, and the current studies then repeated. Such experiments would also be useful for establishing the role of the thalamic input to the STN-GP network during global activation.

6.2.2 *In vitro* study

To examine the dynamics of GABAergic inhibition in the STN, neurons were recorded in brain slices obtained from young animals (16 and 23 days). The interpretations of the *in vitro* data in this thesis are based on the assumption that STN neurons in young animals ("young STN neurons") exhibit similar intrinsic membrane properties to STN neurons in mature animals ("mature STN neurons"). This assumption is validated by the finding that the spontaneous activity and membrane properties of young STN neurons were consistent with the activity and properties reported for mature STN neurons *in vitro* (Nakanishi et al., 1987a; Flores et al., 1995, 1996; Overton and Greenfield, 1995; Abbott et al., 1997; Shen and Johnson, 2000) and *in vivo* (Kita et al., 1983b; Hassani et al., 1996; Urbain et al., 2000). In further support of this assumption, the autorhythmic discharge of STN neurons *in vitro* after blockade of excitatory amino acid neurotransmission was found to be similar to the tonic, regular firing of STN neurons *in vivo* following the ablation of ipsilateral cortex. It is possible that $E_{GABA\text{-}A}$, $E_{IPSP\text{-}A}$, and E_{Cl}, and thus, the efficacy of GABAergic inputs to STN neurons, vary with age. Expression of the K^+/Cl^- co-transporter, KCC2, which is likely the best candidate for the regulation of Cl^- homeostasis in STN neurons (see Chapter 5), in the CNS reaches steady (adult) levels by the end of postnatal week 2 (Rivera et al., 1999), suggesting that this possibility is unlikely. However, this hypothesis is difficult to test directly and thus, age-dependent Cl^- homeostasis cannot be ruled out.

To determine $E_{IPSP\text{-}A}$, $GABA_A$ receptor-mediated IPSPs were evoked in STN neurons by supramaximal stimulation of fibres in the internal capsule or rostral STN. The axons that were stimulated were assumed to be derived from GABAergic neurons in the GP. However, in addition to receiving a massive GABAergic input from the GP (Smith et al., 1990; Bevan et al., 1997), the STN also receives a substantial GABAergic input from VP (Groenewegen and Berendse, 1990; Bevan et al., 1997) and a relatively minor input from the GABAergic neurons of the MTg (Bevan and Bolam, 1995). Thus, it is conceivable that some of the

IPSPs were evoked by stimulation of fibres emanating from these alternative sources of GABAergic input to the STN. One way to minimise the contamination of responses would be to use an alternative parasagittal brain slice preparation that maintains a degree of functional connectivity between the GP and STN; in such a preparation, the GP could be locally stimulated to evoke IPSPs in STN neurons, thus circumventing the stimulation of fibres from the VP and MTg. In this study, no attempt was made to discern the points of origin of evoked IPSPs in STN neurons. Since pallidosubthalamic terminals cover the entire surface of STN neurons (Smith et al., 1990), the evoked IPSPs could have originated at synapses located on the soma and/or dendrites. If E_{Cl} in the dendrites of STN neurons differs from E_{Cl} at the soma (Hara et al., 1992; Staley et al., 1995; Jarolimek et al., 1999), then IPSPs that originated from dendritic sites might have adversely affected the estimation of $E_{IPSP\text{-}A}$ because this parameter was measured only at the soma. Furthermore, IPSPs of dendritic origin may have more readily evoked rebound burst-firing in STN neurons compared to somatic IPSPs since T-channels are preferentially distributed on the dendrites of these neurons (Song et al., 2000). Determination of the kinetics of the evoked IPSPs would be useful in differentiating events with dendritic and somatic points of origin (Spruston et al., 1994) and thus, would facilitate the clarification of these important issues. Although IPSPs were evoked at a frequency (0.1 Hz) that should not facilitate the induction of short- or long-term synaptic plasticity (see Shen and Johnson, 2000), errors introduced by such phenomena during the estimation of $E_{IPSP\text{-}A}$ cannot be completely ruled out. On a similar note, successive pressure-pulse applications of GABA (at a frequency of 0.1 Hz) may have resulted in desensitisation and rundown of $GABA_A$ receptors (Kaila, 1994), thereby affecting the estimation of $E_{GABA\text{-}A}$. The replication of this study using a wide range of stimulation and GABA application frequencies (*e.g.* 0.01-10 Hz) should provide adequate controls for these phenomena.

Brain slices containing the STN were cut at a thickness of 300 μm. Given that the dendrites of STN neurons extend into all planes of the nucleus and are commonly in excess of 300 μm in length (Yelnick and Percheron, 1979; Hammond and Yelnick, 1983; Kita et al., 1983a; Afsharpour, 1985a), it is likely that many of the dendrites of the recorded neurons were severed during the brain slicing procedure. Electrophysiological studies *in vitro* have indicated that T-channels are preferentially distributed on the dendritic processes of STN neurons (Song et al., 2000). Thus, the observed heterogeneity in the rebound burst-firing properties of STN neurons may be due, in part, to the differential loss of dendrites during the preparation of brain slices. One way to test this hypothesis would be to intracellularly label neurons during recording and then subsequently reconstruct the remainder of the dendritic arbor in three-dimensions. The quantification of these anatomical data would then serve as a basis for the correlation of dendritic morphology with intrinsic physiological properties.

In conclusion, brain slice preparations offer unparalleled stability for electrophysiological recordings and allow an investigator to easily manipulate the chemical environment and thus, represent a valuable adjunct to *in vivo* preparations for studying the synaptic mechanisms underlying activity in the STN-GP network. However, these *in vitro* data should be viewed in light of the short-comings of studying young neurons outside of their natural environment, the brain.

6.3 Future Studies

There are a number of logical extensions to these studies that would be of use in further defining the mechanisms underlying activity and hence, information processing in the STN-GP network.

6.3.1 *In vivo* studies

The *in vivo* studies of this thesis provide a stimulus and rationale for additional physiological investigations in anaesthetised and freely-moving animals. To better understand the reciprocal relationship between neurons of the STN-GP network, unit activity should be simultaneously recorded from functionally-related subregions of the STN and GP (identified using the method of Nambu et al., 2000). The utilisation of "tetrodes" or similar mulitelectrode arrays in such experiments would permit a more thorough examination of the synchronisation of neuronal discharge within and between connected regions of the parent nuclei and would also be useful in characterising the pathological alterations of neuronal synchrony that may occur as a result of the depletion of dopamine. Furthermore, preliminary data suggest that the simultaneous recording of LFPs would provide a useful adjunct to multiunit recordings in future experiments since this technique can be used to assess the local synchronisation of oscillatory activity in the STN-GP network. Whilst the experiments described above can be performed in anaesthetised or freely-moving animals, studies using the latter preparation could be potentially more valuable since they may provide information on the dynamics of activity in the STN-GP network and cerebral cortex during the planning, initiation and execution of specific motor commands. On a similar note, studies in freely-moving animals could be used to test whether the activity of the STN-GP network is altered during the learning of a motor task. Furthermore, the effects of pharmacological manipulation of various brain regions on activity in the STN-GP network and ongoing behavioural performance could be directly assessed following the implantation of chronic indwelling cannulae in these animals. For example, it would be possible to determine the influences of the corticosubthalamic and subthalamopallidal projections over neuronal activity and behaviour by injecting excitatory amino acid receptor antagonists into the STN and GP, respectively.

To gain further insight as to whether the processing of cortically-derived information by the STN-GP network is altered in PD, multiunit recordings of the responses of STN and GP neurons to brief cortical stimulation could be carried out in 6-OHDA-lesioned animals anaesthetised with urethane (adapted from the study of Fujimoto and Kita, 1993 in intact animals). In addition, simultaneous LFP recordings could be used to test for the emergence of synchronised, pathological oscillatory activity in the STN-GP network in response to cortical input.

Since extracellular unit recordings can only provide a precise measurement of the times of occurrence of neuronal activity, intracellular recordings techniques should be utilised in anaesthetised animals to further elucidate the roles of extrinsic synaptic inputs and intrinsic membrane properties in shaping the activity of neurons in the STN-GP network. The structure of the burst-like discharges of STN and GP neurons engaged in LFO activity is extremely variable, suggesting that statistical analyses of unit recordings alone are unlikely to yield detailed information on underlying synaptic and intrinsic mechanisms. Similarly, the heterogeneous rebound burst responses of STN neurons will likely confound an estimation of the prevalence of such responses in spike trains. Intracellular recordings would facilitate the identification of sequences of excitation, inhibition and/or disfacilitation that may underlie LFO activity of STN and GP neurons in normal and parkinsonian animals. Furthermore, it would be possible to test whether natural or electrically-evoked synaptic inhibition can generate sufficient hyperpolarisation in STN neurons to produce rebound burst-firing *in vivo*. Such experiments would also be useful for determining whether the (heterogeneous) rebound burst-firing of STN neurons *in vitro* is representative of the rebound responses of STN neurons with intact dendrites *in vivo*.

Although the results of these and other studies have suggested that the corticosubthalamic pathway is of great importance in basal ganglia function and dysfunction, the fundamental physiological characteristics of corticosubthalamic transmission remain to

be established. Thus, detailed intracellular recording studies of the responses of STN neurons to brief cortical stimulation are needed to address a number of key issues, including: (1) the interplay of cortical input with the voltage-dependent and independent properties of STN neurons; (2) the short- and long-term regulation of corticosubthalamic tranmission *i.e.*, synaptic plasticity; (3) the role of dopaminergic, serotonergic, and cholinergic inputs to the STN in the pre- and post-synaptic modulation of cortical input; and (4) the impact of chronic dopamine depletion on corticosubthalamic transmission.

6.3.2 *In vitro* studies

The *in vitro* study of this thesis provides a good starting point for future investigations of the synaptic physiology of the STN-GP network. Recent immunohistochemical (Fritschy et al., 1999; Margeta-Mitrovic et al., 1999; Booth et al., 2000; Charara et al., 2000) and electrophysiological (Booth et al., 1999) data indicate that functional $GABA_B$ receptors are expressed in the STN. The effects of $GABA_A$ and $GABA_B$ receptor activation are dramatically different (for reviews, see Kaila, 1994; Deisz, 1997) and it would be of interest to test whether pre- and/or post-synaptic $GABA_B$ receptors play a role in modulating or mediating GABAergic neurotransmission in the STN. Specifically, it is important to determine whether the long-lasting hyperpolarisations that typically result from post-synaptic $GABA_B$ receptor activation play a part in the generation of rebound burst-firing in STN neurons. Additonal extensions of the current study of $GABA_A$ receptor-mediated inhibition in the STN could include: (1) an examination of the effects of pre-synaptic $GABA_B$ receptor activation on evoked IPSPs; and (2) the utilisation of minimal (rather then supramaximal) stimulation conditions to characterise the responses of STN neurons to input from single pallidosubthalamic axons. The favourable recording conditions in brain slice preparations should also be exploited to study the short- and long-term plasticity of

inhibitory and excitatory inputs to the STN, which may prove to be of critical importance for physiological and pathophysiological activity in the STN-GP network *in vivo*.

These and other *in vivo* studies of animal models of PD have firmly established that the STN is overactive following dopamine depletion. Pathological increases in the activity of STN neurons are generally assumed to be caused by alterations in the activity of afferent systems. However, it is possible that the chronic loss of dopaminergic tone from the basal ganglia results in a switch of physiological phenotype in the STN. In other words, the intrinsic membrane properties of STN neurons may be temporarily or permanently altered, such that neurons become hypersensitive to excitatory input from the cortex and thalamus, or hyposensitive to inhibitory input from the GP. To test this hypothesis, brain slices should be prepared from 6-OHDA-lesioned or MPTP-treated rodents, and the intrinsic properties and response profiles of recovered STN neurons be determined. In light of the present data, it would be particularly interesting to characterise rebound burst-firing and T-channel expression in the parkinsonian STN, and to evaluate the responses of STN neurons to trains of evoked IPSPs and EPSPs.

The *in vitro* study in thesis was limited to the examination of the dynamics of GABAergic inhibition in the STN. To better understand the mechanisms underlying activity in the STN-GP network *in vivo*, it is necessary to perform a complementary study of the dynamics of glutamatergic excitation in the GP because relatively little is known about the physiology and pharmacology of the subthalamic input to GP neurons. Such a study might also serve as a basis for understanding some of more perplexing phenomena that were recorded in the STN-GP network during the course of the *in vivo* studies in this thesis, for example, the observation that activity in the STN is only reflected in the GP under certain conditions.

6.3.3 Anatomical studies

To characterise fully the roles of neurons within their respective networks, it is necessary to correlate observed physiology with known morphology. A "morpho-functional" approach to studying the STN and GP has the potential to greatly increase our understanding of the STN-GP network and the functions that it subserves. Thus, the selective labelling of single neurons with the juxtacellular labelling technique, following physiological characterisation *in vivo*, presents an ideal opportunity for the correlation of observed physiology with detailed morphology at the LM and EM levels (Pinault, 1996; Bevan et al., 1998; Pang et al., 1998). A wealth of information on the functional organisation of the STN-GP network could potentially be derived from the many neurons that were labelled during the course of this research; a small number of STN and GP neurons (two STN and three GP) were probably labelled in their entirety and were histochemically processed for EM analysis, plus the full dendritic and proximal axonal arbors of many more neurons were labelled and processed for LM analysis. These pools of labelled neurons could be used as a starting point for: (1) testing whether the rat STN is composed of a single type of projection neuron; (2) determining the detailed synaptology of single neurons within the STN-GP network; (3) estimating the degree of convergence and divergence of the connections between STN and GP neurons; and (4) characterising the synaptic relationships of single STN and GP neurons with their targets outside the network.

BIBLIOGRAPHY

Abbott A, Wigmore MA, Lacey MG (1997) Excitation of rat subthalamic nucleus neurones *in vitro* by activation of a group I metabotropic glutamate receptor. Brain Res 766:162-167.

Abeles M (1982) Quantification, smoothing, and confidence limits for single-units' histograms. J Neurosci Methods 5:317-325.

Achermann P, Borbély AA (1997) Low-frequency (< 1 Hz) oscillations in the human sleep electroencephalogram. Neuroscience 81:213-222.

Adrian ED, Matthews BHC (1934) The interpretation of potential waves in the cortex. J Physiol 81:440-471.

Afsharpour S (1985a) Light microscopic analysis of Golgi-impregnated rat subthalamic neurons. J Comp Neurol 236:1-13.

Afsharpour S (1985b) Topographical projections of the cerebral cortex to the subthalamic nucleus. J Comp Neurol 236:14-28.

Aghajanian GK, Rasmussen K (1989) Intracellular studies in the facial nucleus illustrating a simple new method for obtaining viable motor neurons in adult rat brain slices. Synapse 3:331-338.

Aizman O, Brismar H, Uhlen P, Zettergren E, Levey AI, Forssberg H, Greengard P, Aperia A (2000) Anatomical and physiological evidence for D1 and D2 dopamine receptor colocalization in neostriatal neurons. Nature Neurosci 3:226-230.

Albe-Fessard D, Condes-Lara M, Kesar S, Sanderson P (1983) Tonic cortical controls acting on spontaneous and evoked thalamic activity. In: Somatosensory integration in the thalamus (Macchi G, Rustioni A, Spreafico R, eds), pp273-285. Amsterdam: Elsevier.

Alberts WW, Wright EW, Feinstein B (1969) Cortical potentials and Parkinsonian tremor. Nature 221:670-672.

Albin RL (1995) The pathophysiology of chorea/ballism and parkinsonism. Parkinson Rel Disord 1:3-11.

Albin RL, Aldrich JW, Young AB, Gilman S (1989a) Feline subthalamic nucleus neurons contain glutamate-like but not GABA-like or glycine-like immunoreactivity. Brain Res 491:185-188.

Albin RL, Young AB, Penney JB (1989b) The functional anatomy of basal ganglia disorders. Trends Neurosci 12:366-375.

Aldridge JW, Gilman S (1991) The temporal structure of spike trains in the primate basal ganglia: afferent regulation of bursting demonstrated with precentral cerebral cortical ablation. Brain Res 543:123-138.

Aldridge JW, Gilman S, Dauth G (1990) Spontaneous neuronal unit activity in the primate basal ganglia and the effects of precentral cerebral cortical ablations. Brain Res 516:46-56.

Alexander GE, Crutcher MD (1990) Functional architecture of basal ganglia circuits: neural substrates of parallel processing. Trends Neurosci 13:266-271.

Alexander GE, Crutcher MD, DeLong MR (1990) Basal ganglia-thalamocortical circuits; parallel substrates for motor, oculomotor, 'prefrontal' and 'limbic' functions. Prog Brain Res 85:119-146.

Amzica F, Steriade M (1995) Short- and long-range neuronal synchronization of the slow (<1 Hz) cortical oscillation. J Neurophysiol 73:20-37.

Amzica F, Steriade M (1998) Cellular substrate and laminar profile of sleep K-complex. Neuroscience 82:671-686.

Andersen P, Eccles JC, Sears TA (1964) The ventro-basal complex of the thalamus: types of cells, their responses and their functional organization. J Physiol 174:370-399.

Anderson ME, Turner RS (1991) A quantitative analysis of pallidal discharge during targeted reaching movement in the monkey. Exp Brain Res 86:623-632.

Angel A, Gratton DA (1982) The effect of anesthetic agents on cerebral cortical responses in the rat. Br J Pharmac 76:541-549.

Anis NA, Berry SC, Burton NR, Lodge D (1983) The dissociative anaesthetics, ketamine and phencyclidine, selectively reduce excitation of central mammalain neurones by N-methyl-aspartate. Br J Pharmac 79:565-575.

Armstrong-James M, Fox K (1983) Similarities in unitary cortical activity between slow-wave sleep and light urethane anaesthesia in the rat. J Physiol 346:55P.

Armstrong DM, Saper CB, Levey AI, Wainer BH, Terry RD (1983) Distribution of cholinergic neurons in rat brain: demonstrated by the immunocytochemical localization of choline acetyltransferase. J Comp Neurol 216:53-68.

Asanuma C, Porter LL (1990) Light and electron microscopic evidence for a GABAergic projection from the caudal basal forebrain to the thalamic reticular nucleus in rats. J Comp Neurol 302:159-172.

Aubert I, Ghoarayeb I, Normand E, Bloch B (2000) Phenotypical characterisation of the neurons expressing the D1 and D2 dopamine receptors in the monkey striatum. J Comp Neurol 418:22-32.

Awad H, Hubert GW, Smith Y, Levey AI, Conn PJ (2000) Activation of metabotropic glutamate receptor 5 has direct excitatory effects and potentiates NMDA receptor currents in neurons of the subthalamic nucleus. J Neurosci 20:7871-7879.

Aziz TZ, Peggs D, Sambrook MA, Crossman AR (1991) Lesion of the subthalamic nucleus for the alleviation of 1-methyl-4-phenyl-1,2,3,6-tetrahydropyridine (MPTP)-induced parkinsonism in the primate. Mov Disord 6:288-292.

Aziz TZ, Peggs D, Agarwal E, Sambrook MA, Crossman AR (1992) Subthalamic nucleotomy alleviates parkinsonism in the 1-methyl-4-phenyl-1,2,3,6-tetrahydropyridine (MPTP)-exposed primate. Br J Neurosurg 6:575-582.

Baez LA, Ahlskog JE, Randall PK (1977) Body weight and regulatory deficits following unilateral nigro-striatal lesions. Brain Res 132:467-476.

Baunez C, Robbins TW (1999) Effects of transient inactivation of the subthalamic nucleus by local muscimol and APV injections on performance on the five-choice serial reaction time task in rats. Psychopharmacology 141:57-65.

Beckstead RM (1983a) A pallidostriatal projection in the cat and monkey. Brain Res Bull 11:629-632.

Beckstead RM (1983b) A reciprocal axonal connection between the subthalamic nucleus and the neostriatum in the cat. Brain Res 275:137-142.

Beckstead RM (1984) The thalamostriatal projection in the cat. J Comp Neurol 223:313-346.

Beckstead RM, Domesick VB, Nauta WJH (1979) Efferent connections of the substantia nigra and ventral tegmental area in the rat. Brain Res 175:191-217.

Bell K, Churchill L, Kalivas PW (1995) GABAergic projection from the ventral pallidum and globus pallidus to the subthalamic nucleus. Synapse 20:10-18.

Benazzouz A, Gross C, Féger J, Boraud T, Bioulac B (1993) Reversal of rigidity and improvement in motor performance by subthalamic high-frequency stimulation in MPTP-treated monkeys. Eur J Neuroscience 5:382-389.

Benazzouz A, Piallat B, Pollak P, Benabid AL (1995) Responses of substantia nigra *pars reticulata* and globus pallidus complex to high frequency stimulation of the subthalamic nucleus in rats: electrophysiological data. Neurosci Letts 189:77-80.

Beninato M, Spencer RF (1988) The cholinergic innervation of rat substantia nigra: a light and electron micoscopic study. Exp Brain Res 72: 178-184.

Bennett BD, Bolam JP (1994) Synaptic input and output of parvalbumin-immunoreactive neurones in the neostriatum of the rat. Neuroscience 62:707-719.

Bentivoglio M, van der Kooy D, Kuypers HGJM (1979) The organization of the efferent projections of the substantia nigra in the rat. A retrograde fluorescent double labeling study. Brain Res 174:1-17.

Berger B, Gaspar P, Verney C (1991) Dopaminergic innervation of the cerebral cortex: unexpected differences between rodents and primates. Trends Neurosci 14:21-27.

Bergman H and DeLong MR (1989) Electro-physiological studies of the connections between the subthalamic nucleus (STN) and globus pallidus (GP) in behaving monkeys. Soc Neurosci Abstr 15:902.

Bergman H, Wichmann T, DeLong MR (1990) Reversal of experimental parkinsonism by lesions of the subthalamic nucleus. Science 249:1436-1438.

Bergman H, Wichmann T, Karmon B, DeLong MR (1994) The primate subthalamic nucleus. II. Neuronal activity in the MPTP model of parkinsonism. J Neurophysiol 72:507-520.

Bergman H, Feingold A, Nini A, Raz A, Slovin H, Abeles M, Vaadia E (1998) Physiological aspects of information processing in the basal ganglia of normal and parkinsonian primates. Trends Neurosci 21:32-38.

Bergstrom DA, Walters JR (1984) Dopamine attenuates the effects of GABA on single unit activity in the globus pallidus. Brain Res 310:23-33.

Beurrier C, Congar P, Bioulac B, Hammond C (1999) Subthalamic nucleus neurons switch from single-spike activity to burst-firing mode. J Neurosci 19:599-609.

Beurrier C, Bioulac B, Hammond C (2000) Slowly inactivation sodium current (I_{NaP}) underlies single-spike activity in rat subthalamic neurons. J Neurophysiol 83:1951-1957.

Beurrier C, Bioulac B, Audin J, Hammond C (2001) High-frequency stimulation produces a transient blockade of voltage-gated currents in subthalamic neurons. J Neurophysiol 85:1351-1356.

Bevan MD, Bolam JP (1995) Cholinergic, GABAergic, and glutamate-enriched inputs from the mesopontine tegmentum to the subthalamic nucleus in the rat. J Neurosci 15:7105-7120.

Bevan MD, Wilson CJ (1999) Mechanism underlying spontaneous oscillation and rhythmic firing in rat subthalamic neurons. J Neurosci 19:7617-7628.

Bevan MD, Bolam JP, Crossman AR (1994a) Convergent synaptic input from the neostriatum and the subthalamus onto identified nigrothalamic neurons in the rat. Eur J Neurosci 6:320-334.

Bevan MD, Crossman AR, Bolam JP (1994b) Neurons projecting from the entopeduncular nucleus to the thalamus receive convergent synaptic input from the subthalamic nucleus and the neostriatum in the rat. Brain Res 659:99-109.

Bevan MD, Francis CF, Bolam JP (1995) The glutamate-enriched cortical and thalamic input to neurons in the subthalamic nucleus of the rat. J Comp Neurol 361:491-511.

Bevan MD, Smith AD, Bolam JP (1996) The substantia nigra as a site of synaptic integration of functionally diverse information arising from the ventral pallidum and the globus pallidus in the rat. Neuroscience 75:5-12.

Bevan MD, Clarke NP, Bolam JP (1997) Synaptic integration of functionally diverse pallidal information in the entopeduncular nucleus and subthalamic nucleus in the rat. J Neurosci 17:308-324.

Bevan MD, Booth PAC, Eaton SA, Bolam JP (1998) Selective innervation of neostriatal interneurons by a subclass of neuron in the globus pallidus of the rat. J Neurosci 18:9438-9452.

Bolam JP (Ed) (1992) Experimental neuroanatomy. Oxford, UK: Oxford University Press.

Bolam JP, Bennett B (1995) The microcircuitry of the neostriatum. In: Molecular and cellular mechanisms of neostriatal functions (Ariano M, Surmeier DJ, eds), pp1-19. Austin, TX, USA: R.G. Landes Company.

Bolam JP, Bevan MD (2000) Microcircuits of the striatum. In: The basal ganglia and thalamus in health and movement disorders (Ilinsky IA, Kultas-Ilinsky K, eds) *in press*.

Bolam JP, Smith Y (1991) The GABA and substance P input to dopaminergic neurones in the substantia nigra of the rat. Brain Res 529:57-78.

Bolam JP, Smith Y (1992) The striatum and globus pallidus send convergent inputs to single cells in the entopeduncular nucleus of the rat: A double anterograde labelling study combined with postembedding immunocytochemistry for GABA. J Comp Neurol 321:456-476.

Bolam JP, Francis CM, Henedrson Z (1991) Cholinergic input to dopaminergic neurons in the substantia nigra: a double immunocytochemical study. Neuroscience 41:483-494.

Bolam JP, Smith Y, Ingham CA, von Krosigk M, Smith AD (1993) Convergence of synaptic terminals from the striatum and globus pallidus onto single neurones in the subtantia nigra and the entopeduncular nucleus. In: chemical signalling in the basal ganglia (Arbuthnott GW, Emson PC, eds), pp73-88. Oxford, UK: Elsevier.

Bolam JP, Hanley JJ, Booth PAC, Bevan MD (2000) Synaptic organisation of the basal ganglia. J Anat 196:527-542.

Booth PAC, Bolam JP, Wilson CJ, Bevan MD (1999) Post-synaptic $GABA_B$ receptor activation inhibits spontaneous activity and hyperpolarises rat subthalamic neurons *in vitro*. Soc Neurosci Abstr 25:1158.

Booth PAC, Bolam, JP, Ige AO, Disney GH, Marshall FH, White JH, Emson PC (2000) $GABA_B$ receptors in the rat brain: cellular and subcellular distribution in the basal ganglia. Eur J Neurosci 12 [Suppl 11]:133.

Boraud T, Bezard E, Guehl D, Bioulac B, Gross C (1998) Effects of L-DOPA on neuronal activity of the globus pallidus externalis (GPe) and globus pallidus internalis (GPi) in the MPTP-treated monkey. Brain Res 787:157-160.

Boraud T, Bezard E, Bioulac B, Gross CE (2000a) Ratio of inhibited-to-activated pallidal neurons decreases dramatically during passive limb movement in the MPTP-treated monkey. J Neurophysiol 83:1760-1763.

Boraud T, Bezard E, Stutzmann JM, Bioulac B, Gross CE (2000b) Effects of riluzole on the electrophysiological activity of pallidal neurons in the 1-methyl-4-phenyl-1,2,3,6-tetrahydropyridine-treated monkey. Neurosci Letts 281:75-78.

Bormann J, Hamill OP, Sakmann B (1987) Mechanism of anion permeation through channels gated by glycine and γ-aminobutyric acid in mouse cultures spinal neurons. J Physiol 386:243-286.

Breese GR, Traylor TD (1971) Depletion of brain noradrenaline and dopamine by 6-hydroxydopamine. Br J Pharmac 42:88-99.

Bringmann A (1995) Different functions of rat's pedunculopontine tegmental nucleus are reflected in cortical EEG. Neuroreport 6:2065-2068.

Brotchie JM, Mitchell IJ, Sambrook MA, Crossman AR (1991a) Alleviation of parkinsonism by excitatory amino acid transmission in the medial segment of the globus pallidus in rat and primate. Movement Disord 6:133-138.

Brotchie P, Iansek R, Horne MK (1991b) Motor function of the monkey globus pallidus. 1. Neuronal discharge and parameters of movement. Brain 114:1667-1683.

Brotchie P, Iansek R, Horne MK (1991c) Motor function of the monkey globus pallidus. 2. Cognitive aspects of movement and phasic neuronal activity. Brain 114:1685-1702.

Brown LL, Makman MH, Wolfson LI, Dvorkin B, Warner C, Katzman R (1979) A direct role of dopamine in the rat subthalamic nucleus and adjacent intrapeduncular area. Science 206:1416-1418.

Buchwald NA, Wyers EJ, Okuma T, Heuser G (1961) The "caudate-spindle" I. Electrophysiological properties. Electroenceph Clin Neurophysiol 13:509-518.

Bunney BS, Aghajanian GK (1976) The precise localization of nigral afferents in the rat determined by a retrograde tracing technique. Brain Res 117:423-235.

Burbaud P, Gross C, Benazzouz A, Coussemacq M, Bioulac B (1995) Reduction of apomorphine-induced rotational behaviour by subthalamic lesion in 6-OHDA lesioned

rats is associated with a normalization of firing rate and discharge pattern in *pars reticulata* neurons. Exp Brain Res 105:48-58.

Bures J, Buresová O, Weiss T, Fifková E (1963) Excitability changes in non-specific thalamic nuclei during cortical spreading depression in the rat. Electroenceph Clin Neurophysiol 15:73-83.

Buzsáki G, Bickford RG, Ponomareff G, Thal LJ, Mandel R, Gage FH (1988) Nucleus basalis and thalamic control of neocortical activity in the freely moving rat. J Neurosci 8:4007-4026.

Buzsáki G (1991) The thalamic clock: emergent network properties. Neuroscience 41:351-364.

Cahusac PMB, Morris R, Salt TE, Hill RG (1990) Sensory responses of caudal trigeminal neurons to thermal and mechanical stimuli and their behavioural correlates in the rat. Neuroscience 36:543-551.

Calabresi P, Misgeld U, Dodt HU (1987) Intrinsic membrane properties of neostriatal neurons can account for their low level of spontaneous activity. Neuroscience 20:293-303.

Calabresi P, Mercuri NB, Stefani A, Bernardi G (1990) Synaptic and intrinsic control of membrane excitability of neostriatal neurons I. An *in vivo* analysis. J Neurophysiol 63:651-662.

Calabresi P, Pisani A, Mercuri NB, Bernardi G (1996) The corticostriatal projection: from synaptic plasticity to dysfunctions of the basal ganglia. Trends Neurosci 19:19-24.

Campbell GA, Eckardt MJ, Weight FF (1985) Dopaminergic mechanisms in subthalamic nucleus of rat: analysis using horseradish peroxidase and microiontophoresis. Brain Res 333:261-270.

Canteras NS, Shammah-Lagnado SJ, Silva BA, Ricardo JA (1988) Somatosensory inputs to the subthalamic nucleus: a combined retrograde and anterograde horseradish peroxidase study in the rat. Brain 458:53-64.

Canteras NS, Shammah-Lagnado SJ, Silva BA, Ricardo JA (1990) Afferent connections to the subthalamic nucleus; a combined retrograde and anterograde horseradish peroxidase study in the rat. Brain Res 513:43-59.

Carpenter MB, Whittier JR, Mettler FA (1950) Analysis of choreoid hyperkinesia in the rhesus monkey: surgical and pharmacological analysis of hyperkinesia resulting from lesions in the subthalamic nucleus of Luys. J Comp Neurol 92:293-332.

Carpenter MB, Fraser RAR, Shriver JE (1968) The organization of pallidosubthalamic fibres in the monkey. Brain Res 11:522-559.

Carpenter MB, Batton RR, Carleton SC, Keller JT (1981) Interconnections and organization of pallidal and subthalamic nucleus neurons in the monkey. J Comp Neurol 197:579-603.

Carpenter MB, Jayaraman A (1990) Subthalamic nucleus of the monkey: connections and immunocytochemical featuresof afferents. J Hirnforsch 31:653-668.

Carter DA, Fibiger HC (1978) The projections of the entopeduncular nucleus and globus pallidus in rat as demonstrated by autoradiography and horseradish peroxidase histochemistry. J Comp Neurol 177:113-124.

Celada P, Paladini CA, Tepper JM (1999) GABAergic control of rat substantia nigra dopaminergic neurons: role of globus pallidus and substantia nigra *pars reticulata*. Neuroscience 89:813-825.

Chang HT, Wilson CJ, Kitai ST (1981) Single neostriatal efferent axons in the globus pallidus: a light and electron microscopic study. Science 213:915-918.

Chang HT, Kita H, Kitai ST (1984) The ultrastructual morphology of the subthalamic-nigral axon terminals intracellularly labeled with horesradish peroxidase. Brain Res 299:182-185.

Charara A, Parent A (1994) Brainstem dopaminergic, cholinergic and serotonergic afferents to the pallidum in the squirrel monkey. Brain Res 640:155-170.

Charara A, Heilman TC, Levey AI, Smith Y (2000) Pre- and postsynaptic localization of GABA(B) receptors in the basal ganglia in monkeys. Neuroscience 95:127-140.

Charpier S, Mahon S, Deniau JM (1999) *In vivo* induction of long-term potentiation by low-frequency stimulation of the cerebral cortex. Neuroscience 91:1209-1222.

Chergui K, Akaoka H, Charléty PJ, Saunier CF, Buda M, Chouvet G (1994) Subthalamic nucleus modulates burst firing of nigral dopamine neurons via NMDA receptors. Neuroreport 5:1185-1188.

Chernyshev BV, Weinberger NM (1998) Acoustic frequency tuning of neurons in the basal forebrain of the waking guinea pig. Brain Res 793:79-94.

Cheruel F, Dormont JF, Amalric M, Schmeid A, Farin D (1994) The role of the putamen and pallidum in motor initiation in the cat. I. Timing of movement-related single-unit activity. Exp Brain Res 100:250-266.

Cheruel F, Dormont JF, Farin D (1996) Activity of neurons of the subthalamic nucleus in relation to motor performance in the cat. Exp Brain Res 108:206-220.

Chesselet MF, Delfs JM (1996) Basal ganglia and movement disorders. Trends Neurosci 19:417-422.

Chevalier G, Deniau JM (1990) Disinhibtion as a basic process in the expression of striatal functions. Trends Neurosci 13:277-280.

Chevalier G, Thierry AM, Shibazaki T, Féger J (1981) Evidence for a GABAergic inhibitory nigrotectal pathway in the rat. Neurosci Letts 21:67-70.

Chevalier G, Vacher S, Deniau JM, Desban M (1985) Disinhibtion as a basic process in the expression of striatal functions. I. The strato-nigral influence on tecto-spinal/tecto-diencephalic neurons. Brain Res 334:215-226.

Clarke NP, Bolam JP, Bevan MD (1996) Glutamate-enriched inputs from the mesopontine tegementum to the entopeduncular nucleus in the rat. Eur J Neurosci 8:1363-1376.

Clarke NP, Bevan MD, Cozzari C, Hartman BK, Bolam JP, (1997) Glutamate-enriched cholinergic synaptic terminals in the entopeduncular nucleus of the rat. Neuroscience 81:371-385.

Contreras D, Steriade M (1995) Cellular basis of EEG slow rhythms: a study of dynamic corticothalamic relationships. J Neurosci 15:604-622.

Contreras D, Steriade M (1997a) Synchronization of low-frequency rhythms in corticothalamic networks. Neuroscience 76:11-24.

Contreras D, Steriade M (1997b) State-dependent fluctuations of low-frequency rhythms in corticothalamic networks. Neuroscience 76:25-38.

Contreras D, Destexhe A, Sejnowski TJ, Steriade M (1996) Control of spatiotemporal coherence of a thalamic oscillation by corticothalamic feedback. Science 274:771-774.

Contreras D, Destexhe A, Steriade M (1997) Spindle oscillations during cortical spreading depression in naturally sleeping cats. Neuroscience 77: 933-936.

Cooper AJ, Stanford IM (2000) Electrophysiological and morphological characteristics of three subtypes of rat globus pallidus neurone *in vitro*. J Physiol 527:291-304.

Corvaja M, Doucet G, Bolam JP (1993) Ultrastructure and synaptic targets of the raphe-nigral projection in the rat. Neuroscience 55:417-427.

Cowan RL, Wilson CJ (1994) Spontaneous firing patterns and axonal projections of single corticostriatal neurons in the rat medial agranular cortex. J Neurophysiol 71:17-32.

Crossman AR, Sambrook MA, Jackson A (1984) Experimental hemichorea/hemiballismus in the monkey. Studies on the intracerebral sites of action in a drug-induced dyskinesia. Brain 107:579-596.

Dafny N, Reyes-Vasquez C, Qiao JT (1990) Modification of nociceptively identified neurons in the thalamic parafascicularis by chemical stimulation of dorsal raphe with glutamate, morphine, serotonin and focal dorsal raphe electrical stimulation. Brain Res Bull 24:717-723.

Dai M, Tepper JM (1998) Do silent dopminergic neurons exist in the rat substantia nigra *in vivo*? Neuroscience 85:1089-1099.

Damlama M, Bolam JP, Tepper JM (1993) Axon collaterals of *pars reticulata* neurons synapse on *pars compacta* neurons. Soc Neurosci Abstr 19:1432.

Deisz RA (1997) Electrophysiology of $GABA_B$ receptors. In: The GABA receptors (Enna SJ, Bowerey NG, eds), pp157-207. Totowa, NJ, USA: Humana Press.

Deisz RA (1999) The $GABA_B$ receptor antagonist CGP 55845A reduces presynaptic $GABA_B$ actions on neocortical neurons of the rat *in vitro*. Neuroscience 93:1241-1249.

Deniau JM, Hammond C, Chevalier G, Féger J (1978a) Evidence for branched subthalamic nucleus projections to substantia nigra, entopeduncular nucleus and globus pallidus. Neurosci Letts 9:117-121.

Deniau JM, Thierry AM, Shibazaki T, Féger J (1978b) Electrophysiological properties of identified output neurons of the rat substantia nigra (*pars compacta* and *pars reticulata*): Evidence for the existence of branched neurons. Exp Brain Res 32:409-422.

Deniau JM, Kitai ST, Donoghue JP, Grofová I (1982) Neuronal interactions in the substantia nigra *pars reticulata* through axon collaterals of the projection neurons. Exp Brain Res 47:105-113.

Deniau JM, Chevalier G (1992) The lamellar organisation of the rat substantia nigra *pars reticulata*: distribution of projection neurons. Neuroscience. 46:361-377.

Deniau JM, Menetray A, Charpier S (1996) The lamellar organization of the rat substantia nigra *pars recticulata*: Segregated patterns of striatal afferents and relationship to the topography of corticostriatal projections. Neuroscience 73:761-781.

DeLong MR (1971) Activity of pallidal neurons during movement. J Neurophysiol 34:414-427.

DeLong MR (1973) Putamen: activity of single units during slow and rapid arm movements. Science 179:1240-1242.

DeLong MR (1990) Primate models of movement disorders of basal ganglia origin. Trends Neurosci 13:281-285.

DeLong MR, Crutcher, MD, Georgopoulos AP (1983) Relations between movement and single cell discharge in the substantia nigra of the behaving monkey. J Neurosci 3:1599-1606.

DeLong MR, Crutcher, MD, Georgopoulos AP (1985) Primate globus pallidus and subthalamic nucleus: functional organization. J Neurophysiol 53:530-543.

Deransart C, Marescaux C, Depaulis A (1996) Involvement of nigral glutamatergic inputs in the control of seizures in a genetic model of absence epilepsy in the rat. Neuroscience 71:721-728.

Deransart C, Le BT, Marescaux C, Depaulis A (1998a) Role of the subthalamo-nigral input in the control of amygdala-kindled seizures in the rat. Brain Res 807:78-83.

Deransart C, Vercueil L, Marescaux C, Depaulis A (1998b) The role of the basal ganglia in the control of generalised absence seizures. Epilepsy Res 32:213-223.

Deschênes M, Roy JP, Steriade M (1982) Thalamic bursting mechanism: an inward current revealed by membrane hyperpolarisation. Brain Res 239:289-293.

Deschênes M, Bourassa J, Doan VD, Parent A (1996) A single-cell study of the axonal projections arising from the posterior intralaminar thalamic nuclei in the rat. Eur J Neurosci 8:329-343.

Destexhe A, Contreras D, Steriade M (1999) Spatiotemporal analysis of local field potentials and unit discharges in cat cerebral cortex during natural wake and sleep states. J Neurosci 19:4595-4608.

Détári L, Vanderwolf CH (1987) Activity of identified cortically projecting and other basal forebrain neurones during large slow waves and cortical activation in anaesthetized rats. Brain Res 437:1-8.

Détári L, Juhasz G, Kukorelli T (1987) Neuronal firing in the pallidal region: firing patterns during sleep-wakefulness cycle in cats. Electroenceph Clin Neurophysiol 67:159-166.

Diana M, Carcia-Munoz M, Richards J, Freed CR (1989) Electrophysiological analysis of dopamine cells from the substantia nigra *pars compacta* of circling rats. Exp Brain Res 74:625-630.

Domich L, Oakson G, Steriade M (1986) Thalamic burst patterns in the naturally sleeping cat: a comparison between cortically projecting and reticularis neurones. J Physiol 379:429-449.

Dostrovsky JO, Levy R, Wu JP, Hutchison WD, Tasker RR, Lozano AM (2000) Microstimulation-induced inhibition of neuronal firing in human globus pallidus. J Neurophysiol 84:570-574.

Dray A, Gonye TJ, Oakley NR (1976) Caudate stimulation and substantia nigra activity in the rat. J Physiol 259:825-849.

Dubé L, Smith AD, Bolam JP (1988) Identification of synaptic terminals of thalamic or cortical origin in contact with distinct medium size spiny neurons in the rat neostriatum. J Comp Neurol 267455-471.

Duque A, Balatoni B, Détári L, Zaborsky L (2000) EEG correlation of the discharge properties of identified neurons in the basal forebrain. J Neurophysiol 84:1627-1635.

Dybdal D, Gale K (2000) Postural and anticonvulsant effects of inhibition of the rat subthalamic nucleus. J Neurosci 20:6728-6733.

Ebihara S, Shirato K, Harata N, Akaike N (1995) Gramicidin-perforated patch recording: GABA response in mammalian neurones with intact intracellular chloride. J Physiol 484:77-86.

Elble RJ, Koller WC (1990) Parkinsonian Tremor. In: Tremor, pp 118-133. Baltimore, MD, USA: Johns Hopkins UP.

Evarts EV (1964) Temporal patterns of discharge of pyramidal tract neurons during sleep and waking in the monkey. J Neurophysiol 27:152-171.

Faull RLM, Mehler WR (1978) The cells of origin of nigrotectal, nigrothalamic and nigrostriatal projections. Neuroscience 3:989-1002.

Fallon JH, Moore RY (1978) Catecholamine innervation of the basal forebrain IV. Topography of the dopamine projection to the basal forebrain and neostriatum. J Comp Neurol 180:545-550.

Féger J, Robledo P (1991) The effects of activation or inhibition of the subthalamic nucleus on the metabolic and electrophysiological activities within the pallidal complex and substantia nigra in the rat. Eur J Neurosci 3:947-952.

Féger J, Hammond C, Rouzaire-Dubois B (1979) Pharmacological properties of acetylcholine-induced excitation of subthalamic neurons. Br J Pharmacol 65:511-515.

Féger J, Bevan MD, Crossman AR (1994) The projections from the parafascicular thalamic nucleus to the subthalamic nucleus and the striatum arise from separate neuronal populations: a comparison with the corticostriatal and corticosubthalamic efferents in a retrograde fluorescent double-labeling study. Neuroscience 60:125-132.

Feige B, Aertsen A, Kristeva-Feige R (2000) Dynamic synchronization between multiple cortical motor areas and muscle activity in phasic voluntary movements. J Neurophysiol 84:2622-2629.

Fibiger HC, Zis AP, McGreer EG (1973) Feeding and drinking deficits after 6-OHDA administration in the rat: similarity to the lateral hypothalamic syndrome. Brain Res 55:135-148.

Fink-Jensen A, Mikkelsen JD (1989) The striato-entopeduncular pathway of the rat. A retrograde transport study with wheat-germ-agglutinin horseradish peroxidase. Brain Res 476:194-198.

Filion M (1979) Effects of interruption of the nigrostriatal pathway and of dopaminergic agents on the spontaneous activity of globus pallidus neurons in the awake monkey. Brain Res 178:425-441.

Filion M, Harnois C (1978) A comparison of projections of the entopeduncular nucleus to the thalamus, the midbrain and the habenular in the cat. J Comp Neurol 181:763-780.

Filion M, Tremblay L (1991) Abnormal spontaneous activity of globus pallidus neurons in monkeys with MPTP-induced parkinsonism. Brain Res 547:142-151.

Filion M, Tremblay L, Bédard PJ (1988) Abnormal influences of passive limb movement on the activity of globus pallidus neurons in parkinsonian monkeys. Brain Res 444:165-176.

Flores G, Valencia J, Rosales MG, Sierra A, Aceves J (1993) Appearance of EMG activity and motor asymmetry after unilateral lesions of the dopaminergic innervation to the subthalamic nucleus in the rat. Neurosci Letts 162:153-156.

Flores G, Rosales MG, Hernández S, Sierra A, Aceves J (1995) 5-hydroxytryptamine increases spontaneous activity of subthalamic neurons in the rat. Neurosci Letts 192:17-20.

Flores G, Hernández S, Rosales MG, Sierra A, Martínez-Fong D, Flores-Hernández J, Aceves J (1996) M3 muscarinic receptors mediate cholinergic excitation of the spontaneous activity of subthalamic neurons in the rat. Neuroscience 203:203-206.

Flores-Hernández J, Galarraga E, Pineda JA, Bargas J (1994) Patterns of excitatory and inhibitory synaptic transmission in the rat neostriatum as revealed by 4-AP. J Neurophysiol 72:2246-2256.

Fonnum F, Grofova I, Rinvik E (1978) Origin and distribution of glutamate decarboxylase in the nucleus subthalamicus of the cat. Brain Res 153:370-374.

Franks NB, Lieb WR (1994) Molecular and cellular mechanisms of general anaesthesia. Nature 367:607-614.

Freeman AS, Meltzer LT, Bunney BS (1985) Firing properties of substantia nigra dopaminergic neurons in freely moving rats. Life Sci 36:1983-1994.

Freund TF, Powell J, Smith AD (1984) Tyrosine hydroxylase-immunoreactive boutons in synaptic contact with identified striatonigral neurons, with particular reference to dendritic spines. Neuroscience 13:1189-1215.

Fritschy JM, Meskenaite V, Weinmann O, Honer M, Benke D, Mohler H (1999) $GABA_B$-receptor splice variants GB1a and GB1b in rat brain: developmental regulation, cellular distribution and extrasynaptic localization. Eur J Neurosci 11:761-768.

Froestl W, Mickel SJ, von Sprecher G, Bittiger H, Olpe HR (1992) Chemistry of new $GABA_B$ antagonists. Pharmac Commun 2:52-56.

Frost JD (1968) EEG-intracellular potential relationships in isolated cerebral cortex. Electroenceph Clin Neurophysiol 24:343-443.

Fujimoto K, Kita H (1992) Response of rat substantia nigra *pars reticulata* units to cortical stimulation. Brain Res 142:105-109.

Fujimoto K, Kita H (1993) Response characteristics of subthalamic neurons to the stimulation of the sensorimotor cortex in the rat. Brain Res 609:185-192.

Gandia JA, Delasheras S, Garciá M, Giménez-Amaya JM (1993) Afferent projections to the reticular thalamic nucleus from the globus pallidus and the substantia nigra in the rat. Brain Res Bull 32:351-358.

Garcia-Rill E (1991) The pedunculopontine nucleus. Prog Neurobiol 36:361-389.

Garcia-Rill E, Hull CD, Levine MS, Buchwald NA (1979) The spontaneous firing patterns of forebrain neurons: IV. Effects of bilateral and unilateral frontal cortical ablations on firing of caudate, globus pallidus and thalamic neurons. Brain Res 165:23-36.

Gardener TW, Kitai ST (1992) Single-unit activity in the globus pallidus and neostriatum of the rat during performance of a trained head movement. Exp Brain Res 88:517-530.

Gauthier J, Parent M, Lévesque M, Parent A (1999) The axonal arborization of single nigrostriatal neurons in rats. Brain Res 834:228-232.

Georgopoulos AP, DeLong MR, Crutcher MD (1983) Relations between parameters of step-tracking movements and single cell discharge in the globus pallidus and subthalamic nucleus of the behaving monkey. J Neurosci 3:1586-1598.

Gerfen CR, Wilson CJ (1996) The basal ganglia. In: Handbook of chemical neuroanatomy 12: integrated systems of the CNS III (Swanson LW, Björklund A, Hökfelt T, eds), pp371-468. London: Elsevier.

Gerfen CR (1985) The neostriatal mosaic. I. Compartmental organization of projections from the neostriatum to the substantia nigra in the rat. J Comp Neurol 236:454-476.

Gerfen CR, Herkenham M, Thibault J (1987) The neostriatal mosiac. II. Patch- and matrix-directed mesostriatal dopaminergic and non-dopaminergic systems. J Neurosci 7:3915-3934.

Gerfen CR, Engber TM, Mahan LC, Susel Z, Chase TN, Monsma FJ, Sibley DR (1990) D1 and D2 dopamine receptor-regulated gene expression of striatonigral and striatopallidal neurons. Science 250:1429-1432.

Gevins AS, Cutillo BA, Bressler SL, Morgan NH, White RM, Illes J, Greer DS (1989) Event-related covariances during a bimanual visuomotor task. II. Preparation and feedback. Electroenceph Clin Neurophysiol 74:147-160.

Gill SS, Heywood P (1997) Bilateral dorsolateral subthalamotomy for advanced Parkinson's disease. Lancet 350:1224.

Giuffrida R, Li Volsi G, Maugeri G, Perciavalle V (1985) Influences of pyramidal tract on the subthalamic nucleus in the cat. Neurosci Letts 54:231-235.

Gonja-Magee T, Anderson ME (1983) An electrophysiological characterization of projections from the pedunculopontine area to entopeduncular nucleus and globus pallidus in the cat. Exp Brain Res 49:269-279.

Grace AA, Bunney BS (1983a) Intracellular and extracellular electrophysiology of nigral dopaminergic neurons. 1. Identification and characterization. Neuroscience 10: 301-316.

Grace AA, Bunney BS (1983b) Intracellular and extracellular electrophysiology of nigral dopaminergic neurons. 1. Action potential generating mechanisms and morphological correlates. Neuroscience 10: 317-331.

Grace AA, Bunney BS (1984a) The control of firing in nigral dopaminergic neurons: single spike firing. J Neurosci 4:2866-2876.

Grace AA, Bunney BS (1984b) The control of firing in nigral dopaminergic neurons: burst firing. J Neurosci 4:2877-2890.

Grace AA, Bunney BS (1985) Opposing effects of striatonigral feedback pathways on midbrain dopamine cell activity. Brain Res 333:271-284.

Graybiel AM (1995) Building action repertoires: memory and learning functions of the basal ganglia. Curr Opin Neurobiol 5:733-741.

Graybiel AM, Aosaki T, Flaherty AW, Kimura M (1994) The basal ganglia and adaptive motor control. Science 265:1826-1831.

Greenamyre JT, Eller RV, Zhang Z (1991) Antiparkinsonian effects of remacemide hydrochloride, a glutamate antagonist, in rodent and primate models of Parkinson's disease. Ann Neurol 48:977-981.

Greengard P, Allen PB, Nairn AC (1999) Beyond the dopamine receptor: the DARPP-32/protein phosphatase-1 cascade. Neuron 23:435-447.

Groenewegen HJ, Berendse HW (1990) Connections of the subthalamic nucleus with ventral striatopallidal parts of the basal ganglia in the rat. J Comp Neurol 294:607-622.

Groenewegen HJ, Berendse HW (1994) Anatomical relationships between the prefrontal cortex and the basal ganglia in the rat. In: Motor and Cognitive Functions of the

Prefrontal Cortex (Thierry AM, Glowinski J, Goldman-Rakic PS, Christen Y, eds), pp52-76. Berlin: Springer-Verlag.

Groenewegen HJ, Berendse HW, Meredith GE, Haber SN, Voorn P, Wolters JG, Lohman AHM (1991) Functional anatomy of the ventral limbic system-innervated striatum. In: The Mesolimbic Dopamine System: From Motivation to Action (Willner P, Scheel-Kruger J, eds), pp19-59. Chichester, UK: John Wiley & Sons Ltd.

Groenewegen HJ, Berendse HW, Haber SN (1993) Organization of the output of the ventral striatiopallidal system in the rat - ventral pallidal efferents. Neuroscience 57:113-142.

Grofová I, Deniau JM, Kitai ST (1982) Morphology of the substantia nigra *pars reticulata* projection neurons intracellularly labeled with HRP. J Comp Neurol 208:352-368.

Grover LM, Lambert NA, Schwartzkronin PA, Teyler TJ (1993) Role of HCO_3^- ions in depolarizing $GABA_A$ receptor-mediated responses in pyramidal cells of rat hippocampus. J Neurophysiol 69:1541-1555.

Hamada I, DeLong MR (1992) Excitotoxic lesions of the primate subthalamic nucleus result in transient dyskinesia of the contralateral limbs. J Neurophysiol 68:1850-1858.

Hammond C, Yelnik J (1983) Intracellular labelling of rat subthalamic neurones with horseradish peroxidase: computer analysis of dendrites and characterization of axon arborization. Neuroscience 8:781-790.

Hammond C, Deniau JM, Rizk A, Féger J (1978a) Electrophysiological demonstration of an excitatory subthalamonigral pathway in the rat. Brain Res 151:235-244.

Hammond C, Deniau JM, Rouzaire-Dubois B, Féger J (1978b) Peripheral input to the rat subthalamic nucleus, an electrophysiological study. Neuroscience Letts 9:171-176.

Hammond C, Féger J, Bioulac B, Souteryrand JP (1979) Experimental hemiballism in the monkey produced by unilateral kainic acid lesion into courpus Luysii. Brain Res 171:577-580.

Hammond C, Rouzaire-Dubois B, Féger J, Jackson A, Crossman AR (1983a) Anatomical and electrophysiological studies on the reciprocal projections between the subthalamic nucleus and nucleus pedunculopontinus in the rat. Neuroscience. 9:41-52.

Hammond C, Shibazaki T, Rouzaire-Dubois B (1983b) Branched output neurons of the rat subthalamic nucleus: electrophysiological study of the synaptic effects on identified cells in the two main target nuclei, the entopeduncular nucleus and the substantia nigra. Neuroscience. 9:511-520.

Hanley JJ, Bolam JP (1997) Synaptology of the nigrostriatal projection in relation to the compartmental organization of the neostriatum in the rat. Neuroscience 81:353-370.

Hara M, Inoue M, Yasukura T, Onishsi S, Mikami Y, Inagaki C (1992) Uneven distribution of intracellular Cl^- in rat hippocampal neurons. Neurosci Letts 143:135-138.

Hari R, Salenius S (1999) Rhythmical corticomuscular communication. Neuroreport 10:1-10.

Hartmann-von Monakow K, Akert K, Kunzle H (1978) Projections of the precentral motor cortex and other cortical areas of the frontal lobe to the subthalamic nucleus in the monkey. Exp Brain Res 33:395-403.

Hassani OK, Féger J (1999) Effects of intrasubthalamic injection of dopamine receptor agonists on subthalamic neurons in normal and 6-hydroxydopamine-lesioned rats: an electrophysiological and c-fos study. Neuroscience 92:533-543.

Hassani OK, Mouroux M, Féger J (1996) Increased subthalamic neuronal activity after nigral dopaminergic lesion independent of disinhibition via the globus pallidus. Neuroscience 72:105-115.

Hassani OK, François C, Yelnick J, Féger J (1997) Evidence for a dopaminergic innervation of the subthalamic nucleus in the rat. Brain Res 749:88-94.

Hattori T, Fibiger HC, McGeer PL (1975) Demonstration of a pallido-nigral projection innervating dopaminergic neurons. J Comp Neurol 162:487-504.

Hazrati LN, Parent A (1991) Projection from the external pallidum to the reticular thalamic nucleus in the squirrel monkey. Brain Res 550:142-146.

Hedreen JC (1999) Tyrosine hydroxylase-immunoreactive elements in the human globus pallidus and subthalamic nucleus. J Comp Neurol 409:400-410.

Hellwig B, Häußler S, Lauk M, Guschlbauer B, Köster B, Krsietva-Feige R, Timmer J, Lücking CH (2000) Tremor-correlated cortical activity detected by electroencephalography. Clin Neurophysiol 111:806-809.

Hladsky SB, Haydon DA (1984) Ion movements in gramicidin channels. Curr Topics Memb Transport 21:327-371

Hollerman JR, Grace AA (1992) Subthalamic nucleus cell firing in the 6-OHDA-treated rat: basal activity and response to haloperidol. Brain Res 590: 291-299.

Holsheimer J, Demuelemeester H, Nuttin B, de Sutter P (2000) Identification of the target neuronal elements in electrical deep brain stimulation. Eur J Neurosci 12:4573-4577.

Horikawa K, Armstrong WE (1988) A versatile means of intracellular labeling: injection of biocytin and its detection with avidin conjugates. J Neurosci Methods 25:1-11.

Horikawa K, Armstrong WE (1991) A biocytin-containing compound *N*-(2-aminoethyl)biotinimide for intracellular labeling and neuronal tracing studies: comparison with biocytin. J Neurosci Methods 37:141-150.

Hornikiewicz O (1998) Biochemical aspects of Parkinson's disease. Neurology 51 [Suppl 2]:S2-S9.

Hsu SM, Raine L (1981) Protein A, avidin and biotin in immunohistochemistry. J Histochem Cytochem 29:1349-1353.

Hsu SM, Soban E (1982) Color modification of diaminobenzidine (DAB) precipitation by metallic ions and its application for double immunohistochemistry. J Histochem Cytochem 30:1079-1082.

Hsu SM, Raine L, Fanger H (1981) Use of avidin-biotin-peroxidase complex (ABC) in immunoperoxidase techniques: a comparison between ABC and unlabeled antibody (PAP) procedures. J Histochem Cytochem 29:577-580.

Hubbard JI, Llinás R, Quastel DMJ (1969) Extracellular field potentials in the central nervous system. In: Electrophysiological analysis of synaptic transmission, pp265-361. Baltimore, MD, USA: Williams and Watkins.

Hudson JL, van Horne CG, Strömberg I, Brock S, Clayton J, Masserano J, Hoffer BJ, Gerhardt GA (1993) Correlation of apomorphine- and amphetamine-induced turning with nigrostriatal dopamine content in unilateral 6-hydroxydopamine lesioned rats. Brain Res 626:167-174.

Huguenard JR (1996) Low-threshold calcium currents in central nervous system neurons. Annu Rev Physiol 58:329-346.

Huguenard JR, Prince DA (1992) A novel t-type current underlies prolonged Ca^{2+}-dependent burst firing in GABAergic neurons of rat thalamic reticular nucleus. J Neurosci 12:3804-3817.

Huguenard JR, Alger BE (1986) Whole-cell voltage-clamp study of the fading of GABA-activated currents in acutely dissociated hippocampal neurons. J Neurophysiol 56:1-18.

Huntsman MM, Porcello DM, Homanics GE, DeLorey TM, Huguenard JR (1999) Reciprocal inhibitory connections and network synchrony in the mammalian thalamus. Science 283:541-543.

Hurtado JM, Gray CM, Tamas LB, Sigvardt KA (1999) Dynamics of tremor-related oscillations in the human globus pallidus. Proc Natl Acad Sci USA 96:1674-1679.

Hutchison WD, Lozano AM, Tasker RR, Lang AE, Dostrovsky JO (1997) Identification and characterization of neurons with tremor-frequency activity in human globus pallidus. Exp Brain Res 113:557-563.

Inase M, Tokuno H, Nambu A, Akazawa T, Takada M (1999) Corticostriatal and corticosubthalamic input zones from the presupplementary motor area in the macaque:

a comparison with the input zones from the supplementary motor area. Brain Res 833:191-201.

Ince E, Ciliax BJ, Levey AI (1997) Differential expression of D1 and D2 dopamine and m4 muscarinic acetylcholine receptor proteins in identified striatonigral neurons. Synapse 27:357-366.

Ingham CA, Bolam JP, Wainer BH, Smith AD (1985) A correlated light and electron microscopic study of identifed cholinergic neurons that project to the cortex in the rat. J Comp Neurol 239:176-192.

Iribe Y, Moore K, Pang KCH, Tepper JM (1999) Subthalamic stimulation-induced synaptic responses in substantia nigra *pars compacta* dopaminergic neurons *in vitro*. J Neurophysiol 82:925-933.

Jackson A, Crossman AR (1981) Subthalamic projection to nucleus tegmenti pedunculopontinus in the rat. Neurosci Letts 22:17-22.

Jackson A, Crossman AR (1983) Nucleus tegmenti pedunculopontinus: efferent connections with special reference to the basal ganglia, studied in the rat by anterograde and retrograde transport of horseradish peroxidase. Neuroscience 10:725-765.

Jackson A, Crossman AR (1984) Experimental choreoathetosis produced by the injection of gamma-aminobutyric acid antagonist into the lentiform nucleus in the monkey. Neurosci Letts 46:41-45.

Jaeger D, Gilman S, Aldridge JW (1993) Primate basal ganglia activity in a precued reaching task: preparation for movement. Exp Brain Res 95:51-64.

Jaeger D, Kita H, Wilson CJ (1994) Surround inhibition among projection neurons is weak or nonexistent in the rat neostriatum. J Neurophysiol 72:2555-2558.

Jaeger D, Gilman S, Aldridge JW (1995) Neuronal activity in the striatum and pallidum of primates related to the execution of externally cued reaching movements. Brain Res 694:111-127.

Jan C, François C, Tandé D, Yelnik Y, Tremblay L, Agid Y, Hirsch EC (2000) Dopaminergic innervation of the pallidum in the normal state, in MPTP-treated monkeys and in parkinsonian patients. Eur J Neurosci 12:4525-4535.

Jahnsen H, Llinás R (1984a) Electrophysiological properties of guinea-pig thalamic neurones: an *in vitro* study. J Physiol 349:205-226.

Jahnsen H, Llinás R (1984b) Ionic basis for the electroresponsiveness and oscillatory properties of guinea-pig thalamic neurones *in vitro*. J Physiol 349:227-247.

Jarolimek W, Lewen A, Misegeld U (1999) A furosemide-sensitive K^+-Cl^- cotransporter counteracts intracellular Cl^- accumulation and depletion in cultured rat midbrain neurons. J Neurosci 19:4685-4704.

Joel D, Weiner I (1997) The connections of the primate subthalamic nucleus: indirect pathways and the open-interconnected scheme of basal ganglia-thalamocortical circuitry. Brain Res Rev 23:62-78.

Joel D, Weiner I (2000) The connections of the dopaminergic system with the striatum in rats and primates: an analysis with respect to the functional and compartmental organization of the striatum. Neuroscience 96:451-474.

Johnson DH (1996) Point process models of single-neuron discharges. J Comput Neurosci 3:275-299.

Johnston D, Wu SMS (1995) Foundations of cellular neurophysiology. London: MIT Press.

Jonsson G (1980) Chemical neurotoxins as denervation tools in neurology. Annu Rev Neurosci 3:169-187.

Kaila K (1994) Ionic basis of $GABA_A$ receptor channel function in the nervous system. Prog Neurobiol 42:489-537.

Kaneoke Y, Vitek JL (1996) Burst and oscillation as disparate neuronal properties. J Neurosci Methods 68:221-223.

Kang Y, Futami T (1999) Arrhythmic firing in dopamine neurons of rat substantia nigra evoked by activation of subthalamic neurons. J Neurophysiol 82:1632-1637.

Kato M, Kimura M (1992) Effects of reversible blockade of basal ganglia on a voluntary arm movement. J Neurophysiol 68:1516-1534.

Kavanau JL (1997) Memory, sleep and the evolution of mechanisms of synaptic efficacy maintenance. Neuroscience 79:7-44.

Kawaguchi Y (1993) Physiological, morphological and histochemical characterisation of three classes of interneurons in rat neostriatum. J Neurosci 13:4908-4923.

Kawaguchi Y (1997) Neostriatal cell subtypes and their functional roles. Neurosci Res 27:1-8.

Kawaguchi Y, Wilson CJ, Emson PC (1989) Intracellular recordings of identified patch and matrix spiny cells in a slice preparation preserving cortical inputs. J Neurophysiol 62:1052-1068.

Kawaguchi Y, Wilson CJ, Emson PC (1990) Projection subtypes of rat neostriatal matrix cells revealed by intracellular injection of biocytin. J Neurosci 10:3421-3438.

Kawaguchi Y, Wilson CJ, Augood SJ, Emson PC (1995) Striatal interneurones: chemical, physiological and morphological characterization. Trends Neurosci 18:527-535.

Kilner JM, Baker SN, Salenius S, Hari R, Lemon RN (2000) Human cortical muscle coherence is directly related to specific motor parameters. J Neurosci 20:8838-8845.

Kincaid AE, Wilson C J (1996) Corticostriatal innervation of the patch and matrix in the rat neostriatum. J Comp Neurol 374:578-592.

Kincaid AE, Penney JB, Young AB, Newman SW (1991a) Evidence for a projection from the globus pallidus to the entopeduncular nucleus in the rat. Neurosci Letts 128:121-125.

Kincaid AE, Penney JB, Young AB, Newman SW (1991b) The globus pallidus receives a projection from the parafascicular nucleus in the rat. Brain Res 553:18-26.

Kirik D, Rosenblad C, Björklund A (1998) Characterization of behavioural and neurodegenerative changes following partial lesions of the nigrostriatal dopamine system induced by intrastriatal 6-hydroxydopamine in the rat. Exp Neurol 152:259-277.

Kita H (1992) Responses of globus pallidus neurons to cortical stimulation: intracellular study in the rat. Brain Res 589:84-90.

Kita H (1993) GABAergic circuits of the striatum. In: Chemical signalling in the basal ganglia (Arbuthnott GW, Emson PC, eds), pp51-72. Oxford, UK: Elsevier.

Kita H (1996) Glutamatergic and GABAergic postsynaptic responses of striatal spiny neurons to intrastriatal and cortical stimulation recorded in slice preparations. Neuroscience 70:925-940.

Kita H, Kitai ST (1987) Efferent projections of the subthalamic nucleus in the rat: light and electron microscopic analysis with the PHA-L method. J Comp Neurol 260:435-452.

Kita H, Kitai ST (1990) Amygdaloid projections to the frontal cortex and the striatum in the rat. J Comp Neurol 298:40-49.

Kita H, Kitai ST (1991) Intracellular study of rat globus pallidus neurons: membrane properties and responses to neostriatal, subthalamic and nigral stimulation. Brain Res 564:296-305.

Kita H, Kitai ST (1994) The morphology of globus pallidus projection neurons in the rat: an intracellular staining study. Brain Res 636:308-319.

Kita H, Chang HT, Kitai ST (1983a) The morphology of intracellularly labeled rat subthalamic neurons: a light microscopic analysis. J Comp Neurol 215:245-257.

Kita H, Chang HT, Kitai ST (1983b) Pallidal inputs to subthalamus: intracellular analysis. Brain Res 264:255-265.

Kita T, Kita H, Kitai ST (1986) Electrical membrane properties of rat substantia nigra compacta neurons in an *in vitro* slice preparation. Brain Res 372:21-30.

Kita H, Kosaka T, Heizmann CW (1990) Parvalbumin-immunoreactive neurons in the rat neostriatum: a light and electron microscopic study. Brain Res 536:1-15.

Kita H, Tokuno H, Nambu A (1999) Monkey globus pallidus external segment neurons projecting to the neostriatum. Neuroreport. 10:1467-1472.

Kitai ST, Deniau JM (1981) Cortical inputs to the subthalamus: intracellular analysis. Brain Res 214:411-415.

Kiyatkin EA, Rebec GV (1999) Modulation of striatal neuronal activity by glutamate and GABA: iontophoresis in awake animals. Brain Res 822:88-106.

Koós T, Tepper JM (1999) Inhibitory control of neostriatal projection neurons by GABAergic interneurons. Nature Neurosci 2:467-472.

Kornhuber J, Kim JS, Kornhuber ME, Kornhuber HH (1984) The cortico-nigral projection: reduced glutamate content in the substantia nigra following frontal cortex ablation in the rat. Brain Res 322:124-126.

Krack P, Benazzouz A, Pollak P, Limousin P, Piallat B, Hoffmann D, Xie J, Benabid AL (1998) Treatment of tremor in Parkinson's disease by subthalamic nucleus stimulation. Mov Disord 13:907-914.

Kreiss DS, Anderson LA, Walters JR (1996) Apomorphine and dopamine D1 receptor agonists increase the firing rates of subthalamic nucleus neurons. Neuroscience 72:863-876.

Kreiss DS, Mastropietro CW, Rawji SS, Walters JR (1997) The responses of subthalamic nucleus neurons to dopamine receptor stimulation in a rodent model of Parkinson's Disease. J Neurosci 17:6807-6819.

Kupsch A, Earl C (1999) Neurosurgical interventions in the treatment of idiopathic Parkinson's disease: neurostimulation and neural implantation. J Mol Med 77:178-184.

Lang AE, Lozano AM (1998a) Parkinson's disease. Part 1. New Eng J Med 339:1044-1053.

Lang AE, Lozano AM (1998b) Parkinson's disease. Part 2. New Eng J Med 339:1130-1143.

Lapper SR, Smith Y, Sadikot AF, Parent A, Bolam JP (1992) Cortical input to parvalbumin-immunoreactive neurones in the putamen of the squirrel monkey. Brain Res 580: 15-224.

Lavoie B, Smith Y, Parent A (1989) Dopaminergic innervation of the basal ganglia in the squirrel monkey as revealed by tyrosine hydroxylase immunohistochemistry. J Comp Neurol 289:36-52.

Lavoie B, Parent A (1990) Immunohistochemical study of the serotonergic innervation of the basal ganglia in the squirrel monkey. J Comp Neurol 299:1-16.

Lawler CP, Gilmore JH, Watts VJ, Walker QD, Southerland SB, Cook LL, Mathis CA, Mailman RB (1995) Interhemispheric modulation of dopamine receptor interactions in unilateral 6-OHDA rodent model. Synapse 21:299-311.

Leão, AAP (1944) Spreading depression of activity in the cerebral cortex. J Neurophysiol 7:359-390.

Leão, AAP (1947) Further observations on the spreading depression of activity in the cerebral cortex. J Neurophysiol 10:409-414.

Lee HJ, Rye DB, Hallanger AE, Levey AI, Wainer BH (1988) Cholinergic vs. non-cholinergic afferents from the mesopontine tegmentum to the extrapyramidal motor system nuclei. J Comp Neurol 275:469-492.

Lee JH, Daud A, Cribbs LL, Lacerda AE, Pereverzev A, Klockner U, Schneider T, Perez-Reyes E (1999) Cloning and expression of a novel member of the low voltage-activated T-type calcium channel family. J Neurosci 19:1912-1921.

Le Moine C, Bloch B (1995) D1 and D2 receptor gene expression in the rat striatum: sensitive cRNA probes demonstrate prominent segregation of D1 and D2 mRNAs in distinct neuronal populations of the dorsal and ventral striatum. J Comp Neurol 355:418-426.

Lévesque M, Parent A (1998) Axonal arborization of corticostriatal and corticothalamic fibers arsing from prelimbic cortex in the rat. Cereb Cortex 8:602-163.

Lévesque M, Gagnon, S; Parent A, Deschênes M (1996) Axonal arborization of corticostriatal and corticothalamic fibers arising from the second somatosensory area in the rat. Cereb Cortex 6:759-770.

Levine MS, Hull CD, Buchwald NA (1974) Pallidal and entopeduncular intracellular responses to striatal, cortical, thalamic, and sensory inputs. Exp Neurol 44:448-460.

Levy R, Hazrati LN, Herrero MT, Vila M, Hassani OK, Mouroux M, Ruberg M, Asensi H, Agid Y, Féger J, Obeso JA, Parent A, Hirsch EC (1997) Re-evaluation of the functional anatomy of the basal ganglia in normal and parkinsonian states. Neuroscience 76:335-343.

Levy R, Hutchison WD, Lozano AM, Dostrovsky JO (2000) High-frequency synchronization of neuronal activity in the subthalamic nucleus of parkinsonian patients with limb tremor. J Neurosci 20:7766-7775.

Limousin P, Pollak P, Benazzouz A, Hoffmann D, Le Bas JF, Broussolle E, Perret JE, Benabid AL (1995) Effect on parkinsonian signs and symptoms of bilateral subthalamic nucleus stimulation. Lancet 345:91-95.

Lindvall O, Björklund A (1979) Dopaminergic innervation of the globus pallidus by collaterals from the nigrostriatal system. Brain Res 172:169-173.

Llinás R, Yarom Y (1981) Properties and distribution of ionic conductances generating electroresponsiveness of mammalian inferior olivary neurones *in vitro*. J Physiol 315:569-584.

Llinás RR, Ribary U, Jeanmonod D, Kronberg E, Mitra PP (1999) Thalamocortical dysrhythmia: A neurological and neuropsychiatric syndrome characterized by magnetoencephalography. Proc Natl Acad Sci USA 96:15222-15227.

Lozano AM, Lang AE, Hutchinson WD, Dostrovsky JO (1998a) New developments in understanding the etiology of Parkinson's disease and in its treatment. Curr Opin Neurobiol 8:783-790.

McAuley JH, Framer SF, Rithwell JC, Marsden CD (1999) Common 3 Hz and 10 Hz oscillations modulate human eye and finger movements while they simultaneously track a visual target. J Physiol 515:905-917.

MacLeod NK, Ryman A, Arbuthnott GW (1990) Electrophysiological properties of nigrothalamic neurons after 6-hydroxydopamine lesions in the rat. Neuroscience 38:447-456.

Magariños-Ascone CM, Buño W, García-Austt E (1992) Activity in monkey substantia nigra neurons related to a simple learned movement. Exp Brain Res 88:283-291.

Magariños-Ascone CM, Figueiras-Mendez R, Riva-Meana C, Córdoba-Fernández A (2000) Subthalamic neuron activity related to tremor and movement in Parkinson's disease. Eur J Neurosci 12:2597-2607.

Maggi CA, Meli A (1986) Suitability of urethane anaesthesia for physiopharmacological investigations in various systems. Part 1: General considerations. Experientia 42:109-210.

Magnin M, Morel A, Jeanmonod D (2000) Single-unit analysis of the pallidum, thalamus and subthalamic nucleus in parkinsonian patients. Neuroscience 96:549-564.

Maloney KJ, Cape EG, Gotman J, Jones BE (1997) High frequency γ electroencephalogram activity in association with sleep-wake states and spontaneous behaviors in the rat. Neuroscience 76:541-555.

Margeta-Mitrovic M, Mitrovic I, Riley RC, Jan LY, Basbaum AI (1999) Immunohistochemical localization of $GABA_B$ receptors in the rat central nervous system. J Comp Neurol 405:299-321.

Matsumura M, Kojima J, Gardner TW, Hikosaka O (1992) Visual and oculomotor functions of monkey subthalamic nucleus. J Neurophysiol 67:1615-1632.

Maurice N, Deniau JM, Glowinski J, Thierry AM (1998a) Relationships between the prefrontal cortex and the basal ganglia in the rat: physiology of the corticosubthalamic circuits. J Neurosci 18:9539-9546.

Maurice N, Deniau JM, Menetrey A, Glowinski J, Thierry AM (1998b) Prefrontal cortex-basal ganglia circuits in the rat: involvement of ventral pallidum and subthalamic nucleus. Synapse 29:363-370.

Maurice N, Deniau JM, Glowinski J, Thierry AM (1999) Relationships between the prefrontal cortex and the basal ganglia in the rat: physiology of the cortico-nigral circuits. J Neurosci 19:4674-4681.

McCormick DA, Bal T (1997) Sleep and arousal: thalamocortical mechanisms. Annu Rev Neurosci 20:185-215.

McDonald AJ (1991) Topographical organization of amygdaloid projections to the caudatoputamen nucleus, accumbens and related striatal-like areas of the rat brain. Neuroscience 44:15-33.

Metherate R, Cox CL, Ashe JH (1992) Cellular bases of neocortical activation: modulation of neural oscillations by the nucleus basalis and endogenous acetylcholine. J Neurosci 12:4701-4711.

Millhouse OE (1986) Pallidal neurons in the rat. J Comp Neurol 254:209-227.

Mink JW (1996) The basal ganglia: focused selection and inhibition of competing motor programmes. Prog Neurobiol 50:381-425.

Mink JW, Thatch WT (1991a) Basal ganglia motor control. I. Nonexclusive relation of pallidal discharge to five movement modes. J Neurophysiol 65:273-300.

Mink JW, Thatch WT (1991b) Basal ganglia motor control. II. Late pallidal timing relative to movement onset and inconsistent pallidal coding of movement parameters. J Neurophysiol 65:301-329.

Mink JW, Thatch WT (1993) Basal ganglia circuits and their role in behaviour. Curr Opin Neurobiol 3:950-957.

Mintz I, Hammond C, Féger J (1986) Excitatory effect of iontophoretically applied dopamine on identified neurons of the rat subthalamic nucleus. Brain Res 375:172-175.

Mori S, Takino T, Yamada H, Sano Y (1985a) Immunohistochemical demonstration of serotonin nerve fibers in the subthalamic nucleus of the rat, cat and monkey. Neurosci Letts 62:305-309.

Mori S, Ueda S, Yamada H, Takino T, Sano Y (1985b) Immunohistochemical demonstration of serotonin nerve fibers in the corpus striatum of the rat, cat and monkey. Anat Embryol 173:1-5.

Moriizumi T, Hattori T (1992) Separate neuronal populations of the rat globus pallidus projecting to the subthalamic nucleus, auditory cortex and pedunculopontine tegmental area. Neuroscience 46:701-710.

Moriizumi T, Nakamura Y, Kitao Y, Kudo M (1987) Ultrastructual analyses of afferent terminals in the subthalamic nucleus of the cat with a combined degeneration and horseradish peroxidase tracing method. J Comp Neurol 265:159-174.

Morison RS, Bassett DL (1945) Electrical activity of the thalamus and basal ganglia in decorticate cats. J Neurophysiol 8: 309-314.

Moruzzi G, Magoun HW (1949) Brain stem reticular formation and activation of the EEG. Electroenceph Clin Neurophysiol 1:455-473.

Mouroux M, Féger J (1993) Evidence that the parafascicular projection to the subthalamic nucleus is glutamatergic. Neuroreport 4:613-615.

Mouroux M, Hassani OK, Féger J (1995) Electrophysiological study of the excitatory parafascicular projection to the subthalamic nucleus and evidence for ipsi- and contralateral controls. Neuroscience 67:399-407.

Mouroux M, Hassani OK, Féger J (1997) Electrophysiological and fos immunohistochemical evidence for the excitatory nature of the parafascicular projection to the globus pallidus. Neuroscience 81:387-397.

Murer MG, Pazo JH (1993) Circling behaviour induced by inactivation of the $GABA_A$ receptors in the subthalamic nucleus. Neuroreport 4:1219-1222.

Murer MG, Riquelme LA, Tseng KY, Pazo JH (1997) Substantia nigra *pars reticulata* single unit activity in normal and 6-OHDA-lesioned rats: effects of intrastriatal apomorphine and subthalamic lesions. Synapse 27:278-293.

Naito A, Kita H (1994a) The cortico-nigral projection in the rat: an anterograde tracing study with biotinylated dextran amine. Brain Res 637:317-322.

Naito A, Kita H (1994b) The cortico-pallidal projection in the rat: an anterograde tracing study with biotinylated dextran amine. Brain Res 653:251-257.

Nakamura S, Sutin J (1972) The pattern of termination of pallidal axons upon cells of the subthalamic nucleus. Exp Neurol 35:254-264.

Nakanishi H, Hori N, Kastuda N (1985) Neostriatal evoked inhibition and effects of dopamine on globus pallidal neurons in rat slice preparations. Brain Res 358:282-286.

Nakanishi H, Kita H, Kitai ST (1987a) Electrical membrane properties of rat subthalamic neurons in an *in vitro* slice preparation. Brain Res 437:35-44.

Nakanishi H, Kita H, Kitai ST (1987b) Intracellular study of rat substantia nigra *pars reticulata* neurons in an *in vitro* slice preparation: electrical membrane properties and response characteristics to subthalamic stimulation. Brain Res 437:45-55.

Nakanishi H, Kita H, Kitai ST (1988) An N-methyl-D-aspartate receptor mediated excitatory postsynaptic potential evoked in subthalamic neurons in an *in vitro* slice preparation of the rat. Neurosci Letts 95:130-136.

Nakanishi H, Kita H, Kitai ST (1990) Intracellular study of rat entopeduncular neurons in an *in vitro* slice preparation: electrical membrane properties. Brain Res 527:81-88.

Nakanishi H, Kita H, Kitai ST (1991) Intracellular study of rat entopeduncular neurons in an *in vitro* slice preparation: response to subthalamic stimulation. Brain Res 549:285-291.

Nambu A, Llinás R (1994) Electrophysiology of globus pallidus neurons *in vitro*. J Neurophysiol 72:1127-1139.

Nambu A, Llinás R (1997) Morphology of globus pallidus neurons: its correlation with electrophysiology in guinea pig brain slices. J Comp Neurol 377:85-94.

Nambu A, Yoshida SI, Jinnai K (1990) Discharge patterns of pallidal neurons with input from various cortical areas during movement in the monkey. Brain Res 519:183-191.

Nambu A, Takada M, Inase M, Tokuno H (1996) Dual somatotopical representations in the primate subthalamic nucleus: evidence for ordered but reversed body-map transformations from the primary motor cortex and the supplementary motor area. J Neurosci 16:2671-2683.

Nambu A, Tokuno H, Inase M, Takada M (1997) Corticosubthalamic input zones from forelimb representations of the dorsal and ventral divisions of the premotor cortex in the macaque monkey: comparison with the input zones from the primary motor cortex and the supplementary motor area. Neurosci Letts 239:13-16.

Nambu A, Tokuno H, Hamada I, Kita H, Imanishsi M, Akazawa T, Ikeuchi Y, Hasegawa N (2000) Excitatory cortical input to pallidal neurons via the subthalamic nucleus in the monkey. J Neurophysiol 84:289-300.

Nauta HJW, Cole M (1978) Efferent projections of the subthalamic nucleus: an autoradiographical study in monkey and cat. J Comp Neurol 180:1-16.

Neher E (1992) Correction for liquid junction potentials in patch clamp experiments. Methods Enzymol 207:123-131.

Ni ZG, Bouali-Benazzouz R, Gao DM, Benabid AL, Benazzouz A (2000) Changes in the firing pattern of globus pallidus neurons after the degeneration of nigrostriatal pathway are mediated by the subthalamic nucleus. Eur J Neurosci 12:4338-4344.

Nicola SM, Surmeier DJ, Malenka RC (2000) Dopaminergic modulation of neuronal excitability in the striatum and nucleus accumbens. Annu Rev Neurosci 23:185-215.

Nicoll RA, Madison DV (1982) General anesthetics hyperpolarise neurons in the vertebrate central nervous system. Science 217:1055-1057.

Nieoullon A, Cheramy A, Glowinski J (1977) Interdependence of the nigrostriatal dopaminergic systems on the two sides of the brain in the cat. Science 198:416-418.

Nieoullon A, Cheramy A, Leviel V, Glowinski J (1979) Effects of the unilateral application of dopaminergic drugs on the *in vivo* release of dopamine in the two caudate nuclei of the cat. Eur J Pharmacol 53:289-196.

Nini A, Feingold A, Slovin H, Bergman H (1995) Neurons in the globus pallidus do not show correlated activity in the normal monkey, but phase-locked oscillations appear in the MPTP model of Parkinsonism. J Neurophysiol 74:1800-1805.

Nisenbaum ES, Wilson CJ (1995) Potassium currents responsible for inward and outward rectification in rat neostriatal spiny projection neurons. J Neurosci 15:4449-4463.

Nishino H, Ono T, Fukuda M, Sasaki K (1985) Monkey substantia nigra (*pars reticulata*) neuron discharges during operant feeding. Brain Res 334:190-193.

Noda H, Manohar S, Adey WR (1968) Responses of cat pallidal neurons to cortical and subcortical stimuli. Exp Neurol 20:585-610.

Nuñez A (1996) Unit activity of rat basal forebrain neurons: relationship to cortical activity. Neuroscience 72:757-766.

Obeso JA, Olanow CW, Nutt JG (2000a) Levodopa motor complications in Parkinson's disease. Trends Neurosci 23 [10 Suppl]:S2-S7.

Obeso JA, Rodríguez-Oroz MC, Rodríguez M, Lanciego JL, Artieda J, Gonzalo N, Olanow CW (2000b) Pathophysiology of the basal ganglia in Parkinson's disease. Trends Neurosci 23 [10 Suppl]:S8-S19.

Oertel WH, Mugnaini E (1984) Immunocytochemical studies of GABAergic neurons in rat basal ganglia and their relations to other neuronal systems. Neurosci Letts 47:233-238.

Ogura M, Kita H (2000) Dynorphin exerts both postsynaptic and presynaptic effects in the globus pallidus of the rat. J Neurophysiol 83:3366-3376.

Ohye C, Le Guyader C, Féger J (1976) Responses of subthalamic and pallidal neurons to striatal stimulation: an extracellular study on awake animals. Brain Res 111:241-252.

Oorschot DE (1996) Total number of neurons in the neostriatal, pallidal, subthalamic, and substantia nigral nuclei of the rat basal ganglia; a stereological study using the cavalieri and optical disector methods. J Comp Neurol 366:580-599.

Overton PG, Greenfield SA (1995) Determinants of neuronal firing pattern in the guinea-pig subthalamic nucleus: an *in vivo* and *in vitro* comparison. J Neural Transm 10:4154.

Paladini CA, Tepper JM (1999) $GABA_A$ and $GABA_B$ antagonists differentially affect the firing pattern of substantia nigra dopaminergic neurons *in vivo*. Synapse 32:165-176.

Pan HS, Walters JR (1988) Unilateral lesion of the nigrostriatal pathway decreases the firing rate and alters the firing pattern of globus pallidus neurons in the rat. Synapse 2:650-656.

Pang K, Tepper JM, Zaborsky L (1998) Morphological and electrophysiological characteristics of noncholinergic basal forebrain neurons. J Comp Neurol 394:186-204.

Parent A, Hazrati LN (1995a) Functional anatomy of the basal ganglia I. The cortico-basal ganglia-thalamocortical loop. Brain Res Rev 20:91-127.

Parent A, Hazrati LN (1995b) Functional anatomy of the basal ganglia II. The place of the subthalamic nucleus and external pallidum in the basal ganglia circuitry. Brain Res Rev 20:128-154.

Parent A, Smith Y (1987) Organization of the efferent projections of the subthalamic nculeus in the squirrel monkey as revealed by retrograde labeling methods. Brain Res 436:296-310.

Parent A, Gravel S, Boucher R (1981) The origin of forebrain afferents to the habenula in rat, cat and monkey. Brain Res Bull 6:23-28.

Parent A, Charara A, Pinault D (1995) Single striatofugal axons arborizing in both pallidal segments and in the substantia nigra in primates. Brain Res 698:280-294.

Park MR, Falls WM, Kitai ST (1982) An intracellular HRP study of the rat globus pallidus. J Comp Neurol 211:284-294.

Paxinos G, Watson C (1986) The rat brain in stereotaxic coordinates (2nd Edn). Sydney, Aus: Academic Press.

Perez-Reyes E, Cribbs LL, Daud A, Lacerda AE, Barclay J, Williamson MP, Fox M, Lee JH (1998) Molecular characterization of a neuronal low-voltage-activated T-type calcium channel. Nature 391:896-900.

Perier C, Agid Y, Hirsch EC, Féger J (2000) Ipsilateral and contralateral subthalamic activity after unilateral dopaminergic lesion. Neuroreport 11:3275-3278.

Perkel DH, Gerstein GL, Moore GP (1967a) Neuronal spike trains and stochastic point processes I. The single spike train. Biophys J 7:391-418.

Perkel DH, Gerstein GL, Moore GP (1967b) Neuronal spike trains and stochastic point processes II. Simultaneous spike trains. Biophys J 7:419-440.

Perkins MN, Stone TW (1980) Subthalamic projections to the globus pallidus: an electrophysiolgical study in the rat. Exp Neurol 68:500-511.

Perkins MN, Stone TW (1981) Iontophoretic studies on pallidal neurones and the projection from the subthalamic nucleus. Quart J Exp Phys 66:225-236.

Perkins MN, Stone TW (1983) Neuronal responses to 5-hydroxytryptamine and dorsal raphe stimulation within the globus pallidus of the rat. Exp Neurol 79:118-129.

Peschanski M, Guilbaud G, Gautron M (1981) Posterior intralaminar region in rat: neuronal responses to noxious and non-noxious cutaneous stimuli. Exp Neurol 72:226-238.

Pinault D (1994) Golgi-like labeling of a single neuron recorded extracellularly. Neurosci Letts 170:255-260.

Pinault D (1996) A novel single-cell staining procedure performed *in vivo* under electrophysiological control: morpho-functional features of juxtacellularly labeled thalamic cells and other central neurons with biocytin or Neurobiotin. J Neurosci Methods 65:113-136.

Plenz D, Kitai ST (1998) Up and down states in striatal medium spiny neurons simultaneously recorded with spontaneous activity in fast-spiking interneurons studied in cortex-striatum-substantia nigra organotypic cultures. J Neurosci 18:266-283.

Plenz D, Kitai ST (1999) A basal ganglia pacemaker formed by the subthalamic nucleus and external globus pallidus. Nature 400:677-682.

Pollak P, Benabid AL, Limousin P, Benazzouz A, Hoffmann D, Le-Bas JF, Perret J (1996) Subthalamic nucleus stimulation alleviates akinesia and rigidity in parkinsonian patients. Adv Neurol 69:591-594.

Precht W, Yoshida M (1971) Blockade of caudate-evoked inhibition of neurons in the substantia nigra by picrotoxin. Brain Res 32:229-233.

Rajakumar N, Elisevich K, Flumerfelt BA (1993) Compartmental organisation of the striatoentopeduncular projection in the rat. J Comp Neurol 331:286-296.

Rajakumar N, Elisevich K, Flumerfelt BA (1994) Parvalbumin-containing GABAergic neurons in the basal ganglia output system of the rat. J Comp Neurol 350:324-336.

Raz A, Vaadia E, Bergman H (2000) Firing patterns and correlations of spontaneous discharge of pallidal neurons in the normal and the tremulous 1-methyl-4-phenyl-1,2,3,6-tetrahydropyridine vervet model of parkinsonism. J Neurosci 20:8559-8571.

Ricardo JA (1980) Efferent connections of the subthalamic region in the rat. I. The subthalamic nucleus of Luys. Brain Res 202:257-271.

Richards CD, Shiroyama T, Kitai ST (1997) Electrophysiological and immunocytochemical characterization of GABA and dopamine neurons in the substantia nigra of the rat. Neuroscience 80:545-557.

Rinvik E, Ottersen OP (1993) Terminals of subthalamonigral fibres are enriched with glutamate-like immunoreactivity: an electron microscopic immunogold analysis in the cat. J Chem Neuroanat 6:19-30.

Rinvik E, Grofovâ I, Hammond C, Féger J, Deniau JM (1979) A study of the afferent connections to the subthalamic nucleus in the monkey and cat using the HRP technique. Adv Neurol 24:53-70.

Rivera C, Voipio J, Payne JA, Ruusvuori E, Lahtinen H, Lamsa K, Pirvola U, Saarma M, Kaila K (1999) The K^+/Cl^- co-transporter KCC2 renders GABA hyperpolarising during neuronal maturation. Nature 397:251-255.

Robledo P, Féger J (1990) Excitatory influence of rat subthalamic nucleus to substantia nigra *pars reticulata* and the pallidal complex: electrophysiological data. Brain Res 518:47-54.

Rodríguez M, González-Hernández T (1999) Electrophysiological and morphological evidence for a GABAergic nigrostriatal pathway. J Neurosci 19:4682-4694.

Rodriguez MC, Guridi OJ, Alvarez L, Mewes K, Macias R, Vitek J, DeLong MR, Obeso JA (1998) The subthalamic nucleus and tremor in Parkinson's disease. Mov Disord 13 [Suppl 3]:111-118.

Rohlfs A, Nikkah G, Rosenthal C, Rundfeldt C, Brandis A, Samii M, Loscher W (1997) Hemispheric asymmetries in spontaneous firing characteristics of substantia nigra *pars reticulata* neurons following a unilateral 6-hydroxydopamine lesion of the rat nigrostriatal pathway. Brain Res 761:352-356.

Romanski KV, Usunoff KG, Ivanov DP, Galabov GP (1979) Corticosubthalamic projections in the cat: an electron microscopic study. Brain Res 163:319-322.

Romo R, Schultz W (1990) Dopamine neurons of the monkey midbrain: contingencies of responses to active touch during self-initiated arm movements. J Neurophysiol 63:592-606.

Rothblat DS, Schneider JS (1995) Alterations in pallidal neuronal responses to peripheral sensory and striatal stimulation in symptomatic and recovered Parkinsonian cats. Brain Res 705:1-14.

Rouzaire-Dubois B, Scarnati E (1985) Bilateral corticosubthalamic nucleus projections: electrophysiological study in rats with chronic cerebral lesions. Neuroscience 15:69-79.

Rouzaire-Dubois B, Scarnati E (1987) Pharmacological study of the cortical-induced excitation of subthalamic neurons in the rat: evidence for amino acids as putative neurotransmitters. Neuroscience 21:429-440.

Rouzaire-Dubois B, Hammond C, Hamon B, Féger J (1980) Pharmacological blockade of the globus pallidus-induced inhibitory response of subthalamic cells in the rat. Brain Res 200:321-329.

Ruskin DN, Bergstrom DA, Kaneoke Y, Patel BN, Twery MJ, Walters JR (1999) Multisecond oscillations in firing rate in the basal ganglia: robust modulation by dopamine receptor activation and anesthesia. J Neurophysiol 81:2046-2055.

Ryan LJ, Clark KB (1991) The role of the subthalamic nucleus in the response of globus pallidus neurons to stimulation of the prelimbic and agranular frontal cortices in rats. Exp Brain Res 86:641-651.

Ryan LJ, Clark KB (1992) Alteration of neuronal responses in the subthalamic nucleus following globus pallidus and neostriatal lesions in rats. Brain Res Bull 29:319-327.

Ryan LJ, Sanders DJ (1993) Subthalamic nucleus lesion regularizes firing patterns in globus pallidus and substantia nigra *pars reticulata* neurons in rats. Brain Res 626:327-331.

Ryan LJ, Sanders DJ (1994) Subthalamic nucleus and globus pallidus lesions alter activity in nigrothalamic neurons in rats. Brain Res Bull 34:19-26.

Ryan LJ, Tepper JM, Young SJ, Groves PM (1986) Frontal cortex stimulation evoked neostriatal potentials in rats: intracellular and extracellular analysis. Brain Res Bull 17:751-758.

Ryan LJ, Sanders DJ, Clark KB (1992) Auto- and cross-correlation analysis of subthalamic nucleus neuronal activity in neostriatal- and globus pallidal-lesioned rats. Brain Res 583:253-261.

Sachdev RNS, Gilman S, Aldridge JW (1989) Effects of excitotoxic striatal lesions on single unit activity in globus pallidus and entopeduncular nucleus of the cat. Brain Res 501:295-306.

Sadikot AF, Parent A, Smith Y, Bolam JP (1992) Efferent connections of the centromedian and parafascicular nuclei in the squirrel monkey. A light and electron microscopic study of the thalamostriatal projection in relation to striatal heterogeneity. J Comp Neurol 320:228-242.

Sanderson P, Mavoungou R, Albe-Fessard D (1986) Changes in substantia nigra *pars reticulata* activity following lesions of the substantia nigra *pars compacta.* Neurosci Letts 6:25-30.

Saper CB, Loewy AD (1982) Projections of the pedunculopontine tegemental nucleus in the rat: evidence for extrapyramidal circuitry. Brain Res:252:-367-372.

Sato F, Lavallée P, Lévesque M, Parent A (2000a) Single-axon tracing study of neurons of the external segment of the globus pallidus in primate. J Comp Neurol 417:17-31.

Sato F, Parent M, Lévesque M, Parent A (2000b) Axonal branching pattern of neurons of the subthalamic nucleus in primates. J Comp Neurol 424:142-152.

Scarnati E, Proia A, Campana E, Pacitti C (1986) A microiontophoretic study on the nature of the putative synaptic neurotransmitter involved in the pedunculopontine-substantia nigra *pars compacta* excitatory pathway of the rat. Exp Brain Res 62:470-478.

Schultz W (1986) Activity of *pars reticulata* neurons of monkey substantia nigra in relation to motor, sonsory, and complex events. J Neurophysiol 55:660-667.

Schultz W (1998) Predictive reward signal of dopamine neurons. J Neurophysiol 80:1-27.

Schultz W, Romo R (1987) Responses of nigrostriatal dopamine neurons to high-intensity somatosensory stimulation in the anesthetized monkey. J Neurophysiol 57:201-217.

Schultz W, Romo R (1988) Neuronal activity in the monkey neostriatum during the initiation of movements. Exp Brain Res 71:431-436.

Schultz W, Romo R (1990) Dopamine neurons of the monkey midbrain: contingencies of responses to stimuli eliciting immediate behavioural reactions. J Neurophysiol 63:607-623.

Schultz W, Dayan P, Montague PR (1997) A neural substrate of prediction and reward. Science 275:1593-1599.

Schwarting RKW, Huston JP (1996a) Unilateral 6-hydroxydopamine lesions of meso-striatal dopamine neurons and their physiological sequelae. Prog Neurobiol 49:215-266.

Schwarting RKW, Huston JP (1996b) The unilateral 6-hydroxydopamine lesion model in behavioral brain research. Analysis of functional deficits, recovery and treatments. Prog Neurobiol 50:275-331.

Schwarz M, Sontag KH, Wand P (1984) Sensory-motor processing in substantia nigra *pars reticulata* in conscious cats. J Physiol 347:129-147.

Shammah-Lagnado SJ, Alheid GF, Heimer L (1996) Efferent connections of the caudal part of the globus pallidus in the rat. J Comp Neurol 376:489-567.

Shen KZ, Johnson SW (2000) Presynaptic dopamine D2 and muscarine M3 receptors inhibit excitatory and inhibitory transmission to rat subthalamic neurones *in vitro*. J Physiol 525:331-341.

Shink E, Smith Y (1995) Differential synaptic innervation of neurons in the internal and external segments of the globus pallidus by the GABA- and glutamate-containing terminals in the squirrel monkey. J Comp Neurol 358:119-141.

Shink E, Bevan MD, Bolam JP, Smith Y (1996) The subthalamic nucleus and the external pallidum: two tightly interconnected structures that control the output of the basal ganglia in the monkey. Neuroscience 73:335-357.

Sidibé M, Smith Y (1996) Differential synaptic innervation of striatofugal neurones projecting to the internal or external segments of the globus pallidus by thalamic afferents in the squirrel monkey. J Comp Neurol 365:445-465.

Sloan TB (1998) Anesthetic effects on electrophysiological recordings. J Clin Neurophysiol 15:217-226.

Smith Y, Bolam JP (1989) Neurons of the substantia nigra *pars reticulata* receive a dense GABA-containing input from the globus pallidus in the rat. Brain Res 493:160-167.

Smith AD, Bolam JP (1990a) The neural network of the basal ganglia as revealed by the study of synaptic connections of identified neurones. Trends Neurosci 13:259-265.

Smith Y, Bolam JP (1990b) The output neurons and the dopaminergic neurons of the substantia nigra receive a GABA-containing input from the globus pallidus in the rat. J Comp Neurol 296:47-64.

Smith Y, Bolam JP (1991) Convergence of synaptic inputs from the striatum and the globus pallidus onto identified nigrocollicular cells in the rat: a double anterograde labelling study. Neuroscience 44:45-73.

Smith ID, Grace AA (1992) Role of subthalamic nucleus in the regulation of nigral dopamine neuron activity. Synapse 12:287-303.

Smith Y, Kieval JZ (2000) Anatomy of the dopamine system in the basal ganglia. Trends Neurosci 23 [10 Suppl]:S28-33.

Smith Y, Parent A (1988) Neurons of the subthalamic nucleus in primates display glutamate but not GABA immunoreactivity. Brain Res 453:353-356.

Smith Y, Parent A, Seguela P, Descarries L (1987) Distribution of GABA-immunoreactive neurons in the basal ganglia of the squirrel monkey (*Saimiri sciureus*). J Comp Neurol 259:50-64.

Smith Y, Bolam JP, von Krosigk (1990) Topographical and synaptic organization of the GABA-containing pallidosubthalamic projection in the rat. Eur J Neurosci 2:500-511.

Smith Y, Bevan MD, Shink E, Bolam JP (1998) Microcircuitry of the direct and indirect pathways of the basal ganglia. Neuroscience 86:353-387.

Soghomonian JJ, Descarries L, Watkins KC (1989) Serotonin innervation in adult rat neostriatum. II. Ultrastructural features: a radioautographic and immunocytochemical study. Brain Res 481:67-86.

Soltis RP, Anderson LA, Walters JR, Kelland MD (1994) A role for non-NMDA excitatory amino acid receptors in regulating the basal activity of rat globus pallidus neurons and their activation by the subthalamic nucleus. Brain Res 666:21-30.

Soltysik S, Hull CD, Buchwald NA, Fekete T (1975) Single unit activity in basal ganglia of monkeys during performance of a delayed response task. Elecetroenceph Clin Neurophysiol 39:65-78.

Somogyi P, Bolam JP, Smith AD (1981) Monosynaptic cortical input and local axon collaterals of identified striatonigral neurons. A light and electron microscopic study using the Golgi-peroxidase transport-degeneration procedure. J Comp Neurol 195:567-584.

Song WJ, Baba Y, Otsuka T, Murakami F (2000) Characterization of Ca^{2+} channels in rat subthalamic nucleus neurons. J Neurophysiol 84:2630-2637.

Spooren WP, Helfrich SE, Cools AR (1995) Interactions of the subthalamic nucleus and the subpallidal area in oro-facial dyskinesia: role of GABA and glutamate. Psychopharmacology 119:20-26.

Spooren WP, Lynd-Balta E, Mitchell S, Haber SN (1996) Ventral pallidostriatal pathway in the monkey: evidence for modulation of basal ganglia circuits. J Comp Neurol 370:295-312.

Spruston N, Jaffe DB, Johnston D (1994) Dendritic attentuation of synaptic potentials and currents: the role of passive membrane properties. Trends Neurosci 17:161-166.

Staines WA, Fibiger HC (1984) Collateral projections of neurons of the rat globus pallidus to the striatum and substantia nigra. Exp Brain Res 56:217-220.

Staines WA, Atmadja S, Fibiger HC (1981) Demonstration of a pallidostriatal pathway by retrograde transport of HRP-labeled lectin. Brain Res 206:446-450.

Staley KJ, Soldo BL, and Proctor WR (1995) Ionic mechanisms of neuronal excitation by inhibitory $GABA_A$ receptors. Science 269:977-981.

Stanford IM, Cooper AJ (1999) Presynaptic μ and δ opioid receptor modulation of $GABA_A$ IPSCs in the rat globus pallidus *in vitro*. J Neurosci 19:4796-4803.

Stephenson FA (1995) The $GABA_A$ receptors. Biochem J 310:1-9.

Steriade M (1999) Coherent oscillations and short-term plasticity in corticothalamic networks. Trends Neurosci 22:337-345.

Streiade M (2000) Corticothalamic resonance, states of vigilance and mentation. Neuroscience 101:243-276.

Steriade M, Amzica F (1998) Coalescence of sleep rhythms and their chronology in corticothalamic networks. Sleep Res Online 1:1-10.

Steriade M, Jones EG, Llinás RR (1990) Thalamic oscillations and signaling. New York: Wiley-Interscience.

Steriade M, Amzica F, Nuñez A (1993a) Cholinergic and noradrenergic modulation of the slow (≈ 0.3 Hz) oscillation in neocortical cells. J Neurophysiol 70:1385-1400.

Steriade M, Contreras D, Curró Dossi R, Nuñez A (1993b) The slow (< 1 Hz) oscillation in reticular thalamic and thalamocortical neurons: scenario of sleep rhythm generation in interacting thalamic and neocortical networks. J Neurosci 13:3284-3299.

Steriade M, Nuñez A, Amzica F (1993c) A novel slow (< 1 Hz) oscillation of neocortical neurons *in vivo*: depolarizing and hyperpolarizing components. J Neurosci 13:3252-3265.

Steriade M, Nuñez A, Amzica F (1993d) Intracellular analysis of relations between the slow (< 1 Hz) neocortical oscillation and other sleep rhythms of the electroencephalogram. J Neurosci 13:3266-3283.

Steriade M, Contreras D, Amzica F, Timofeev I (1996) Synchronization of fast (30-40 Hz) spontaneous oscillations in intrathalamic and thalamocortical networks. J Neurosci 16:2788-2808.

Stern EA, Kincaid AE, Wilson CJ (1997) Spontaneous subthreshold membrane potential fluctuations and action potential variability of rat corticostriatal and striatal neurons *in vivo*. J Neurophysiol 77:1697-1715.

Stern EA, Jaeger D, Wilson CJ (1998) Membrane potential synchrony of simultaneously recorded striatal spiny neurons *in vivo*. Nature 394:475-478.

Stuart G (1999) Voltage-activated sodium channels amplify inhibition in neocortical pyramidal neurons. Nature Neurosci 2:144-150.

Sugimoto T, Hattori T, Mizuno N, Itoh K, Sato M (1983) Direct projections from the centre median-parafascicular complex to the subthalamic nucleus in the cat and rat. J Comp Neurol 214:209-216.

Surmeier DJ, Eberwine J, Wilson CJ, Cao Y, Stefani A, Kitai ST (1992) Dopamine receptor subtypes colocalize in rat striatonigral neurons. Proc Natl Acad Sci USA 89:10178-10182.

Surmeier DJ, Song WJ, Yan Z (1996) Coordinated expression of dopamine receptors in neostriatal medium spiny neurons. J Neurosci 16:6579-6591.

Svoboda K, Helmchen F, Denk W, Tank, D (1999) Spread of dendritic excitation in layer 2/3 pyramidal neurons in rat barrel cortex *in vivo*. Nature Neurosci 2:65-73.

Taira T, Lamsa K, Kaila K (1997) Posttetanic excitation mediated by $GABA_A$ receptors in rat CA1 pyramidal neurons. J Neurophysiol 77: 2213-2218.

Takada M, Nishihama MS, Nishihama CC, Hattori T (1988) Two separate neuronal populations of the rat subthalamic nucleus project to the basal ganglia and pedunculopontine tegmental region. Brain Res 442:72-80.

Talley EM, Cribbs LL, Lee JH, Daud A, Perez-Reyes E, Bayliss DA (1999) Differential distribution of three members of a gene family encoding low voltage-actived (T-type) calcium channels. J Neurosci 19:1895-1911.

Tepper JM, Trent F (1993) *In vivo* studies of the postnatal development of rat neostriatal neurons. In: Chemical signalling in the basal ganglia (Arbuthnott GW, Emson PC, eds), pp35-50. Oxford, UK: Elsevier.

Tepper JM, Sawyer SF, Groves PM (1987) Electrophysiologically identified nigral dopaminergic neurons intracellularly labeled with HRP: light microscopic analysis. J Neurosci 7:2794-2806.

Tepper JM, Trent F, Nakamura S (1990) Postnatal development of the electrical activity of nigrostriatal dopaminergic neurons. Dev Brain Res 54:21-33.

Tepper JM, Martin LP, Anderson DR (1995) $GABA_A$ receptor-mediated inhibition of rat substantia nigra dopaminergic neurons by *pars reticulata* projection neurons. J Neurosci 15:3092-3103.

Thesleff S (1980) Aminopyridines and synaptic transmission. Neuroscience 5:1413-1419.

Thompson SM, Gähwiler BH (1989) Activity dependent inhibition III. Desensitization and $GABA_B$ receptor-mediated presynaptic inhibition in the hippocampus *in vitro*. J Neurophysiol 61:524-533.

Toan DL, Schultz W (1985) Responses of rat pallidum cells to cortex stimulation and effects of altered dopaminergic activity. Neuroscience 15:683-694.

Totterdell S, Bolam JP, Smith AD (1984) Characterization of pallidonigral neurons in the rat by a combination of Golgi impregnation and retrograde transport of horseradish peroxidase: their monosynaptic input from the neostriatum. J Neurocytol 13:593-616.

Tseng KY, Riquelme LA, Belforte JE, Pazo JH, Murer MG (2000) Substantia nigra *pars reticulata* units in 6-hydroxydopamine-lesioned rats: responses to striatal D2 dopamine receptor stimulation and subthalamic lesions. Eur J Neurosci 12:247-256.

Tsubokawa T, Sutin J (1972) Pallidal and tegmental inhibition of oscillatory slow waves and unit activity in the subthalamic nucleus. Brain Res 41:101-118.

Ulrich D, Huguenard JR (1997a) Nucleus-specific chloride homeostasis in rat thalamus. J Neurosci 17:2348-2354.

Ulrich D, Huguenard JR (1997b) $GABA_A$-receptor-mediated rebound burst firing and burst shunting in thalamus. J Neurophsyiol 78:1748-1751.

Ungerstedt U (1968) 6-hydroxy-dopamine induced degeneration of central monoamine neurons. Eur J Pharm 5:107-110.

Urbain N, Gervasoni D, Soulière F, Lobo L, Rentéro N, Windels F, Astier B, Savasta M, Fort P, Renaud B, Luppi PH, Chouvet G (2000) Unrelated course of subthalamic nucleus and globus pallidus neuronal activities across vigilance states in the rat. Eur J Neurosci 12:3361-3374.

Van der Kooy D, Carter DA (1981) The organization of the efferent projections and striatal afferent of the entopeduncular nucleus and adjacent areas in the rat. Brain Res 211:15-36.

Van der Kooy D, Hattori H (1980) Single subthalamic nucleus neurons project to both the globus pallidus and substantia nigra in rat. J Comp Neurol 192:751-768.

Van der Kooy D, Kolb B (1985) Non-cholinergic globus pallidus cells that project to the cortex but not to the subthalamic nucleus in rat. Neurosci Letts 57:113-118.

Van der Kooy D, Hattori H, Shannak K, Hornykiewicz O (1981) The pallido-subthalamic projection in rat: anatomical and biochemical studies. Brain Res 204:253-268.

Velísková J, Velsek L, Moshé SL (1996) Subthalamic nucleus: a new anticonvulsant site in the brain. Neuroreport 7:1786-1788.

Vila M, Périer C, Féger J, Yelnik Y, Faucheux B, Ruberg M, Raisman-Vozari R, Agid Y, Hirsch EC (2000) Evolution of changes in neuronal activity in the subthalamic nucleus of rats with unilateral lesions of the substantia nigra assessed by metabolic and electrophysiological measurements. Eur J Neurosci 12:337-344.

Villa AEP, Bajo Lorenzana VM (1997) Ketamine modulation of the temporal pattern of discharges and spike train interactions in the substantia nigra *pars reticulata*. Brain Res Bull 43:525-535.

Volkmann J, Joliot M, Mogilner A, Ioannides AA, Lado F, Fazzini E, Ribary U, Llinás R (1996) Central motor loop oscillations in parkinsonian resting tremor revealed by magnetoencephalography. Neurology 46:1359-1370.

Von Krosigk M, Smith Y, Bolam JP, Smith AD (1992) Synaptic organization of GABAergic inputs from the striatum and the globus pallidus onto neurons in the substantia nigra and retrorubral field which project to the medullary reticular formation. Neuroscience 50:531-549.

Walker RH, Arbuthnott GW, Wright AK (1989) Electrophysiological and anatomical observations concerning the pallidostriatal pathway in the rat. Exp Brain Res 74:303-310.

Waszczak BL, Bergstrom DA, Walters JR (1981) Single unit responses of substantia nigra and globus pallidus neurons to GABA agonist and antagonist drugs. Adv Biochem Psychopharmacol 30:79-94.

Waszczak BL, Lee EK, Tamminga CA, Walters JR (1984) Effect of dopamine system activation on substantia nigra *pars reticulata* output neurons: variable single-unit responses in normal rats and inhibition in 6-hydroxydopamine-lesioned rats. J Neurosci 4:2369-2375.

Weiss T, Fifková E (1961) Bioelectric activity in the thalamus and hypothalamus of rats during cortical spreading EEG depression. Electroenceph Clin Neurophysiol 13:734:744.

Whittier JR (1947) Ballism and the subthalamic nucleus (nucleus hypothalamicus, corpus Luysii). Arch Neurol Psychiatry 58: 672-692.

Wichmann T, DeLong MR (1996) Functional and pathophysiological models of the basal ganglia. Curr Opin Neurobiol 6:751-758.

Wichmann T, Bergman H, DeLong MR (1994a) The primate subthalamic nucleus. I. functional properties in intact animals. J Neurophysiol 72:494-506.

Wichmann T, Bergman H, DeLong MR (1994b) The primate subthalamic nucleus. III. Changes in motor behaviour and neuronal activity in the internal pallidum induced by subthalamic inactivation in the MPTP model of Parkinsonism. J Neurophysiol 72:521-530.

Wichmann T, Bergman H, Starr PA, Subramanian T, Watts RL, DeLong MR (1999) Comparison of MPTP-induced changes in spontaneous neuronal discharge in the internal pallidal segment and in the substantia nigra *pars reticulata* in primates. Exp Brain Res 125:397-409.

Wickens JR, Wilson CJ (1998) Regulation of action-potential firing in spiny neurons of the rat neostriatum *in vivo*. J Neurophysiol 79:2358-2364.

Wigmore MA, Lacey MG (2000) A Kv3-like persistent, outwardly rectifying, Cs^+-permeable, K^+ current in rat subthalamic nucleus neurons. J Physiol 527:493-506.

Wilson CJ (1986) Postsynatpic potentials evoked in spiny neostriatal neurons by stimulation of ipsilateral and contralateral neocortex. Brain Res 367:201-213.

Wilson CJ, Groves PM (1980) Fine structure and synaptic connections of the common spiny neuron of the rat neostriatum: a study employing intracellular injection of horseradish peroxidase. J Comp Neurol 194:599-615.

Wilson CJ, Groves PJ (1981) Spontaneous firing patterns of identified spiny neurons in the rat striatum. Brain Res 220:67-80.

Wilson CJ, Phelan KD (1982) Dual topographic representation of neostriatum in the globus pallidus of rats. Brain Res 243:354-359.

Wilson CJ, Kawaguchi Y (1996) The origins of two-state spontaneous membrane potential fluctuations of neostriatal spiny neurons. J Neurosci 16:2397-2410.

Wilson CJ, Young SJ, Groves PM (1977) Statistical firing properties of neuronal spike trains in the substantia nigra: cell types and their interactions. Brain Res 136:243-260.

Windels F, Bruet N, Poupard A, Urbain N, Chouvet G, Feuerstein C, Savasta M (2000) Effects of high frequency stimulation of subthalamic nucleus on extracellular glutamate and GABA in substantia nigra and globus pallidus in the normal rat. Eur J Neurosci 12:4141-4146.

Winters WD, Ferrar-Allado T (1972) The cataleptic state induced by ketamine: a review of the neuropharmacology of anesthesia. Neuropharmacology 11:303-315.

Woolf NJ, Butcher LL (1986) Cholinergic systems in the rat brain: III. Projections from the pontomesencephalic tegmentum to the thalamus, tectum, basal ganglia, and basal forebrain. Brain Res Bull 16:603-637.

Xu ZC, Wilson CJ, Emson PC (1991) Restoration of thalamostriatal projections in rat neostriatal grafts: An electron microscopic analysis. J Comp Neurol 303:22-34.

Yamada H, Fujimoto K, Yoshida M (1995) Neuronal mechanism underlying dystomina induced by bicuculline injection into the putamen of the cat. Brain Res:333-336.

Yelnik J, Percheron G (1979) Subthalamic neurons in primates: a quantitative and comparative analysis. Neuroscience 4:1717-1743.

Yen CT, Fu TC, Chen RC (1989) Distribution of thalamic nociceptive neurons activated from the tail of the rat. Brain Res 498:118-122.

Yoshida M, Nagatsuka Y, Muramatsu S, Niijima K (1991) Differntial roles of the caudate nucleus and putamen in motor behaviour of the cat as investigated by local injection of GABA antagonists. Neurosci Res 10:34-51.

Yoshida S, Nambu A, Jinnai K (1993) The distribution of the globus pallidus neurons with input from various cortical areas in the monkey. Brain Res 611:170-174.

Yung WH, Häusser MA, Jack JJB (1991) Electrophysiology of dopaminergic and non-dopaminergic neurons of the guinea pig substantia nigra *pars compacta in vitro*. J Physiol 436:643-667.

Yung KKL, Bolam JP, Smith AD, Hersch SM, Ciliax BJ, Levey AI (1995) Immunocytochemical localization of D1 and D2 dopamine receptors in the basal ganglia of the rat: light and electron microscopy. Neuroscience 65:709-730.

Yung KKL, Smith AD, Levey AI, Bolam JP (1996) Synaptic connections between spiny neurons of the direct and indirect pathways in the neostriatum of the rat: evidence from dopamine receptor and neuropeptide immunostaining. Eur J Neurosci 8:861-869.

Zahm DS, Williams E, Wohltmann C (1996) Ventral striatopallidothalamic projection: IV. Relative involvements of neurochemically distinct subterritories in the ventral pallidum and adjacent parts of the rostoventral forebrain. J Comp Neurol 364:6965-6974.

Zigmond MJ, Abercrombie ED, Berger TW, Grace AA, Stricker EM (1990) Compensations after lesions of central dopaminergic neurons: some clinical and basic implications. Trends Neurosci 13:290-295.